



University  
of Glasgow

Woods, Kerry Louise (2009) *Regulators of autophagy in Leishmania major*. PhD thesis.

<http://theses.gla.ac.uk/1211/>

Copyright and moral rights for this thesis are retained by the author

A copy can be downloaded for personal non-commercial research or study, without prior permission or charge

This thesis cannot be reproduced or quoted extensively from without first obtaining permission in writing from the Author

The content must not be changed in any way or sold commercially in any format or medium without the formal permission of the Author

When referring to this work, full bibliographic details including the author, title, awarding institution and date of the thesis must be given

# **Regulators of Autophagy in *Leishmania major***

Kerry Louise Woods  
MSc, BSc

Submitted in fulfilment of the requirements for the  
Degree of PhD

University of Glasgow  
Department of Infection and Immunity

February 2009

## Abstract

Autophagy is a conserved lysosomal degradation pathway for recycling long-lived proteins and organelles that is thought to be required for life cycle progression and virulence of *Leishmania*. ATG8 is a ubiquitin like protein that is required for the formation of autophagosomes, and *Leishmania* uniquely possesses a set of ATG8-like proteins in addition to ATG8, that are distributed in three multi-gene families called ATG8A, ATG8B and ATG8C. The localisation and expression of ATG8A, ATG8B and ATG8C were analysed using GFP fusion proteins and affinity purified antibodies. ATG8A exhibited a dramatic relocalisation to punctate structures under starvation conditions, suggestive of a specific role for ATG8A in starvation induced autophagy. Although ATG8 and ATG8A both participate in a response to starvation, they differed in their sensitivity to the PI(3) kinase inhibitor wortmannin, responded differently to the presence of energy sources, and labelled distinct subsets of vesicles. When the data generated in this thesis was considered together with recent analyses of the functions of the cysteine peptidases ATG4.1 and ATG4.2, evidence for distinct roles of ATG8 and ATG8A emerged. ATG8B and ATG8C localised to single punctate structures close to the flagellar pocket in a small proportion of promastigotes grown under nutrient rich conditions. The distribution of ATG8B and ATG8C labelled structures did not change during differentiation or starvation, suggestive of a role distinct from autophagy. ATG8B labelled structures appeared to be duplicated during cell division, and might be derived from endosomal membranes.

ATG8A, ATG8B and ATG8C expression was shown to be developmentally regulated with all expressed at high levels in stationary phase promastigotes. Conjugation of ATG8 to phosphatidylethanolamine (PE) is required for the

association of ATG8 with autophagosome membranes, and while ATG8 was shown to be conjugated to a phospholipid, no evidence was obtained to suggest that ATG8 paralogues are modified by a lipid. High molecular weight proteins were detected by western blot with anti-ATG8, ATG8A, ATG8B and ATG8C antibodies, perhaps indicating associations with other proteins in complexes. Two ubiquitin fusion proteins and a putative SNARE were identified in co-immunoprecipitation experiments performed with anti-ATG8B antibodies, although further experiments are required to determine the validity of these interactions.

To analyse the role of a predicted presenilin-1 (PS1) homologue in *L. major*,  $\Delta ps1$  null mutants were generated. These mutants were not defective in their ability to differentiate into infective metacyclic promastigotes, and could establish infections *in vivo* and *in vitro*, demonstrating that PS1 is not essential and is not a good target for drug development. Large autophagosomes accumulated in  $\Delta ps1$  mutants suggesting that PS1 might be involved in the regulation of autophagy, although it seemed that the parasites could compensate for this, as autophagy was restored to normal levels in  $\Delta ps1$  mutants that had undergone differentiation into amastigotes. Antibodies were raised against a PS1 peptide that recognised *L. major* PS1 only when over-expressed, suggesting that endogenous PS1 is expressed at a low level. PS1-HA that was stably integrated into the genome localised to a structure close to the flagellar pocket, although a different localisation was observed when PS1-GFP was over-expressed, and investigation is required to clarify the subcellular localisation.

In summary, the regulation of autophagy in *L. major* has been investigated from two different angles, leading to the characterisation of a unique family of ATG8-like proteins and an aspartic peptidase, presenilin-1.

# Table of Contents

<b>CHAPTER 1: INTRODUCTION .....</b>	
1.1 Leishmania.....	17
1.1.1 Leishmaniasis - the disease .....	17
1.1.2 Cutaneous leishmaniasis (CL).....	17
1.1.3 Visceral leishmaniasis.....	18
1.1.4 Geographical distribution and disease burden .....	18
1.1.5 Treatment of Leishmaniasis .....	20
1.1.6 Transmission of <i>Leishmania</i> and Life cycle.....	21
1.2 <i>Leishmania</i> Differentiation.....	24
1.2.1 Changes in surface molecule expression during differentiation....	25
1.2.2 Developmentally regulated protein expression and post-translational modifications .....	26
1.2.3 Developmentally regulated changes in endocytic and lysosomal structure and function .....	27
1.2.4 The role of Peptidases in <i>Leishmania</i> Differentiation .....	28
1.3 Autophagy .....	31
1.3.1 General Introduction to Autophagy.....	31
1.3.2 The Selectivity of Autophagy .....	33
1.3.3 The molecular machinery of autophagy .....	34
1.3.4 Regulation and induction of autophagy .....	36
1.3.5 Autophagosome formation .....	37
1.3.6 Atg12-Atg5 conjugation .....	38
1.3.7 Atg8 modification .....	39
1.3.8 Proteins involved in the regulation of autophagosome fusion.....	40
1.3.9 A putative role for Presenilin-1 in Autophagy.....	41
1.3.10 Autophagy in trypanosomatids .....	42
1.3.11 Multiple Atg8 genes in higher eukaryotes and <i>L. major</i> .....	46
1.4 Aims of this project .....	47
<b>CHAPTER 2: MATERIALS AND METHODS .....</b>	
2.1 Bacterial strains and culture methods.....	49
2.1.1 Bacterial strains .....	49
2.1.2 Bacterial culture .....	49
2.1.3 Long term storage of bacteria.....	49
2.1.4 Generation of heat shock competent <i>E. coli</i> .....	50
2.1.5 Heat-shock transformation .....	50
2.2 Vectors used in this study .....	51
2.2.1 Expression vectors for <i>Leishmania</i> .....	51
2.2.2 Ribosomal integration vector for <i>Leishmania</i> (pRIB).....	52
2.2.3 Gene knock-out vector for <i>Leishmania</i> .....	52
2.2.4 Plasmids generated or used in this study .....	53
2.2.5 Oligonucleotides used in this study.....	54
2.3 Molecular biology techniques .....	54
2.3.1 Polymerase chain reaction (PCR) .....	54
2.3.2 Restriction digest.....	55
2.3.3 DNA gel electrophoresis and DNA gel extraction .....	56

2.3.4	Ligations .....	56
2.3.5	Verification of ligations .....	56
2.3.6	Plasmid purification.....	57
2.3.7	Sequence alignments and phylogenetic analyses.....	57
2.4	<i>Leishmania</i> culture methods.....	57
2.4.1	Cell lines used .....	57
2.4.2	Cultivation of <i>L. major</i> .....	57
2.4.3	Preparation of stabilates for long term storage of <i>L. major</i> cell lines	58
2.4.4	Estimation of cell density .....	58
2.4.5	DNA preparation for transfection.....	58
2.4.6	Transfection of <i>Leishmania</i> .....	59
2.4.7	Selection and Cloning of Transfected <i>Leishmania</i> .....	59
2.4.8	Isolation of genomic DNA from <i>Leishmania</i> .....	59
2.4.9	Isolation of total RNA and synthesis of cDNA from <i>Leishmania</i> and	5' RACE
		60
2.4.10	Verification of <i>Leishmania</i> species by PCR .....	60
2.4.11	Southern blot analysis .....	60
2.4.12	Production of <i>Leishmania</i> cell lysates.....	61
2.4.13	Subcellular fractionation.....	61
2.4.14	Purification of <i>L. major</i> metacyclic promastigotes.....	62
2.4.15	Extraction of peritoneal macrophages from BALB/C mice .....	62
2.4.16	Macrophage infection assay.....	63
2.4.17	Footpad infection of BALB/C mice.....	63
2.4.18	Alamar blue test with promastigote cells .....	63
2.4.19	Analysis and Induction of Autophagy .....	64
2.5	Statistical Analysis.....	64
2.6	Fluorescence microscopy.....	64
2.6.1	4,6-Diamidino-2-phenylindole (DAPI) staining.....	65
2.6.2	Green fluorescent protein (GFP) and red fluorescent protein (RFP)	65
		65
2.6.3	FM4-64 labelling .....	65
2.6.4	Lysotracker labelling.....	66
2.6.5	ER-tracker labelling.....	66
2.6.6	Immunofluorescence analysis .....	66
2.7	Biochemical methods .....	67
2.7.1	Purification of His and GST tagged proteins.....	67
2.7.2	Peptide synthesis and antibodies production .....	68
2.7.3	Affinity purification of antibodies .....	68
2.7.4	SDS-PAGE .....	69
2.7.5	Coomassie gel staining .....	69
2.7.6	Western blotting .....	69
2.7.7	Co-immunoprecipitation experiments.....	70
2.7.8	Incorporation of [ <sup>3</sup> H] ethanolamine into <i>L. major</i> promastigotes..	71

### CHAPTER 3: ANALYSIS OF THE LOCATION OF *L. MAJOR* ATG8-LIKE PROTEINS ..

3.1	Introduction .....	73
3.1.1	Multiple Atg8 homologues in eukaryotic organisms .....	73
3.1.2	The roles of Human Atg8 homologues.....	74
3.1.3	The roles of <i>Arabidopsis</i> Atg8 homologues .....	76
3.2	Phylogenetic analysis of ATG8-like proteins in <i>Leishmania</i> .....	77
3.3	Sequence and Structure of <i>L. major</i> ATG8 like proteins.....	82

3.3.1	ATG8 residues required for interaction with ATG4.....	83
3.3.2	ATG8 residues required for the interaction with ATG7 .....	83
3.3.3	ATG8 residues that bind to the ubiquitin core.....	83
3.4	Localisation of ATG8-like proteins during life cycle progression .....	85
3.4.1	Production of GFP and RFP expressing <i>L. major</i> .....	85
3.4.2	Promastigote stages .....	87
3.4.3	Intracellular amastigote stages .....	89
3.5	Localisation of ATG8-like molecules during the starvation response ...	91
3.5.1	GFP-ATG8A is redistributed to multiple punctate structures in a time dependent manner .....	93
3.5.2	Partial colocalisation of ATG8A and ATG8 during starvation .....	95
3.5.3	<i>L. major</i> ATG8A puncta formation is inhibited by the addition of an energy source, but is insensitive to autophagic inhibitors.....	97
3.5.4	ATG8A is not associated with turnover of glycosomes during starvation .....	98
3.6	Localisation of ATG8B and ATG8C.....	100
3.6.1	Co-localisation of ATG8B with other ATG8-like molecules.....	101
3.6.2	Co-localisation of GFP-ATG8B with the endocytic tracer FM4-64 .	103
3.7	Immunofluorescence analysis of ATG8, ATG8A, ATG8B and ATG8C....	104
3.7.1	ATG8B does not co-localise with markers of the Golgi .....	108
3.8	Discussion .....	108

#### CHAPTER 4: POST-TRANSLATIONAL MODIFICATIONS OF ATG8-LIKE PROTEINS ..

4.1	Introduction .....	115
4.1.1	Post translational processing of Atg8 homologues by the cysteine peptidase Atg4 .....	115
4.1.2	Modification of yeast and mammalian Atg8 homologues with a phospholipid .....	118
4.1.3	Subcellular localisation of yeast and mammalian Atg8 homologues	119
4.2	Optimisation of <i>L. major</i> ATG8, ATG8A, ATG8B and ATG8C specific antibodies for western blot analysis .....	120
4.2.1	Detection of ATG8 paralogues in wild type <i>L. major</i> .....	121
4.2.2	Subcellular fractionation of <i>Leishmania</i> promastigotes and immunodetection of ATG8-like proteins.....	126
4.3	An analysis of the potential lipidation of <i>Leishmania</i> ATG8-like proteins	129
4.3.1	Treatment of GFP tagged ATG8 like proteins with phospholipase D	129
4.3.2	Treatment of wild type promastigotes with phospholipase D .....	130
4.3.3	Incorporation of radioactively labelled ethanolamine into <i>Leishmania</i> and immunoprecipitation of ATG8-like proteins .....	133
4.4	Co-immunoprecipitation of <i>Leishmania</i> ATG8B with interacting partners	136
4.5	Discussion .....	145

#### CHAPTER 5: CHARACTERISATION OF *L. MAJOR* PRESENILIN-1 .....

5.1	Introduction .....	150
5.1.1	General Introduction.....	150

5.1.2	Presenilin-1 and it's role in Alzheimer's Disease .....	151
5.1.3	Expression and Localisation of Presenilin-1 .....	152
5.1.4	Structure and Processing of Presenilin-1 .....	152
5.1.5	Activity and Specificity of Presenilin-1 .....	154
5.1.6	Biological Roles of Presenilin-1 independent of the $\gamma$ -secretase complex 155	
5.1.7	Aspartyl peptidase activity in <i>Leishmania</i> .....	156
5.2	Alignments and phylogenetic analyses of <i>L. major</i> presenilin-1 .....	157
5.3	Expression of <i>L. major</i> PS1 mRNA .....	159
5.4	Localisation of <i>L. major</i> PS1 .....	160
5.4.1	Production of <i>L. major</i> expressing GFP and HA tagged PS1 .....	160
5.4.2	Analysis of the localisation of PS1-GFP and PS1-HA .....	164
5.5	Expression of <i>L. major</i> PS1 protein .....	166
5.5.1	Attempts to express a His tagged PS1 fragment .....	166
5.5.2	Expression of GST tagged PS1 fragment .....	166
5.5.3	Peptide synthesis and antibody production .....	167
5.6	Production of PS1 null mutant cell lines .....	171
5.6.1	Confirmation of <i>Leishmania</i> species by PCR .....	171
5.6.2	Generation of $\Delta ps1$ null mutants and confirmation by PCR and Southern blot .....	172
5.7	Analysis of growth and virulence of $\Delta ps1$ mutants .....	179
5.7.1	Growth curves .....	179
5.7.2	Differentiation into metacyclic promastigotes .....	180
5.7.3	Infectivity to mammalian cells .....	183
5.8	Analysis of Autophagy in $\Delta ps1$ mutant promastigotes .....	185
5.9	Analysis of endocytosis and protein trafficking in PS1 null mutants ...	191
5.9.1	Internalisation of the endocytic tracer FM4-64 in $\Delta ps1$ mutants ..	192
5.9.2	Localisation of syntaxin 5 and syntaxin 1A in $\Delta ps1$ mutants .....	193
5.9.3	Trafficking of the vacuolar proton pyrophosphatase (V-H <sup>+</sup> -PPase) in $\Delta ps1$ mutants .....	194
5.10	Other aspartyl peptidases in <i>L. major</i> .....	196
5.11	Discussion .....	198
<b>CHAPTER 6: GENERAL DISCUSSION .....</b>		<b>207</b>
6.1	A role for ATG8A in an autophagy-like starvation response? .....	209
6.2	An association of ATG8B and ATG8C with vesicle-trafficking? .....	212
6.3	Do ATG8 paralogues form conjugates with other proteins rather than a phospholipid? .....	214
6.4	A putative role for PS1 in the regulation of autophagy requires further confirmation .....	218

# List of Tables

## Chapter 1: Introduction

Table 1-1. Core Autophagy Machinery and putative <i>Leishmania</i> orthologues. .	35
---	----

## Chapter 2: Materials and Methods

Table 2-1 Vectors used in this study.....	51
Table 2-2 Plasmids used or generated in this study.....	53
Table 2-3 Oligonucleotides used in this study.....	54

## Chapter 3: Analysis of the location of *L. major* ATG8-like proteins

Table 3-1 <i>Leishmania</i> ATG8 like genes. ....	79
Table 3-2 Percentage sequence identity between yeast, human and <i>Leishmania</i> ATG8 proteins.. ....	81
Table 3-3 Plasmids used for the expression of GFP and RFP tagged ATG8 like proteins in <i>Leishmania</i> . ....	86

## Chapter 4: Post-translational modifications of *L. major* ATG8-like proteins

Table 4-1 Potential interacting partners of ATG8B, experiment one.....	139
Table 4-2 Potential interacting partners of ATG8B, experiment two.....	140
Table 4-3 Potential interacting partners of ATG8B, experiment three.....	142

## Chapter 5: Characterisation of *Leishmania major* Presenilin-1

Table 5-1- Cell lines to study subcellular localisation of PS1 .....	161
Table 5-2 Oligos and Enzymes used for PCR and Southern blot analysis of <i>PS1</i> mutants and re-expressing cell lines .....	175
Table 5-1 LD <sub>50</sub> values for $\gamma$ -secretase and SPP inhibitors on wild type and $\Delta ps1$ <i>L. major</i> .....	197

# List of Figures

## CHAPTER 1: INTRODUCTION

Figure 1-1 Global distribution of Leishmaniasis. ....	19
Figure 1-2 A) Development of <i>Leishmania</i> species in the sandfly vector and mammalian host .....	23
Figure 1-3 <i>Leishmania</i> Life Cycle.....	24
Figure 1-4 Schematic representation of the main intracellular organelles from <i>Leishmania</i> promastigote (left) or amastigote (right) forms.....	28
Figure 1-5 Clans and families of <i>Leishmania major</i> peptidases (taken from Besteiro <i>et al.</i> , 2007). . . . .	30
Figure 1-6 Schematic depiction of Autophagy (taken from Xie and Klionsky, 2007). . . . .	32
Figure 1-7 Regulatory complex for Autophagy induction.. . . .	36
Figure 1-8 Atg12 and Atg8 conjugation systems in vesicle formation . . . . .	38
Figure 1-9 Two conjugation systems involving the ubiquitin like proteins Atg8 and Atg12 are required for the formation of autophagosomes. . . . .	40

## CHAPTER 3: ANALYSIS OF THE LOCATION OF L. MAJOR ATG8-LIKE PROTEINS

Figure 3-1 <i>L. major</i> Gene Arrays for ATG8A, ATG8B and ATG8C. ....	80
Figure 3-2 Phylogenetic analysis of ATG8-like proteins from yeast, human and <i>Leishmania major</i> .....	81
Figure 3-3 Sequence alignment of yeast, human and <i>Leishmania</i> ATG8 proteins	82
Figure 3-4 Maps of the plasmids used for the transient expression of GFP-ATG8A and RFP-ATG8A.. . . .	86
Figure 3-5 Localisation of GFP tagged ATG8 homologues in <i>L. major</i> promastigotes grown in nutrient rich media. ....	88
Figure 3-6 Distribution of GFP-ATG8, GFP-ATG8A, GFP-ATG8B and GFP-ATG8C during growth in nutrient rich media.....	89
Figure 3-7 Localisation of GFP-ATG8A, ATG8B and ATG8C in differentiating parasites within macrophages, 24 hours post infection. ....	90
Figure 3-8 The effect of nutrient deprivation on the localisation of GFP-ATG8, GFP-ATG8A, GFP-ATG8B and GFP-ATG8C. ....	92
Figure 3-9 Starvation response of ATG8A. ....	94
Figure 3-10 Starvation response of ATG8A.....	95
Figure 3-11 Partial colocalisation of GFP-ATG8A with RFP-ATG8. ....	96
Figure 3-12 The response of GFP-ATG8A to starvation in the presence of glucose, proline and wortmannin. ....	98
Figure 3-13 GFP-ATG8A does not co-localise with glycosomes .....	100
Figure 3-14 RFP-ATG8B and GFP-ATG8C localisation over-laps near the flagellar pocket.....	102
Figure 3-15 Co-localisation of GFP-ATG8B with the endocytic tracer FM4-64... 104	104
Figure 3-16 Immunofluorescence analysis of ATG8, ATG8A, ATG8B and ATG8C in promastigotes.. . . .	107
Figure 3-17 Immunofluorescence analysis of ATG8B and the Golgi marker ARL1 .....	108

## CHAPTER 4: POST-TRANSLATIONAL MODIFICATIONS OF ATG8-LIKE PROTEINS

Figure 4-1 Hydrolysis of <i>L. major</i> ATG8s by <i>L. major</i> ATG4s <i>in vitro</i> (Williams <i>et al.</i> , 2009). .....	117
Figure 4-2 The distribution of GFP-ATG8A in $\Delta atg4.2$ null mutants after 4 hours in nutrient deprived medium.. .....	117
Figure 4-3 Specificity of anti-ATG8, anti-ATG8A, anti-ATG8B and anti-ATG8C antibodies. ....	121
Figure 4-4 Immunodetection of endogenous ATG8, ATG8A, ATG8B, and ATG8C in <i>Leishmania</i> promastigotes.. .....	123
Figure 4-5 Immunodetection of endogenous ATG8, ATG8A, ATG8B and ATG8C in <i>Leishmania</i> promastigotes and amastigotes.. .....	125
Figure 4-6 Subcellular fractionation of wild type <i>L. major</i> and detection of endogenous ATG8, ATG8A and ATG8B. ....	128
Figure 4-7 Western blot analysis of GFP-ATG8, GFP-ATG8A and GFP-ATG8B. ....	130
Figure 4-8 Phospholipase D treatment of wild type <i>L. major</i> promastigotes and detection of endogenous ATG8, ATG8A and ATG8B. ....	132
Figure 4-9 Immunoprecipitation of radioactively labelled ATG8, ATG8B and ATG8B. ....	135
Figure 4-10 Immunoprecipitation of ATG8B from wild type <i>L. major</i> . ....	138

## CHAPTER 5: ANALYSIS OF *L. MAJOR* PRESENILIN-1

Figure 5-1 The role of the $\gamma$ -secretase complex in amyloid plaque formation in Alzheimer's Disease. (taken from de Strooper <i>et al.</i> , 2003).....	152
Figure 5-2 A model of human PS1 (taken from Xia and Wolfe, 2003).....	154
Figure 5-3 Sequence analysis of <i>L. major</i> PS1.....	158
Figure 5-4 Phylogenetic analysis of PS1 proteins from <i>C. elegans</i> , humans, <i>T. brucei</i> , <i>T. cruzi</i> and <i>Leishmania</i> spp.....	159
Figure 5-5- Expression of PS1 mRNAs in promastigote and amastigote life cycle stages. ....	160
Figure 5-6 Maps of plasmids for the expression of PS1-GFP and PS1-HA and integration of PS1-HA into the 18S rRNA locus.....	162
Figure 5-7 Confirmation of PS1-HA cell lines by PCR and western blot.. .....	163
Figure 5-8- Localisation of PS1-GFP (C terminal tag) in live <i>L. major</i> promastigotes. ....	164
Figure 5-9 Immunofluorescence analysis of <i>L. major</i> promastigotes expressing PS1-HA. ....	165
Figure 5-10 Purification of GST-PS1 from <i>E. coli</i> cells.. .....	167
Figure 5-11 Testing pre-immune rabbit serum and anti-PS1 rabbit serum by western blot.....	169
Figure 5-12 Testing affinity purified rabbit anti-PS1 serum by western blot. . .	170
Figure 5-13 Schematic of strategy used to produce PS1 null mutants. ....	171
Figure 5-14 - PCR confirmation of the <i>Leishmania</i> species used in this study... ..	172
Figure 5-15 Maps of wild type <i>PS1</i> locus, <i>PS1</i> loci with integration of <i>BSD</i> and <i>HYG</i> resistance genes, and the 18S ribosomal locus with integration of <i>PS1</i> .....	174
Figure 5-16 PCR analysis of $\Delta ps1$ mutant clones.. .....	176
Figure 5-17 Southern blot analysis of $\Delta PS1$ -5 and $\Delta PS1$ -B. ....	177
Figure 5-18 Southern Blot Analysis of <i>L. major</i> $\Delta ps1$ null mutants, heterozygotes and re-expressing cell lines. ....	179
Figure 5-19 Growth curve for $\Delta ps1$ mutants.....	180
Figure 5-20 Analysis of metacyclogenesis in $\Delta ps1$ null mutants. ....	182

Figure 5-21 Infection and survival of <i>L. major</i> wild type and $\Delta ps1$ promastigotes within peritoneal macrophages .....	184
Figure 5-22 Formation of footpad lesions in BALB/c mice infected with wild type and $\Delta PS1$ mutant <i>L. major</i> .. .....	185
Figure 5-23. Analysis of autophagy in $\Delta ps1$ mutant promastigotes (experiment one).....	188
Figure 5-24 Abnormally large autophagosomes accumulate in $\Delta ps1$ mutant promastigotes. ....	189
Figure 5-25 Analysis of autophagy in $\Delta ps1$ mutant promastigotes (experiment two). ....	190
Figure 5-26 Localisation of GFP-ATG8, GFP-ATG8A, GFP-ATG8B and GFP-ATG8C in $\Delta PS1$ mutants.. .....	191
Figure 5-27 Uptake of the endocytic tracer FM4-64 in $\Delta ps1$ mutants.....	193
Figure 5-28 Localisation of syntaxin 1A and syntaxin 5 in $\Delta ps1$ promastigotes..	194
Figure 5-29 Localisation of wild type and mutated V-H <sup>+</sup> -PPase in $\Delta ps1$ mutants.. .....	196

## Acknowledgements

First, I would like to thank my supervisors Prof. Jeremy Mottram and Prof. Graham Coombs for giving me the opportunity to carry out my PhD in their labs, and in particular to Jeremy for the day to day advice and regular helpful discussions. I especially appreciate having had the opportunities to present my work at various conferences in the past year. I would also like to acknowledge the MRC for funding this research.

A huge thankyou is due to Dr Rod Williams who has been involved in the autophagy project from the start, and who shared many ideas with me and always found the time to offer practical advice in the lab.

Thanks also to my assessor, Dr Tansy Hammarton, who offered helpful input throughout the project. Dr Richard Burchmore carried out mass spec analysis on the samples obtained in co-IP experiments and gave lots of helpful advice, so thanks go to him. Dr Lawrence Tetley and Margaret helped me to try immuno-EM analyses, and I am grateful for their time and patience.

Thanks to all members of the Mottram lab for making it an enjoyable place to work - particularly to Elaine for keeping me sane at times and helping out with some last minute cloning disasters, and to Jim Scott, Jim Hilley, Cathy, Lesley, Elmarie, Esther, Jane, Rod, Daniela, Will, Yuk-Chen, Seb and Audrey and everyone else for lots of help (and fun) over the past few years.

Finally, thanks to Alex for being so supportive throughout the whole project.

## Author's Declaration

The research reported in this thesis is the result of my own original work, except where stated otherwise, and has not been submitted for any other degree.

Some of the results contained in this thesis have been presented at conferences, as follows:

Woods, KL., Williams, RA., Coombs, GH., Mottram, JC. Regulators of Autophagy in *Leishmania*. British Society of Parasitology Annual Meeting, Newcastle 2008.

Woods, KL., Williams, RA., Coombs, GH., Mottram, JC. Regulators of Autophagy in *Leishmania*. 19<sup>th</sup> Annual Molecular Parasitology Meeting. Woods Hole, USA, 2008.

Woods, KL., Williams, RA., Coombs, GH., Mottram, JC. The roles of ATG8-like proteins in *Leishmania major*. Northern UK Kinetoplastid Meeting, Liverpool 2008.

Some of the results presented in chapter 3 have been published in Autophagy journal.

Williams, RAM., Woods., KL., Juliano, L., Mottram, JC., Coombs, GH. Characterisation of unusual families of ATG8-like proteins and ATG12 in the protozoan parasite *Leishmania major* (2009). *Autophagy* 5(2): 1-14

## List of Abbreviations

APP	amyloid precursor protein
APLP1	amyloid precursor protein relatd protein
ATG	<u>autophagy</u> related
bp	base pair
BSA	Bovine serum albumin
BSD	blasticidin S
CL	cutaneous leishmaniasis
CMA	chaperone mediated autophagy
CPA	cysteine peptidase A
CPB	cysteine peptidase B
CTF	C-terminal fragment
DABCO	4-diazabicyclo[2.2.2]octane
DAPI	4,6-diamidino-2-phenylindole
DAPT	<i>N</i> -[ <i>N</i> -(3,5-difluorophenacetyl)- <i>L</i> -alanyl]- <i>S</i> -phenylglycine t-butyl ester
DMSO	dimethyl sulfoxide
E-64	<i>trans</i> -epoxysuccinyl- <i>L</i> -leucylamido(4-guanidino)butane
EDTA	ethylenediamine tetra acetic acid
EF1- $\alpha$	elongation factor alpha from <i>T. brucei</i>
ER	endoplasmic reticulum
FT	flow through
GABARAP	$\gamma$ -aminobutyric-acid-type-A (GABA <sub>A</sub> )-receptor associated protein
GATE-16	Golgi-associated ATPase enhancer of 16kDa
GFP	green fluorescent protein
GIPL	glycosylinositol phospholipid
GPI	glycoinositol-phopholipid
HYG	hygromycin B
HIFCS	heat inactivated foetal calf serum
HRP	horseradish peroxidase
IPTG	isopropyl- $\beta$ -D-thiogalactopyranoside
K11777	<i>N</i> -methyl-piperazine-Phe-homoPhe-vinylsulfone-phenyl
Kb	kilo base
kDa	kilo Dalton
LB	Luria-Bertani medium
LC3	microtubule-associated protein 1 light chain 3
LD50	lethal dose to kill 50%
LPG	lipophosphoglycan
$\mu$	micro
m	milli / metre
M	molar
MAP-LC3	microtubule-associated protein 1 light chain 3
Min	minute
ms	millisecond
MVT	multivesicular tubule
NEO	neomycin (G418)
NSF	<i>N</i> -ethylmaleimide-sensitive factors
OD	optical density
PBS	phosphate buffered saline
PCR	polymerase chain reaction
PE	phosphatidylethanolamine

PEM	peritoneal exudate macrophage
PI3K	phosphoinositide 3-kinase
PLD	phospholipase D
PM	peritrophic matrix
PMSF	phenylmethylsulfonyl fluoride
PSG	promastigote secretory gel
PS1	presenilin-1
PV	parasitophorous vacuole
RFP	red fluorescent protein
SDS-PAGE	sodium dodecylsulphate polyacrylamide gel electrophoresis
SEM	standard error of mean
SNAP	Soluble NSF attachment protein
SNARE	N-ethylmaleimide-sensitive factors adaptor protein receptors
SPP	signal peptide peptidase
Triton X-100	t-Octylphenoxypolyethoxyethanol
V-H-P-Pase	vacuolar proton pyrophosphatase
VSG	variant surface glycoprotein
WHO	world health organisation
WT	wild type
X-Gal	5-bromo-4-chloro-3-indolyl- $\beta$ -[D]-galactopyranoside

# 1 Introduction

## 1.1 Leishmania

### 1.1.1 Leishmaniasis – the disease

The Leishmaniasis are parasitic diseases with a diverse array of clinical forms, a widespread geographical distribution, and a great epidemiological diversity. Obligate intracellular parasites of the genus *Leishmania* (order Kinetoplastida), of which 21 out of 30 species infect man (Herwaldt, 1999), are the cause of the disease. Leishmaniasis occurs in two main clinical forms, cutaneous and visceral, which are associated with a broad range of symptoms (Herwaldt, 1999).

### 1.1.2 Cutaneous leishmaniasis (CL)

Cutaneous leishmaniasis (CL) affects the skin and mucous membranes, and is a public health and a social problem in many countries in the New and Old World. CL in the Old World is caused mainly by *Leishmania major*, *L. tropica* and *L. aethiopica*, and also less commonly in the Mediterranean area by *L. infantum* and *L. donovani* (Gonzalez *et al.*, 2008). The main causative agents in the New World are *L. braziliensis*, *L. guyanensis*, *L. amazonensis*, *L. panamensis*, *L. mexicana* and *L. peruviana* (Tuon *et al.*, 2008). CL has been categorised into four different clinical forms, localised CL, recidivans, diffuse CL and mucocutaneous CL.

In localised CL the parasite is confined to the skin where it causes the formation of lesions, typically 0.5 - 3 cm in diameter, which usually heal spontaneously over several months or years. However, secondary bacterial infection is common and can cause severe pain and disability (Gonzalez *et al.*, 2008).

Recidivans is a chronic form of CL is caused by *L. tropica* that affects approximately 5% of patients infected with this species. It is characterised by an extreme cellular immune response and frequent development of microsatellite lesions that relapse and ulcerate on previous scars. The disease is difficult to treat and extremely disfiguring (Reithinger *et al.*, 2007).

Diffuse cutaneous leishmaniasis (DCL) due to *L. aethiopica*, *L. amazonensis* and *L. mexicana* is characterised by disseminated lesions that resemble those of

lepromatous leprosy. These lesions can cover the entire body of an individual, and are not self healing (Reithinger *et al.*, 2007)

Mucocutaneous leishmaniasis (MCL), which mostly occurs in the New World, causes extensive destruction of nasal and pharyngeal cavities causing extremely disfiguring lesions and mutilation of the face. Secondary bacterial infections are common, and this form of the disease can be fatal (Reithinger *et al.*, 2007).

### **1.1.3 Visceral leishmaniasis**

Visceral leishmaniasis is characterised by fever, splenomegaly, hepatomegaly and anaemia and is the most severe form of the disease, almost always fatal if untreated. The disease, called “Kala-azar” in India, is caused by *L. donovani* in Africa, India and Asia, *L. infantum* in the Mediterranean basin, and *L. chagasi* in the New World. A complication of visceral disease is post-kala-azar dermal leishmaniasis (PKLD). PKLD is characterised by a nodular rash and has been reported in patients from India and Sudan after treatment for VL (Zijlstra *et al.*, 2003)

### **1.1.4 Geographical distribution and disease burden**

Leishmaniasis affects around 12 million people and is endemic in 88 countries (72 of which are developing countries), putting an estimated 350 million people at risk. Annual incidence is estimated at 500,000 new cases of visceral leishmaniasis, and as many as 1 - 1.5 million for cutaneous leishmaniasis (Desjeux, 2004). The leishmaniases cause an estimated 70,000 deaths each year, and an estimated 2.4 million disability-adjusted life years (Reithinger *et al.*, 2007). 90% of CL cases occur in Afghanistan, Algeria, Brazil, Pakistan, Peru, Saudi Arabia and Syria, while 90% of VL cases occur in Bangladesh, north eastern India, Nepal, Sudan and north eastern Brazil (Desjeux, 2004) (figure 1.1).

The number of cases reported globally has increased over the past 10 years, in part due to improved diagnosis, but also due to an increase in anti-leishmanial drug resistance and a lack of adequate vector or reservoir control tools (Reithinger *et al.*, 2007). The distribution of leishmaniasis has been modified since the emergence of the HIV/AIDS pandemic, and co-infection of HIV/*Leishmania*, which can lead to uncommon clinical forms of the disease and

resistance against current treatment, has been reported in 35 countries (Cruz *et al.*, 2006; Santos *et al.*, 2008). Until the introduction of highly active antiretroviral therapy (HAART) in the late 1990s, up to 70% of all cases of visceral leishmaniasis in the Mediterranean basin were associated with HIV. Co-infection with HIV/*Leishmania* is becoming an increasing problem in countries including Ethiopia, Sudan, Brazil and India (Cruz *et al.*, 2006).

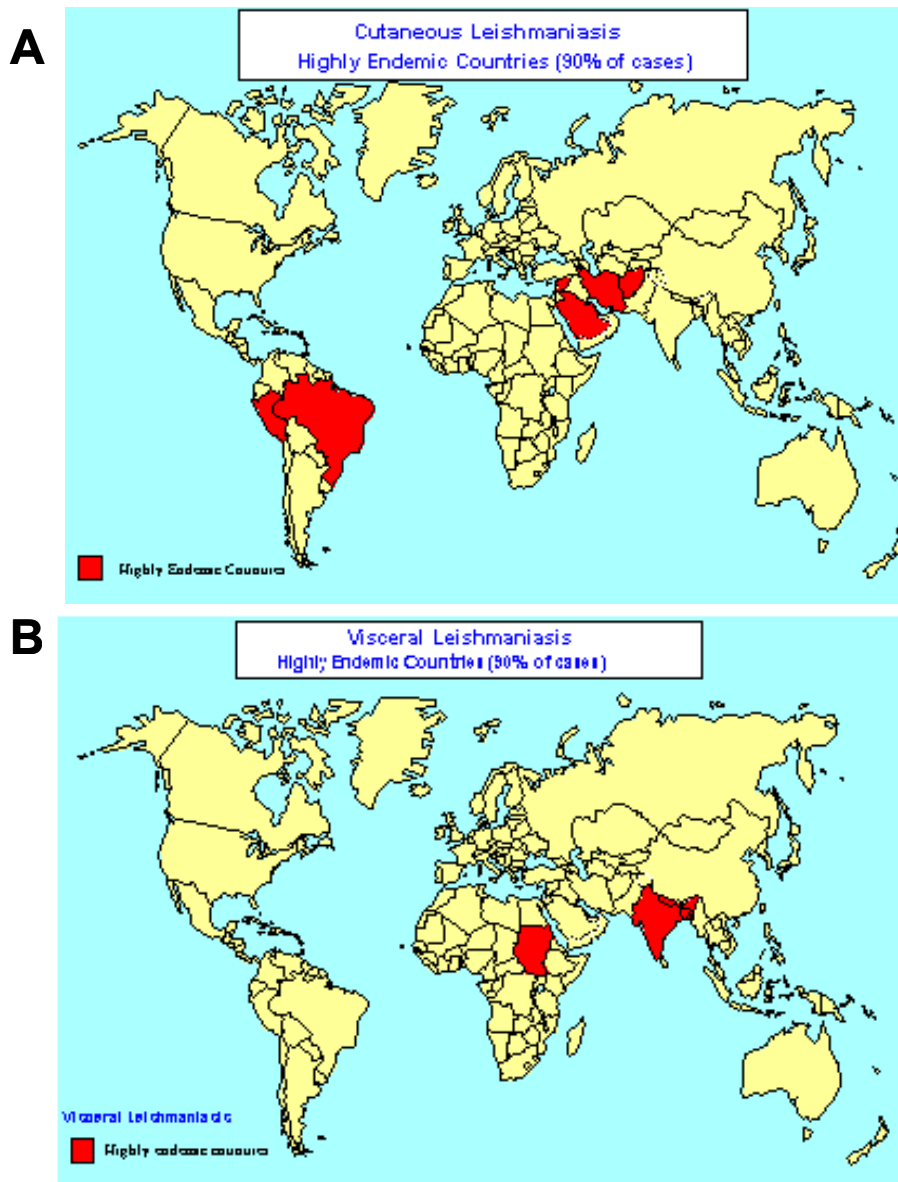


**Figure 1-1 Global distribution of Leishmaniasis.** A) Countries highly endemic (90% of cases) for cutaneous Leishmaniasis. B) Countries highly endemic (90% of cases) for visceral Leishmaniasis. Source: [http://www.who.int/leishmaniasis/leishmaniasis\\_maps/en/index2.html](http://www.who.int/leishmaniasis/leishmaniasis_maps/en/index2.html)

### 1.1.5 Treatment of Leishmaniasis

The development of safe, affordable and effective drugs for the treatment of Leishmaniasis is still urgently required. The fact that recovery from infection leads to resistance against further infection suggests that the production of a successful vaccine is feasible. However, although recent investigations into the possibility of live attenuated vaccines have been promising, no vaccine is currently available (Silvestre *et al.*, 2008).

Primary treatment against leishmaniasis is usually with pentavalent antimonials (sodium stibogluconate (Pentostam<sup>TM</sup>, GlaxoSmith Kline) and meglumine antimoniate (Glucantime, Aventis)), which have been in use since the 1940s (Santos *et al.*, 2008). Though pentavalent antimonials are effective against some forms of leishmaniasis, increasing levels of resistance have been reported (Ouellette *et al.*, 2004). Second line drugs such as pentamidine (Aventis) and amphotericin B (Bristol-Myers Squibb) are used where resistance to antimonials is found, but these drugs are expensive, highly toxic to the host, and resistance to pentamidine has also been reported (Bray *et al.*, 2003; Santos *et al.*, 2008). Lipid-associated formulations of amphotericin B (for example AmBiosome®, Gilead) have reduced toxicity, but prohibitively high costs limit their usefulness (Croft and Coombs, 2003).

A number of drugs are currently in clinical development. Miltefosine, originally developed as an anticancer drug, was first registered for the oral treatment of visceral leishmaniasis in India in 2002, and is currently recommended for use against visceral and cutaneous leishmaniasis in a number of other countries including Ethiopia, Bolivia and Colombia (Berman, 2008). However, there are concerns about the teratogenicity that limit its use in women of child bearing age and also its long half life which is feared may lead to the emergence of drug resistance (Croft *et al.*, 2006). Paromomycin, an aminoglycoside antibiotic, was originally identified as an antileishmanial drug in the 1960s, and phase IV trials are currently ongoing in India and in East Africa (Sundar *et al.*, 2007). With both miltefosine and paromomycin, resistance could be induced in *L. donovani* promastigotes *in vitro* (Maarouf *et al.*, 1998; Seifert *et al.*, 2003). Sitamaquine (an 8-aminoquinoline derivative) is another oral drug currently in development at GlaxoSmithKline (GSK), and appears to be only mildly toxic to the host (Croft

and Coombs, 2003). Although progress has been made in recent years, the development of drugs that are affordable, have low or no toxic effects, and that are less likely to lead to the acquirement of drug resistance in the parasite takes many years, so continued research regarding *Leishmania* cell biology is still desperately needed.

### **1.1.6 Transmission of *Leishmania* and Life cycle**

Transmission of *Leishmania* occurs between female phlebotomine sandflies and mammalian hosts. About 30 species of phlebotomine sandflies (family Psychodidae, subfamily *Phlebotominae*) are proven vectors (Desjeux, 1996). Leishmaniasis can be anthroponotic, where humans are the main reservoir (for example visceral disease due to *L. donovani* in India), or zoonotic (for example visceral disease due to *L. chagasi* in Brazil, where dogs are important reservoirs for the disease). There are two main lifecycle stages. Amastigotes, the disease causing stage of the parasite, are intracellular, non-motile parasites that reside and replicate within the mature phagolysosome compartment of macrophages of the mammalian host, and promastigotes are flagellated forms that develop in the sandfly vector.

When the sandfly takes a bloodmeal, amastigotes, which are found in macrophages in the skin of the host, are taken up by the fly. Parasites that are present within the liver or spleen are not accessible to the sandfly. The development of the parasite within the vector is triggered by an increase in pH and a decrease in temperature in the sandfly midgut (Bates, 2007), and takes between six and nine days, depending on the species (Kamhawi, 2006, figure 1.2B). There are at least five developmental stages which occur within the sandfly vector, each with morphological and functional variations that occur to maximise survival in the sandfly (Gossage *et al.*, 2003, figure 1.2A).

Firstly, the amastigote differentiates into weakly motile procyclic promastigotes that are relatively resistant to sandfly digestive enzymes. These replicate in the bloodmeal, which is separated from the midgut by a peritrophic matrix (PM) (Kamhawi, 2006). After a few days, replication of the parasites is reduced and they differentiate into strongly motile nectomonad promastigotes, which accumulate at the anterior end of the peritrophic matrix, and whose function is

to break out of the PM in a process that is facilitated by a parasite secretory chitinase (Bates, 2007). Nectomonads migrate towards the anterior thoracic midgut with some of them attaching themselves to the microvilli of the midgut epithelium until they reach the stomodeal valve at the junction between the foregut and midgut. It is the ability of these nectomonads to attach to the epithelium cells and avoid expulsion during defecation that allows the infection to persist beyond the bloodmeal phase. At the stomodeal valve, the nectomonads differentiate into replicating leptomonad forms, which secrete promastigote secretory gel (PSG), a parasite derived product that is important for establishing infection (Bates, 2007). Some leptomonads attach themselves to the surface of the stomodeal valve and differentiate into haptomonad promastigotes, and others differentiate into metacyclic promastigotes, the mammalian infective form. These highly motile metacyclic promastigotes have a small body with a long flagellum and are resistant to complement mediated lysis, allowing their survival within the mammalian host while they differentiate into amastigotes.

Metacyclic promastigotes are injected into the skin of the mammalian host by the sandfly and are phagocytosed either directly by macrophages or by neutrophils, the first cells to be recruited to the site of infection, which undergo apoptosis after 2-4 days and are subsequently phagocytosed by macrophages (Laskay *et al.*, 2008). Immediately after phagocytosis, the metacyclic promastigotes are located within macrophage derived phagosomes that fuse with endocytic organelles resulting in the formation of an acidic compartment known as the parasitophorous vacuole (PV) (Antoine *et al.*, 1998). Within the PV the metacyclic promastigotes differentiate into replicative amastigotes that periodically escape from the host cell to reinfect other phagocytic cells (macrophages or dendritic cells) or non-phagocytic cells (fibroblasts) (McConville *et al.*, 2007).

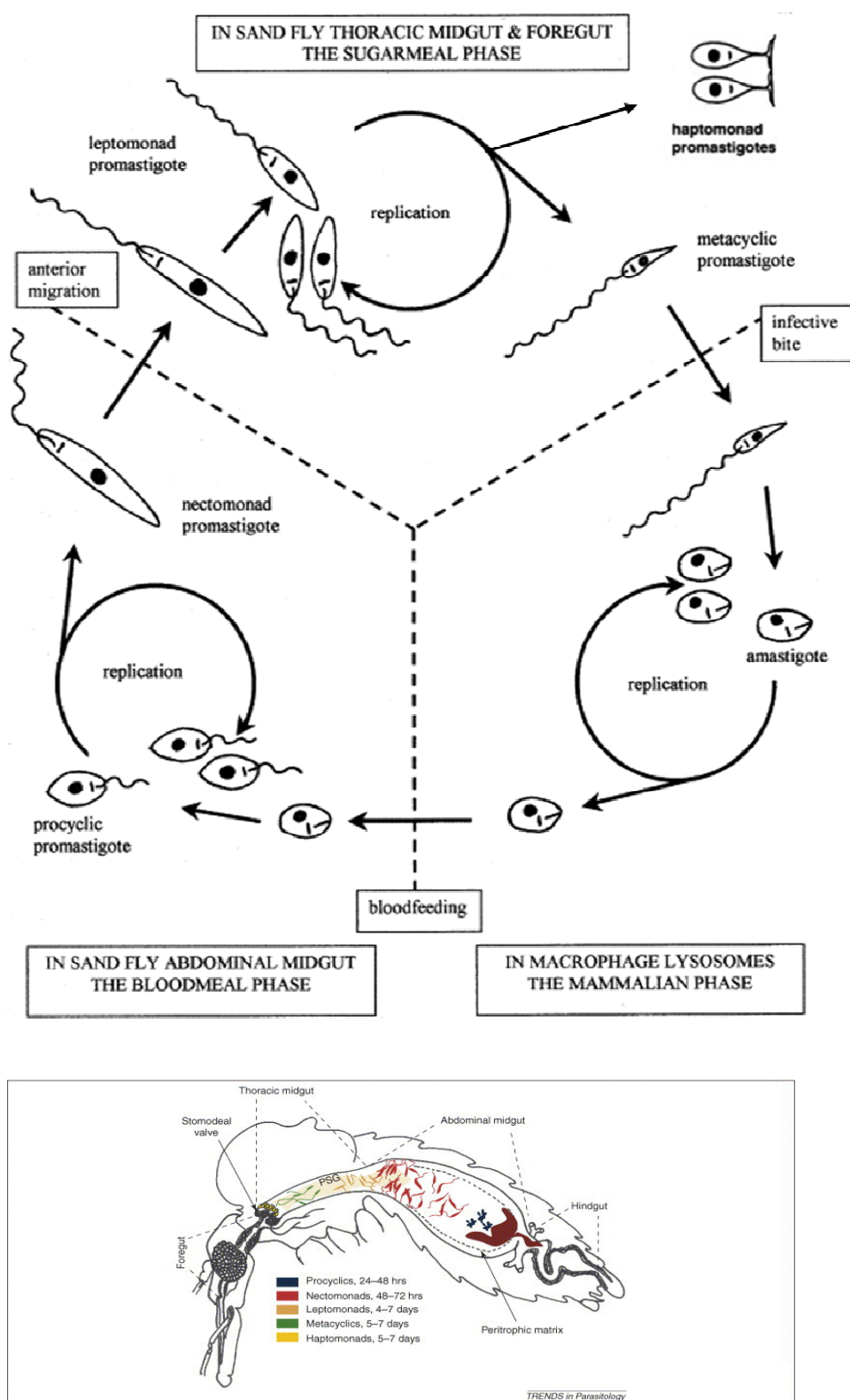


**Figure 1-2 A) Development of *Leishmania* species in the sandfly vector and mammalian host** (adapted from Gossage *et al.*, 2003). There are three replicative stages, amastigotes in the macrophage; procyclic promastigotes in the abdominal midgut; and leptomonad promastigotes in the thoracic midgut. Nectomonad promastigotes are strongly motile and elongated and are migratory forms that break out of the bloodmeal. Some leptomonad promastigotes differentiate into metacyclic promastigotes which are the mammalian infective form, and others attach themselves to the cuticle lined surface of the stomodaeal valve and differentiate into haptomonad promastigotes. **Figure 2B) The timing of the appearance of distinct morphological forms of promastigotes within the sandfly gut.** (adapted from Kamhawi, 2006).

## 1.2 *Leishmania* Differentiation

During lifecycle progression between the sandfly vector and mammalian host, *Leishmania* parasites must adapt to survive changeable environmental conditions, having to cope with varying nutrient and oxygen availability, pH and temperature. Such requirements have resulted in life cycle stages that are morphologically and functionally distinct. Procyclic promastigotes are motile, flagellated cells with a spindle shaped body with a length of approximately 20  $\mu\text{m}$ , and their flagellum approximately equal in length to the body. The characteristic shape of each life cycle stage is maintained by a sheath of cross-linked subpellicular microtubules (Gull, 1999). The infective metacyclic promastigotes maintain a similar shape, but their body is shorter and their flagellum longer. By contrast, amastigotes are smaller (approximately 5  $\mu\text{m}$  in diameter), ovoid cells with a greatly reduced flagellum that does not extend outside the flagellar pocket (figure 1.3).

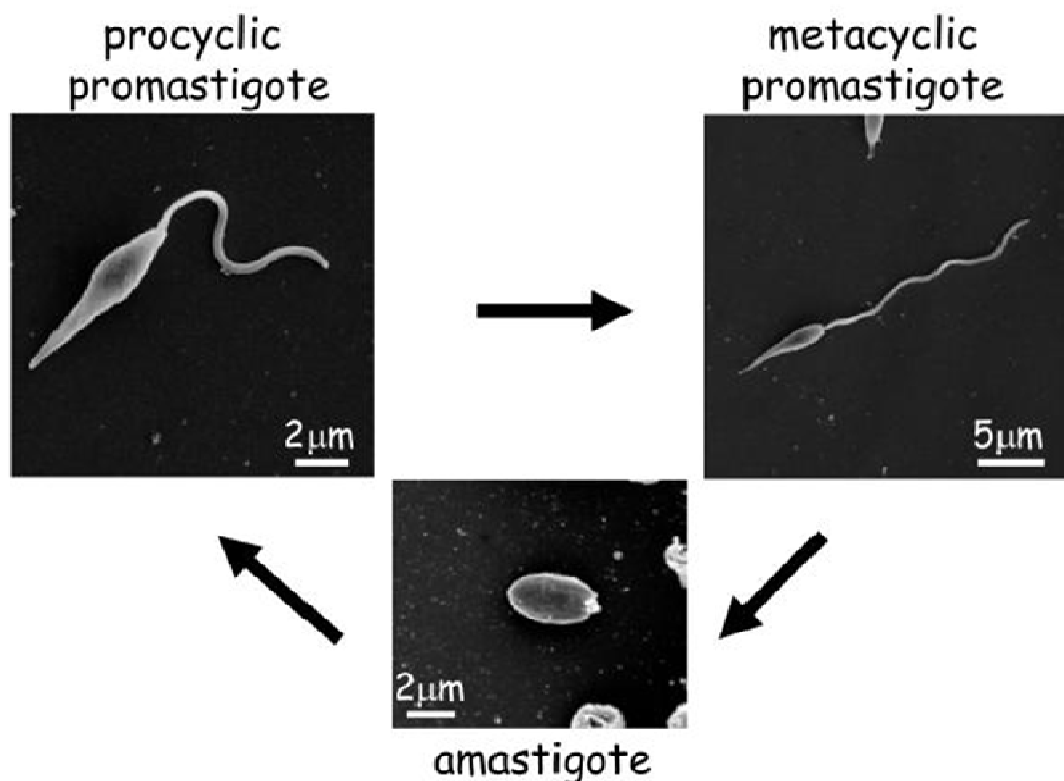


**Figure 1-3 *Leishmania* Life Cycle** (taken from Besteiro *et al.*, 2007). Scanning electron microscope images of the main *Leishmania major* life cycle stages, the procyclic and metacyclic promastigotes were grown in culture, the amastigote was isolated from an infected macrophage isolated from a mouse.

### 1.2.1 Changes in surface molecule expression during differentiation

*Leishmania* are exposed to a hydrolytic environment in both the sandfly midgut and the macrophage phagolysosome, and as such require the expression of a number of stage specific virulence factors. The surface of *Leishmania* promastigotes is coated by a dense glycocalyx (literally “sugar coat”) that is rich in glycosylated phosphatidylinositol (GPI) glycolipids and that covers the entire promastigote and is visible by electron microscopy (Pimenta *et al.*, 1991). This glycocalyx contains lipophosphoglycan (LPG), proteophosphoglycans (PPGs), low molecular weight glycoinositol phospholipids (GIPLs), and GPI anchored proteins such as the abundant 63-kDa surface proteinase, gp63, (McConville *et al.*, 1993). In contrast to promastigote stages, amastigotes downregulate the expression of LPG and other surface macromolecules and have a much reduced surface coat, although a glycocalyx of parasite derived GIPLS and host derived sphingolipids is retained (McConville *et al.*, 1993, McConville and Blackwell, 1991; Naderer *et al.*, 2004).

LPG, the major surface glycoconjugate of promastigote stages and expressed at approximately  $5 \times 10^6$  molecules per cell, consists of a polymer of repeating Gal $\beta$ 1,4Man-PO $_4$  units attached to a glycan core that is inserted into the membrane via a lipid anchor (Lodge and Descoteaux, 2005). Although the glycan core and lipid anchor of LPG are identical in all *Leishmania* species, LPGs from some species possess additional oligosaccharide side chains. During differentiation from procyclic promastigotes to metacyclic promastigotes, certain structural changes occur to LPG that are required to aid the detachment of metacyclic promastigotes from the sandfly midgut, and that contribute to the ability of metacyclic promastigotes to withstand complement mediated lysis in the mammalian host (Puentes *et al.*, 1988; Sacks, 2001). LPG elongates during differentiation, doubling the number of repeating units from about 15 in procyclic promastigotes to 30 in metacyclic promastigotes, and in some species, substitutions to the repeating units occur (Descoteaux and Turco, 1999). LPG expression is down regulated by at least three orders of magnitude in amastigote stages (Moody *et al.*, 1993; Turco and Sacks, 1991). Analysis of *Leishmania* mutants that lack individual or multiple surface components indicates that LPG plays a critical role in macrophage infection, while promastigote virulence in the

mammalian host is not significantly affected by loss of other surface components (McConville *et al.*, 2007).

The expression of gp63 (also called promastigote surface protease or leishmanolysin), a zinc metalloprotease, is up regulated in metacyclic promastigotes and down regulated in amastigotes (Ramamoorthy *et al.*, 1992). GP63 is thought to be required for the infection of mammals by enhancing phagocytosis of promastigotes by macrophages, and conferring resistance to lysis by host complement (Joshi *et al.*, 1998; Yao *et al.*, 2003). Evidence also exists suggesting that gp63 plays a role in promastigote adhesion to epithelial cells within the sandfly gut (Santos *et al.*, 2006).

A family of hydrophilic surface proteins encoded by the *LmcDNA16* gene locus, HASPA1, HASPA2, HASPB, SHERP1 and SHERP2 have been implicated as possible virulence factors with HASP proteins being expressed exclusively at the surface of metacyclic and amastigote stages and SHERP proteins expressed by metacyclic promastigotes only (Knuepfer *et al.*, 2001; McKean *et al.*, 2001).

### **1.2.2 Developmentally regulated protein expression and post-translational modifications**

One peculiarity of trypanosomatids is that the regulation of gene expression does not occur at the level of transcription initiation (Campbell *et al.*, 2003a).

Kinetoplastid open reading frames are arranged in long arrays that are transcribed into polycistronic RNA precursors before being further processed into individual mRNAs by *trans* splicing in which an identical short leader sequence, the spliced leader (SL) is spliced onto the 5' ends of multiple mRNAs (Bonen, 1993) and polyadenylation occurs at the 3' end (Clayton, 2002). No evidence has been found for the regulation of transcription by RNA polymerase II, therefore it is thought that all regulation of trypanosomatid protein expression must occur at the post-transcriptional level via mechanisms including modulation of mRNA stability, regulation of translation, post-translational modifications and proteolysis of proteins (Campbell *et al.*, 2003a; Clayton and Shapira, 2007).

Proteomics studies have revealed an increase in enzymes involved in uptake of amino acids, fatty acid oxidation and gluconeogenesis in parasites undergoing

differentiation into amastigotes (as compared to glucose oxidation in promastigotes) (Naderer and McConville, 2008; Rosenzweig *et al.*, 2008). The enzymatic contents of *Trypanosoma brucei* glycosomes, (organelles that contain many of the enzymes involved in carbohydrate metabolism and that are characteristic of kinetoplastids) differs between life cycle stages, and recent evidence suggests that glycosomes are degraded and recycled during the differentiation process (Herman *et al.*, 2008).

### **1.2.3 Developmentally regulated changes in endocytic and lysosomal structure and function**

In both life cycle stages, the flagellar pocket is a specialised invagination of the plasma membrane that encloses the base of the flagellum. Organelles of the secretory and endocytic pathway are found to localise close to the flagellar pocket that is thought to be the sole site of exocytosis and endocytosis in the cell (Landfear and Ignatushchenko, 2001; McConville *et al.*, 2002b). Although components of the endocytic and exocytic machinery are present in all life cycle stages, there are notable differences (figure 1.4).

The differentiation from promastigote to amastigote stages is associated with a change in the relative abundance and distribution of secretory and endocytic organelles. Lesion derived amastigotes possess much reduced ER and Golgi apparatus compared to promastigotes, while the lysosomal compartments fill a large proportion of the amastigote cell volume as compared to promastigotes (Waller and McConville, 2002). The *Leishmania* lysosome, the site of degradation for proteins trafficked through the endocytic pathway, is an unusual structure that undergoes extensive remodelling during lifecycle progression (Waller and McConville, 2002). In early log phase, dividing procyclic promastigotes, the weakly acidic lysosomal compartment exists as a single vesicular structure located at the anterior end of the cell, while in metacyclic promastigotes it exists as a long, tubular structure termed the multivesicular tubule (MVT) (Besteiro *et al.*, 2006a; Mullin *et al.*, 2001). The MVT of metacyclic promastigotes was first identified in an ultrastructural study of *L. mexicana* as a post-Golgi tubulovesicular compartment (Weise *et al.*, 2000), and confirmed to be lysosomal by the accumulation of the endocytic tracer FM4-64 and by the presence of both serine and cysteine peptidases (Mullin *et al.*, 2001).

In amastigote stages, the lysosome undergoes further morphological transformation into large, electron dense vacuoles termed megasomes that fill a large proportion of the cytoplasm. The size and number of megasomes vary depending on species. For example, megasomes represent up to 15% of total cell volume of lesion derived amastigotes of *L. mexicana* (Coombs *et al.*, 1986), and only ~5% of the cell volume of *L. amazonensis* amastigotes (Ueda-Nakamura *et al.*, 2002).

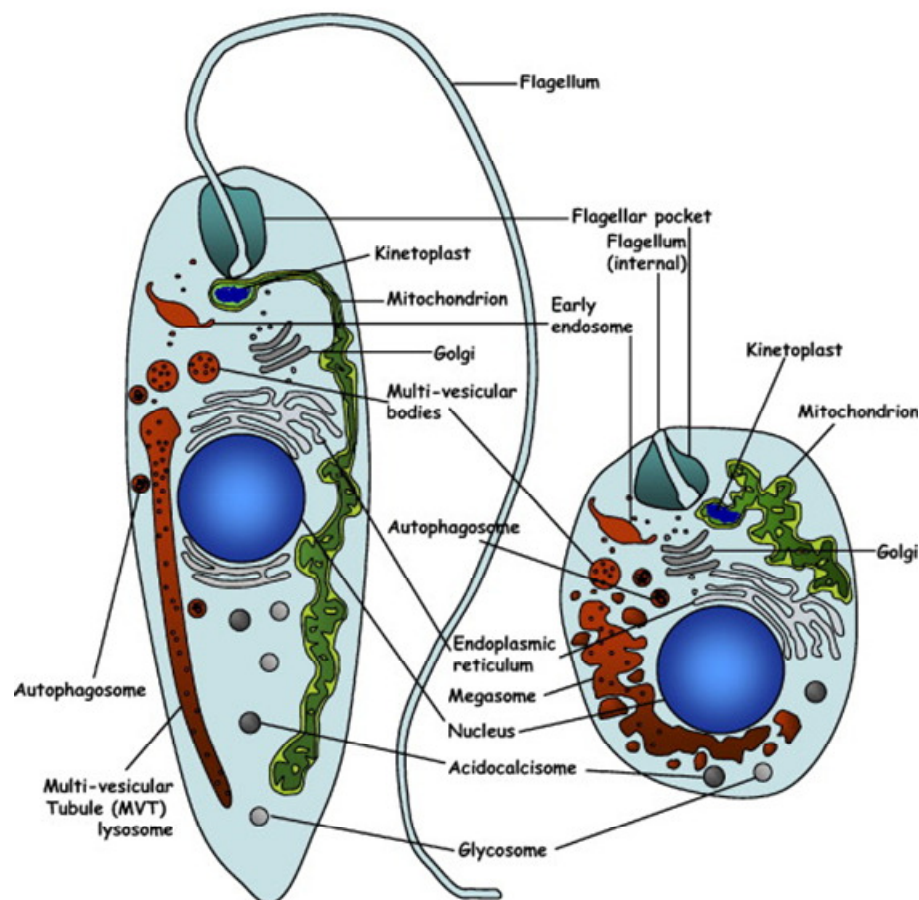


**Figure 1-4 Schematic representation of the main intracellular organelles from *Leishmania* promastigote (left) or amastigote (right) forms.** The flagellar pocket marks the anterior end of the cell. Taken from Besteiro *et al.*, (2007).

### 1.2.4 The role of Peptidases in *Leishmania* Differentiation

Accompanying the differentiation associated morphological changes that occur in the *Leishmania* lysosome is a change in lysosomal peptidase content.

Peptidases (or proteases) are enzymes responsible for proteolysis; that is causing

the hydrolysis of the peptide bonds that link amino acids together in polypeptide chains. Peptidases are classified as serine, threonine, cysteine, aspartic, metallo- or glutamic depending on the type of catalysis used for peptide bond hydrolysis. The mechanism of proteolysis involves the production of a nucleophilic amino acid residue or water molecule that attacks the carboxyl group of the peptide. In serine and threonine peptidases the catalytic nucleophile is the reactive hydroxyl group (of a serine or threonine residue, respectively); while in cysteine peptidases the nucleophile is a reactive sulfhydryl group. Aspartic and metallo-peptidases rely on the activation of a water molecule for the production of a nucleophile, mediated either by two aspartate residues in the case of aspartic peptidases, or by a metal ion in the metallo-peptidases (zinc, cobalt or manganese). Approximately 1.8% of the *L. major* genome encodes peptidases, encoding at least 154 peptidases; 2 aspartic, 62 cysteine, 55 metallo, 13 serine, 21 threonine, and one peptidase of unknown catalytic type (figure 1.5) (Ivens *et al.*, 2005). Trypanosomatids lack the pepsin-like aspartic peptidases (such as plasmepsins) that are so abundant in apicomplexans, but have many cysteine peptidase genes that have been identified as virulence factors, including the abundant cathepsin L-like enzymes (CPA and CPB) and cathepsin B-like enzymes (CPC) (Mottram *et al.*, 2004).

The differentiation of metacyclic promastigotes into amastigotes is accompanied by the formation of megasome structures and an increase in cathepsin L-like cysteine peptidase activity (CPB) (Brooks *et al.*, 2001; Courret *et al.*, 2001; Ueda-Nakamura *et al.*, 2002). Similarly, an overall increase in proteolytic activity occurs during differentiation from procyclic to metacyclic promastigotes, which is concurrent with the formation of the MVT-lysosome, known to contain serine and cysteine peptidases (Mullin, 2001). Although definitive data is relatively limited, it is thought that peptidases could play a role in nutrient acquisition, either when secreted into the host environment or within the endosomal / lysosomal system (Opperdoes and Coombs, 2007).

In addition to being the final destination for proteins trafficked through the endocytic pathway, the lysosome is also the end point of the autophagy pathway. Over the past few years, evidence has accumulated demonstrating that autophagy plays an important role in protein turnover during *Leishmania* differentiation.

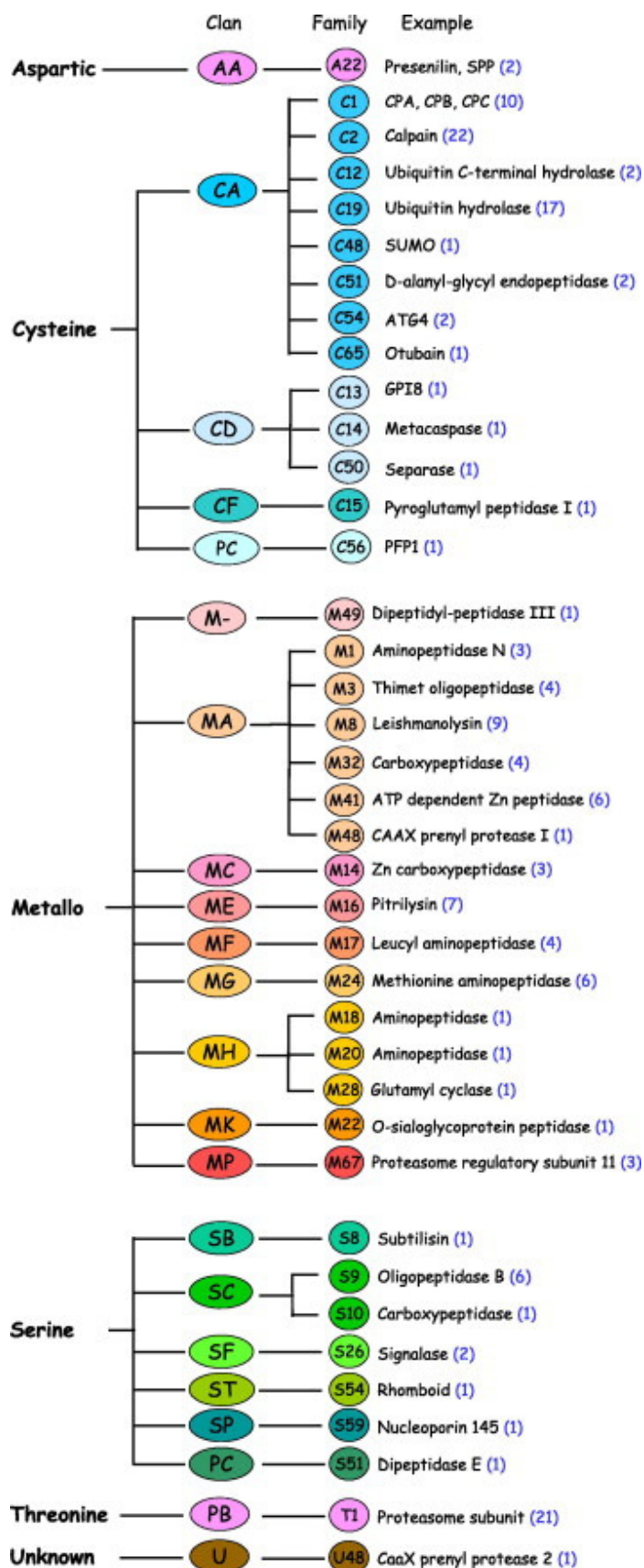


**Figure 1-5 Clans and families of *Leishmania major* peptidases (taken from Besteiro et al., 2007).** Nomenclature is based on the MEROPS database (<http://merops.sanger.ac.uk/>). Numbers in brackets represent the estimated number of peptidases in each family, as based on information in Ivens et al., (205) and the MEROPS database (release 7.7, January 2007).

## 1.3 Autophagy

### 1.3.1 General Introduction to Autophagy

Autophagy, literally “self-eating”, is a lysosomal degradation pathway for proteins and organelles that results in the complete and irreversible break down of a substrate into its essential constituents (e.g. amino acids) that can then be recycled and reused by the cell (Cuervo, 2004). The biological functions of autophagy are wide ranging, and as such the roles and regulation of autophagy have received huge amounts of scientific interest in the past few decades.

A basal level of autophagy is required in all cells for the maintenance of cellular homeostasis, where the continuous turnover of long-lived cytosolic proteins and certain organelles occurs alongside the removal of damaged and unwanted cellular components. Autophagy is upregulated when cells need to generate intracellular nutrients during starvation (Onodera and Ohsumi, 2005; Tsukada and Ohsumi, 1993), or when damaging cytoplasmic components accumulate, for example during infection or in response to oxidative stress (Orvedahl and Levine, 2009; Scherz-Shouval and Elazar, 2007). The deregulation of autophagy has been implicated in the pathogenesis of various human diseases including cancer and neurodegenerative disease (He and Klionsky, 2006; Huang and Klionsky, 2007; Komatsu *et al.*, 2006). Studies in the model organisms *Dictyostelium discoideum*, *Caenorhabditis elegans* and *Drosophila melanogaster* provided evidence for a role of autophagy in architectural remodelling during cellular differentiation and development (Melendez *et al.*, 2003; Otto *et al.*, 2003, Scott *et al.*, 2004), and in more recent years autophagy has been shown to be involved in the differentiation and life cycle progression of *Leishmania* (Besteiro *et al.*, 2006b; Williams *et al.*, 2006). The occurrence of autophagy in trypanosomatids will be discussed in detail in section 1.3.10.

Degradation by autophagy involves the formation of cytosolic double-membrane vesicles which sequester portions of the cytoplasm (Klionsky, 2005). Initially a “C” shaped double membrane structure appears in the cytosol. This membrane expands at both ends, eventually closing to form a double membrane vesicle (called the autophagosome), into which cytoplasm and certain organelles are sequestered (Yang *et al.*, 2005). The autophagosome is then targeted to the

lysosome, where the external membrane fuses with the lysosomal membrane, and the internal vesicle together with its cargo is released into the interior of the lysosome to be degraded by hydrolases (figure 1.5) (Klionsky, 2005; Reggiori and Klionsky, 2005; Xie and Klionsky, 2007; Yang *et al.*, 2005).

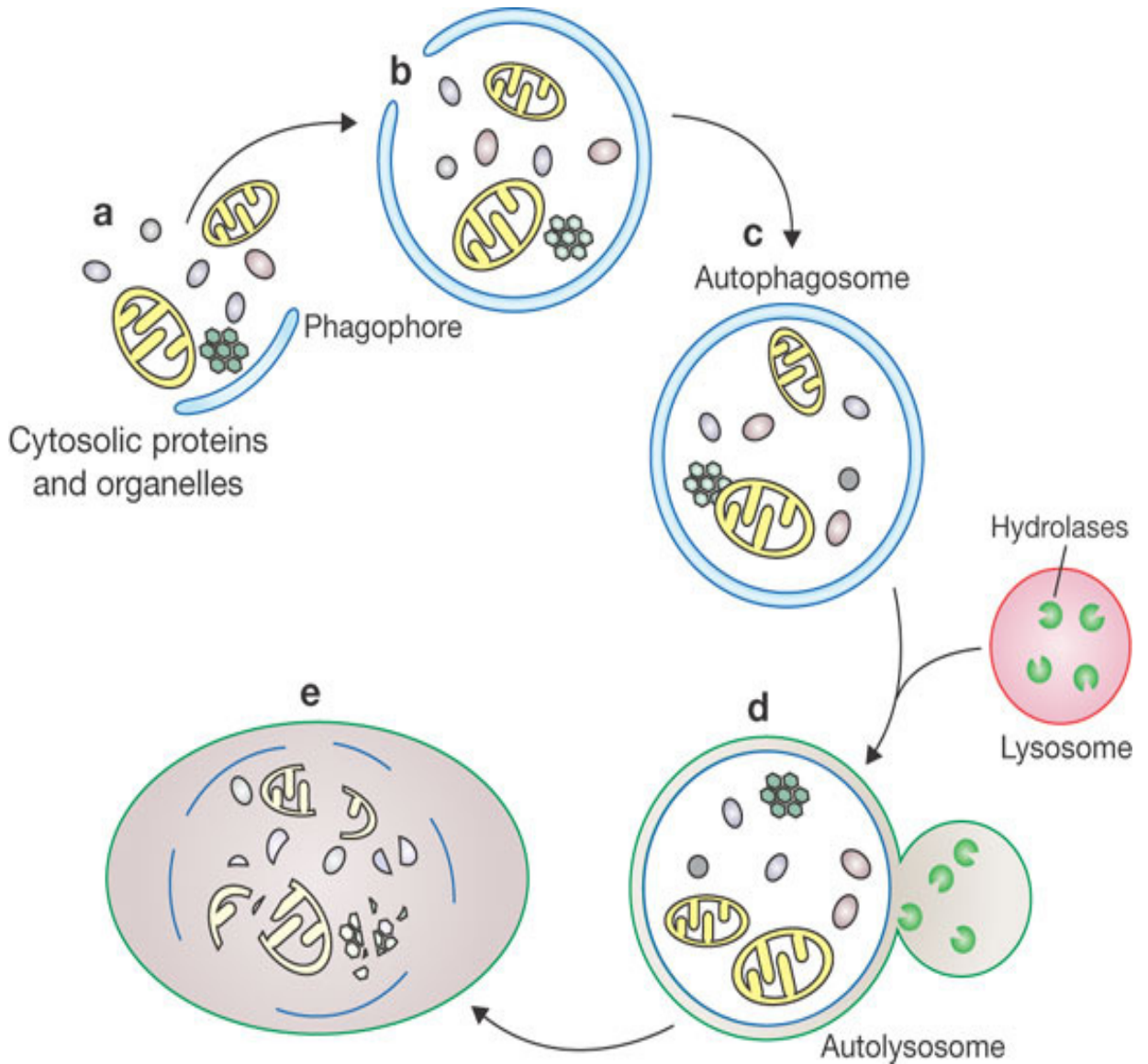


**Figure 1-6 Schematic depiction of Autophagy (taken from Xie and Klionsky, 2007).** Cytosolic material is sequestered by an expanding sac, the phagophore (also referred to as the pre-autophagosome structure, PAS) (a, b), resulting in the formation of a double membrane vesicle (c). The outer membrane of the autophagosome fuses with a lysosome (it is now called an autolysosome), exposing the inner single membrane of the autophagosome to lysosomal hydrolases (d), resulting in degradation of the contents of the autophagosome (e).

### 1.3.2 The Selectivity of Autophagy

Autophagy can be selective, where a specific cargo is targeted in response to an intracellular signal, or nonselective when cytoplasmic components are randomly engulfed by autophagosomes in response to environmental stimuli. Several types of selective and non-selective autophagy have been described, including macroautophagy, microautophagy, chaperone mediated autophagy, mitophagy, pexophagy and cytoplasm to vacuole targeting (Cvt) pathway of yeast.

Macroautophagy, where proteins or entire organelles are engulfed in a double membrane vesicle termed the autophagosome and subsequently degraded by lysosomal enzymes, is the most prevalent form of autophagy and is usually referred to simply as “autophagy”. Microautophagy is a process in which cytoplasm is directly engulfed at the surface of the degradative organelle (the vacuole or lysosome) without the production of autophagosomes. The membrane invaginates, and pinches off to form an internal autophagic vesicle containing cytoplasmic material (Kunz *et al.*, 2004). In addition to microautophagy of soluble cytosolic components, larger particles can also be taken up by vacuoles, for example during piecemeal microautophagy of the nucleus (PMN), during which parts of the nucleus are degraded within vacuoles (Roberts *et al.*, 2003). The selective autophagy of particular organelles has been described, for example “mitophagy” is the selective degradation of mitochondria by autophagy, and “pexophagy” describes the selective turnover of peroxisomes by micro- or macroautophagy (Dunn *et al.*, 2005; Kanki and Klionsky, 2008; Tuttle and Dunn, 1995).

Chaperone-mediated autophagy (CMA) is a selective form of autophagy, so far only detected in mammalian cells, that is activated during long term nutrient deprivation. CMA does not involve the formation of double membrane vesicles. Instead, substrate proteins containing a KFERQ-like sequence motif bind to a chaperone molecular complex containing Hsc70 and other co-chaperones, which then associates directly with the lysosomal surface receptor Lamp2. Most known substrates for CMA contain a peptide sequence biochemically related to KFERQ, and it was reported that such sequences are present in 30% of cytosolic proteins in fibroblasts (Chiang and Dice, 1988; Dice, 2007).

Finally, the cytoplasm to vacuole (Cvt) targeting pathway is an example of a selective, autophagy-like pathway that is specific to yeast, in which the hydrolases aminopeptidase 1 and  $\alpha$ -mannosidase are selectively transported to the vacuole (Huang and Klionsky, 2002). Cvt vacuoles resemble autophagosomes morphologically, and much of the molecular machinery is shared between autophagy and Cvt pathway, and so it seems that the Cvt pathway is a specific form of autophagy that evolved uniquely in yeast (Scott *et al.*, 1996). While many autophagy genes are conserved between the Cvt pathway and autophagy, those involving Cvt selectivity are restricted to yeast (Meijer *et al.*, 2007).

Throughout this thesis, “autophagy” refers to the process of macroautophagy.

### **1.3.3 The molecular machinery of autophagy**

Although the morphology of autophagy was first characterised in mammalian cells, most of our current understanding of the molecular components of the pathway comes from studies in *S. cerevisiae*, due in part to the relative ease with which high through put genetic analyses can be carried out. Independent genetic screens were carried out in several laboratories to identify mutants defective in the autophagy pathway, leading to a range of names given to autophagy genes including APG, AUT and ATG. A unified nomenclature for the description of autophagy genes and proteins in yeast was proposed, with *ATG* and *Atg* (AuTophagy related) being the names given for the genes and proteins involved in the process (Klionsky *et al.*, 2003). There are currently 30 *ATG* genes described in yeast, and orthologues of many *ATG* gene products have been identified and characterised in higher eukaryotes including mammals, insects, worms and plants, and have been shown to have similar functions in autophagy (Xie and Klionsky, 2007). Among the *ATG* genes, a core set of machinery seems to be conserved and required for all types of autophagy (Xie and Klionsky, 2007). This set of core autophagy proteins is summarised in table 1, and putative *Leishmania* orthologues are provided.

<i>S. cerevisiae</i> gene	Description	<i>Leishmania</i> orthologue?
<b>INDUCTION OF AUTOPHAGY</b>		
<i>TOR1, TOR2</i>	PIK-kinase family Ser/Thr protein kinase, rapamycin target	LmjF36.6320 LmjF34.4530
<i>ATG1</i>	Ser/Thr protein kinase	Many potential homologues
<i>ATG13</i>	Phosphoprotein component of Atg1 complex	None identified
<b>PHAGOPHORE INITIATION</b>		
<i>ATG2</i>	Membrane protein, interacts with Atg9	None identified
<i>ATG9</i>	Membrane protein, interacts with Atg2. Required for phagophore initiation	LmjF27.0390
<i>ATG18</i>	Membrane protein	LmjF29.1575
<i>ATG6</i>	Component of Vps34 complex	LmjF08.0400
<i>Vps34</i>	Class III PtdIns 3 kinase	LmjF24.2010
<i>Vps15</i>	Ser/Thr protein kinase, component of Vps34 complex.	LmjF28.1760
<b>AUTOPHAGOSOME COMPLETION</b>		
<i>ATG3</i>	E2-like enzyme, conjugates PE to ATG8	LmjF33.0295
<i>ATG4</i>	Cysteine protease, cleaves ATG8	LmjF32.3890 LmjF30.0270
<i>ATG5</i>	Conjugated to ATG12	LmjF30.0980
<i>ATG7</i>	E1-like enzyme, activates Atg8 and Atg12	LmjF07.0010
<i>ATG8</i>	Ubiquitin-like protein conjugated to PE	LmjF19.1630
<i>ATG10</i>	E2-like enzyme, conjugates Atg5 and Atg12	LmjF31.3105
<i>ATG12</i>	Ubiquitin-like protein, conjugated to Atg5	LmjF21.1300
<i>ATG16</i>	Component of Atg5-Atg12 complex	LmjF33.1410

**Table 1-1 Core Autophagy Machinery and putative *Leishmania* orthologues.** The list of core autophagy genes was generated based on Xie and Klionsky, 2007, and *Leishmania* orthologues were identified as in Herman *et al.*, 2006 and Williams *et al.*, 2006.

### 1.3.4 Regulation and induction of autophagy

The protein kinase Tor (Target of rapamycin) is a sensor for two metabolites known to regulate autophagy; ATP and amino acids (Ogier-Denis and Codogno, 2003). The inhibition of Tor with rapamycin leads to the stimulation of autophagy in yeast (Noda and Ohsumi, 1998) indicating that Tor is a negative regulator of autophagy. In yeast and mammals, Tor controls the phosphorylation state of Atg13 and its subsequent interaction with the protein kinase Atg1, a complex required for the initiation of autophagy. Under nutrient rich conditions, where autophagy is inhibited, Tor causes the hyperphosphorylation of the protein Atg13, resulting in it having a lower affinity for Atg1. During starvation, or following inhibition of Tor with rapamycin, Atg13 is dephosphorylated, resulting in its association with Atg1 and Atg17 (Kabeya *et al.*, 2005; Kamada *et al.*, 2000). The organisation of several autophagy proteins including Atg5, Atg12 and Atg8 seems to be dependent on the inhibition of Tor and the activation of Atg1 kinase (Ogier-Denis and Codogno, 2003).

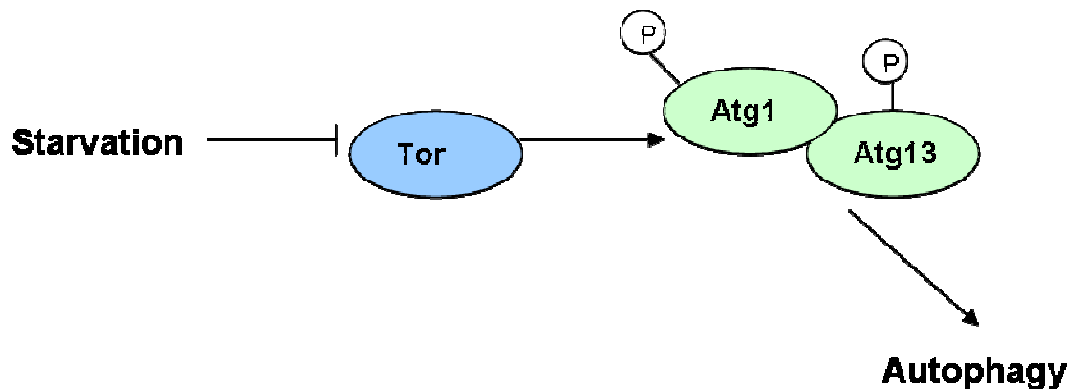


**Figure 1-7 Regulatory complex for Autophagy induction.** (Adapted from Yorimitsu and Klionsky, 2005). The inhibition of Tor when nutrients are scarce leads to the partial dephosphorylation of Atg13, causing it to have increased affinity for Atg1 and Atg17.

### 1.3.5 Autophagosome formation

The proposed site of autophagosome formation is the phagophore assembly site (PAS), and most core autophagy proteins co-localise at this structure (Kim *et al.*, 2002; Suzuki *et al.*, 2001). A population of Atg9, a transmembrane protein, localises to the PAS, and in the absence of Atg9, the ubiquitin like proteins Atg8 and Atg12 that are required for the completion of autophagosomes are not recruited to this site (Suzuki *et al.*, 2001). Atg1 is known to regulate Atg9 trafficking from the PAS (Reggiori *et al.*, 2004), and is thought to have additional, broader functions in autophagy (Xie and Klionsky, 2007). An autophagy specific phosphoinositide 3-kinase (PI(3)K) complex, consisting of Vps34, Vps15 and Atg6 localises to the PAS, and is thought to be required for autophagosome formation, although the mechanisms underlying this are unclear (Kihara *et al.*, 2001; Obara *et al.*, 2006).

Many of the autophagy proteins isolated and characterized from yeast and mammals are involved in two ubiquitylation-like conjugation systems, the first of which results in the formation of an Atg12-Atg5-Atg16 complex and the second results in the conjugation of Atg8 to phosphatidylethanolamine (PE). Both conjugation systems are essential for the formation of autophagosomes and highly conserved among eukaryotes (Geng and Klionsky, 2008; Xie and Klionsky, 2007). The Atg12-Atg5-Atg16 complex is localised on the expanding phagophore and dissociates before or immediately after autophagosome completion (Mizushima *et al.*, 2001; Mizushima *et al.*, 2003). The Atg12-Atg5 conjugate is essential for promoting the lipidation and correct localisation of Atg8, and it has been suggested that the Atg12-Atg5 complex might provide the E3-like activity required for Atg8 lipidation (section 1.3.7, Fujita *et al.*, 2008; Hanada *et al.*, 2007). Atg8 is thought to control phagophore expansion during autophagosome formation, and to act as a scaffold protein for the expanding autophagosome membrane (figure 1.7, Nakatogawa *et al.*, 2007; Xie *et al.*, 2008).

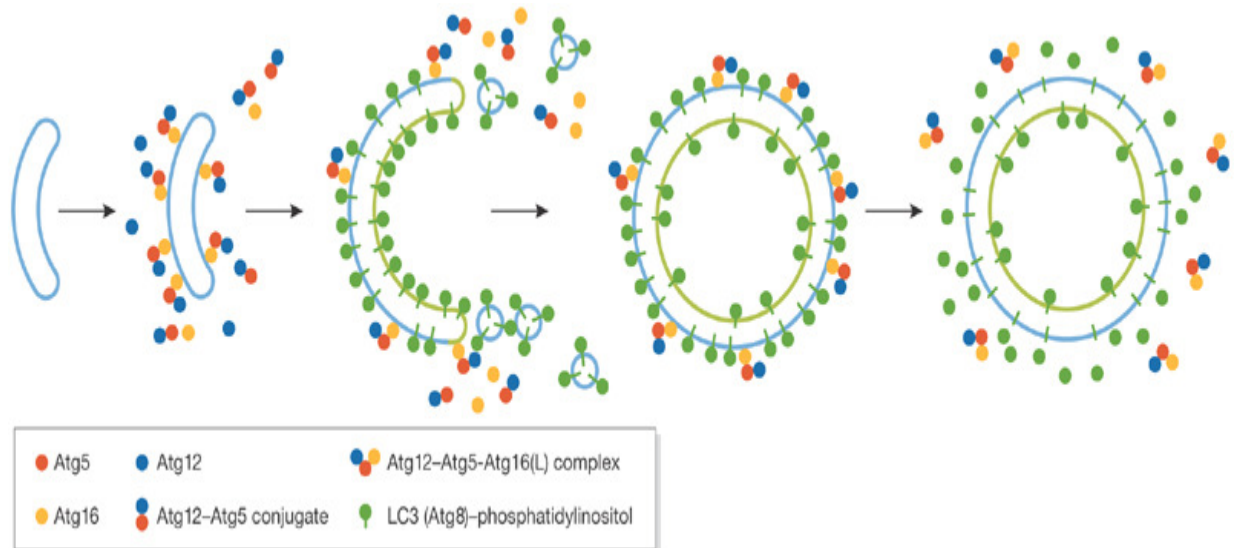


**Figure 1-8 Atg12 and Atg8 conjugation systems in vesicle formation.** Taken from Geng and Klionsky, 2008. The Atg12-Atg5-Atg16 complex is recruited to the early-stage phagophore and redistributed to the outer surface of the phagophore. The Atg12-Atg5-Atg16 complex is thought to direct Atg8-PE to this site, and the presence of Atg8 is thought to support the expansion of the phagophore. Upon fusion of the autophagosome, Atg8 on the internal surface remains sealed within the autophagosome, while external Atg8 is released by the proteolytic action of Atg4. LC3 is the mammalian orthologue of Atg8.

### 1.3.6 Atg12-Atg5 conjugation

Atg12 is a small, hydrophilic, ubiquitin-like protein (UBL) that becomes covalently linked to Atg5, its target protein. All UBLs become attached to their substrates via related enzyme pathways. Ubiquitin and most UBLs are synthesised as inactive precursors that require proteolytic processing by specific peptidases to expose a carboxyl glycine residue, the site of substrate conjugation. The E1 or E1-like enzyme binds ATP-MgCl<sub>2</sub> and ubiquitin, and catalyses ubiquitin C-terminal acyl-adenylation. Then the catalytic Cys in the E1 enzyme attacks the ubiquitin-adenylate to form a high energy thioester bond between the C terminus of the UBL and E1. The UBL is passed to the active site cysteine of an E2 or E2-like enzyme, before finally the UBL is conjugated to its protein substrate via the action of an E3 protein ligase (Kerscher *et al.*, 2006).

Atg12 is first activated by the E1 like enzyme Atg7 in an ATP-dependent manner, resulting in the formation of a thioester bond between the C terminal Gly<sup>186</sup> of Atg12 and the Cys<sup>507</sup> of Atg7 (Tanida *et al.*, 1999). Atg12 is then transferred to the E2-like enzyme Atg10 (Shintani *et al.*, 1999), before being finally conjugated to its target protein Atg5 via an isopeptide bond at Lys<sup>149</sup> (Mizushima *et al.*,

1998). No E3-like enzyme appears to be involved in Atg12-Atg5 conjugation (Geng and Klionsky, 2008). Atg12 and Atg5 are barely detectable in their free forms, as a conjugate forms immediately and irreversibly after their synthesis (Yang *et al.*, 2005). Atg16 then binds to Atg5 forming the Atg12-Atg5-Atg16 complex (Mizushima *et al.*, 1999) (figure 1.8).

### 1.3.7 Atg8 modification

Atg8 is another ubiquitin like protein that is essential for the formation of autophagosomes. Whereas ubiquitin and other UBLs (including Atg12) interact with other proteins, Atg8 interacts with a phospholipid, phosphatidylethanolamine (PE), making it unique among UBLs (Ichimura *et al.*, 2000). Full length Atg8 undergoes proteolytic processing by the cysteine peptidase Atg4, removing the carboxy terminal arginine residue, and exposing the carboxyl glycine residue, Gly<sup>116</sup> (Kirisako *et al.*, 2000). Atg7 has E1-like activity for Atg8 as well as Atg12, and a thioester bond is formed between the exposed glycine residue of Atg8 and Cys<sup>507</sup> of Atg7 (Ichimura *et al.*, 2000). Atg8 is then transferred to the E2 conjugating enzyme Atg3 via a thioester bond before being finally conjugated at Gly<sup>116</sup> to PE via an amide bond (Ichimura *et al.*, 2000). This lipidation process results in the conversion of Atg8 from a soluble to a tightly membrane bound protein. Upon completion of the autophagosome, the Atg8 which is attached to the outer membrane is released by the deconjugating action of Atg4, and the Atg8 on the inner membrane remains sealed within the autophagosome, making it a specific marker protein for autophagic vacuoles (figure 1.8). Transgenic mice expressing LC3, the mammalian homologue of Atg8, conjugated to green fluorescent protein have been used to study autophagy in different tissues in response to starvation (Mizushima *et al.*, 2004).

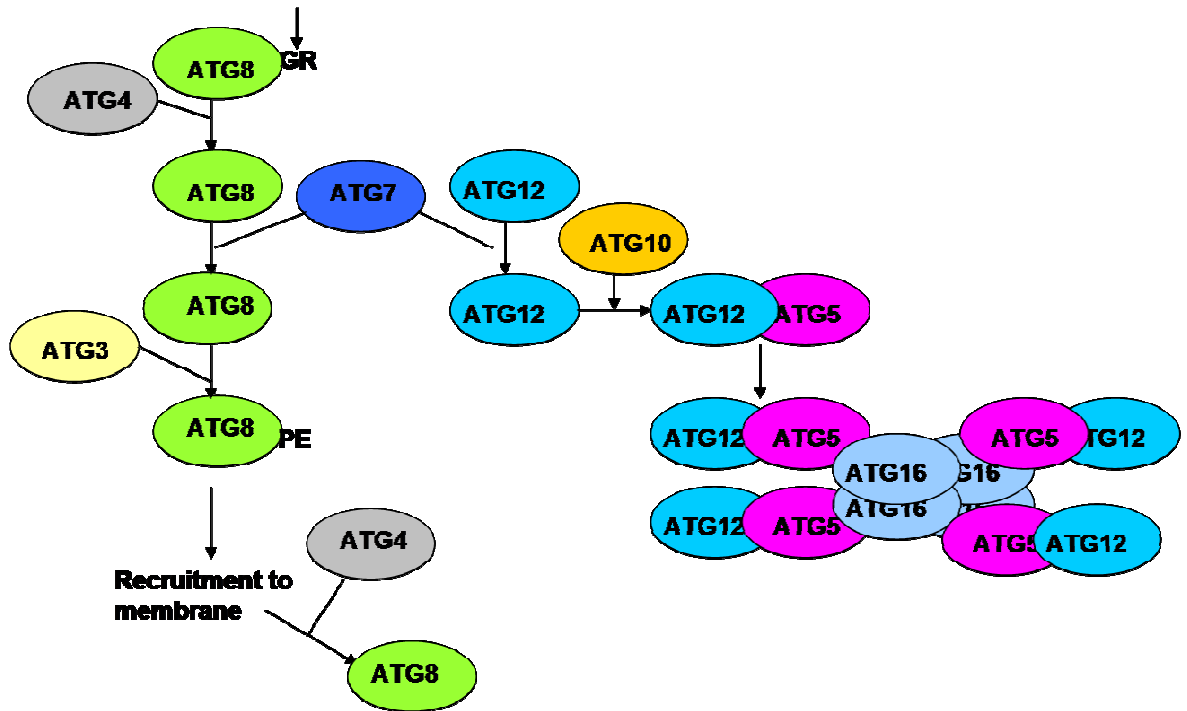


**Figure 1-9 Two conjugation systems involving the ubiquitin like proteins Atg8 and Atg12 are required for the formation of autophagosomes.**

In the first conjugation system required for autophagosome formation, Atg12 is activated by Atg7, and then covalently conjugated to Atg5 via Atg10. In the second ubiquitin-like cascade, full length Atg8 (Atg8GR) is first cleaved by the cysteine peptidase Atg4, removing the carboxyl arginine residue and exposing Gly<sup>116</sup>. The cleaved form of Atg8 is then activated by Atg7, transferred to the conjugating enzyme Atg3, and finally conjugated to phosphatidylethanolamine (PE) via an amide bond. Atg8-PE is tightly associated with autophagosome membranes. Atg7 has E1-like activity for both Atg8 and Atg12, Atg10 is the E2-like enzyme in Atg12 conjugation while Atg3 is the E2-like enzyme required for Atg8 conjugation. No E3-like activity has been identified for Atg12 conjugation, while the Atg12-Atg5 is thought to have E3 like activity for Atg8. Diagram drawn based on Klionsky *et al.*, 2005).

### 1.3.8 Proteins involved in the regulation of autophagosome fusion

Autophagosomes can reportedly fuse with early or late endosomes, and with lysosomes, (Berg *et al.*, 1998; Lawrence and Brown, 1992; Liou *et al.*, 1997; Lucocq and Walker, 1997; Tooze *et al.*, 1990), suggesting that the maturation of autophagosomes in mammals is a step-wise process. An autophagosome which has fused with an endosome is termed an “amphisome”, and an “autolysosome” describes an autophagosome or an amphisome which has fused to a lysosome (Eskelinen, 2005). While fusion events between autophagic vacuoles and multivesicular endosomes are frequently observed in mammalian cells (Eskelinen *et al.*, 2002), this does not occur in yeast. Instead, the autophagosome and

endosome both fuse with the vacuole, the yeast equivalent of the lysosome, and their contents mix at this point.

Various proteins have been identified in yeast which are required for this fusion event, including Ypt (the yeast homologue of Rab7) (Kirisako *et al.*, 1999), Vam3 (a syntaxin homologue) (Darsow *et al.*, 1997), Sec18 (yeast homologue of N-ethylmaleimide sensitive factor, NSF), and Vti1 (a SNARE protein) (Ishihara *et al.*, 2001). Mammalian proteins with a potential involvement in autophagosome maturation include the SKD1 AAA ATPase (a Vps4 homologue) (Nara *et al.*, 2002), Vti1 (Atlashkin *et al.*, 2003), Rab7 (Gutierrez *et al.*, 2004), Lamp2 (lysosomal membrane protein 2, Tanaka *et al.*, 2000), lysosomal enzymes cathepsin D, B and L (Felbor *et al.*, 2002; Koike *et al.*, 2000), and the aspartic peptidase Presenilin-1 (Esselens *et al.*, 2004; Wilson *et al.*, 2004). The vacuolar sorting protein Vps4, and the cathepsin L-like cysteine peptidases CPA/CPB have been found to be involved in the regulation of autophagy in *Leishmania* (Besteiro *et al.*, 2006b; Williams *et al.*, 2006, discussed in section 1.3.10).

### 1.3.9 A putative role for Presenilin-1 in Autophagy

Of the 154 known peptidases encoded in the *L. major* genome, just two of these are aspartic peptidases (Ivens *et al.*, 2005). One of these shares sequence identity with signal peptide peptidase (SPP) that cleaves signal peptides within their transmembrane region (Xia and Wolfe, 2003), and the other is presenilin 1 (PS1). Presenilin-1 (PS1) is a polytopic integral membrane protein, and the catalytic core of the mammalian  $\gamma$ -secretase complex (Dewji, 2005). PS1-like peptidases have been described in mammals, worms and *Dictyostelium*, but have not been detected in yeast or in *Plasmodium falciparum*.

The best known role for Presenilin 1 (PS1) is in the intramembrane proteolysis of the amyloid precursor protein, leading to the liberation of amyloid  $\beta$  peptide, a major feature and initiator of pathogenesis in Alzheimer's disease (De Strooper and Woodgett, 2003). PS1 has also been implicated in a wide range of biological processes including calcium channel regulation ((Leissring *et al.*, 2000, Yoo *et al.*, 2000), trafficking of secretory proteins to the cell surface (Kaether *et al.*, 2002; Naruse *et al.*, 1998), and a role in the maturation of autophagic vacuoles has tentatively been suggested (Eskelinen, 2005).

Wilson *et al* (2004) demonstrated that a PS1 deficiency in neuronal cells led to the mislocalisation and accumulation of  $\alpha$ - and  $\beta$ -synuclein proteins in degradative vacuoles resembling autophagic vacuoles. Esselens *et al* (2004) reported the accumulation of telencephalin in large vacuoles which are positive for the markers LC3 (the mammalian homologue of Atg8) and Atg12 (which normally dissociates from mature autophagosomes), but lack endosomal and lysosomal markers. Finally, Yu *et al* (2006) describe impaired protein turnover by autophagy in the fibroblast cells of familial AD patients and in blastocysts in *Δps1* mice, despite seeing an overall increase in the numbers of autophagic vacuoles and in the levels of LC3 expression. Together, these results indicate a possible involvement of presenilin-1 in the autophagic pathway, potentially in the maturation of autophagic vacuoles (Eskelinen, 2005).

### 1.3.10 Autophagy in trypanosomatids

An analysis of the *L. major*, *T. brucei* and *T. cruzi* genomes using autophagy related yeast genes as a query was published in 2005, and orthologues for many of the important genes involved in autophagy induction (for example TOR) and autophagosome formation (for example members of the ATG8 conjugation pathway) were identified (table 1.1, Rigden *et al.*, 2005). Although proteins with sequence identity to TOR were identified, no putative Atg13 orthologue was found, nor was a clear candidate for Atg1 discovered, although many serine/threonine protein kinases were identified as putative hits. The absence of Atg13 might suggest that autophagy is regulated via a different mechanism to autophagy in yeast or mammalian cells. Most key proteins involved in autophagosome formation were identified, including Vps34, Vps15 and Atg6, and those involved in the Atg8 conjugation pathway (table 1.1, Herman *et al.*, 2006). ATG19 and ATG11, two proteins specifically associated with the Cvt pathway (Meijer *et al.*, 2007), were absent from *L. major*, *T. brucei* and *T. cruzi*, suggestive that the Cvt pathway does not exist in trypanosomatids (Herman *et al.*, 2006). In that analysis, ATG12, ATG5, ATG10 and ATG16, components of the ATG12 ubiquitin-like conjugation cascade and thought to be essential for autophagosome formation, were found to be absent from trypanosomatids, raising the question as to whether autophagy could function in these parasites.

An independent analysis of the *L. major* genome using yeast Atg8 proteins as a query confirmed the presence of proteins of the ATG8 conjugation system (ATG3, ATG4, ATG7 and ATG8), and additionally identified proteins with some sequence similarity to ATG5, ATG10, ATG12 and ATG16 (Williams *et al.*, 2006). Although identities for these proteins were low, particular characteristics of the proteins were used to tentatively assign them as autophagy orthologues. The *L. major* genes encoding possible *ATG5*, *ATG10* and *ATG12* homologues were recently shown to complement their respective *S. cerevisiae* mutants, and ATG12 fused to RFP was shown to localise in part to ATG8-containing puncta, suggesting that *Leishmania* does in fact possess functioning, albeit divergent, components of the ATG12 conjugation system (Williams *et al.*, 2009). Only a truncated version of the *ATG12* gene with an exposed carboxyl glycine (*ATG12g*) could complement yeast  $\Delta atg12$  mutants, suggesting that *Leishmania* ATG12 is unusual in that it requires processing by an as yet unidentified peptidase. In addition to a clear Atg8 homologue (LmjF19.1630), a set of proteins that shared some sequence identity with yeast Atg8 (between 21 and 27% identity) were identified. These proteins clustered into three multi-gene families and were designated ATG8A, ATG8B and ATG8C (Williams *et al.*, 2006).

The use of GFP-ATG8 as a marker of autophagosomes in *Leishmania* has been demonstrated in *L. major* and *L. mexicana* (Besteiro *et al.*, 2006b; Williams *et al.*, 2006). A detailed analysis of the occurrence of autophagy in *Leishmania* was performed using *L. mexicana* as a model (Williams *et al.*, 2006). This study demonstrated that autophagy was up regulated during both major differentiation processes; from procyclic to metacyclic promastigotes, and from metacyclic promastigotes to amastigotes, and played an additional role in starvation induced autophagy. The use of GFP-ATG8 as a marker of autophagy in *Leishmania* was validated based on the appearance of double membrane bound vesicles (as observed with transmission electron microscopy) which coincided with an increase in GFP-ATG8 labelled puncta upon starvation. Additionally it was shown that wortmannin, a known inhibitor of autophagy in *S. cerevisiae* and in mammals, inhibited the appearance of autophagosomes in *Leishmania* (although only when used at a concentration 1000 fold higher than that required for yeast), providing further evidence that the GFP labelled punctate structures observed were indeed autophagosomes.

Treatment of *L. mexicana* promastigotes with an inhibitor of clan CA, family C1 cysteine peptidases known as K11777 (N-methyl-piperazine-phe-homophe-vinylsulfone-phenyl) for 24 hours led to an accumulation of GFP-labelled autophagosomes (with an average of 6 autophagosomes per cell compared to 1-2 per cell in control cells), suggesting that peptidases involved in lysosomal degradation are required for the normal progression of autophagy in *Leishmania* (Williams *et al.*, 2006). In an *L. mexicana* lysosomal cysteine peptidase double null mutant ( $\Delta cpa/cpb$ , Mottram *et al.*, 1996), RFP-ATG8 was found to localise to autophagosomes as normal during early stages of growth. However, as the parasites entered stationary phase, a single large punctus was formed which enlarged during stationary phase in place of the normal MVT, providing evidence that these cysteine peptidases are required for the degradation of autophagosomes in the MVT (Williams *et al.*, 2006).  $\Delta cpa/cpb$  promastigotes are unable to differentiate into infective metacyclic promastigotes (Mottram *et al.*, 1996) and were found to be less able to withstand nutrient deprivation than wild type cells, suggesting that a functioning autophagy pathway is required for both parasite differentiation and in withstanding starvation.

Besteiro *et al.*, (2006) demonstrated that *L. major* parasites deficient in the autophagy gene *ATG4.2* were defective in their ability to differentiate into infective metacyclic promastigotes, indicating that autophagy is essential for differentiation and virulence of the parasite. It was also shown that mutant parasites deficient in endosome sorting (mutants over expressing a dominant-negative ATPase *VPS4*) could not differentiate into metacyclic promastigotes, and that the autophagy pathway, monitored by the expression of the autophagosome marker GFP-ATG8, was disrupted. This study led to the suggestion that in *L. major* the autophagy pathway requires an interaction with the endosomal network in order to function. Autophagy has been shown to overlap with endocytosis by demonstrating the presence of endocytosed material in autophagic vacuoles in mammalian cells (Gordon *et al.*, 1992). The ATPase *SKD1* (which is the mouse homologue of the yeast *Vps4*), has been implicated in transport from endosomes to the vacuole, and has been shown to be important in the autophagic pathway (Nara *et al.*, 2002), as it was in *L. major* (Besteiro *et al.*, 2006b).

The occurrence of autophagy was also demonstrated in *T. cruzi* and shown to be associated with starvation and with differentiation from non-infective epimastigotes into infective metacyclic trypomastigotes (Alvarez *et al.*, 2008a; Alvarez *et al.*, 2008b). These authors identified an Atg8 homologue termed TcAtg8.1 that was able to complement an *S. cerevisiae*  $\Delta$ atg8 mutant, and immunofluorescence analysis using polyclonal antibodies raised against recombinant Atg8.1 showed that Atg8.1 was associated with autophagosomes, the formation of which was upregulated during differentiation and in response to starvation. Another putative Atg8 homologue was identified, TcAtg8.2, that had a lower level of sequence identity to yeast Atg8, could not rescue a yeast  $\Delta$ atg8 mutant, and did not localise to autophagosomes. Two Atg4 homologues were identified, both of which complemented an *S. cerevisiae*  $\Delta$ atg4 mutant, and which were both shown to process Atg8.1 and Atg8.2 in an *in vitro* assay, although Atg4.1 showed much higher affinity for both Atg8 proteins (Alvarez *et al.*, 2008a).

Autophagy has been implicated in the turnover of glycosomes during *T. brucei* differentiation (Herman *et al.*, 2008). Glycosomes were found to associate with the lysosome during differentiation from long slender bloodstream cells to stumpy forms and to a much greater extent during differentiation from stumpy forms to the insect stage procyclic trypanosomes. The proportion of glycosomes being degraded in the lysosome was much higher in procyclic forms, in which glycolysis is considerably less active. Electron microscopy analysis revealed that glycosomes clustered around the lysosome during differentiation, while glycosomes were never seen within autophagosomal membranes, leading the authors to suggest that a process analogous to micropexophagy was occurring in *T. brucei*. Most of the ATG proteins specifically involved in yeast micropexophagy were identified in *T. brucei* (Herman *et al.*, 2006). The association of glycosomes in the lysosome could also be induced by starvation, suggesting that micropexophagy can be induced by starvation in *T. brucei*.

Recently, it was shown that the growth of *T. brucei* bloodstream forms is controlled by two functional independent TOR kinases, TbTOR1 and TbTOR2. TbTOR1 was found to promote cell growth and proliferation by positively regulating cell size, cell cycle progression and RNA polymerase I localisation to the nucleolus, while TbTOR2 regulated actin polarisation towards the endocytic

pathway, and was crucial for endocytosis and cytokinesis (Barquilla *et al.*, 2008). Autophagy was induced in cells depleted for TbTOR1, as seen by electron microscopy analysis, suggesting that autophagy is induced upon inhibition of TOR, as in other eukaryotic cells (Barquilla and Navarro, 2009). TbTOR1 was found to be insensitive to rapamycin, so autophagy could not be induced in these organisms by the addition of rapamycin. These authors found that *T. brucei* Atg8 homologues, TbAtg8A or TbAtg8B, when fused with a yellow protein did not localise to autophagosomes, and so confirmation of the data obtained by ultrastructural analysis was not achieved.

### 1.3.11 Multiple Atg8 genes in higher eukaryotes and *L. major*

While there is just a single *ATG8* gene in *S. cerevisiae*, higher eukaryotes possess gene families with multiple copies of *ATG8* genes (Slavikova *et al.*, 2005).

Mammals possess four families of Atg8-related proteins, all of which possess a conserved Gly residue near the C-terminus corresponding to the PE receptor site in yeast Atg8. These gene families are: microtubule-associated protein 1 light chain 3 (MAP1-LC3), Golgi-associated ATPase enhancer of 16kDa (GATE16),  $\gamma$ -aminobutyric-acid-type-A (GABA<sub>A</sub>)-receptor associated protein (GABARAP) and Atg8L (Kabeya *et al.*, 2004). LC3 has been well characterised as a functional Atg8 homologue (Mizushima *et al.*, 2004). On the other hand, while GABARAP, GATE-16 and Atg8L are all able to localise to autophagosome membranes, a role in autophagy *in vivo* has not been assigned to these proteins, and it seems that they function in cellular processes distinct from autophagy (Kabeya *et al.*, 2004; Tanida *et al.*, 2004c). In *Arabidopsis*, nine Atg8 homologues have been identified which appear to have distinct roles in differentiation and starvation induced autophagy (Slavikova *et al.*, 2005).

The *L. major* genome encodes, in addition to the previously characterised *L. major* ATG8 (LmjF19.1630), 25 additional genes encoding proteins with low levels of similarity to ATG8 and its other homologues. Based on phylogenetic analysis, these proteins have been grouped into three families named *ATG8A*, *ATG8B* and *ATG8C* (Williams *et al.*, 2006). Members of the *ATG8A*, *ATG8B* and *ATG8C* families are absent from mammals, yeast and other protozoan parasites, including the closely related parasites *T. brucei* and *T. cruzi*, thus the presence of these “ATG8-like” proteins is apparently unique to *Leishmania spp.* It should

be noted that the *T. brucei* Atg8 proteins named TbAtg8A and TbAtg8B are not related to the *L. major* ATG8A or ATG8B, rather they represent two copies an Atg8 homologue.

## 1.4 Aims of this project

There are still many unanswered questions about the molecular processes that accompany *Leishmania* differentiation, a process vital for parasite virulence, and the recent demonstration of the important role of autophagy in differentiation events has led to an interest in studying proteins potentially involved in regulating this process.

The availability of the published *L. major* genome (Ivens *et al.*, 2005) led to the identification of three multi-gene families of “ATG8-like” proteins, of unknown function and apparently unique to *Leishmania* species. Additionally, a homologue of presenilin-1 (PS1), a protein implicated in the regulation of autophagy in mammalian cells, was identified in the *L. major* genome.

The two main aims of this project were:

1. To analyse the location, expression, and post-translational processing of ATG8-like proteins in *L. major* to investigate a potential role in autophagy.
2. To analyse the location, expression and role of PS1 in *L. major* using genetic manipulation techniques, with the hypothesis that PS1 may be involved in the regulation of autophagy.

## **2 Materials and Methods**

## 2.1 Bacterial strains and culture methods

### 2.1.1 Bacterial strains

For the cloning of plasmids, host strains *E. coli* XL1- Blue (*recA1 endA1 gyrA96 thi-1 hsdR17 supE44 relA1 lac* [F'*proAB lacIqlacZΔM15 Tn10* (Tetr)]) (Stratagene) or *E. coli* DH5α (F- $\phi$ 80*lacZΔM15 Δ(lacZYA-argF)U169 recA1 endA1 hsdR17*(rk-, mk+) *phoA supE44 thi-1 gyrA96 relA1 λ-*) (Invitrogen) were used. Both strains are endonuclease deficient, improving the quality of miniprep DNA, and are recombination (*recA*) deficient, improving insert stability. The *hsdR* mutation prevents the cleavage of cloned DNA by the *EcoK* nuclease, and the *lacZΔM15* gene on the F' episome allows blue white screening.

For the expression of proteins, *E. coli* BL21(DE3) (F- *ompT hsdSB*(rB- mB-) *gal dcm* (DE3)) (Novagen) cells were used. DE3 strains contain an IPTG-inducible gene for the T7 RNA polymerase, and are specially designed for the high level expression of proteins.

### 2.1.2 Bacterial culture

After transformation with the desired plasmid, *E. coli* cells were spread using a glass spreader sterilised with ethanol onto LB-agar plates containing the relevant antibiotic (100  $\mu\text{g ml}^{-1}$  ampicillin). After overnight incubation at 37°C, bacteria colonies were maintained on plates which were sealed with parafilm for up to 4 weeks at 4°C. Single colonies were picked with a sterile cocktail stick and used to inoculate 5- 10 ml LB-medium, and grown overnight at 37°C in a rotary incubator. From this “starter culture” larger volumes of LB-medium were inoculated and grown at 37°C for the desired length of time.

### 2.1.3 Long term storage of bacteria

A single colony was used to inoculate 5 ml LB supplemented with the appropriate antibiotic and grown overnight at 37°C. 500  $\mu\text{l}$  of the overnight culture was mixed with an equal volume of 2% peptone (w/v) 40% (v/v) glycerol solution, and the cells stored at -80°C.

## **2.1.4 Generation of heat shock competent *E. coli***

### **2.1.4.1 Rubidium chloride method**

A single colony of the strain of interest was used to inoculate 5 ml of LB-media (containing tetracycline in the case of XL1 blue cells), and grown at 37°C overnight. The culture was diluted 1:100 in 50 ml fresh LB medium and grown at 37°C until an optical density of 0.6 was reached at a wavelength of 600 nm (O.D.<sub>600nm</sub>). The culture was incubated on ice for 10 minutes and harvested at 2000 X g for 15 minutes at 4°C. The cell pellet was resuspended in 16 ml chilled RF1 buffer (100 mM rubidium chloride, 50 mM MnCl<sub>2</sub>·4H<sub>2</sub>O, 30 mM potassium acetate, 10 mM CaCl<sub>2</sub>, 15% glycerol, with a final pH of 5.8, adjusted with 0.2 M acetic acid), mixed by slow vortexing and incubated on ice for 15 minutes. The suspension was harvested at 4°C, and the cell pellet resuspended in 4 ml chilled RF2 buffer (10 mM MOPS pH 6.8, 10 mM rubidium chloride, 75 mM CaCl<sub>2</sub>, 15% glycerol, with a final pH of 6.8, adjusted with NaOH). The suspension was incubated on ice for one hour, aliquoted for single use, and snap-frozen in ethanol on dry-ice. Competent cells were stored at -80°C.

### **2.1.4.2 Calcium chloride method**

In some cases competent cells were prepared using calcium chloride. A 25 ml culture was grown to an O.D.<sub>600nm</sub> of 0.4 as described above. The culture was harvested at 2000 X g for 10 minutes at 4°C, and the pellet resuspended in 12.5 ml chilled, sterile 50 mM CaCl<sub>2</sub> by slow pipetting and stored on ice for 30 minutes. The suspension was harvested at 2000 X g for 10 minutes at 4°C and the cell pellet resuspended in 2.5 ml chilled, sterile 50 mM CaCl<sub>2</sub> with glycerol added to a final concentration of 10%. Cells were frozen and stored as described above.

### **2.1.5 Heat-shock transformation**

The DNA of interest (ligation mixture or plasmid) was added to 50 µl of heat shock competent *E. coli* cells which had been allowed to defrost on ice, and incubated on ice for 15 minutes. Transformation was then performed by incubating the cell-DNA mix at 42°C for 45 seconds. The suspension was allowed to recover by incubating on ice for 15-30 minutes before being spread onto LB agar plates containing the relevant antibiotic. Where BL21 cells were

transformed, LB medium was added to the transformed cells for one hour at 37°C to aid their recovery prior to plating.

## 2.2 Vectors used in this study

The DNA vectors that were used throughout this study are described in table 2.1. Some more detail about the pNUS, pRIB and *Leishmania* knock out vectors is provided below.

Vector	Description	Manufacturer / Reference
PGEM-T Easy	Gene cloning vector	Promega
Pet-21a	His tagged protein expression construct (N terminal His-tag)	Novagen
pGEX-5X1	GST-tagged protein expression construct	GE Healthcare
pNUS	For the expression of fluorescently tagged proteins in <i>Leishmania</i> (RFP and GFP, N terminal and C terminal)	(Tetaud <i>et al.</i> , 2002)
pRIB (pGL631)	Ribosomal integration expression construct for <i>Leishmania</i> .	(Benzel <i>et al.</i> , 2000)
pGL345	Knock out construct for <i>Leishmania</i>	(Mottram <i>et al.</i> , 1996)

Table 2-1 Vectors used in this study

### 2.2.1 Expression vectors for *Leishmania*

The expression of biologically active proteins fused to fluorescent proteins in *Leishmania* was achieved using the pNUS expression vectors (Tetaud *et al.*, 2002). 5'-Trans-splicing signals and some poorly defined regions within the 3'-untranslated regions of genes are required for optimal expression of genes in trypanosomatids. The pNUS vectors therefore include the intergenic region of the *Crithidia fasciculata* phosphoglycerate kinase (PGK) genes A and B which allow the polyadenylation of the target gene and spliced leader addition to the selectable marker. To permit the trans-splicing of the target gene, part of the intergenic regions of the PGK locus was added upstream. Finally a 3'-untranslated sequence from the *Crithidia* glutathionylspermidine synthetase (GSPS) was added to allow the polyadenylation of the selectable marker gene. In this study, pNUS-GFPcN (pGL1132, for the production of C terminal GFP tags), pNUS-GFPnN (pGL1135, for the production of N terminal GFP tags) and pNUS-REDnD (pGL1043, for the production of N terminal RFP tags) were used.

### **2.2.2 Ribosomal integration vector for *Leishmania* (pRIB)**

The pRIB vector is based on the pFW31 vector (Benzel *et al.*, 2000), and was used in this study for the re-expression of PS1 in  $\Delta ps1$  null mutant cell lines, and for the stable integration of PS1 with an HA tag into wild type cells. Following linearization with *PacI* and *PmeI* of the plasmid, transfection and cloning, the gene of interest is stably expressed at the 18S ribosomal RNA small subunit (18S rRNA locus, GeneDB identifier LmjF27.rRNA.06) under the control of the rRNA promoter (pol1). This allows homogenous expression of the gene in both promastigote and amastigote forms (Misslitz *et al.*, 2000), and avoids problems that may be associated with high levels of over expression of a particular gene on an episome (Benzel *et al.*, 2000). This vector uses the 5' trans-splicing signals and 3'-polyadenylation sites of the *L. major* cysteine peptidase B (CPB) gene to allow the gene of interest to be expressed.

### **2.2.3 Gene knock-out vector for *Leishmania***

The backbone vector used in this study for generating a PS1 knock out is based upon pGL345, a construct designed for the knock out of the *L. mexicana* cysteine peptidase B array (lmcpcb) (Mottram *et al.*, 1996). In this vector, the 5' and 3' untranslated regions (UTRs) of *L. major* dihydrofolate reductase (DHFR) allow the optimal expression of the antibiotic selectable marker. In this study the flanking regions of lmcpcb were replaced with the flanking regions of PS1 by digestion with *HindIII/SalI* and *XmaI/BglII* (plasmid produced prior to the start of the project) to allow homologous recombination into the chromosomal locus (following linearization of the plasmid with *HindIII* and *BglII* and transfection) producing a knock out cell line.

## 2.2.4 Plasmids generated or used in this study

Plasmid	Backbone	Description
pGL1184	Pet-21a	For expression of His tagged PS1 protein, AMP resistant. (Produced by C. McKelvie)
pGL1078	pGL1135	Episomal expression of GFP-ATG8 (HYG resistant). Produced by Dr S. Besteiro.
pGL1410	pGL1135	Episomal expression of GFP-ATG8A (NEO resistant)
pGL1411	pGL1043	Episomal expression of RFP-ATG8A (BSD resistant)
pGL1412	pGL1135	Episomal expression of GFP-ATG8B (NEO resistant)
pGL1413	pGL1043	Episomal expression of RFP-ATG8B (BSD resistant)
pGL1414	pGL1135	Episomal expression of GFP-ATG8C (NEO resistant)
pGL1415	pGL1043	Episomal expression of RFP-ATG8C (BSD resistant)
pGL1161	pGL897	Knockout construct for PS1 (HYG resistant). (Produced by C. McKelvie)
pGL1162	pGL897	Knockout construct for PS1 (BSD resistant). (Produced by C. McKelvie)
pGL1443	pGEX-5X1	For expression of GST tagged PS1, factor Xa cleavage site
pGL1564	pRIB	Integrative vector for the stable expression of PS1-HA (PUR resistant)
pGL1566	pGL1132	Episomal expression of PS1-GFP (NEO resistant)
pGL1567	pRIB	Integrative vector for re-expressing PS1 (PUR resistant)
pGL1686	pGL1078	Episomal expression of GFP-ATG8 (NEO resistant)
pGL1662	pGL1043	Episomal expression of RFP-ATG8 (BSD resistant)
pGL1601	pGL1043	RFP-SQL episome for labelling glycosomes. (Produced by Dr R. Williams).
pGL1431	pGL1135	Episomal expression of GFP-LmjF28.1470 (Produced by Dr S Besteiro)
pGL1433	pGL1135	Episomal expression of GFP-32.0070 (Produced by Dr S Besteiro)
pGL1681	pGL1132	Episomal expression of GFP-V-H <sup>+</sup> -PPase (Produced by D Tonn)
pGL1704	pGL1132	Episomal expression of GFP-V-H <sup>+</sup> -PPase <sup>Y437AY439A</sup> (Produced by D Tonn)

Table 2-2 Plasmids used or generated in this study

## 2.2.5 Oligonucleotides used in this study

Oligonucleotide	Sequence	Restriction site
NT250 (5')	<u>AGATCT</u> ATGTCCATGTACCAGTCGC TGATCCCTGCCGAC	<i>Bgl</i> II
NT251 (3')	<u>GGTACCT</u> TACAAGGAGCCAAGCAGG TCCGGGTTATTCTC	<i>Kpn</i> I
NT252 (5')	<u>AGATCT</u> ATGTCCGCCTACCACAGCA GCAACCCTGTGAGGCC	<i>Bgl</i> II
NT266 (3')	<u>GATATC</u> CCTAAGCGACGGAGAAGCAC GGACTCGCAAAGGC	<i>Eco</i> RV
NT256 (5')	<u>AGATCT</u> ATGTCCGCCTACGTGTTGT CGACGCCGCTG	<i>Bgl</i> II
OL1857 (3')	ACATGAG <u>GATATC</u> CCTAGTTCAAGGCG CACGAGCCGCACGA	<i>Eco</i> RV
OL2034 (5')	GGGTGTTGCTTCACTAAAGCCG	
OL2035 (3')	GTCGCTTTGCTCGTCGTAGTTC	
OL2036(5')	<u>GCGGATCC</u> ACGACGTGGGCGTTGC TGATG	<i>Bam</i> HI
OL2037 (3')	<u>GCCTCGAG</u> TAGCTTGAATGGAGTG GCGTG	<i>Xho</i> I
OL2204 (5')	<u>CCATATG</u> ATGTCGAGCATGCCTCTC TTAG	<i>Nde</i> I
OL2205 (3')	CAT <u>GGTACCG</u> AGCACCAGCAGGTGA TGACTC	<i>Kpn</i> I
OL2207(5')	<u>CCTCGAG</u> ATGTCGAGCATGCCTCTC TTAG	<i>Xho</i> I
OL2208 (3')	GCAGATCT <u>BCAGGCATAGTCCGGG</u> <u>ACGTCGTAGGGGTA</u> GAGCACCAGC AGGTGATGACTC	<i>Bgl</i> II, stop codon (blue), HA tag (red)
OL1760 (5')	AACTAACGCTATATAAGTATCAGTTT CTGTACTTTATTG	Splice leader primer
OL2588 (3')	GCTCAGCGACTCCACAATTAGC	Gene specific primer for PS1 5'RACE
OL1853 (5')	CTGGATCATTTTCCGATG	<i>Leishmania</i> species test primer
OL1854 (3')	TGATACCACTTATCGCACTT	<i>Leishmania</i> species test primer

Table 2-3 Oligonucleotides used in this study

## 2.3 Molecular biology techniques

### 2.3.1 Polymerase chain reaction (PCR)

PCR reactions were performed using either the *Taq* DNA polymerase (NEB) for analytical PCRs, or *Phusion* high fidelity DNA polymerase (Finnzymes) where a proof-reading polymerase was required for cloning. For cloning, the gene of

interest was amplified from genomic DNA using oligonucleotides that were designed to contain particular restriction sites at their 5' end, allowing subsequent transfer of the gene of interest between sub-cloning vectors and the final expression vector.

Analytical PCR reactions were typically performed in a 20  $\mu$ l volume containing approximately 100 ng DNA, 10 pmol of each oligonucleotide, 0.5 units of *Taq* polymerase and 2  $\mu$ l of 10 X PCR mix (1.13 mg ml<sup>-1</sup> BSA, 450 mM Tris pH 8.8, 110 mM ammonium sulphate, 45 mM MgCl<sub>2</sub>, 68.3 mM  $\beta$ -mercaptoethanol, 44  $\mu$ M EDTA pH 8.0, 10 mM dCTP, 10 mM dATP, 10 mM dGTP, 10 mM dTTP, water). Typically amplifications were performed in a PCR Express machine (Hybaid) using the following reaction: DNA denaturation (95°C, 5 minutes), then (95°C 1 min, 55°C 1 min, 72°C y min) x 25 cycles, and finally DNA extension at 72°C for 10 minutes, where the extension time (y) was estimated based on the size of the fragment to be amplified, assuming that typical polymerases synthesise approximately 1 Kb DNA per minute.

Proof reading PCR reactions for amplification of genomic DNA were typically performed in a 50  $\mu$ l reaction containing approximately 100 ng template DNA, 10 pmol of each oligonucleotide, 10 mM dNTPs, 3% DMSO and 20% 5 X *Phusion* HF buffer (containing 1.5 mM MgCl<sub>2</sub>). In these cases, denaturation was carried out at 98°C for 30 seconds. *Phusion* High-Fidelity DNA Polymerase produces blunt end PCR products, so where the PCR products were to be ligated into the sub-cloning vector pGEMT-Easy, 3' A-overhangs were added to the blunt-end fragments by adding 1 unit of *Taq* polymerase directly to the PCR tube and incubating for 20 minutes at 72°C.

### **2.3.2 Restriction digest**

Restriction enzymes were obtained from New England Biolabs (NEB) and used according to manufacturer's instructions with the buffers supplied. Plasmid digestions were typically performed in 20 - 50  $\mu$ l reaction volumes for 2 - 3 hours at 37°C. Where a large amount of purified DNA was required, the reaction was scaled up in volume, and sometimes carried out overnight. Reactions were stopped by the addition of DNA loading buffer to a 1 x final concentration, and analysed by DNA gel electrophoresis.

### 2.3.3 DNA gel electrophoresis and DNA gel extraction

DNA agarose gels were prepared by melting (in the microwave) powdered agarose in 0.5 x TBE buffer (20 mM Tris, 20 mM boric acid, 0.5 mM EDTA pH 7.2). Gels contained 0.8-1.5% agarose (w/v) according to the size of the DNA fragment to be separated. Ethidium bromide (0.2 mg ml<sup>-1</sup>) or SYBR® Safe (1 in 5000 dilution) (Invitrogen) was added to the agarose prior to the gel setting. DNA samples were mixed with 6 x DNA loading buffer (15% Ficoll, 0.25% bromophenol blue, 0.25% xylene cyanol FF) and electrophoresed at 60-120 volts, until the dye front was approximately two thirds of the length of the gel. A 1 kb molecular weight marker (Invitrogen) was used at a concentration of 0.5 µg per lane to determine the size and concentration of the analysed DNA fragments. Gels were viewed under ultra violet illumination (Gel Doc 2000, Bio-Rad) or a Safe Imager™ blue light transilluminator (for use with SYBR® Safe). Avoiding exposure of the DNA to UV light was particularly important when preparing DNA for cloning or for transfection into *Leishmania* cells. Following PCR reactions or enzymatic digestion, DNA fragments of interest were isolated and purified using a Gel Extraction Kit (Qiagen) following manufacturer's instructions.

### 2.3.4 Ligations

PCR products were ligated into the pGEMT-Easy (Promega) vector following the manufacturer's guidelines. For ligation into the final cloning vector, digested and purified plasmid and DNA insert were mixed together at a ratio of 1:3 in a 10 µl reaction containing 200 units of T4 DNA ligase (NEB) and 1 X T4 DNA ligase buffer (50 mM Tris-HCl, 10 mM MgCl<sub>2</sub>, 1 mM ATP, 10 mM Dithiothreitol, pH 7.5, supplied with enzyme), and incubated overnight at 16°C.

### 2.3.5 Verification of ligations

Where the vector pGEMT-Easy was used for sub-cloning, the addition of 0.5 mM IPTG and 80 µg ml<sup>-1</sup> X-gal to transformant plates allowed blue / white screening of bacterial colonies and the identification of cells potentially containing the desired DNA insert. Plasmid DNA was subsequently purified from white colonies, and the success of the ligation verified by restriction digest or sequencing.

Where blue / white screening was not possible (for example when cloning into final vectors such as the pNUS vectors), the presence of the insert in the vector was assessed either by DNA purification and subsequent restriction digest, or

when a high number of colonies were obtained, by colony PCR analysis. For screening the presence of insert in pGEMT-Easy, the SP6 / T7 primer pair was used. When a different vector was used, primer pairs were determined using the Vector-NTI program.

### **2.3.6 Plasmid purification**

High purity plasmid DNA (up to 20 µg) was purified from 5 ml cultures of *E. coli* cells using a QIAprep Spin Miniprep Kit (Qiagen), following manufacturer's guidelines. Where larger quantities of DNA were required, for example for the preparation of DNA for transfection of *Leishmania* cells, 50 ml of bacterial culture was grown and the DNA extracted using a MidiPrep kit (Qiagen). Plasmids were sequenced using The Sequencing Service at the University of Dundee, and AlignX (a module of Vector NTI Advance 10, Invitrogen) was used to analyse the sequence data.

### **2.3.7 Sequence alignments and phylogenetic analyses**

Amino acid sequences were imported into Vector NTI Advance 10 from the GeneDB ([www.genedb.org](http://www.genedb.org)) or the National Centre for Biotechnology Information (NCBI) (<http://www.ncbi.nlm.nih.gov/>) websites. Alignments were performed using the Clustal W algorithm of the Align X program (Vector NTI, Invitrogen). The data was exported as a multiple sequence file (MSF) format and used to build phylogenetic trees with the MEGA3.1 software (Kumar *et al.*, 2004), using the Neighbor-Joining method. The reliability of the tree obtained was tested by bootstrap analysis (1000 pseudoreplicates).

## **2.4 *Leishmania* culture methods**

### **2.4.1 Cell lines used**

Wild type *L. major* (Friedlin strain: WHO designation MHOM/JL/81/Friedlin) were used throughout this study.

### **2.4.2 Cultivation of *L. major***

*L. major* promastigotes were grown at 25°C in HOMEM medium (Invitrogen) supplemented with 10% (v/v) heat inactivated foetal calf serum (HIFCS) and 1% (v/v) penicillin/streptomycin antibiotics (Sigma). Cells were sub-passaged into

fresh medium at a concentration of approximately  $1 \times 10^6$  cells  $\text{ml}^{-1}$  twice each week. Transgenic *L. major* cell lines were maintained with appropriate antibiotics: hygromycin B (Calbiochem) at  $50 \mu\text{g ml}^{-1}$ , puromycin (Calbiochem) at  $50 \mu\text{g ml}^{-1}$ , blasticidin S hydrochloride (Calbiochem) at  $10 \mu\text{g ml}^{-1}$ , and neomycin (G418, Calbiochem) at  $50 \mu\text{g ml}^{-1}$ .

### **2.4.3 Preparation of stabilates for long term storage of *L. major* cell lines**

Stabilates were prepared by mixing 500  $\mu\text{l}$  cells with 500  $\mu\text{l}$  HOMEM + 20% HIFCS + 10% DMSO in a 1.5 ml cryotube and storing overnight at  $-80^\circ\text{C}$  before transferring to liquid nitrogen for long term storage.

### **2.4.4 Estimation of cell density**

Cell density was determined by counting cells diluted with an equal volume of 2% formaldehyde (v/v) in PBS in an improved Neubauer haemocytometer (Weber Scientific) under microscopy. To produce a growth curve, a fresh culture was set up at a density of  $1 \times 10^5$  cells  $\text{ml}^{-1}$ , and counted at the same time each day until stationary phase was reached.

### **2.4.5 DNA preparation for transfection**

Prior to transfection, the purified DNA of interest was ethanol precipitated by adding 2 volumes of 100% ethanol and 10% (final volume) 3M NaAc pH 5.2 and incubating for at least one hour (usually overnight) at  $-20^\circ\text{C}$ , prior to centrifugation at  $13,000 \times g$  for 30 minutes at  $4^\circ\text{C}$ . The DNA pellet was subsequently washed with ice-cold 70% ethanol, air-dried under a sterile hood for 5 minutes, and resuspended in sterile water. Where an episomal construct was to be transfected, approximately 10 - 20  $\mu\text{g}$  of circular plasmid was precipitated with ethanol. For knock out or integrative constructs, approximately 50  $\mu\text{g}$  of plasmid was linearised by digestion with the appropriate restriction enzymes. The digested DNA fragments were separated by electrophoresis on an agarose gel containing SYBR® Safe, cut from a gel under Safe Imager™ blue light, purified using the Qiaquick gel extraction kit (QIAGEN), and then ethanol precipitated as above.

### **2.4.6 Transfection of *Leishmania***

Transfections were performed using a human T-cell Amaxa nucleofector kit (Amaxa Biosystems) following manufacturer's instructions. For one transfection,  $5 \times 10^7$  cells in their mid-log phase of growth were harvested at  $1000 \times g$  for 10 minutes at room temperature and resuspended in 100  $\mu$ l of the Amaxa nucleofector buffer. Approximately 10  $\mu$ g of DNA, prepared in 10  $\mu$ l sterile water was added to the cells and gently mixed. Cells were electroporated using the U-033 Amaxa programme before being transferred to 10 ml of fresh HOMEM medium with 20% HIFCS. The culture was immediately split into two flasks to select for independent transfection events and allowed to recover overnight in a 25°C incubator. The following day the appropriate antibiotics were added and cells were cloned in 96 well plates as described below. For each transfection, a negative control was performed using water in place of DNA.

### **2.4.7 Selection and Cloning of Transfected *Leishmania***

To select for a population of transfectants when using non-integrative vectors, the overnight culture was diluted at least 1 in 4 in fresh HOMEM with 20% HIFCS with the appropriate antibiotics. For cells transfected with integrative vectors, serial dilutions of 1 in 5, 1 in 50 and 1 in 500 were obtained from each of the overnight cultures and plated out on 96 well microplates. Based on calculated transfection efficiencies approximately 20 clones should be obtained from a 1 in 50 dilution, and 2 clones should be obtained from a 1 in 500 dilution (Protocols for handling and working with *Leishmania* species, Mottram laboratory 2008). Plates and flasks were maintained at 25°C for 2 - 6 weeks while awaiting the growth of transfectants. When clones grew to log phase, they were transferred to 10 ml cultures for subsequent analysis and stabilate preparation.

### **2.4.8 Isolation of genomic DNA from *Leishmania***

Genomic DNA was prepared from *L. major* promastigotes using the "cultured animal cells" protocol of the DNeasy tissue kit (Qiagen) following manufacturer's instructions. In most cases, a 10 ml *Leishmania* culture (approximately  $1 \times 10^8$  cells) yielded approximately 3  $\mu$ g DNA.

### **2.4.9 Isolation of total RNA and synthesis of cDNA from *Leishmania* and 5'RACE**

Total RNA from *L. major* promastigotes was isolated using ready-to-use TRIzol (Life Technologies), which is a monophasic solution of phenol and guanidine isothiocyanate. The method was carried out following manufacturer's instructions. The introduction of RNase during RNA isolation was prevented by using RNase-free tips, sterile disposable plastic-ware and RNase free water; prepared by adding diethylpyrocarbonate (DEPC) to 0.01% (v/v), leaving overnight and then autoclaving. First strand cDNA was synthesised from poly A<sup>+</sup> mRNA contained in the total RNA by priming with Oligo (dT), which is used to hybridise to 3' poly(A) tails, and the enzyme Superscript III reverse transcriptase (Life technologies), following manufacturer's instructions. When synthesis was complete, the reaction was terminated by incubation at 85°C, and RNA was removed by the addition of RNaseH (Life technologies). *L. major* PS1 was amplified from cDNA using reverse transcriptase PCR (RT-PCR) with a splice leader specific primer that targets the spliced leader (OL1760) with a PS1 specific primer (OL2588). The product was then sequenced to determine the splice leader addition site.

### **2.4.10 Verification of *Leishmania* species by PCR**

The species of *Leishmania* used in this study was confirmed by PCR amplification of the ribosomal internal spacer locus with OL1853 and OL1854 and subsequent analysis of *Hae*III restriction fragment length polymorphisms by agarose gel electrophoresis, following the method described by Schonian *et al.*, 2003.

### **2.4.11 Southern blot analysis**

For the analysis of PS1 heterozygotes and null mutants, 3 µg of genomic DNA was digested with the restriction enzyme *Pci*I, and separated overnight by electrophoresis in a 0.8 % agarose gel in TBE buffer at 30 V. The gel was nicked, denatured, and neutralised by incubation for 10 minutes in depurination solution (0.25 N HCl), denaturation solution (0.5 M NaOH, 1.5 M NaCl) and neutralisation solution (1.5 M NaCl, 0.5 M Tris HCl, pH 7.5). The gel was blotted onto a Hybond<sup>TM</sup>-N<sup>+</sup> nylon membrane in 20 X SSC (3 M NaCl, 0.3 M NaCitrate, pH 7.0) by capillary transfer overnight. The transferred DNA fragments were covalently

attached to the membrane by UV crosslinking. 10 ng of the desired probe (either the PS1 5' flanking region of the PS1 open reading frame) was purified, labelled with Alk-Phos<sup>TM</sup> Direct labelling kit (Amersham) following manufacturer's instructions, and incubated with the membrane overnight. The signal was detected using a CDP-Star detection reagent (Amersham) and exposed using a Kodak film or a Typhoon imager (GE healthcare).

#### **2.4.12 Production of *Leishmania* cell lysates**

*Leishmania* cells were counted and centrifuged at 1000 x g for 10 minutes, washed twice with 10 ml filter sterile PBS, and the cell pellet either lysed immediately or stored at -20°C. Cells were normally resuspended in lysis buffer containing 0.2 % triton X-100 in PBS and a mixture of peptidase inhibitors and incubated on ice for 30 minutes. Peptidase inhibitor mix contained: Cysteine protease inhibitor E-64 (trans-epoxysuccinyl-L-leucylamido(4-guanidino)butane) (10 µM), metalloprotease inhibitor 1,10-phenanthroline (400 µM), aspartic protease inhibitor pepstatin A (2 µM), serine protease inhibitor phenylmethylsulphonyl fluoride (PMSF) (1 mM), metal ion chelator ethylenediamine tetra acetic acid (EDTA) (2 mM) and the cysteine / serine protease inhibitor leupeptin (10 µM). Protein concentration was estimated using the Micro BCA Protein Assay kit (Pierce) following manufacturer's instructions. In some cases (highlighted in results sections), cells were lysed without detergent prior to subcellular fractionation as described below.

#### **2.4.13 Subcellular fractionation**

*Leishmania* lysates were prepared and fractionated from early stationary phase cells as in Coombs *et al.*, (1982). Parasites were harvested by centrifugation at 2000 x g for 10 minutes, washed twice in 0.25 M sucrose, and lysed in the presence of peptidase inhibitors without the use of detergent by mixing to a thick paste with alumina (Sigma). When more than 99% of the parasites were lysed (assessed by phase contrast microscopy) the paste was washed in 4 volumes of 0.25 M sucrose and the resultant supernatant was fractionated by differential centrifugation resulting in four fractions. The fraction termed P1 (pellet 1) was collected by centrifugation at 2000 x g for 10 minutes, P2 was collected by centrifugation at 13000 x g for 30 minutes, and finally a one hour high-speed centrifugation step at 100,000 x g resulted in the pellet, P3, and the

supernatant, S. Each pellet was subsequently solubilised in 0.2% Triton X-100, the amount of protein estimated using the BCA assay (Pierce) and each fraction diluted to equal protein concentrations for comparative analysis by SDS-PAGE. Where specified, phospholipid moieties were removed from the protein of interest by incubating 20 µg of cell lysate with 10 units of phospholipase D (sigma) for one hour at 37°C.

#### **2.4.14 Purification of *L. major* metacyclic promastigotes**

Parasites were harvested at 1000 x g for 10 minutes, washed and resuspended in PBS at a density of  $1 \times 10^8$  cells ml<sup>-1</sup>. Peanut lectin (Sigma, stock solution is stored at 100 mg ml<sup>-1</sup> at -20°C) was added to a final concentration of 50 µg ml<sup>-1</sup> and incubated at room temperature for 10 minutes. Metacyclic promastigotes were separated from the agglutinated procyclic promastigotes by centrifugation at 100 x g for 5 minutes, and the supernatant containing the metacyclic promastigotes recovered for use.

#### **2.4.15 Extraction of peritoneal macrophages from BALB/C mice**

Institute for Cancer Research (ICR) mice were killed by inhalation of CO<sub>2</sub> gas prior to their necks being broken. Mice were laid on their backs and sprayed with 70% ethanol, a small incision was made with scissors at the abdomen, and their skin was pulled away from the body. After sterilising the mouse again with 70% ethanol, the membrane at the sternum was pulled taught with forceps and a 21G needle was inserted just underneath the membrane with the bevel facing upwards, filling the cavity with 10 ml RPMI 1640 media (PAA cat no. E15-842) and 1% (v/v) gentamicin antibiotic. After shaking the mouse for 30 seconds to release the macrophages, a 26G needle with an empty 10 ml syringe was inserted into the mouse's side with the bevel facing into the body, and the fluid was removed. Macrophages were harvested at 1000 x g for 10 minutes at 4°C and resuspended in fresh RPMI supplemented with 10% HIFCS and 1% gentamicin and the cell density was determined by counting with an improved Neubauer haemocytometer (Weber Scientific) under microscopy. Macrophages were diluted to a cell density of  $5 \times 10^5$  cells ml<sup>-1</sup> in RPMI supplemented with 10% HIFCS and 100 µl macrophages were added to each well of a 16 well Lab-tek™

cavity slides (50,000 macrophages per well) where they were maintained for up to a week at 37°C, 5% CO<sub>2</sub>.

#### **2.4.16 Macrophage infection assay**

Peritoneal macrophages were harvested as described above and incubated at 37°C, 5% CO<sub>2</sub> for 24 hours. The next day, *L. major* cells were diluted to a density of  $5 \times 10^6$  cells ml<sup>-1</sup> in RPMI 1640 medium supplemented with 10% HIFCS and 100 µl added to each well of the cavity slide, resulting in a 10 to 1 infection ratio. After 3 hours the slides were washed at least three times with RPMI to remove non-internalised parasites. At 24 hours and 120 hours post infection, cells were fixed with 100% methanol and stained with 10% Giemsa's stain (BDH) for 10 minutes. The percentage of infected macrophages and the average number of amastigotes per infected macrophage were determined for various cell lines at each time point by light microscopy under oil immersion. For fluorescence microscopy, macrophages were isolated as above and adhered to 13 mm circular coverslips overnight in 12 well plates. The following day stationary phase promastigotes were added as described above. At the desired time points the coverslide was gently lifted with forceps, washed at least three times in filter sterilised PBS and settled onto a microscope slide for analysis (described in section 2.6).

#### **2.4.17 Footpad infection of BALB/C mice**

Groups of 5 female BALB/c mice were inoculated in the footpad with  $5 \times 10^5$  stationary phase promastigotes resuspended in 20 µl PBS, pH 7.4. The thickness of the footpad was measured each week until the footpad reached a thickness of 5 mm, at which point the experiment was terminated and the mice culled.

#### **2.4.18 Alamar blue test with promastigote cells**

*L. major* cells were diluted to a concentration of  $2 \times 10^6$  cells ml<sup>-1</sup> in HOMEM medium with 10% HIFCS. Drugs (stock solutions prepared at 10 or 50 mM in DMSO) were diluted in HOMEM with 10% HIFCS at the desired concentrations, ranging from 1.5 µM to 50 µM. Tests were completed in 96 well plates with 100 µl of the appropriate drug concentration and 100 µl of *Leishmania* cells added to each well. Control wells contained 100 µl of HOMEM with 10% HIFCS and DMSO to a matching concentration to the test wells. Plates were incubated for 5 days

at 25° with air as the gas phase. After 5 days, 20 µl sterile resazurin solution (0.0125% (w/v) resazurin salt (Sigma) in PBS, filter sterilised) was added and the plates incubated for a further 24 hours. Plates were read using an EnVision plate reader (Perkin Elmer, Beaconfield, UK) at emission wavelength of 535 nm, excitation of 620 nm, with a general mirror. LD<sub>50</sub> values were determined by comparison to the control wells, using GraFit 5 data analysis software (Erithacus Software, Horley, UK).

#### **2.4.19 Analysis and Induction of Autophagy**

Autophagy was monitored in *L. major* promastigotes by counting the number of autophagosomes labelled with GFP-ATG8 by fluorescence microscopy (Besteiro *et al.*, 2006b) (preparation of cells for microscopy is described below). For analysis of autophagy during procyclic promastigote to metacyclic promastigote differentiation, a minimum of 200 cells were counted on each day of a growth curve and the number of cells containing autophagosomes, and the average number of autophagosomes per cell, were recorded. To induce autophagy by starvation, promastigotes were harvested at 1000 x g, washed twice in PBS, resuspended in nutrient free media (PBS) at a density of 1 x 10<sup>8</sup> cells ml<sup>-1</sup>, and incubated at 25°C for 2 to 4 hours. The addition of extra sources of energy or inhibitors of autophagy is described in chapter 3.

### **2.5 Statistical Analysis**

Data were expressed as means ± standard error of the mean (SEM). Levels of significance were calculated by unpaired t tests using the Data Analysis add-on of Microsoft Excel. Differences were considered significant at a p value of <0.5.

### **2.6 Fluorescence microscopy**

Images were obtained using an Applied Precision DeltaVision Deconvolution microscope system. Cells were viewed under UV light with the DAPI (λ = 480 nm), FITC (λ = 540 nm) or rhodamine (λ = 580 nm) filters, and images captured using a CoolSnap HQ camera. DeltaVision softWoRx image acquisition and display software was used for deconvolution and image processing.

Alternatively, slides were examined under UV light using a Zeiss Axioplan microscope where images were processed using a Hamamatsu ORCA-ER digital camera and Openlab version 3.5 software.

### **2.6.1 4,6-Diamindino-2-phenylindole (DAPI) staining**

200  $\mu\text{l}$  of live cells were incubated with DAPI at a final concentration of  $1 \mu\text{g ml}^{-1}$  for one minute in the dark. After washing twice in PBS (by centrifugation at  $1000 \times g$  for 2 minutes), cells were resuspended in 20 - 50  $\mu\text{l}$  ice cold PBS, spread onto a Twin frosted 76 x 26 mm microscope slide (BDH) with a 22 x 64 mm coverglass (BDH), and sealed with nail varnish. Alternatively, cells were fixed in 2% formaldehyde in PBS for ten minutes, washed twice, resuspended in PBS and treated with DAPI and settled on a slide as described above. Where fixed cells were analysed, 0.01% of 1,4-diazabicyclo[2.2.2]octane (DABCO) was spread onto the slide as an anti-fading agent. The fluorescence was observed with the DAPI filter ( $\lambda = 480 \text{ nm}$ ) of the UV microscope and pictures were taken with an exposure time of 40 ms. Phase was observed against bright visible light and pictures were taken with an exposure time of 50 ms.

### **2.6.2 Green fluorescent protein (GFP) and red fluorescent protein (RFP)**

Live cells were prepared for microscopy as described above. GFP fluorescence was observed with the FITC filter ( $\lambda=540 \text{ nm}$ ) and pictures were typically taken with an exposure time of 100 - 200 ms, depending on the intensity of the protein. RFP fluorescence was observed with the Rhodamine filter ( $\lambda=580 \text{ nm}$ ), and a similar exposure time was used.

### **2.6.3 FM4-64 labelling**

500  $\mu\text{l}$  of promastigotes were pelleted and washed in HOMEM ( $1000 \times g$  for 5 minutes) and resuspended in 100  $\mu\text{l}$  HOMEM containing 40  $\mu\text{M}$  FM4-64 (16 mM stock in dimethyl sulfoxide [DMSO] Molecular Probes) and incubated for 15 minutes at  $4^\circ\text{C}$ , resulting in labelling of the flagellar pocket. Cells were then either prepared for microscopy as described above, or washed with HOMEM, resuspended in 500  $\mu\text{l}$  HOMEM and incubated for 15 minutes at  $25^\circ\text{C}$  to label components of the early endosomal system. FM4-64 fluorescence was observed

with the Rhodamine filter ( $\lambda=580$  nm) and pictures were taken with an exposure time of 50 ms.

#### **2.6.4 LysoTracker labelling**

Approximately  $1 \times 10^7$  promastigotes were pelleted and washed as described above, and resuspended in 100  $\mu$ l of HOMEM with 1  $\mu$ l LysoTracker Red DND-99 (1 mM stock in DMSO, Molecular Probes) and incubated for 30 minutes at 25°C. Cells were then washed and prepared for microscopy as described above, and lysotracker fluorescence observed with the Rhodamine filter ( $\lambda=580$  nm) and pictures were taken with an exposure time of 50 ms.

#### **2.6.5 ER-tracker labelling**

Promastigotes were incubated with 0.5  $\mu$ M ER-Tracker™ Red (Molecular Probes, M7512, in DMSO) for approximately 30 minutes at 25°C (1 mM stock in DMSO). Cells were then processed for microscopy as described above, and ER-tracker fluorescence was observed with the Rhodamine filter ( $\lambda=580$  nm) and pictures were taken with an exposure time of 50 - 100 ms.

#### **2.6.6 Immunofluorescence analysis**

Promastigotes were washed twice in PBS before fixation in 200  $\mu$ l of 1% formaldehyde / PBS for 15 - 30 minutes at room temperature. The cells were permeabilised by the addition of 20  $\mu$ l of 1% Triton X-100 / PBS for 10 minutes, and then 20  $\mu$ l of 1 M glycine / PBS was added for a further 10 minutes in order to neutralise the free aldehyde groups resulting from formaldehyde fixation to reduce background fluorescence. Finally the cells were washed twice and resuspended in fresh PBS. Glass slides were washed in 70% ethanol and coated with 0.01% poly-L-lysine (0.1% stock, Sigma). The fixed cells were allowed to adhere to the slides for 15 - 30 minutes in a dark box containing PBS-soaked tissues to prevent the cells from drying.

The cells were incubated with blocking solution (10% HIFCS in TB buffer (0.1% Triton-X-100, 0.1% BSA)) for 30 minutes. Primary antibodies were diluted in TB buffer and incubated with the cells for 1 hour at room temperature, or overnight at 4°C. Cells were washed with at least 10 ml PBS, and excess liquid removed by blotting with a tissue at the corner of the slide. Alexa Fluor 488 (green) or Alexa

Fluor 594 (red) - conjugated secondary antibodies (Molecular Probes) were diluted 1 in 1000 in TB buffer and incubated with the cells in the dark for 1 hour at room temperature. DAPI (Sigma) was diluted in TB buffer at  $0.5 \mu\text{g ml}^{-1}$  and incubated with the cells for one minute, prior to washing the slides with 10 ml PBS and removing excess liquid. 15  $\mu\text{l}$  of mounting solution (2.5 % DABCO in 50% glycerol / PBS) was applied to a coverslide which was laid on the slide and sealed with nail varnish. Fluorescence was observed and images obtained as described above

## 2.7 Biochemical methods

### 2.7.1 Purification of His and GST tagged proteins

*E. coli* BL21 (DE3) cells were transformed with the relevant DNA plasmid and plated onto an LB-agar plate supplemented with the relevant antibiotics. An overnight starter culture of 5 ml was set up in LB media, and from this fresh cultures were inoculated and grown at  $37^{\circ}\text{C}$  to an  $\text{O.D.}_{600\text{nm}}$  of 0.7. Cultures were moved to their induction temperature for 30 minutes and protein expression was induced for the appropriate length of time (specified in the relevant chapters) using Isopropyl- $\beta$ -D-Thiogalactopyranoside (IPTG) at the appropriate concentration (specific conditions are specified in the relevant results chapters). Cells were harvested at  $4000 \times g$  for 15 minutes and resuspended in ice-cold PBS, pH 7.4, supplemented with DNase-I ( $10 \mu\text{g ml}^{-1}$ ), Lysozyme ( $100 \mu\text{g ml}^{-1}$ ) and protease inhibitors (complete EDTA-free protease inhibitor cocktail tablets, Roche), and incubated for 60 minutes on ice. The cell lysate was sonicated 5 x 15 seconds (1sec. on/1sec. off) to break open the cells, centrifuged at  $12000 \times g$  for 20 minutes, and the soluble fraction (supernatant) collected.

For purification of GST tagged proteins the soluble fraction (40 ml volume from a 1 l culture) was incubated with 4 ml glutathione sepharose 4B at room temperature for 30 - 60 minutes. The resin was washed three times in PBS, and the protein eluted in elution buffer (50 mM Tris, 20 mM glutathione, pH 7.0).

For purification of His tagged proteins, the soluble lysate was incubated with Ni-NTA-agarose beads (200  $\mu\text{l}$  for 40 ml soluble lysate) for 20 minutes at  $4^{\circ}\text{C}$  with gentle agitation, and centrifuged at  $1000 \times g$  for 5 minutes at  $4^{\circ}\text{C}$ . The column

was washed twice with ice-cold PBS pH 7.4 with 20 mM imidazole, and eluted in 100 µl fractions with 100 mM NaPi pH 7.4, 10 mM NaCl, 0.5 M imidazole.

Purified proteins were analysed by SDS-PAGE.

### **2.7.2 Peptide synthesis and antibodies production**

Full length recombinant His-ATG8, His-ATG8A, His-ATG8B and His-ATG8C protein was produced in *E. coli* (protein produced by Dr R. Williams) and used to raise polyclonal antiserum in a rabbit (ATG8) or sheep (ATG8A, ATG8B and ATG8C) using standard procedures.

A 10 KDa C terminal fragment of PS1 tagged with GST was produced in *E. coli* as described above and used to raise polyclonal antiserum in a sheep. Additionally, a peptide corresponding to 15 amino acids in the C terminal domain of the predicted PS1 sequence (CRLIVESLSSFTSHH) was synthesised (BioGenes GmbH, Koepenicker Str. 325, D-12555 Berlin, Germany) and used to immunise a rabbit (BioGenes).

### **2.7.3 Affinity purification of antibodies**

1 mg of recombinant protein or peptide was covalently linked to 500 µl of Aminolink Coupling Gel (Pierce) following manufacturer's instructions. The peptide/aminolink resin mixture was equilibrated with 10 ml of IgG binding buffer (0.14 M NaCl, 8 mM sodium phosphate buffer pH 7.5, 2 mM potassium phosphate buffer pH 7.5, 0.1 M KCl) and incubated with 4 ml of antiserum overnight at 4°C. The resin was washed with 20 ml of IgG binding buffer before bound antibodies were eluted with multiple 500 µl fractions of Immunopure IgG elution buffer (Pierce). 25 µl of 1M Tris-HCl pH 9.5 was instantly added to each collection tube to neutralise the acidic pH of the elution buffer. The protein content of each elution was quantified using a BCA protein assay (Pierce), and the fractions containing the most protein were pooled and concentrated on a Vivaspin 2 ultrafiltration unit (regenerated cellulose 10,000 MWCO, Vivascience) at 3000 x g. The filter was washed three times with 2 ml PBS, and finally 200 µl of concentrated antibodies were recovered and stored at -20°C in aliquots.

### **2.7.4 SDS-PAGE**

Protein samples were mixed with 5 x SDS-PAGE sample buffer (10% w/v SDS, 10 mM beta-mercapto-ethanol, 20% v/v glycerol, 0.2 M Tris-HCl, pH 6.8, 0.05% bromophenol blue), denatured by boiling at 100°C for five minutes and separated by SDS-PAGE (sodium dodecyl sulfate polyacrylamide gel electrophoresis). Depending on the size of the protein to be analysed, polyacrylamide gels containing 12% or 15% (w/v) polyacrylamide (Bio-Rad) were prepared using a gel casting cassette system (Invitrogen). When stated in the results chapters, acrylamide gels were prepared containing 6 M urea. This was achieved by dissolving the appropriate weight of urea powder in the Tris and acrylamide (with gentle heating) before adding the remaining ingredients. Proteins were electrophoresed in an XCell SureLock Mini-Cell (Invitrogen) with 1 x SDS-PAGE running buffer (10 x Running buffer: 25 mM Tris, 192 mM glycine and 0.1% SDS) at 180 volts for approximately one hour until the dye front reached the foot of the gel.

### **2.7.5 Coomassie gel staining**

SDS-PAGE acrylamide gels were incubated with agitation in Coomassie blue R250 stain (45% ethanol, 45% distilled water, 10% glacial acetic acid, 0.25% Coomassie blue R250) for approximately one hour and rinsed with milli-Q water. The stain was removed by incubating gels with agitation in destain solution (45% ethanol, 45% distilled water, 10% glacial acetic acid) for several hours or overnight, changing the destain solution as required. For analysis of immunoprecipitated proteins, Brilliant Blue G - colloidal concentrate (Sigma, B2025) was used as it is reported to be 10 fold more sensitive than Coomassie stains. In such cases, the proteins were fixed prior to staining for one hour in 7% glacial acetic acid in 40% (v/v) methanol.

### **2.7.6 Western blotting**

Following SDS-PAGE, separated proteins were transferred to a Hybond-C nitrocellulose membrane (Amersham) by electroblotting using the Mini Trans-Blot Electrophoretic Transfer Cell System for one hour at 100 volts or the Trans-Blot Semi-Dry System for 30 minutes at 20 volts. In each case the gel, membrane and filter paper were soaked in transfer buffer (20 mM Tris/HCl, 15 mM glycine, 20% (v/v) methanol). The membranes were subsequently incubated

in blocking solution of 5% milk in TBS/Tween (TBST: 25 mM Tris-HCl, pH 8.0, 125 mM NaCl, 0.1% Tween 20) for one hour (at room temperature) or overnight (at 4°C) to prevent non-specific binding of antibodies to the membrane. The membrane was then incubated with primary antibodies in fresh blocking solution for one hour to overnight (at 4°C). The relevant concentrations of primary antibodies are provided in results chapters. After at least three washes of 10 minutes each in TBST, the membrane was then incubated with goat anti-mouse, goat anti-rabbit or donkey anti-sheep Horse Radish Peroxidase (HRP) conjugated antibodies at 1 in 5000 dilution for one hour at room temperature. After at least three washes, the western blots were revealed using an ECL kit (SuperSignal West Pico Chemoluminescent Substrate, PIERCE).

### **2.7.7 Co-immunoprecipitation experiments**

Parasite lysate enriched for ATG8B was obtained from 200 ml early stationary phase cells by physical lysis with alumina, ultracentrifugation at 100,000 x g at 4°C for 60 minutes, and solubilisation of the pellet in 0.2% NP-40 (section 2.4.13). A reusable column for immunoprecipitation was produced by crosslinking 1 mg of purified antibody to aldehyde-activated beaded agarose (Pierce Profound™ Co-Immunoprecipitation Kit). The lysate was incubated with the immobilised antibody overnight at 4°C. The column was washed six times in PBS, and 6 100 µl elutions were collected from the column in 0.2 M glycine, pH2.5. Eluted proteins were analysed by SDS-PAGE and staining with Brilliant Blue G - colloidal concentrate (Sigma) and by western blotting. Proteins detected as coomassie stained bands by SDS-PAGE were cut from the gel using a clean scalpel and stored at -20°C. Samples (coomassie stained protein bands excised from the gel and elutions) were sent to the Sir Henry Wellcome Functional Genomics Facility (SHWFGF) for analysis where the samples were subjected to proteolysis with the enzyme trypsin and analysed by electrospray ionisation mass spectrometry on a Q-STAR® Pulsar i hybrid MS/MS System. The data was analysed at the SHWFGF using Applied Biosystems Analyst QS (v1.1) software and the automated Matrix Science Mascot Daemon server (v2.1.06), and protein identifications were assigned using the Mascot search engine.

### **2.7.8 Incorporation of [<sup>3</sup>H] ethanolamine into *L. major* promastigotes**

2 x 10<sup>8</sup> dividing promastigotes were resuspended in 10 ml fresh HOMEM, 10% HIFCS and incubated with 20 µCi [<sup>3</sup>H] ethanolamine for 24 hours. Autophagy was induced by starvation in PBS for four hours prior to immunoprecipitation as described above. Samples were loaded onto two gels, one of which was stained with Brilliant Blue G - colloidal concentrate (Sigma), impregnated with NAMP100 Amplify Fluorogenic Reagent (GE Healthcare) for 30 minutes, dried and exposed to a Kodak film for one week at -80°C. The second gel was subjected to western blot (as described above) to confirm the success of the immunoprecipitation.

### **3 Analysis of the Location of *L. major* ATG8-like proteins**

### 3.1 Introduction

The occurrence and importance of autophagy in *Leishmania* has been clearly demonstrated. Besteiro *et al.*, (2006b) showed that the disruption of endosomal sorting in *Leishmania* by the overexpression of a dominant negative ATPase, VPS4, led to de-regulation of autophagy (monitored by GFP-ATG8) and caused the parasites to be unable to differentiate into infective metacyclic promastigotes. In the same paper, an *ATG4.2* null mutant ( $\Delta atg4.2$ ) was analysed and also found to be defective in both autophagy and the ability to differentiate (Besteiro *et al.*, 2006b). A detailed analysis of autophagy in *L. mexicana* was performed making use of GFP-ATG8 as a marker of autophagosomes, and it was demonstrated that autophagy is clearly upregulated during both major differentiation processes of the parasite life cycle; from procyclic to metacyclic promastigote, and from metacyclic promastigote to the mammalian amastigote form, and also in response to starvation (Williams *et al.*, 2006).

#### 3.1.1 Multiple Atg8 homologues in eukaryotic organisms

While there is just a single *Atg8* gene in *S. cerevisiae*, higher eukaryotes possess multiple *Atg8* like genes, suggesting that different *Atg8* proteins may have different functions in addition to autophagy (Slavikova *et al.*, 2005). In *Arabidopsis*, nine *Atg8* homologues have been identified that appear to have distinct roles in differentiation and starvation induced autophagy (Slavikova *et al.*, 2005). Four families of mammalian ATG8-related proteins exist (MAP1-LC3, GABARAP, GATE-16 and Atg8L), all of which are able to localise to autophagosome membranes, but which have additional divergent functions. In *L. major*, in addition to the previously characterised ATG8, twenty five additional “ATG8-like” proteins have been described based on sequence similarity (Williams *et al.*, 2006). Given the crucial role of autophagy in the life cycle progression and virulence of *Leishmania* parasites (Besteiro *et al.*, 2006b), the roles of these putative ATG8 paralogues were studied, with the working hypothesis that they have distinct roles in autophagy related processes, which may be important for parasite virulence.

### 3.1.2 The roles of Human Atg8 homologues

Humans possess four families of Atg8-related proteins, all of which possess a conserved Gly residue near the C-terminus corresponding to the site of attachment to phosphatidylethanolamine (PE) in yeast Atg8. These gene families are: microtubule-associated protein 1 light chain 3 (MAP1-LC3) (henceforth referred to as LC3), Golgi-associated ATPase enhancer of 16 kDa (GATE16),  $\gamma$ -aminobutyric-acid-type-A (GABA<sub>A</sub>)-receptor associated protein (GABARAP) (Kabeya *et al.*, 2004) and Atg8L (Hemelaar *et al.*, 2003). These four Atg8 homologues are all cleaved after synthesis by the cysteine peptidase Atg4B (Hemelaar *et al.*, 2003). All were shown to interact with the E1 and E2 enzymes Atg7 and Atg3, and to generate modified (perhaps lipidated) forms that are associated with autophagosome membranes (Tanida *et al.*, 2006; Tanida *et al.*, 2002; Tanida *et al.*, 2001). Together these observations suggest that humans possess a divergent set of proteins which are all capable of functioning in the Atg8 conjugation system.

LC3 has been well described as a universal autophagosome membrane marker, and thus a functional homologue of yeast Atg8. Using transgenic mice expressing GFP-LC3 systemically it was shown that upon starvation LC3 was recruited to punctate structures corresponding to autophagosomes and autolysosomes in many tissues (Mizushima *et al.*, 2004). Starvation induced autophagy was clearly observed in skeletal and heart muscles, while GFP-LC3 localisation in the brain was not affected by starvation. In the lens and thymus widespread punctate fluorescence was observed irrespective of nutrient availability, suggesting that autophagy is constitutively active in certain tissues.

Two forms of LC3 exist which can be distinguished by SDS-PAGE. The post-translational processing of LC3 by ATG4 results in a truncated version of LC3 in which the carboxyl glycine residue is exposed. This form is referred to as LC3-I. Upon induction of autophagy LC3-I becomes covalently attached to the lipid modifier PE via the action of ATG3 and ATG7. The modified form of the protein is termed LC3-II, and can be differentiated from LC3-I by SDS-PAGE. The transition of LC3-I to LC3-II was found to coincide with the differentiation of cultured podocytes (Asanuma *et al.*, 2003), suggesting a possible role in the differentiation process. LC3 was first identified as a subunit of microtubule

associated proteins MAP1A and MAP1B, and recombinant LC3 was shown to co-sediment with taxol-stabilised microtubules or purified tubulin *in vitro* (Mann and Hammarback, 1994).

While GABARAP and GATE-16, when modified by Atg7 and Atg3 and converted into form II, have been shown to localise to LC3 positive autophagosome membranes under starvation conditions in transiently transfected F9 teratocarcinoma cells (Kabeya *et al.*, 2004), a detailed role for these proteins in autophagy has still not been described. The distribution of Atg8 homologues in rats that had been subjected to starvation was analysed by immunoblotting with specific antibodies, and was found to be divergent. LC3 was abundantly expressed in brain, liver and skeletal muscles, with LC3-II found predominantly in pellet fractions and LC3-I found mostly in supernatant fractions. GABARAP was relatively abundant in the spleen and kidney, and GATE-16 was enriched in the brain, skeletal muscles and the heart. Whereas only LC3-II (and not LC3-I) localises to membrane compartments, GABARAP-I and GATE16-I were found to localise to membrane compartments prior to modification to GABARAP-II and GATE16-II form (Tanida *et al.*, 2003). These data have led to suggestions that GABARAP and GATE-16 may play a role in autophagy that is tissue dependent, or that these proteins have tissue-specific functions that are distinct from autophagy.

GATE16 has been shown to promote intra-Golgi trafficking and post-mitotic reassembly of Golgi fragments, and is thought to act as a Golgi-SNARE protector in various physiological membrane fusion events (Elazar *et al.*, 2003; Muller *et al.*, 2002). GATE-16 is a soluble transport factor that modulates intra-Golgi transport through interactions with N-ethylmaleimidine sensitive factor (NSF) and v-SNARE GOC-28, and was shown to localise to the Golgi apparatus and to be predominately membrane bound (Sagiv *et al.*, 2000).

GABARAP interacts with the  $\gamma$ -amino butyric acid receptor (GABA<sub>A</sub>R) and tubulin in nerve cells, suggesting a role in modulating anchoring and clustering of GABA receptors in post-synaptic regions (Wang *et al.*, 1999). However, GABARAP is expressed in many tissues in addition to neuronal tissues, suggesting an additional function. GABARAP has been shown to localise mainly to intracellular punctate structures including the Golgi apparatus and to interact with NSF

(Kittler *et al.*, 2001) suggesting a possible role for GABARAP in intracellular trafficking of GABA<sub>A</sub>P-containing transport vesicles towards the cell membrane along microtubules (Chen and Olsen, 2007).

### 3.1.3 The roles of *Arabidopsis* Atg8 homologues

A family of nine *ATG8* genes termed *AtATG8a* to *8i* have been identified in *Arabidopsis* plants (Doelling *et al.*, 2002). The proteins are between 41 and 99% similar to each other, and share between 33 and 73% identity with yeast and human Atg8 homologues. AtAtg8 proteins can be sub-divided into three families based on sequence similarity, the first consisting of four proteins; Atg8a, c, d and f, the second consists of three proteins; AtAtg8b, e and g, and the third consists of two proteins; AtAtg8h and Atg8i (Slavikova *et al.*, 2005). AtAtg8a and AtAtg8d have been shown to complement yeast  $\Delta atg8$  strains which are defective in autophagy, and to interact with AtAtg4 in a yeast-2-hybrid assay (Ketelaar *et al.*, 2004).

By tagging five AtAtg8 proteins representing each AtAtg8 family with GFP, it was determined that AtAtg8 proteins localise to structures which resemble autophagosomes and that they were processed at their C-termini in a manner similar to yeast Atg8 (Slavikova *et al.*, 2005). Cellular processes involving Atg8 were found to operate both under favourable growth conditions and under starvation stress. Under favourable growth conditions, all five Atg8 homologues were expressed in the roots, with members of different groups showing differential expression patterns in various root regions, suggestive that members of different Atg8 families could possess non-redundant functions, perhaps associated with root differentiation and development. The Atg8 genes were weakly expressed in young shoots under favourable growth conditions, but in response to prolonged darkness or starvation, the expression of AtAtg8a and AtAtg8i was up regulated (Slavikova *et al.*, 2005). As with LC3, AtAtg8a and AtAtg8d were found to co-sediment with microtubules, indicative of an interaction between microtubules and the autophagy pathway (Ketelaar *et al.*, 2004).

## 3.2 Phylogenetic analysis of ATG8-like proteins in *Leishmania*

A search of the *L. major* genome using *S. cerevisiae* ATG8 as a query led to, in addition to the previously characterised *L. major* ATG8 (LmjF19.1630), the tentative identification of 25 genes encoding proteins with some similarity to ATG8 (Williams *et al.*, 2006). Phylogenetic analysis shows that these proteins cluster into three distinct families, which have been named *ATG8A*, *ATG8B* and *ATG8C* (figure 3.2). *Leishmania* ATG8 exists as a single copy gene, and encodes the protein which shows the highest degree of identity to yeast Atg8 (50% sequence identity at the protein level). The other 25 ATG8-like genes cluster into three multigene families designated *ATG8A* (3 copies), *ATG8B* (9 copies) and *ATG8C* (13 copies) (table 3.1, figure 3.1). *ATG8A* and *ATG8B* occur in a tandem array on chromosome 19, while *ATG8C* exists as an array on chromosome 9. Within families, *ATG8A* proteins are 98.8% identical, *ATG8B* are 91.8% identical, and *ATG8C* genes are 87.9% identical (table 3.2). *L. major* ATG8, *ATG8A*, *ATG8B* and *ATG8C* proteins respectively share 50%, 27%, 26% and 21% identity with the *S. cerevisiae* Atg8, and *ATG8A*, *ATG8B* and *ATG8C* are between 22 - 29% identical to *L. major* ATG8 (table 3.2).

No clear homologues for ATG5, ATG12, ATG10 and ATG16 are present in trypanosomatid genomes. In one bioinformatics analysis of autophagy genes in *L. major*, *T. cruzi* and *T. brucei*, genes encoding these proteins were reported to be absent (Herman *et al.*, 2006). An independent study, however, did identify proteins with some similarity to yeast and human ATG5, ATG10, ATG12 and ATG16 (Williams *et al.*, 2006). The identities were low, but some characteristic features of each protein led to the tentative identification of LmjF30.0980 as ATG5, LmjF31.3105 as ATG10, LmjF22.1300 as ATG12 and LmjF33.1410 as ATG16.

LmjF22.1300 is 25% identical to yeast Atg8, and 29% similar to *L. major* ATG8 (table 3.2). It possesses the carboxyl-terminus scissile that is exposed by cleavage with the cysteine peptidase ATG4 and is the site of conjugation to PE, and possesses amino acids C-terminal to the scissile glycine. All this leads to the identification of LmjF22.1300 as an ATG8 protein. However, LmjF22.1300 also possesses a 58 amino acid insertion that is somewhat typical of ATG12 proteins.

Based on sequence analyses alone therefore, LmjF22.1300 could be predicted to be either an ATG8 or an ATG12 (Williams *et al.*, 2006). In a phylogenetic tree, Lmj22.1300 lies between most ATG8 and ATG12 proteins (figure 3.2). Recent functional studies found that the full length open reading frame of LmjF22.1300 was not capable of rescuing yeast autophagy mutants which lacked ATG8 or ATG12 (*atg8Δ* and *atg12Δ* respectively). However, a mutated version of the gene in which the scissile glycine was exposed was capable of rescuing the *atg12Δ* yeast mutant and not the *atg8Δ* mutant, suggesting that LmjF22.1300 encodes an unusual ATG12 protein which requires post translational processing by an as yet unidentified peptidase to be functional (Williams *et al.*, 2009). Therefore, LmjF22.1300 (henceforth referred to as ATG12) was not considered in this study, the focus of which was to investigate the roles of ATG8A, ATG8B and ATG8C.

ATG8A, ATG8B and ATG8C appear to be unique to *Leishmania* species, and were not identified in other trypanosomatids. One ATG8 homologue was identified in *T. cruzi* (*TcATG8.1*) that was found to complement yeast autophagy mutant strains (*Δatg8*) and characterised as an autophagosome marker (Alvarez *et al.*, 2008a). Autophagy was found to be up regulated in *T. cruzi* during differentiation from epimastigote to metacyclic promastigotes. A second ATG8-like gene in *T. cruzi* of which there are two copies (*TcATG8.2A* and *TcATG8.2B*) did not localise to autophagosomes or rescue yeast autophagy mutants (Alvarez *et al.*, 2008a). Two copies of a putative ATG8 gene exist in *T. brucei* (termed *ATG8.1A* and *ATG8.1B*) which are 53% identical to the *L. major* ATG8 gene. Another gene termed *TbATG8.2* is identical to *L. major* ATG12 and *T. cruzi* ATG8.2, and so could potentially encode an ATG12 protein. Representatives of ATG8A, ATG8B and ATG8C are present in other *Leishmania* species. *L. infantum* possesses 1 ATG8A gene (M19\_V3.0840), 3 ATG8B genes (M19\_V3.0820, M19\_V3.0850 and M19\_V3.0860) and 4 ATG8C genes (J09\_V3.0170, J09\_V3.0180, J09\_V3.0190 and J09\_V3.0200), while *L. braziliensis* possesses 1 ATG8A gene (M19\_V2.1140), 2 ATG8B genes (M19\_V2.1170 and M19\_V2.1180) and 2 ATG8C genes (M09\_V2.0170 and M09\_V2.0180). In *L. infantum* and *L. braziliensis*, as in *L. major*, ATG8A and ATG8B are found interspersed on the same chromosome, and ATG8C is found on a separate chromosome.

<i>L. major</i> gene name	Systematic name in GeneDB	Size (bp)	Size (aa)	Identity within groups (%)
ATG8	LmjF19.1630	378	125	
ATG12	LmF22.1300	612	203	
ATG8A.1	LmjF19.0840	411	136	98.8%
ATG8A.2	LmjF19.0844	411	136	
ATG8A.3	LmjF19.0848	411	136	
ATG8B.1	LmjF19.0820	366	121	91.8%
ATG8B.2	LmjF19.0842	366	121	
ATG8B.3	LmjF19.0846	366	121	
ATG8B.4	LmjF19.0850	366	121	
ATG8B.5	LmjF19.0860	378	125	
ATG8B.6	LmjF19.0870	378	125	
ATG8B.7	LmjF19.0880	366	121	
ATG8B.8	LmjF19.0900	378	125	
ATG8B.9	LmjF19.0910	366	121	
ATG8C.1	LmjF09.0150	405	134	87.9%
ATG8C.2	LmjF09.0152	375	124	
ATG8C.3	LmjF09.0154	405	134	
ATG8C.4	LmjF09.0156	375	124	
ATG8C.5	LmjF09.0158	405	134	
ATG8C.6	LmjF09.0160	375	124	
ATG8C.7	LmjF09.0162	405	134	
ATG8C.8	LmjF09.0164	375	124	
ATG8C.9	LmjF09.0166	405	134	
ATG8C.10	LmjF09.0170	405	134	
ATG8C.11	LmjF09.0172	375	124	
ATG8C.12	LmjF09.0174	405	134	
ATG8C.13	LmjF09.0180	369	123	

**Table 3-1 *Leishmania* ATG8 like genes.**

The *Leishmania* gene name and the designated GeneDB identifier are provided for all 25 putative ATG8 paralogues, and a putative ATG12 paralogue. The numbers of base pairs (bp) and amino acids (aa) which make up their DNA and protein sequences were obtained from GeneDB and are provided. The extent of sequence identity within families was determined using the Clustal W algorithm of the Align X program (Vector NTI Advance 10 package, <http://www.informaxinc.com/>).

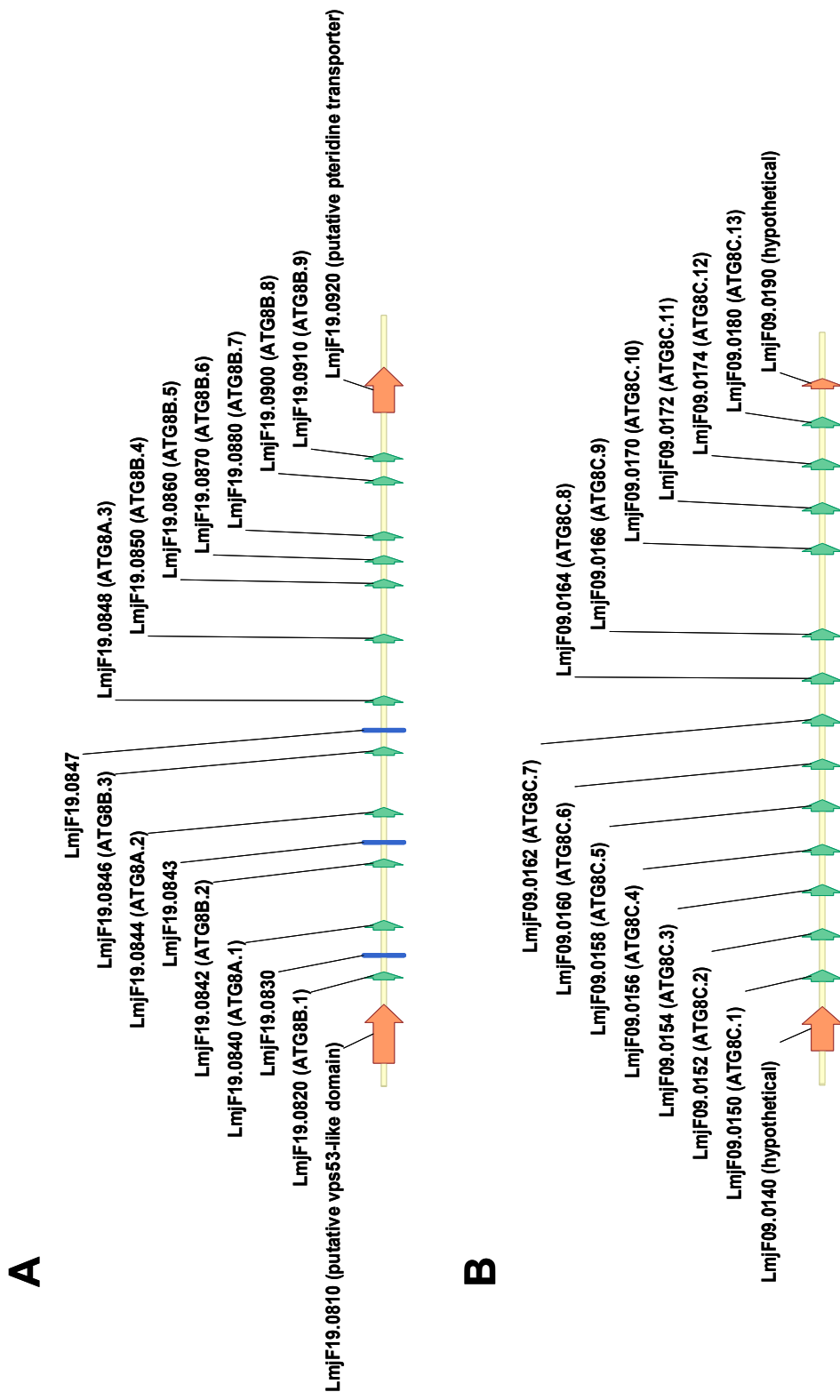


**Figure 3-1 *L. major* Gene Arrays for ATG8A, ATG8B and ATG8C.** A) The distribution of ATG8A and ATG8B genes on chromosome 19. B) The distribution of ATG8C genes on chromosome 9. Genes encoding ATG8A, ATG8B and ATG8C are represented as green arrows. Genes outside the arrays are represented as orange arrows. Genes encoding hypothetical proteins interspersed in the ATG8A/ATG8B array are represented in blue.

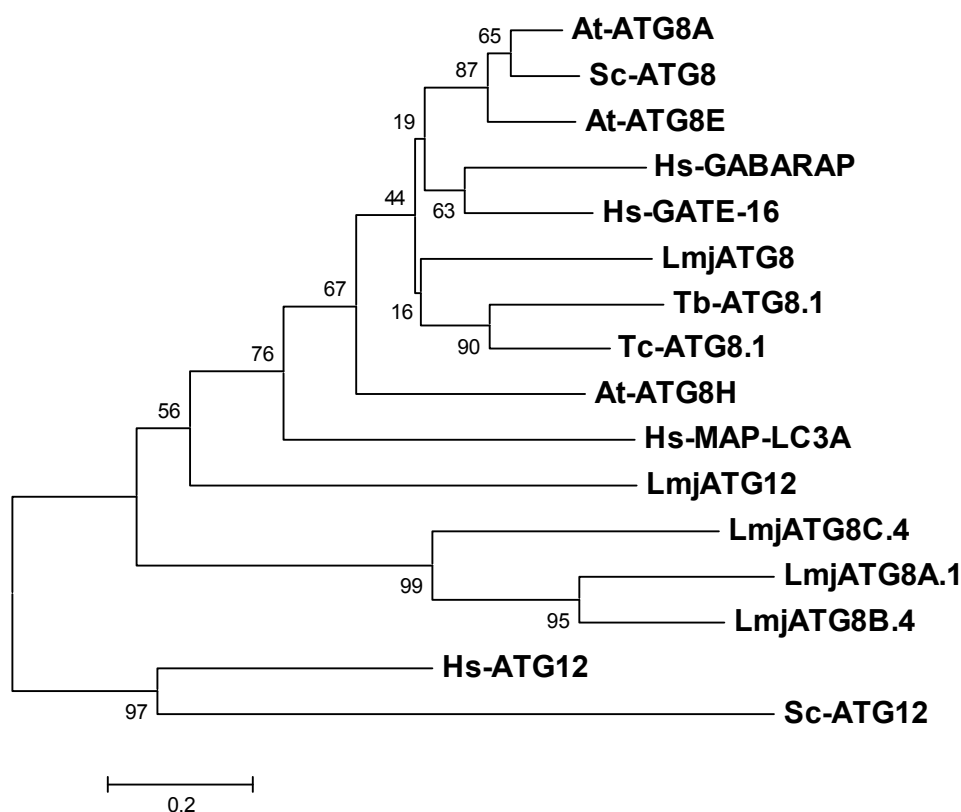


**Figure 3-2 Phylogenetic analysis of ATG8-like proteins from yeast, human and *Leishmania major*.** The relationship between ATG8 proteins from *Leishmania major* (*Lmj*), *Trypanosoma brucei* (*Tb*), *Trypanosoma cruzi*, *Saccharomyces cerevisiae* (*Sc*), *Arabidopsis thaliana* (*At*) and *Homo sapiens* (*Hs*) are shown on this tree. Bootstrap values from 10,000 pseudoreplicates are shown on the nodes. The scale bar represents a distance of 0.1 substitutions per site. The phylogenetic tree was produced using MEGA 3.1 software. The accession numbers and geneDB designations are as follows: ScATG8 (YBL078C), HsGABARAP (NP\_113600), HsGATE-16 (P60521), HsLC3A (NP\_115903), AtATG8A (NP\_567642), AtATG8E (NP\_850431), AtATG8H (NP\_566518) TbATG8A (Tb927.7.5900), TbATG8B (Tb927.7.5910), TcATG8.1 (Tc00.1047053508173.47), LmATG8 (LmjF19.1630), LmATG8A.1 (LmjF19.0840), LmATG8B.4 (LmjF19.0850), LmATG8C.4 (LmjF09.0156). LmjATG12 (LmjF22.1300), Hs-ATG12 (AAH12266), ScAtg12 (P38316)

	GABARAP	GATE 16	LC3	Lmj ATG8	Lmj ATG8A	Lmj ATG8B	Lmj ATG8C	Lmj ATG12
ScATG8	55	56	36	50	27	26	21	25
GABARAP		64	33	48	25	25	23	27
GATE-16			40	50	25	26	26	34
LC3				34	20	18	15	25
LmATG8					29	25	22	29
LmATG8A						57	31	18
LmATG8B							40	22
LmjATG8C								25

**Table 3-2 Percentage sequence identity between yeast, human and *Leishmania* ATG8 proteins.** The extent of sequence similarity between selected ATG8 proteins was determined using the Clustal W algorithm of the Align X program (Vector NTI Advance 10 package, <http://www.informaxinc.com/>). The accession numbers and geneDB designations are as follows: ScATG8 (YBL078C), HsGABARAP (NP\_113600), HsGATE-16 (P60521), HsLC3A (NP\_115903), LmATG8 (LmjF19.1630), LmATG8A.1 (LmjF19.0840), LmATG8B.4 (LmjF19.0850), LmATG8C.4 (LmjF09.0156).



### 3.3.1 ATG8 residues required for interaction with ATG4

Two sites have been identified in Atg8 that are essential for autophagy in yeast due to their interaction with the cysteine peptidase ATG4. Phe<sup>77</sup> and Phe<sup>19</sup> have been shown to be part of the recognition site for ATG4, while Tyr<sup>49</sup> and Leu<sup>50</sup> are important for the post-lipidation step (Amar *et al.*, 2006). The equivalent residues in human LC3, Phe<sup>52</sup> and Leu<sup>53</sup>, and Phe<sup>80</sup> and Leu<sup>82</sup>, were also found to be required for autophagy (Fass *et al.*, 2007). These residues are marked with a (+) symbol in figure 3.3. Each of these residues is conserved in *L. major* ATG8 (Phe<sup>53</sup>, Leu<sup>54</sup>, Phe<sup>81</sup> and Phe<sup>83</sup>), but none are conserved in ATG8A, ATG8B and ATG8C. In ATG8A the residues are substituted with Leu<sup>42</sup>, Ala<sup>43</sup>, Ala<sup>70</sup> and Ala<sup>72</sup>, in ATG8B with Leu<sup>44</sup>, Ala<sup>45</sup>, Thr<sup>72</sup> and Ala<sup>74</sup>, and in ATG8C with Ser<sup>42</sup>, Ala<sup>43</sup>, Ala<sup>71</sup> and Thr<sup>73</sup>. Due to these substitutions, it was unclear whether ATG8A, ATG8B or ATG8C could be functional as ATG8 proteins.

### 3.3.2 ATG8 residues required for the interaction with ATG7

Recently the structure of the ubiquitin like protein NED88 bound to its E1 enzyme the APPBP1-UBA3 complex was reported, and three hydrophobic residues were reported to be essential for binding to the E1 enzyme (Walden *et al.*, 2003). Based on structural alignments, residues Tyr<sup>38</sup>, Leu<sup>82</sup> and Ala<sup>114</sup> in LC3 (Val<sup>36</sup>, Phe<sup>79</sup> and Ser<sup>110</sup> in GATE-16 and Ala<sup>36</sup>, Phe<sup>79</sup> and Ser<sup>110</sup> in GABARAP) were predicted to be required for the binding to the E1 protein ATG7 (Sugawara *et al.*, 2004). These residues are marked with a # symbol on figure 3.3. The first of these residues is a conserved alanine in each of the *L. major* ATG8 proteins (Ala<sup>36</sup> in ATG8A, ATG8B and ATG8C and Ala<sup>40</sup> in ATG8), as is the case for GATE-16. The second (Leu<sup>83</sup> in ATG8) is conserved in all *L. major* ATG8 paralogues. The third residue is a serine in ATG8 (Ser<sup>114</sup>), as in GABARAP and GATE-16, and an alanine in ATG8A (Ala<sup>104</sup>) as in LC3. The equivalent residues in ATG8B and ATG8C are an arginine (Arg<sup>105</sup>) and a threonine (Thr<sup>105</sup>) respectively. Based on these alignments it seems that ATG8 and ATG8A possess all the residues predicted to be required for interaction with ATG7, while ATG8B and ATG8C possess two out of three.

### 3.3.3 ATG8 residues that bind to the ubiquitin core

The crystal structure of LC3 (rat LC3) was reported to contain a five-stranded central  $\beta$ -sheet ( $\beta$ 1-5 as a core) flanked by two pairs of  $\alpha$ -helices ( $\alpha$ 1 and  $\alpha$ 2,

and  $\alpha 3$  and  $\alpha 4$ ). The LC3 structure was largely similar to those of GATE-16 and GABARAP, and the  $\alpha 1$  and  $\alpha 2$  helices in particular are found to be characteristic of LC3 family proteins (Sugawara *et al.*, 2004, Paz *et al.*, 2000, Bavro *et al.*, 2002).  $\alpha 1$  and  $\alpha 2$  are tethered to the ubiquitin core via hydrophilic interactions between certain residues forming hydrogen bonds and salt bridges. Most of the residues involved in such interactions are conserved in the LC3 family proteins, including Lys<sup>8</sup>, Arg<sup>16</sup>, Ile<sup>23</sup>, Pro<sup>32</sup>, Ile<sup>34</sup>, Glu<sup>36</sup>, Leu<sup>53</sup>, Asp<sup>106</sup>, Phe<sup>108</sup> and Tyr<sup>110</sup> (marked with an asterisk \* on figure 3.3), implying that  $\alpha 1$  and  $\alpha 2$  helices are essential for the biological function of LC3 family proteins (Sugawara *et al.*, 2004). Eight out of ten of these residues are conserved in *L. major* ATG8 (Lys<sup>10</sup>, Arg<sup>18</sup>, Ile<sup>36</sup>, Glu<sup>38</sup>, Leu<sup>55</sup>, Asp<sup>108</sup>, Phe<sup>110</sup> and Tyr<sup>112</sup>) with just Ile<sup>23</sup> and Pro<sup>32</sup> being replaced by Val<sup>25</sup> and Leu<sup>35</sup>. Five of the marked residues are conserved in ATG8A and ATG8C, while seven residues are conserved in ATG8C.

Interactions of particular importance in maintaining the ubiquitin folds of LC3 are salt bridges between Lys<sup>8</sup> and Asp<sup>104</sup>, and between Arg<sup>16</sup> and Asp<sup>106</sup>. Interestingly, all of these residues are conserved in ATG8, and the residues involved in the second interaction are conserved in ATG8 paralogues, suggesting that they could maintain an ubiquitin-like structure. Other hydrophobic residues required for the attachment of  $\alpha 2$  to the ubiquitin core are conserved in some but not all of the paralogues; Pro<sup>32</sup> is conserved in ATG8A but not others, Ile<sup>34</sup> and Leu<sup>53</sup> are conserved in ATG8 but not others, Phe<sup>108</sup> is conserved in all but ATG8C, while Tyr<sup>110</sup> is conserved in all but ATG8A.

In summary, *L. major* ATG8 paralogues appear to share many characteristics (at the protein sequence level) with Atg8 and LC3, but also exhibit some potentially important differences. The carboxyl-terminal scissile glycine, the proposed site of hydrolysis by ATG4, is conserved in all of the *L. major* ATG8 paralogues. However, while *L. major* ATG8 possesses all four of the residues found to be important for the interaction with ATG4, these residues are not conserved in ATG8A, ATG8B and ATG8C raising the question as to whether these proteins can be processed by ATG4. Secondly, ATG8 and ATG8A both possess all conserved residues required for an interaction with the E1 enzyme ATG7, while ATG8B and ATG8C only possess two out of three conserved residues, potentially pointing to differences in function. Finally, many of the residues involved in the attachment of  $\alpha 1$  and  $\alpha 2$  to the ubiquitin core are conserved in ATG8, and

partially conserved in ATG8A, ATG8B and ATG8C. 3D structures of *L. major* ATG8 paralogues will be required in order to determine whether these conserved residues are sufficient to maintain the characteristic structure of ubiquitin and LC3 family members.

### **3.4 Localisation of ATG8-like proteins during life cycle progression**

#### **3.4.1 Production of GFP and RFP expressing *L. major***

In order to investigate the possibility that *L. major* ATG8-like proteins associate with autophagosomes in *L. major in vivo*, constructs were produced to express GFP tagged ATG8A, ATG8B and ATG8C in *L. major* promastigotes. Plasmids were produced based on the pNUS vectors which were designed for the optimal expression of fluorescently tagged proteins in *Leishmania spp* and *Crithidia spp* (Tetaud *et al.*, 2002, please see section 2.2.1 for more details). Plasmids containing RFP (dsRED) tagged proteins were also produced for use in co-localisation studies (figure 3.4). An N terminal tag was chosen so as not to interfere with the C-terminal processing required for ATG8 modification.

LmjF19.0840 (ATG8A.1), LmjF19.0850 (ATG8B.4) and LmjF09.0160 (ATG8C.4) were amplified from genomic *L. major* DNA using the primer pairs NT250 / NT251, NT252 / NT266, and NT256 / OL1857, respectively. The PCR products were inserted into the subcloning vector pGEMT-Easy from where they were sequenced and cloned into pGL1135 (pNUS-GFP) and pGL1043 (pNUS-RFP) by restriction digest with the enzymes *Bgl*III and *Kpn*I or *Bgl*III with *Eco*RI (table 3.3).

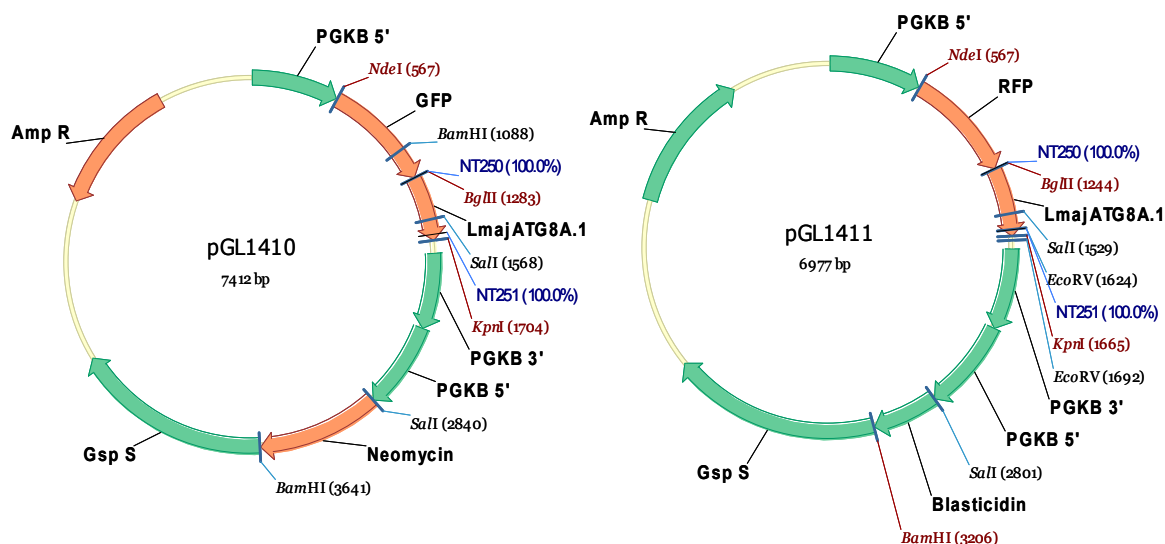


**Figure 3-4 Maps of the plasmids used for the transient expression of GFP-ATG8A and RFP-ATG8A.** Plasmids for the expression of *L. major* ATG8A, ATG8B and ATG8C with an N-terminal GFP or RFP tag were produced by introducing the open reading frame of the gene of interest into the episomal expression vectors pGL1135 or pGL1043, based on the pNUS system (Tetaud *et al.*, 2002). Vector NTI was used to produce vector maps containing information of the restriction enzymes and oligos used during the cloning process. pGL1410 and pGL1411 represent ATG8A tagged to GFP or RFP respectively and are shown as examples.

Plasmid	Gene of interest	Primer pair	Restriction enzymes	Antibiotic resistance marker
pGL1410	GFP-ATG8A	NT250/NT251	<i>Bgl</i> III / <i>Kpn</i> I	Neomycin (G418)
pGL1411	RFP-ATG8A	NT250/NT251	<i>Bgl</i> III / <i>Kpn</i> I	Blasticidin
pGL1412	GFP-ATG8B	NT252/NT266	<i>Bgl</i> III / <i>Eco</i> RV	Neomycin (G418)
pGL1413	RFP-ATG8B	NT252/NT266	<i>Bgl</i> III / <i>Eco</i> RV	Blasticidin
pGL1414	GFP-ATG8C	NT256/OL1857	<i>Bgl</i> III / <i>Eco</i> RV	Neomycin (G418)
pGL1415	RFP-ATG8C	NT256/OL1857	<i>Bgl</i> III / <i>Eco</i> RV	Blasticidin

**Table 3-3 Plasmids used for the expression of GFP and RFP tagged ATG8 like proteins in Leishmania.** A description of the expression plasmids used in this study is provided, including the name of the plasmid (pGL number), antibiotic resistance marker, and the primer pairs and restriction enzymes used for cloning.

GFP tagged ATG8A, ATG8B and ATG8C were expressed in *L. major* promastigotes (designated WT[pN-ATG8A], WT[pN-ATG8B], WT[pN-ATG8C]) and their localisation was analysed by fluorescence microscopy. Promastigotes expressing GFP-ATG8 (WT[pN-ATG8]) have previously been characterised and were used as a control (Besteiro *et al.*, 2006b).

### 3.4.2 Promastigote stages

The localisation of GFP-ATG8A, GFP-ATG8B and GFP-ATG8C was analysed in parasites that were maintained in serum rich medium and monitored over a nine day growth cycle. A previous analysis of GFP-ATG8 revealed that the number of promastigotes in which GFP-ATG8 localised to autophagosome membranes peaked during the differentiation of parasites from procyclic to metacyclic promastigote forms (Besteiro *et al.*, 2006b).

Most early log phase promastigotes of WT[pN-ATG8A], WT[pN-ATG8B] and WT[pN-ATG8C] in nutrient-rich medium had the GFP-tagged proteins evenly distributed throughout the cytoplasm, similar to the diffuse pattern described previously for GFP-ATG8 transgenic cell lines at logarithmic phase of growth (Besteiro *et al.*, 2006b). GFP-ATG8A was nearly always localised in the cytoplasm under nutrient rich conditions (figure 3.5A), with punctate structures only being observed in a small proportion of cells (0-6%), most of which were rounded in shape and appeared to be dying. GFP-ATG8B and GFP-ATG8C localised to a single punctate structure in 2-10% of healthy cells under nutrient rich conditions. Interestingly, the single punctum in WT[pN-ATG8B] and WT[pN-ATG8C] was always located close to the flagellar pocket (Figure 3.5), the only site of endocytosis and exocytosis in the cell. In contrast to the pattern described previously for GFP-ATG8, no peak in the occurrence of punctate structures was observed for GFP-ATG8A, GFP-ATG8B or GFP-ATG8C during metacyclogenesis, and the proportion of cells containing puncta remained consistently low during growth in nutrient rich medium (figure 3.6). These data suggest that the recruitment of ATG8A, ATG8B and ATG8C to autophagosome-like structures is not associated with metacyclogenesis, indicating distinct roles from ATG8 (Besteiro *et al.*, 2006b; Williams *et al.*, 2009).

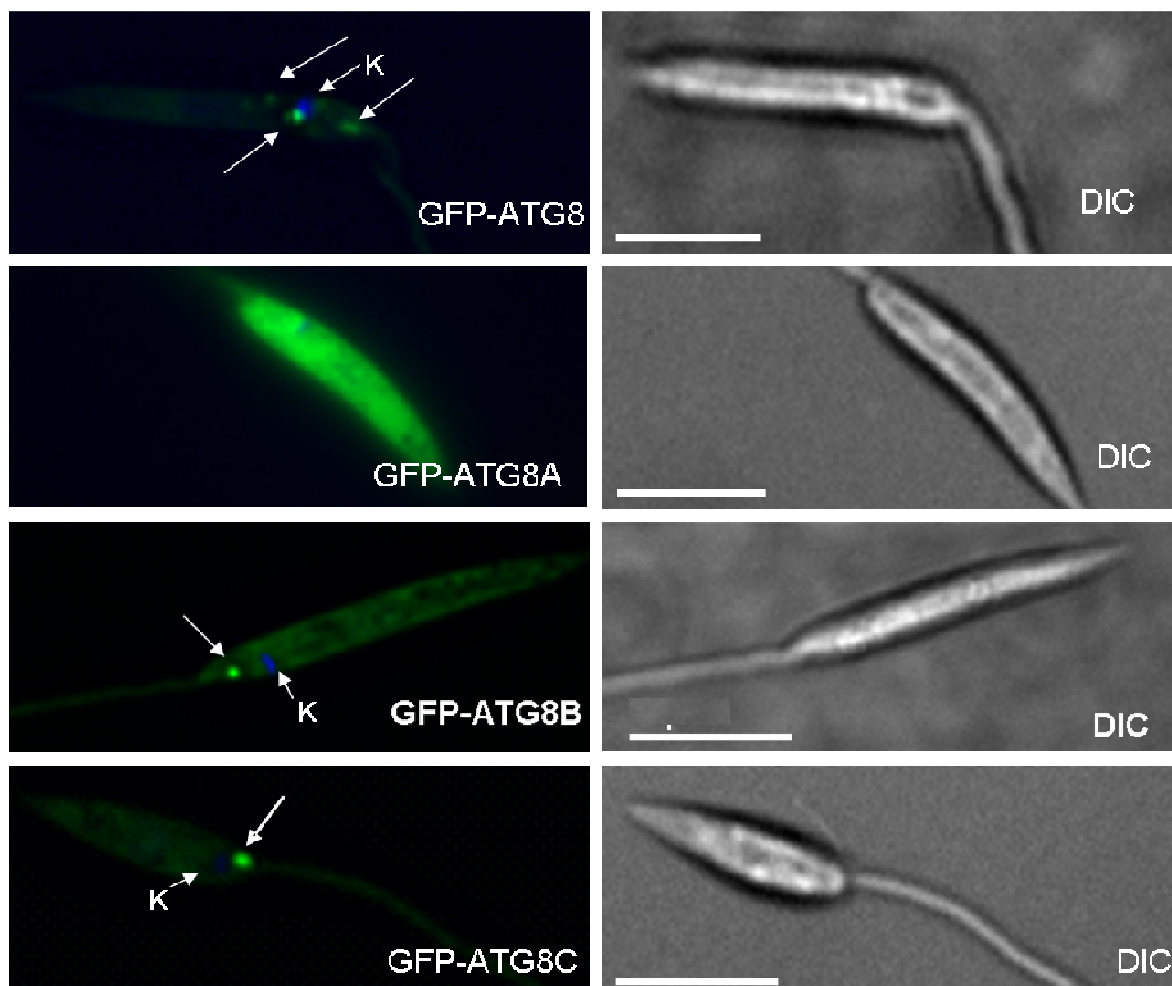


**Figure 3-5 Localisation of GFP tagged ATG8 homologues in *L. major* promastigotes grown in nutrient rich media.**

Live promastigotes expressing GFP tagged ATG8, ATG8A, ATG8B and ATG8C which were grown in nutrient rich media were analysed by fluorescence microscopy. Cells were incubated with DAPI at  $1\mu\text{g ml}^{-1}$  for one minute to stain the nucleus and kinetoplast, washed twice in PBS and then resuspended in ice-cold PBS, settled onto glass slides and viewed using an Applied Precision DeltaVision microscope. The kinetoplast is labelled with K for orientation, and GFP labelled puncta are labelled with arrows. Scale bar is  $5\mu\text{m}$ .

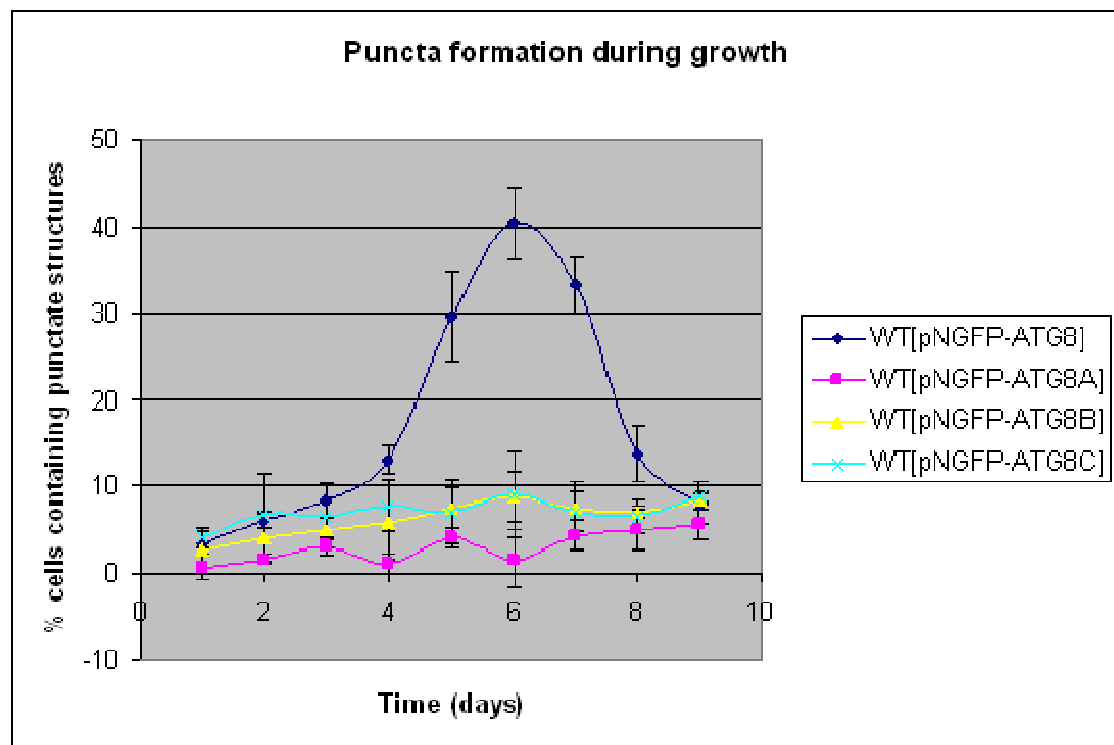


**Figure 3-6 Distribution of GFP-ATG8, GFP-ATG8A, GFP-ATG8B and GFP-ATG8C during growth in nutrient rich media**

Promastigotes were maintained in nutrient rich media and the localisation of the GFP tagged ATG8 proteins was monitored on a daily basis by fluorescence microscopy. The percentage of cells containing punctate structures was determined by counting 200 cells for each time point. Data shown are the averages of three experiments and error bars represent standard deviation from the mean.

### 3.4.3 Intracellular amastigote stages

*Leishmania* ATG8 has also been shown to be associated with parasite differentiation from promastigote to amastigote stages, and all *L. mexicana* cells undergoing *in vitro* differentiation into axenic amastigotes were found to contain multiple autophagosomes (Williams *et al.*, 2006). The formation of autophagosomes in *L. mexicana* undergoing differentiation within macrophages *in vitro* was also assessed, and the number of intracellular parasites containing GFP labelled autophagosomes was found to peak at around 18 hours post infection (Williams *et al.*, 2006). *L. major* ATG8A, ATG8B and ATG8C do not appear to be involved in the differentiation of procyclic promastigotes into metacyclic promastigotes *in vitro*, so a potential involvement in the differentiation from promastigotes into amastigotes was investigated.

Peritoneal macrophages from ICR mice were adhered overnight in RPMI (Sigma) medium at 37°C in 5% CO<sub>2</sub> / 95% air onto 12 well plates, and then infected using late stationary phase promastigotes at a ratio of 10 to 1 for three hours. Non

phagocytosed parasites were then removed by gentle washing with RPMI, the cells incubated in the same conditions until required. Infected macrophages were analysed by fluorescence microscopy at 0, 12, 24 and 72 hours post infection.

In the majority of cells, GFP-ATG8A, GFP-ATG8B and GFP-ATG8C were distributed in the cytoplasm of differentiating parasites. However, at 24 hours post infection a small proportion of WT[pN-ATG8A] (1.2%) and WT[pN-ATG8C] (8%) cells contained GFP labelled punctate structures (figure 3.7). GFP-ATG8B was never observed in punctate structures. These data suggest that ATG8B is not recruited to autophagosome membranes during differentiation from metacyclic promastigotes to amastigotes. The fact that the association of ATG8A and ATG8C with single punctate structures in differentiating cells was relatively rare and that no peak in puncta formation was associated with the onset of differentiation suggests that, unlike ATG8, ATG8A and ATG8C are unlikely to play a significant role in differentiation associated autophagy.

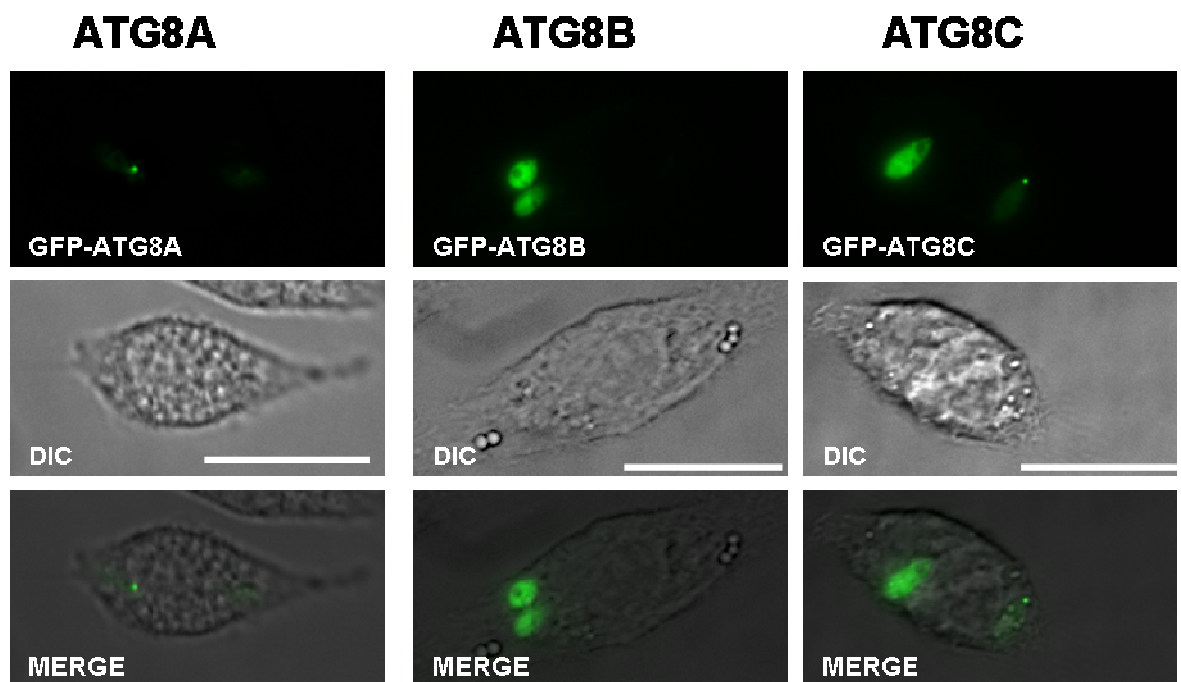


**Figure 3-7 Localisation of GFP-ATG8A, ATG8B and ATG8C in differentiating parasites within macrophages, 24 hours post infection.**

Live macrophages were adhered to 13 mm coverslides within 12 well plates and infected with stationary phase WT[pN-ATGA], WT[pN-ATG8B] or WT[pN-ATG8C]. At the desired time points, coverslides with adhered macrophages were washed twice in PBS and settled onto glass slides and viewed using an Applied Precision DeltaVision microscope. GFP-ATG8B was always expressed in the cytoplasm (panel A). A small percentage of differentiating WT[pN-ATG8A] cells (1.2%) and WT[pN-ATG8C] (8%) contained punctate structures at 24 hours post infection. Scale bar is 15  $\mu$ m.

### 3.5 Localisation of ATG8-like molecules during the starvation response

Autophagy has been shown to be induced by starvation in several organisms, including *Leishmania* (Besteiro *et al.*, 2006b, Williams *et al.*, 2006), so the hypothesis that *Leishmania* ATG8 homologues could play a particular role in starvation induced autophagy was investigated. WT[pN-ATG8], WT[pN-ATG8A], WT[pN-ATG8B] and WT[pN-ATG8C] promastigotes were incubated in nutrient-deprived medium (PBS) for four hours, and the number of cells containing punctate structures was recorded (figure 3.8). After four hours in such conditions, the parasites had reduced motility and appeared sluggish, although were clearly still alive and were normal in shape and appearance. The proportion of WT[pN-ATG8] promastigotes containing punctate structures increased from 15% to 39% after starvation (average of three experiments), supporting previously published data (Besteiro *et al.*, 2006b) and providing a useful control for these experiments. Starvation of WT[pN-ATG8A] promastigotes resulted in the re-localisation of most of GFP-ATG8A into punctate structures (79-93% promastigotes contained punctate structures after four hours). In contrast, there was no significant increase in the occurrence of puncta in WT[pN-ATG8B] and WT[pN-ATG8C] upon starvation (figure 3.8). These data suggest that ATG8A, like ATG8, is associated with starvation-induced autophagosomes, but that ATG8B and ATG8C are associated with other structures in the cell.

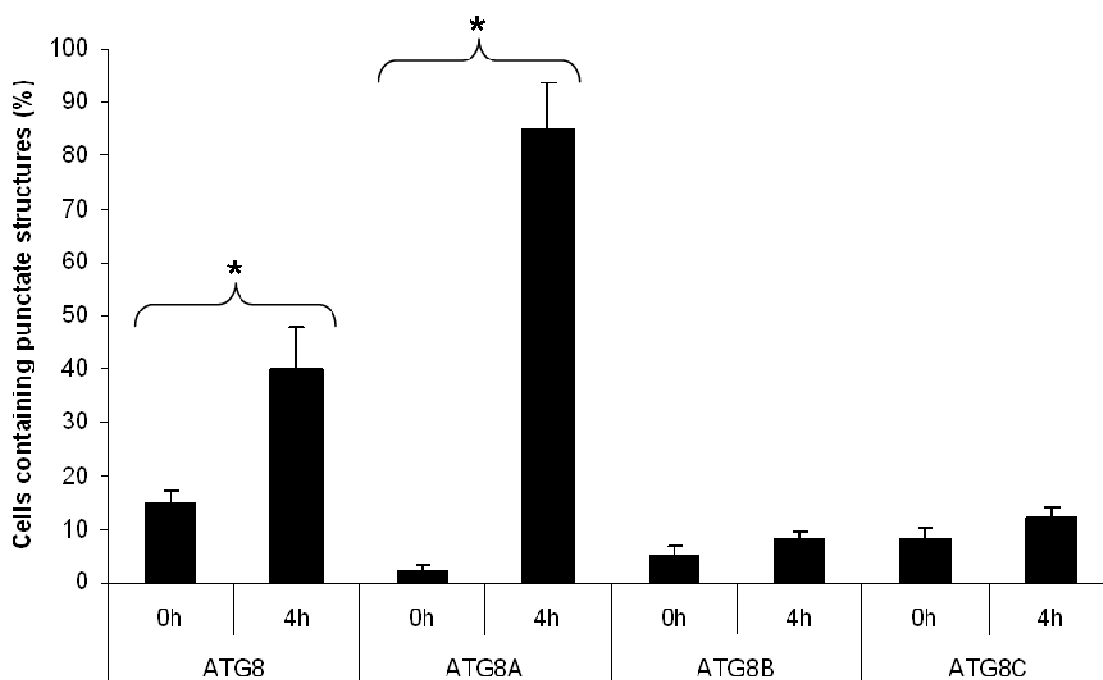


**Figure 3-8 The effect of nutrient deprivation on the localisation of GFP-ATG8, GFP-ATG8A, GFP-ATG8B and GFP-ATG8C.**

WT[pN-ATG8], WT[pN-ATG8A], WT[pN-ATG8B], and WT[pN-ATG8C] promastigotes in logarithmic growth phase were washed twice in pre-warmed PBS and resuspended at a concentration of  $1 \times 10^8$  cells  $\text{ml}^{-1}$  in pre-warmed PBS. Live cells were viewed with an Applied Precision DeltaVision microscope before and after starvation, and the proportion of GFP labelled punctate structures was recorded. Values shown are the mean  $\pm$  S.D from three independent experiments. An asterisk (\*) indicates where data after starvation differed significantly from those for cells maintained in nutrient rich medium ( $p < 0.1$ ).

### **3.5.1 GFP-ATG8A is redistributed to multiple punctate structures in a time dependent manner**

The starvation of promastigotes resulted in the redistribution of GFP-ATG8 to one, two or three punctate structures in approximately 40% of cells. The average number of puncta per cell after starvation was 2.2 in *L. major* (figure 3.9B) and 1.8 in *L. mexicana* (Williams *et al.*, 2006). Interestingly, starvation resulted in the dramatic redistribution of GFP-ATG8A to multiple punctate structures (between 4 and 9) in the majority of starved cells, with the average number of puncta per cell after four hours of starvation being 6.8 (figure 3.9B and 3.10C).

A closer look at the formation of GFP-ATG8A punctate structures during starvation revealed that the process is time dependent. After four hours incubation at a high density in nutrient deprived medium, the majority of cells (79-93%) contained five or more punctate structures (figure 3.9 A, B and 3.10C). After a shorter incubation in PBS (two hours), far fewer cells contained punctate structures (19-30%), and of those most contained between one and three puncta (figure 3.9 A, B and 3.10B). The redistribution of GFP-ATG8 to autophagosomes appears to occur at a steady rate, with a gradual increase both in the proportion of cells containing punctate structures and the average number of puncta per cell occurring (figure 3.9A and B). The time dependent nature of the response of ATG8A to starvation might suggest that ATG8 and ATG8A have distinct roles in the cell, with ATG8A being most significantly involved in surviving extreme starvation.

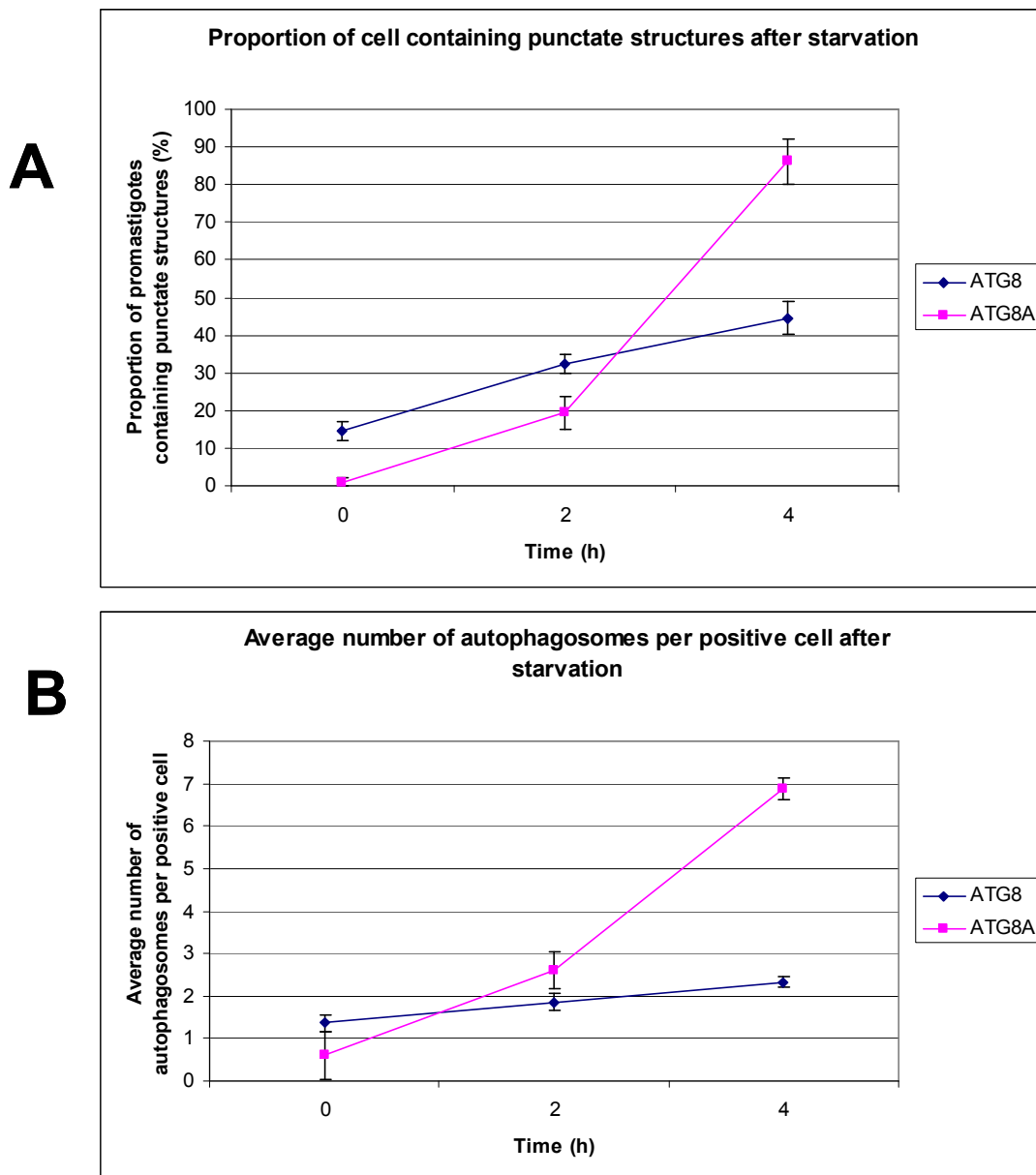


**Figure 3-9 Starvation response of ATG8A.** Mid-log phase cells expressing GFP-ATG8 or GFP-ATG8A were washed twice in PBS and resuspended in pre-warmed PBS at a density of  $1 \times 10^8$  cells  $\text{ml}^{-1}$ . Cells were prepared for microscopy after two and four hours, viewed using an Applied Precision DeltaVision microscope, and the number of autophagosome like structures per cell were counted at each time point. A) The percentage of WT[pN-ATG8] and WT[pN-ATG8A] promastigotes containing punctate structures after two and four hours starvation B) Average number of autophagosomes per cell after starvation. Values shown are the mean  $\pm$  S.D from three independent experiments

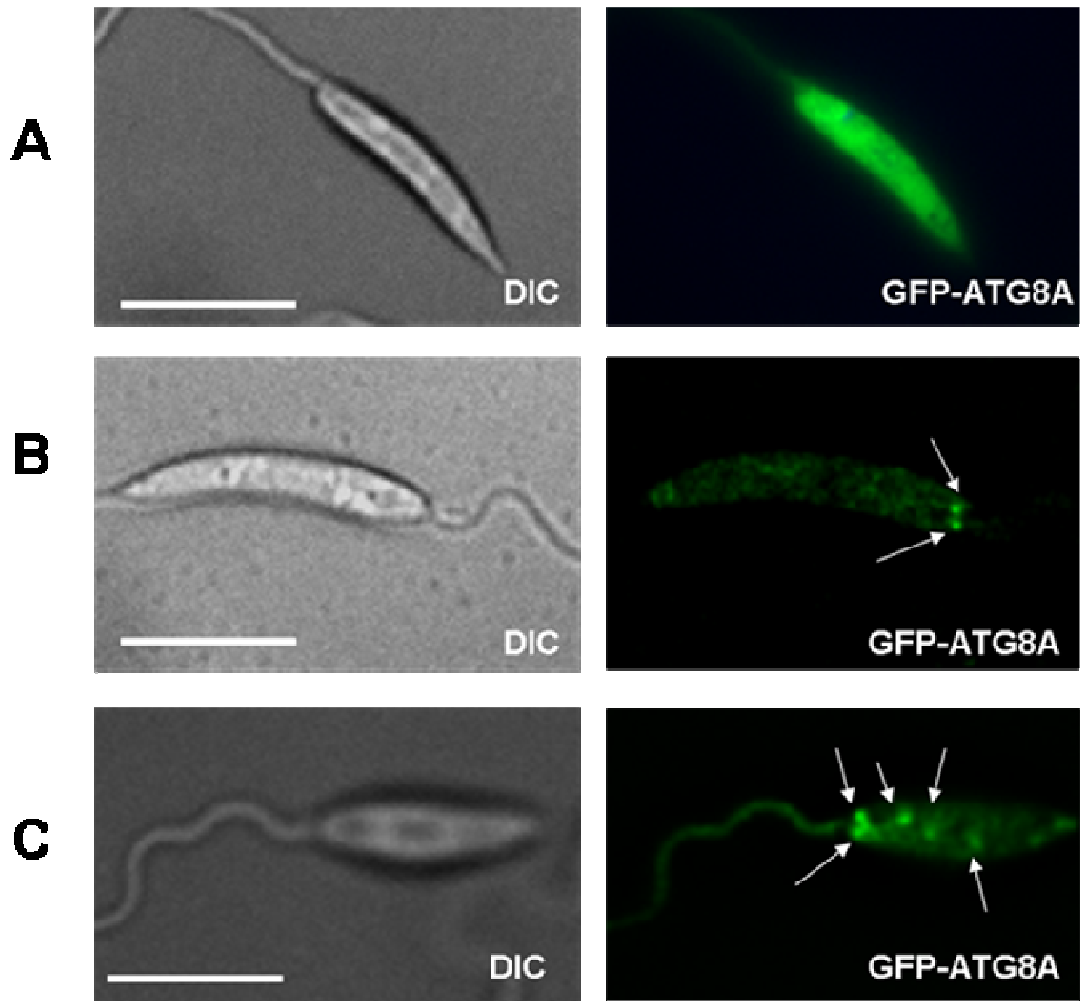


**Figure 3-10 Starvation response of ATG8A**

Mid-log phase cells expressing GFP-ATG8A were washed twice in PBS and resuspended in pre-warmed PBS at a density of  $1 \times 10^8$  cells  $\text{ml}^{-1}$ . Cells were prepared for microscopy after two and four hours, and images obtained using an Applied Precision DeltaVision microscope with SoftWorx deconvolution software. A) Typical localisation of WT[pN-ATG8A] grown in nutrient rich media, B) after two hours starvation, and C) after four hours starvation.

### 3.5.2 Partial colocalisation of ATG8A and ATG8 during starvation

GFP-ATG8 has previously been validated as a marker of autophagosomes (Williams *et al.*, 2006), and so cells were transfected with RFP-ATG8 together with GFP-ATG8A to investigate potential co-localisation. When these cells were starved, GFP-ATG8A and RFP-ATG8 were found to co-localise at some punctate structures in many, but not all, cells (figure 3.11). Co-localisation of RFP-ATG8 with GFP-ATG8A was never observed to occur on all punctate structures within a cell, with GFP-ATG8A labelling far greater numbers of puncta than RFP-ATG8. However, where co-localisation did occur on a particular punctate structure the overlap was almost complete. For example in the figure shown, Pearson's

correlation coefficient was calculated for the selected punctate structure using SoftWorx software, and found to be 0.94, indicating almost complete co-localisation (figure 3.11).

It was previously shown that the punctate structures labelled by GFP-ATG8 in *Leishmania* are likely to be autophagosomes based on electron microscopy analysis of wild type cells, and the fact that the recruitment of ATG8 to such structures was inhibited by known inhibitors of autophagy (Williams *et al.*, 2006). The recruitment of *L. major* ATG8A to puncta which are also labelled by ATG8 provided some evidence that at least some of the structures labelled by *L. major* ATG8A were likely to be autophagosomes. The localisation of GFP-ATG8A on some puncta that are not labelled with RFP-ATG8, and the fact that GFP-ATG8A labels more puncta per cell after starvation than GFP-ATG8 or RFP-ATG8 suggest that, in addition to a recruitment to autophagosome membranes, ATG8A may be recruited to a distinct subset of autophagosomes or perhaps to a different type of vesicle.

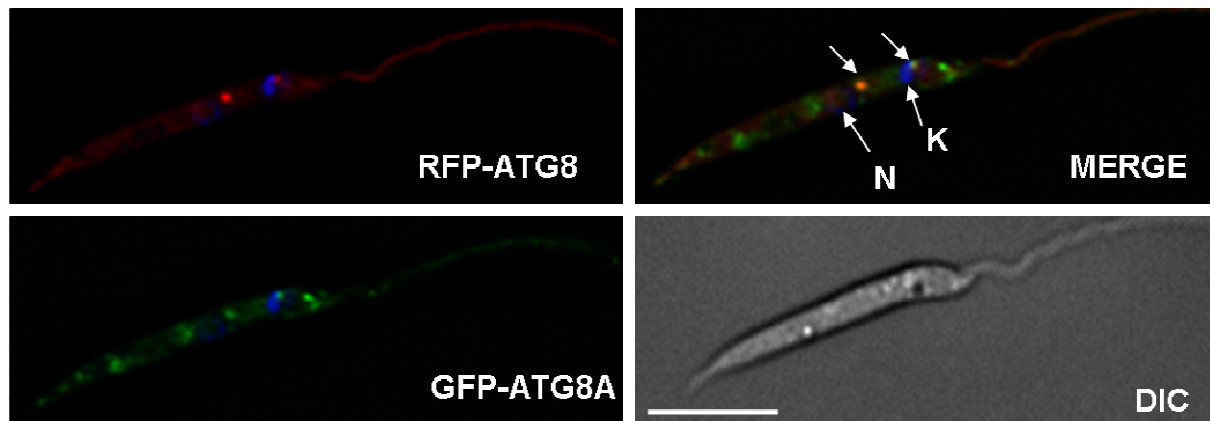


**Figure 3-11 Partial colocalisation of GFP-ATG8A with RFP-ATG8.**

Cells which co-expressed RFP-ATG8 with GFP-ATG8A were washed twice and resuspended in pre-warmed PBS at a concentration of  $1 \times 10^8$  cells  $\text{ml}^{-1}$ . After four hours, cells were incubated with DAPI at  $1 \mu\text{g ml}^{-1}$  for one minute to stain the nucleus and kinetoplast, washed twice in PBS and then resuspended in ice-cold PBS, settled onto glass slides and viewed using an Applied Precision DeltaVision microscope. Arrows indicate the site of co-localisation, and the kinetoplast (K) and nucleus (N) for orientation. Pearson's correlation coefficient was calculated at 0.94 using SoftWorx software, demonstrating almost complete colocalisation. Scale bar is  $5 \mu\text{m}$ .

### **3.5.3 *L. major* ATG8A puncta formation is inhibited by the addition of an energy source, but is insensitive to autophagic inhibitors**

To investigate the nature of the involvement of ATG8A in the response to starvation, starvation experiments were carried out in the presence of either proline, glucose, or the PI3 kinase inhibitor wortmannin. In yeast and mammalian cells, 10 nM wortmannin is sufficient to inhibit autophagy (Munafò and Colombo, 2001, Blommaert *et al.*, 1997), and the recruitment of ATG8 to autophagosomes in both *L. major* and *L. mexicana* was inhibited by wortmannin at concentrations of 10  $\mu$ M (Williams *et al.*, 2006, Besteiro *et al.*, 2006b). The reduced sensitivity of *Leishmania* promastigotes to wortmannin compared to other cells could point either to an alternative pathway for the induction of autophagy *Leishmania* (perhaps not involving PI3K signalling), or a reduced sensitivity of *Leishmania* PI3Ks to wortmannin. Incubation of promastigotes in 10  $\mu$ M wortmannin for twenty four hours prior to and during starvation did not inhibit the response of ATG8A to starvation (figure 3.12), possibly pointing to the occurrence of a survival starvation mechanism that is distinct from autophagy. While the relocalisation of GFP-ATG8A to multiple punctate structures during starvation appeared to be identical either in the presence or absence of wortmannin, a detailed count of the absolute numbers of puncta per cell was not performed in this case, and might be useful in identifying the proportion of GFP-ATG8A labelled puncta that are also labelled with GFP-ATG8 (and therefore likely to be conventional autophagosomes).

The redistribution of GFP-ATG8A during starvation was inhibited when promastigotes were resuspended in PBS supplemented with either glucose (10 mM) or proline (5 mM) (figure 3.12), suggesting that the response of ATG8A is due to nutrient limitation.

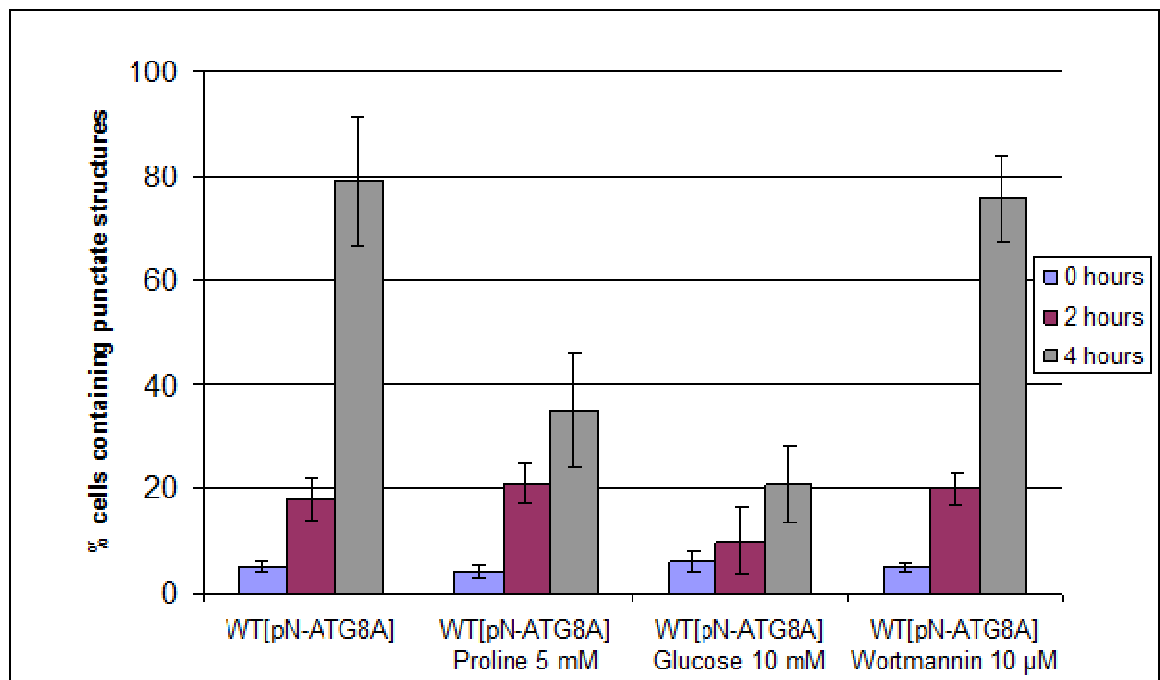


**Figure 3-12 The response of GFP-ATG8A to starvation in the presence of glucose, proline and wortmannin.**

Promastigotes were washed twice and resuspended in pre-warmed PBS at a concentration of  $1 \times 10^8$  cells  $\text{ml}^{-1}$  alone or in the presence of proline (5 mM), glucose (10 mM) or the PI3K inhibitor wortmannin (10  $\mu\text{M}$ ) for four hours. Cells were prepared for microscopy, viewed with an Applied Precision DeltaVision microscope, and the percentage of cells containing punctate structures was recorded. Values shown are the mean  $\pm$  S.D from three independent experiments.

### 3.5.4 ATG8A is not associated with turnover of glycosomes during starvation

In trypanosomatids, the process of glycolysis occurs within organelles similar to yeast peroxisomes, termed glycosomes due to the abundance of glycolytic enzymes contained within (Michels *et al.*, 2006). The turnover of glycosomes by autophagy (pexophagy) has been implicated in trypanosome differentiation and in response to starvation, although the process involved resembled micropexophagy as opposed to macropexophagy (Herman *et al.*, 2008). During adaptation from a methanol medium to one containing glucose or ethanol, the yeasts *Pichia pastoris* and *Hansenula polymorpha* both specifically sequester superfluous peroxisomes via the selective processes of pexophagy that is distinct

from non-selective autophagy induced by nitrogen starvation (Bellu *et al.*, 2001; Kiel *et al.*, 2003; Sakai *et al.*, 1998; Tuttle and Dunn, 1995; Tuttle *et al.*, 1993).

The distribution of ATG8A in multiple punctate structures resembled that of glycosomes in *Leishmania* (Zheng *et al.*, 2004), so in order to investigate a potential role for ATG8A in the selective turnover of glycosomes in response to a shift in nutrient availability, GFP-ATG8A expressing cells were co-transfected with a plasmid encoding RFP-SQL. SQL is an amino acid sequence sufficient to target proteins to the glycosomes in *Leishmania* (Plewes *et al.*, 2003; Sommer *et al.*, 1993). Within one cell, the population of or peroxisomes is heterogeneous, with only some being capable of importing proteins. This is because peroxisome receptor proteins (e.g. Pex5p and Pex7p) have a dual subcellular localisation *in vivo* that cycles between cytosolic and peroxisomal (Dodt and Gould, 1996., Grou *et al.*, 2009). Therefore it was important that RFP-SQL was expressed constitutively rather than transiently, to allow the labelling of all glycosomes in the population.

While the expression patterns of GFP-ATG8A was similar to that of glycosomes, co-localisation between ATG8A and the labelled glycosomes was never observed (figure 3.13), suggesting that ATG8A is not involved in the turnover of glycosomes during starvation. Interestingly, in an *L. mexicana*  $\Delta cpa/cpb$  null mutant, in which autophagosomes accumulate (Williams *et al.*, 2006), GFP-ATG8 occasionally co-localises with RFP-SQL (Dr R Williams, unpublished data), suggesting that glycosomes might be selectively degraded by autophagy during differentiation, as has been suggested for *T. brucei* (Herman *et al.*, 2008).

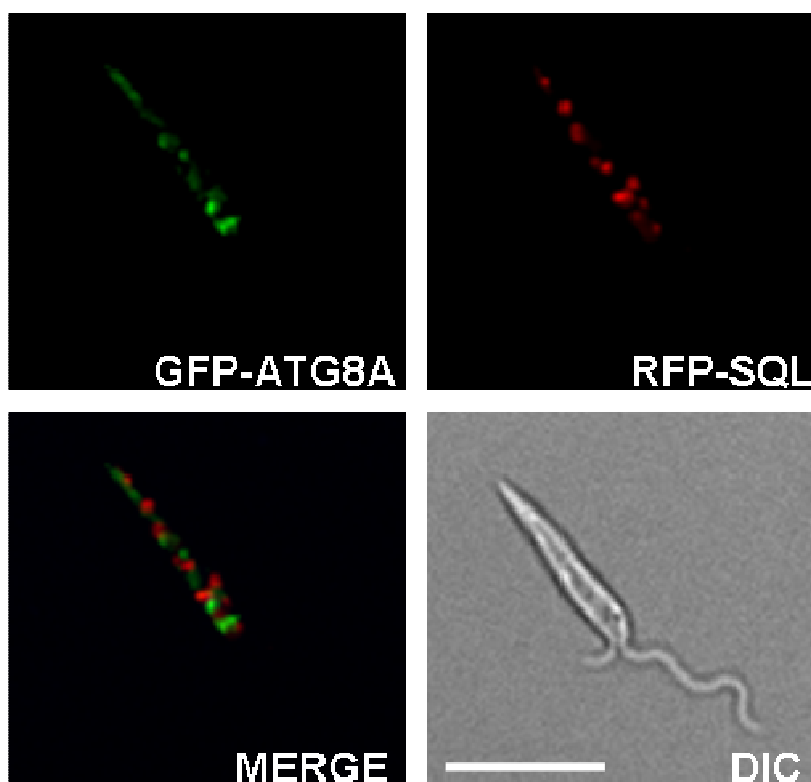


**Figure 3-13 GFP-ATG8A does not co-localise with glycosomes**

Cells which co-expressed RFP-SQL with GFP-ATG8A were washed twice and resuspended in pre-warmed PBS at a concentration of  $1 \times 10^8$  cells  $\text{ml}^{-1}$ . After four hours, cells were washed and resuspended in ice-cold PBS, settled onto glass slides and viewed using an Applied Precision DeltaVision microscope. GFP-ATG8A was not observed to co-localise with RFP-SQL. Scale bar is  $5\mu\text{m}$ .

### 3.6 Localisation of ATG8B and ATG8C

*Leishmania* are apically polarized cells, with all endocytosis and exocytosis occurring at the anterior end of the parasite via the flagellar pocket. This is an invagination of the plasma membrane where the flagellum enters the cell body, and known to be the sole site of endocytosis and exocytosis in kinetoplastids (McConville *et al.*, 2002b; Morgan *et al.*, 2002). All membrane bound compartments and organelles which are associated with endocytosis and membrane turnover are concentrated in the region between the nucleus and flagellar pocket (Field *et al.*, 1998), which contains a complex network of tubules, vesicles, a stacked Golgi complex and other membranous structures close to the flagellar pocket (Duszenko *et al.*, 1988). Even within this region, secretory organelles are highly organised, with the nucleus, ER exit sites, the Golgi apparatus and the flagellar pocket lying in a conserved order along an axis (Morgan *et al.*, 2002). The consistent localisation of both ATG8B and ATG8C

near the flagellar pocket raised the possibility that these proteins were associated with the process of endocytosis or exocytosis, processes relatively understudied in *Leishmania*.

The 2-10% of cells with punctate ATG8B and ATG8C could indicate that the involvement of these proteins with vesicle-associated cell processes is transient, perhaps associated with a particular stage of the cell cycle. Alternatively, the over-expression of GFP tagged proteins could be masking the true localisation of the protein with strong cytosolic expression of the fluorescent protein. In addition to this, only one of the nine or thirteen family members of the ATG8B or ATG8C families respectively was expressed as a GFP fusion protein. Therefore, it is possible that other ATG8B or ATG8C family members are localised to vesicular structures in the other 90-98% of cells in the population, and that competition with untagged isoforms is preventing the GFP tagged proteins from localising to punctate structures.

### **3.6.1 Co-localisation of ATG8B with other ATG8-like molecules**

ATG8B and ATG8C were never seen to co-localise with ATG8 suggesting that they are unlikely to localise to autophagosomes. The localisation of GFP-ATG8B is very similar to that of GFP-ATG8C, indicating that they may co-localise to the same organelle or vesicle (figures 3.5). Co-transfection of GFP-ATG8C with RFP-ATG8B resulted in an overlap of the two signals near the flagellar pocket in all cells that contained GFP-ATG8C labelled puncta (figure 3.14). In most cells transfected with RFP-ATG8B, the red fluorescent protein, in addition to labelling a punctum near the flagellar pocket, accumulated in a long tubular structure, presumably the lysosome, possibly due to misfolding of the protein (figure 3.14).

RFP (or dsRED) has been reported to be inferior to GFP as an *in vivo* marker, as it is slow to mature, tends to form oligomers, and its fluorescence *in vivo* is low compared to GFP (Baird *et al.*, 2000). However, RFP has proved to be useful in this study, for example in the tagging of ATG8 (figure 3.11) and the labelling of glycosomes (figure 3.13). The apparent accumulation of RFP-ATG8B in the lysosomal system of *Leishmania* could be due to the slow maturation of the RFP protein causing disruption of normal endosome function. An alternative to RFP is mCherry of the mFruits series, which are derived from monomeric red

fluorescent proteins (mRFP) and are reported to have improved brightness and photostability (Shu *et al.*, 2006). The localisation of mCherry-ATG8B should be analysed, to see if the mislocalisation problems are solved, and if these constructs could be useful for co-localisation studies.

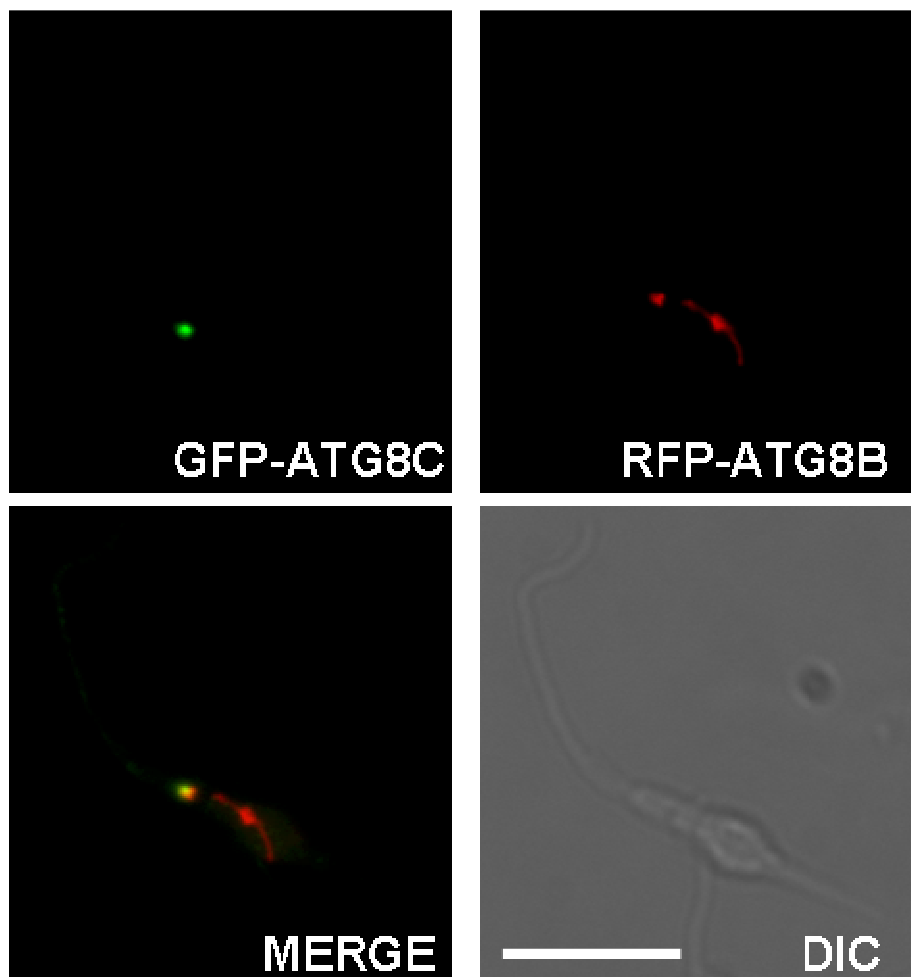


**Figure 3-14 RFP-ATG8B and GFP-ATG8C localisation over-laps near the flagellar pocket.** Cells which co-expressed RFP-ATG8B with GFP-ATG8C were washed and resuspended in ice-cold PBS, and viewed using an Applied Precision DeltaVision microscope. A yellow signal indicates co-localisation. Scale bar is 10  $\mu$ M.

### 3.6.2 Co-localisation of GFP-ATG8B with the endocytic tracer FM4-64

The localisation of ATG8B near the flagellar pocket prompted an investigation into the possible co-localisation of ATG8B with markers of the flagellar pocket or the endosomal system using FM4-64, a dye which is used as a nonselective marker of the endocytic pathway in yeast (Vida and Emr, 1995). In *Leishmania*, this dye is known to be incorporated in a time dependent manner into the flagellar pocket, early endosomes and finally the MVT (Mullin *et al.*, 2001, Besteiro *et al.*, 2006b). Incubation of promastigotes with the dye for fifteen minutes at 4°C resulted in labelling of the flagellar pocket, and while ATG8B consistently resides close to the flagellar pocket, it was never seen to over-lap (figure 3.15A). However, in some cells a second GFP-ATG8B labelled structure was occasionally observed between the nucleus and kinetoplast (figure 3.15B), and this did co-localise with FM4-64 upon incubation for 15 minutes at 4°C and chased for a further 15 minutes at 25°C. This data suggests that some ATG8B could be associated with the early endosomal system of *Leishmania*, or that ATG8B labels vesicles that are derived from endosomal membranes. Some examples of duplication of the ATG8B labelled signal were observed in cells undergoing division, suggesting that ATG8B might be associated with an organelle that is replicated and divided during cell division (figure 3.15B; the most anterior vesicle is undergoing duplication in a cell in which a second flagellum is emerging). However, very few examples were seen in which GFP-ATG8B labelled a structure in dividing cells. Because ATG8B and ATG8C were shown to localise to the same structure (figure 3.14), only the location of ATG8B was studied in detail.

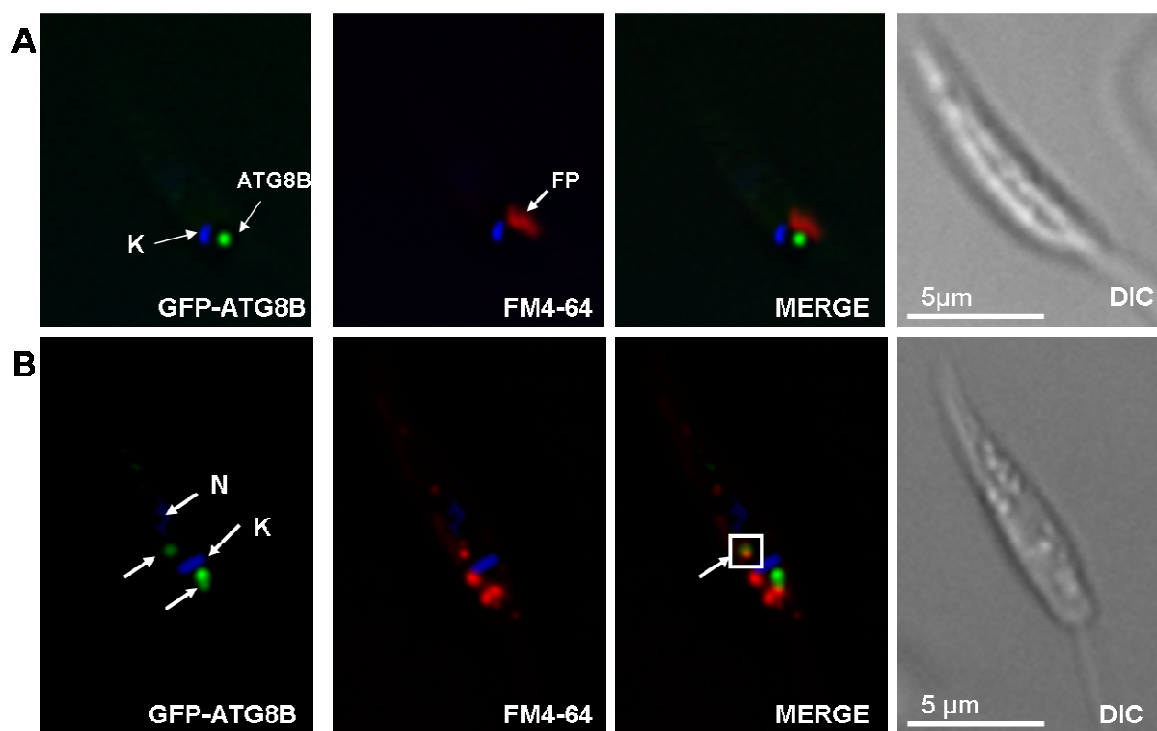


**Figure 3-15 Co-localisation of GFP-ATG8B with the endocytic tracer FM4-64.**

**A) GFP-ATG8B does not co-localise with the flagellar pocket.** Cells which expressed GFP-ATG8B were washed and resuspended in serum free homem media with 12 $\mu$ M FM4-64 for 15 minutes at 4 $^{\circ}$ C, and then immediately prepared for microscopy. The flagellar pocket is labelled and marked with an arrow, and does not co-localise with GFP-ATG8B, also marked with an arrow.

**B) GFP-ATG8B partially co-localises with components of the early endosomal system.**

Cells were treated with FM4-64 as before, but then resuspended in serum supplemented media and chased in the absence of FM4-64 at 25  $^{\circ}$ C for 20 minutes to label components of the early endosomal system. Cells were viewed using an Applied Precision DeltaVision microscope. Arrows point to GFP-ATG8B, and the kinetoplast (K) and nucleus (N) for orientation, and the site of co-localisation is marked with a white box. Scale bar is 5 $\mu$ m.

### 3.7 Immunofluorescence analysis of ATG8, ATG8A, ATG8B and ATG8C

Recombinant His tagged ATG8, ATG8A, ATG8B and ATG8C were expressed by Dr R Williams and used for the production of antibodies in rabbit ( $\alpha$ -ATG8) or sheep ( $\alpha$ -ATG8A,  $\alpha$ -ATG8B and  $\alpha$ -ATG8C). The affinity purification of these antibodies and their optimisation for use in western blot analysis is discussed in chapter 4. The purified antibodies were tested for immunofluorescence, with the aim of supporting localisation and expression data obtained using GFP tagged proteins *in vivo*. In all cases, the primary antibody dilution which gave the most promising results was 1 in 100, and with both  $\alpha$ -rabbit and  $\alpha$ -sheep controls

(with no primary antibody), nothing more than low level background fluorescence was observed (figures 3.16G and H).

$\alpha$ -ATG8 antibodies labelled punctate structures, particularly in cells which had been starved (figure 3.16B). In non-starved cells the signal was generally distributed in the cytoplasm (figure 3.16A), suggesting that the antibody specifically recognises endogenous ATG8. However, these antibodies did not produce a strong signal and a significant amount of background fluorescence signal was seen, suggesting that further purification and optimisation of these antibodies is required if they are to be useful for consistent and reliable immunofluorescence analysis. Additionally, when anti-ATG8 antibodies were used in western blot analysis (chapter 4), multiple proteins were detected in addition to ATG8 (figures 4.5, 4.6, 4.8), perhaps reducing its utility for immunofluorescence localisation studies.

The punctate pattern obtained with  $\alpha$ -ATG8A antibodies on starved, fixed promastigotes resembled that seen with GFP tagged proteins in live cells (figure 3.16 D), indicating that the antibody is specific, supporting the data obtained using cells that expressed GFP-ATG8A. However, a similar pattern was observed in promastigotes which had been grown in nutrient rich media (figure 3.16C), suggesting that the pattern seen was non-specific, and that these antibodies are not useful for immunofluorescence analysis. Alternatively, the antibodies may be detecting a constitutive level of ATG8A recruitment to autophagosome like structures that is not observed when GFP-ATG8A is over-expressed in live cells. Another possibility is that the fixation process may have affected the distribution of endogenous ATG8A. Null mutant cell lines are required to determine whether the immunofluorescence signals detected do represent the localisation of ATG8A *in vivo*.

Antibodies raised against ATG8B recognised punctate structures in ~5% of the cells in the region close to the flagellar pocket in some cells which do look similar to the localisation discovered using GFP tagged proteins (figure 3.16E). In the majority of cells (90-95%),  $\alpha$ -ATG8B detected a signal mostly distributed throughout the cytoplasm as would be expected from the GFP data, indicating that the profile of expression obtained for GFP-ATG8B reflects that of the endogenous protein, and that the fact that ATG8B is localised to puncta in so

few cells is not due to competition of GFP tagged protein with endogenous ATG8B. Deconvolution of images obtained with an Applied Precision DeltaVision microscope was required to reduce background and non-specific staining.

Although  $\alpha$ -ATG8C detected a signal with a localisation like that of the GFP-ATG8C in live cells (figure 3.16F), this antibody also recognised multiple punctate structures throughout some cells which was quite unlike the localisation of GFP-ATG8C. As the background signal could not be reduced by deconvolution of the images, the immunofluorescence data obtained with  $\alpha$ -ATG8C antibodies was thought to be unreliable. The lack of specificity of  $\alpha$ -ATG8C antibodies is discussed further in chapter 4.

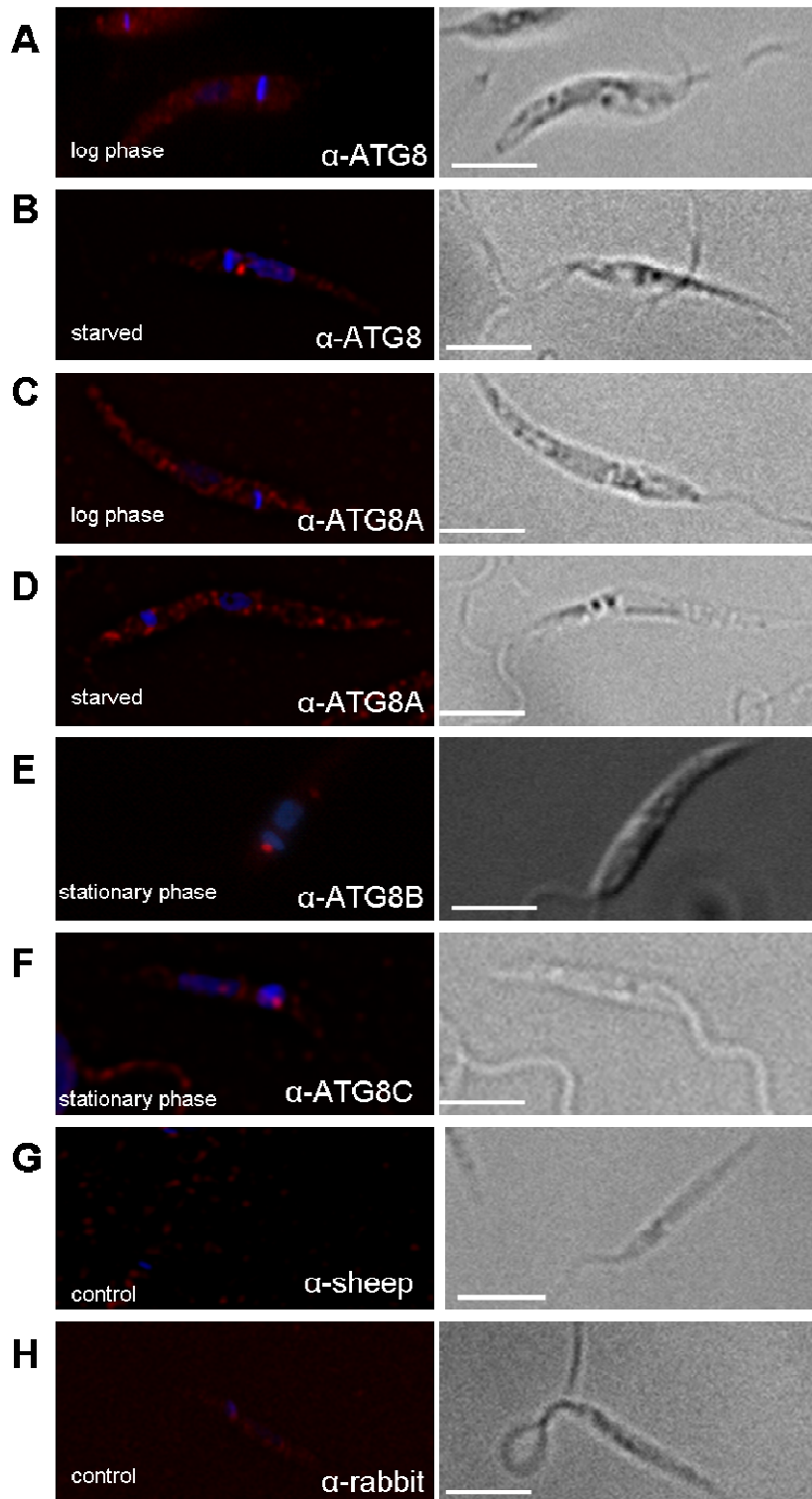


**Figure 3-16 Immunofluorescence analysis of ATG8, ATG8A, ATG8B and ATG8C in promastigotes.** Fixed wild type promastigotes were labelled with anti-ATG8A, ATG8B or ATG8C and Alexa-Fluor 548 (red)- conjugated anti sheep antibodies, or anti-ATG8 antibodies with Alexa-Fluor 548 conjugated anti-rabbit antibodies. In all cases the primary antibody was diluted 1 in 100 prior to use, and the secondary antibodies used at a 1 in 2000 dilution. DAPI staining of the nucleus and kinetoplast are shown in blue. A) Log phase promastigotes probed with anti-ATG8, B) starved promastigotes labelled with anti-ATG8, C) Log phase promastigotes labelled with anti-ATG8A, D) starved promastigotes probed with anti-ATG8A, E) stationary phase promastigotes probed with anti-ATG8B, F) stationary phase promastigotes labelled with anti-ATG8C. Negative controls were performed using G) anti-rabbit secondary antibody alone or H) anti-sheep antibody alone. The scale bar represents 5 μm. Deconvolution was performed using the Deltavision SoftWorx software.

### 3.7.1 ATG8B does not co-localise with markers of the Golgi

The Golgi apparatus of *Leishmania* resides in the region between the nucleus and the flagellar pocket (McConville *et al.*, 2002a, Sahin *et al.*, 2008), leading to an investigation into the possible co-localisation of ATG8B with the Golgi. Anti-ATG8B antibodies and anti-ARL1 antibodies, which have been shown to localise to the trans-Golgi network (Sahin *et al.*, 2008), were used to investigate the relative localisation of ATG8B to the Golgi. No co-localisation between the two signals was ever observed, suggesting that ATG8B is not associated with the Golgi (figure 3.17).

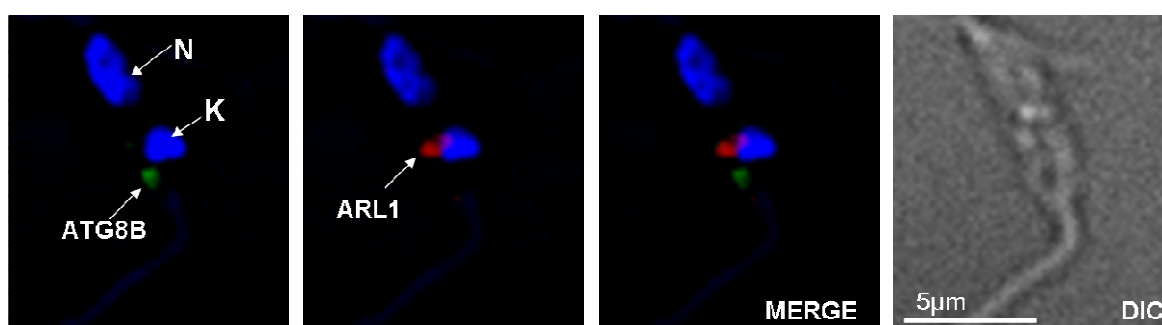


**Figure 3-17 Immunofluorescence analysis of ATG8B and the Golgi marker ARL1**

Fixed wild type promastigotes were labelled with primary antibodies anti-ATG8B (1 in 100 dilution) and anti-ARL1 (1 in 1000 dilution) and Alexa-Fluor 488 (green)- conjugated anti sheep and Alexa-Fluor 548 (red) conjugated anti-rabbit antibodies at a 1 in 2000 dilution. DAPI staining of the nucleus and kinetoplast are shown in blue. The scale bar is 5  $\mu\text{m}$ .

## 3.8 Discussion

*Leishmania major* possess, in addition to the basic components of the autophagy pathway, 25 additional ATG8 like proteins which cluster into three distinct families, and that appear to be unique to *Leishmania* species (Williams *et al.*, 2006). The analysis of GFP tagged ATG8A, ATG8B and ATG8C revealed that, under particular circumstances, representatives of each family of *L. major* ATG8 paralogues localise to punctate structures that resemble GFP-ATG8 labelled autophagosomes.

Through the analysis of the localisation and expression of GFP tagged proteins, an involvement of ATG8A in an autophagy-like response to starvation has been discovered. ATG8A exhibits a dramatic relocalisation in response to nutrient depletion, but no change in distribution was observed during differentiation,

suggestive of a role distinct from *L. major* ATG8. The inhibition of the starvation response of ATG8A by the addition of either glucose or proline suggested that the recruitment of ATG8A to punctate structures is a survival response for when energy sources are scarce. Glucose and proline are both present in the sandfly gut (Hamilton and El Naiem, 2000, Cunningham and Slater, 1974), and *Leishmania* promastigotes have been found to be capable of using both as an energy source (Opperdoes and Coombs, 2007; Burchmore *et al.*, 2003; Blum, 1993; Mazareb *et al.*, 1999; Ter Kuile and Opperdoes, 1992). However, it is not known whether metabolism occurs in promastigotes maintained *in vitro* in the same way as in a natural sandfly environment. Interestingly, the recruitment of GFP-ATG8 to autophagosomes was enhanced when promastigotes were incubated in PBS with added glucose or proline in *L. mexicana* (Dr R Williams, unpublished observations). These data suggest that, while ATG8 and ATG8A are both involved in a response to starvation, they have distinct roles.

The upregulation of ATG8 associated autophagy during both differentiation *in vitro* and in response to starvation perhaps suggests an intimate link between low nutrient availability and the onset of differentiation in the sandfly vector. In fact, nutritional depletion of tetrahydrobiopterin has been shown to be a trigger of metacyclogenesis (Cunningham *et al.*, 2001). One hypothesis could be that ATG8A is required for withstanding periods of starvation within the promastigote secretory gel in the thoracic midgut of infected sandflies, while ATG8 is involved in autophagy associated with differentiation, possibly triggered by changes in their nutritional environment. Detailed analysis of the response of ATG8 in *L. major* to starvation in the presence or absence of energy sources is required to ensure that the effects are not species specific.

Autophagy is known to be an adaptive response to amino acid starvation (Meijer, 2008; Munafo and Colombo, 2001; Onodera and Ohsumi, 2005). Supplementing starvation media with various individual amino acids inhibited the recruitment of GFP-ATG8 to autophagosomes in *L. mexicana* (Dr R Williams, unpublished observation), supporting available data that ATG8 is involved in a classical autophagy pathway (Williams *et al.*, 2006). The analysis of the response of both ATG8 and ATG8A in *L. major* when resuspended in starvation media

supplemented with individual amino acids might uncover further differences between the starvation responses of ATG8 and ATG8A.

Treatment of promastigotes with the autophagy inhibitor wortmannin prior to and during starvation inhibited the response of ATG8 but not ATG8A to starvation, suggesting that ATG8A is involved in a starvation response that is distinct from autophagy. In mammalian cells, 10 nM wortmannin, a PI3 kinase inhibitor, is sufficient to inhibit autophagy (Blommaert *et al.*, 1997; Munafo and Colombo, 2001), and the recruitment of ATG8 to autophagosomes in *Leishmania* was inhibited by wortmannin at concentrations of 10  $\mu$ M (Williams *et al.*, 2006, Besteiro *et al.*, 2006b). PI3 kinases of two different classes have been shown to control autophagy, and it is through the inhibition of PI3Ks that autophagy is inhibited by wortmannin (Petiot *et al.*, 2000). To cause inhibition of autophagy in *Leishmania*, concentrations of wortmannin one thousand fold higher than that which is used in mammalian cells was required (Williams *et al.*, 2006), suggesting either that autophagy in *Leishmania* is regulated via a novel mechanism, or else that perhaps PI3 kinases are regulated in a different manner to mammalian PI3Ks. The difference in sensitivity of ATG8A and ATG8 to wortmannin provides further evidence that they are involved in distinct starvation response pathways.

The possibility that ATG8A is involved in the specific, starvation induced degradation of glycosomes in *Leishmania* was investigated by analysing the localisation of GFP-ATG8A compared with glycosomes labelled with RFP-SQL. The two signals were never shown to overlap, suggesting that ATG8A is not involved in the specific degradation of glycosomes during nutrient deprivation. An occasional co-localisation of GFP-ATG8 labelled autophagosomes with RFP-SQL labelled glycosomes in *L. mexicana*  $\Delta$ *cpa/cpb* mutants (Dr R Williams, unpublished observation) suggests that the selective degradation of glycosomes via macroautophagy might occur in *Leishmania* during differentiation. In addition to this, the apparent increase in ATG8 mediated autophagy in the presence of additional energy sources (glucose or proline) might in fact be an indicator that ATG8 is involved in the turnover of glycosomes during adaptation to changing environments, as the enzymatic content of glycosomes would be expected to vary dependent on the nature of the available nutrients.

Chaperone mediated autophagy (CMA) is a form of autophagy in which selected cytosolic proteins are recognised by a chaperone complex and delivered to the lysosome in response to prolonged starvation, oxidative stress or exposure to toxic compounds (Massey *et al.*, 2004). A cytosolic chaperone, heat shock protein of 70 kDa recognises a pentapeptide (amino acid) motif in the CMA substrate, and it is this interaction which confers the specificity of CMA (Massey *et al.*, 2006). The substrate-chaperone complex is trafficked to the lysosomal surface where it interacts with the lysosome-associated membrane protein LAMP2A, leading to the unfolding and degradation of the substrate protein in the lysosomal lumen (Kaushik *et al.*, 2008). The sequential induction of macroautophagy and chaperone mediated autophagy in response to starvation has been reported. For example, macroautophagy-dependent protein degradation is not observed beyond 4-6 hours of starvation of liver cells and confluent fibroblasts in culture, with chaperone mediated autophagy being the main response to prolonged starvation (Massey *et al.*, 2006). While ATG8A appears to respond to prolonged starvation, GFP-ATG8A was never observed to localise with the lysosome in *Leishmania*, suggesting that a role in CMA is unlikely.

ATG8A, ATG8B and ATG8C do not appear to associate with autophagosome membranes during the differentiation from metacyclic promastigote to amastigote stages. However, when GFP-ATG8A or GFP-ATG8C did localise to punctate structures it was always to a single punctum which appeared to reside close to the flagellar pocket, which has been shown to be involved in endocytosis of nutrients from the PV in amastigotes (Russell *et al.*, 1992; Schaible *et al.*, 1999). Host derived autophagosomes have been shown to fuse with the parasitophorous vacuole (PV) of *L. mexicana* and to be involved in the transport of large molecules, such as fluorescent dextrans, into the PV (Schaible *et al.*, 1999). In that study, the uptake of biotin labelled dextran was studied by immuno-electron microscopy (Schaible *et al.*, 1999). After four hours the dextran label was concentrated in macrophage LAMP-1 positive vesicles containing membranous debris which were autophagosome-like in structure and found in close proximity to the PV. After twenty four hours, the dextran was abundant within the PVs and surrounding vesicles, and was detected in the flagellar pocket of the amastigotes. The uptake of dextran was inhibited by 3-

methyladenine (10 mM), a known inhibitor of autophagy (Schaible *et al.*, 1999). The localisation of occasionally observed puncta close to the flagellar pocket could point to a possible role in the endocytosis of nutrients from the host cytosol, although to support this hypothesis it will be necessary to analyse the localisation of fluorescently labelled molecules that are endocytosed from the PV via the flagellar pocket (e.g. dextran) in comparison to that of GFP-ATG8A or GFP-ATG8C.

ATG8B and ATG8C recruitment to punctate structures did not appear to be associated with progression through the life cycle, nor was it affected by starvation, suggesting that these proteins function in processes that are distinct from autophagy. The localisation of ATG8B and ATG8C in the region near the flagellar pocket, and the partial over-lap of GFP-ATG8B with components of the early endosomal system pointed to a potential role for these proteins in endocytosis or some vesicle dependent intracellular trafficking processes. However, the number of markers investigated in this study for potential co-localisation with ATG8B was limited and should be expanded.

Immunofluorescence analysis of wild type *L. major* cells with anti-ATG8B antibodies was useful in confirming the localisation and distribution of ATG8B obtained from analysing cells over-expressing GFP-ATG8B (figure 3.16). However, the localisation pattern of ATG8A remains to be confirmed. Immunofluorescence analysis of wild type cells with anti-ATG8A antibodies identified multiple punctate structures distributed throughout the cell, similar to the pattern observed with GFP-ATG8A after nutrient deprivation. However, the same pattern was observed in untreated promastigotes, suggesting either that the distribution of endogenous ATG8A may be masked by the over-expression of the GFP-ATG8A plasmid, or that the punctate distribution observed by IFA was in fact an artefact due to fixation.

Episomal expression of tagged proteins in live cells has proven to be useful in many cases, for example in the analysis of autophagy using GFP-ATG8 as a marker (Besteiro *et al.*, 2006b). However, episomal expression can be problematic, with varying levels of protein expression and GFP intensity sometimes leading to misinterpretation, and the possibility that over-expressing a particular protein can lead to its mislocalisation (Benzel *et al.*, 2000). Though

the analysis of GFP tagged Atg8 or LC3 is an established and effective method of analysing autophagy (Klionsky *et al.*, 2008), the formation of GFP-LC3 positive aggregates containing ubiquitinated proteins has been reported even in autophagy deficient cells (Kuma *et al.*, 2007). Lacking definitive confirmation of the distribution of ATG8A by direct immunofluorescence, the analysis of tagged ATG8A (with GFP and perhaps the smaller immunogenic tag HA) that has been stably integrated at the endogenous locus could be useful in supporting data produced in this chapter.

## **4 Post-translational modifications of *L. major* ATG8-like proteins**

## 4.1 Introduction

In order to further characterise *Leishmania* ATG8 like proteins, antibodies raised against recombinant ATG8, ATG8A, ATG8B and ATG8C were used to analyse the expression of endogenous ATG8-like proteins during the life cycle of the parasite, and to investigate their subcellular localisation by cellular fractionation. The recruitment of Atg8 to autophagosomal membranes requires the post translational processing of Atg8 by the cysteine peptidase Atg4 and the subsequent conjugation to the phospholipid phosphatidylethanolamine (PE). It has recently been shown that *L. major* ATG8, ATG8A, ATG8B and ATG8C are selectively cleaved *in vitro* by the cysteine peptidases ATG4.1 and ATG4.2 (Williams *et al.*, 2009) (described below). In this chapter, the possibility that *Leishmania* ATG8-like proteins are modified by a phospholipid after processing by ATG4 was investigated by analysing their mobility by SDS-PAGE in the presence of urea, their sensitivity to phospholipase D, and the incorporation of radioactively labelled ethanolamine into purified ATG8, ATG8A and ATG8B. Additionally co-immunoprecipitation experiments were performed using anti-ATG8B in order to search for potential interacting partners that may provide clues as to the function of this protein.

### 4.1.1 Post translational processing of Atg8 homologues by the cysteine peptidase Atg4

The post-translational processing of Atg8 was studied in yeast by expressing Atg with a myc tag at the N or C terminus, i.e. myc-Atg8 or Atg8-myc respectively, in yeast  $\Delta atg8$  null mutants (Kirisako *et al.*, 2000). No signal was detected upon immunoblotting with anti-myc antibodies in cells expressing Atg8-myc, indicating C terminal processing of Atg8. Atg8-myc was unprocessed in  $\Delta atg4$  null mutant cells, suggesting that Atg4 was the cysteine protease responsible for the C terminal processing of Atg8. The expression of various Atg8-myc constructs with a mutation in the carboxyl region of Atg8 led to the discovery that the carboxyl glycine residue (Gly<sup>116</sup>) is essential for processing by Atg4, whereas the mutation of the carboxy-terminal Arg did not affect the cleavage (Kirisako *et al.*, 2000). The cleaved form of Atg8 in which the carboxyl glycine is exposed is referred to as Atg8FG in yeast.

The human Atg8 homologues, LC3, GABARAP and GATE-16 have all also been shown to be post-translationally cleaved resulting in a form of the protein with an exposed C terminal glycine, referred to respectively as LC3-I, GABARAP-I and GATE-16-I respectively (Tanida *et al.*, 2003; Tanida *et al.*, 2004b). An *in vitro* assay utilising recombinant LC3B-3XFLAG and myc-LC3B-His showed that their carboxyl termini were cleaved, and that this cleavage was almost completely abolished in mutant proteins containing an Ala in place of Gly<sup>120</sup>, indicating that this conserved residue is required for post translational processing and modification of MAP1-LC3 (Tanida *et al.*, 2004b). The post-translational cleavage of GABARAP and GATE-16 exposing Gly116 in both was shown to be dependent on Leu<sup>117</sup> and Phe<sup>117</sup> residues respectively (Tanida *et al.*, 2003).

Based on similarity with the yeast cysteine peptidase Atg4, four human Atg4 proteins have been identified. These are Atg4A (autophagin-2), Atg4B (autophagin-1), Atg4C (autophagin-3) and Atg4D (autophagin-4) (Hemelaar *et al.*, 2003). Atg4B was found to be the cysteine protease responsible for the specific, C terminal processing of LC3, GABARAP, GATE-16, and an additional novel mammalian Atg8 homologue, Atg8L (Hemelaar *et al.*, 2003; Tanida *et al.*, 2006). The roles of Atg4A, Atg4C and Atg4D remain unclear, although Atg4A has been reported to be able to process the GATE-16 C terminus *in vitro* (Scherz-Shouval *et al.*, 2003).

Despite the absence of residues in ATG8 paralogues thought to be required for processing by ATG4 (section 3.3.1), it was recently shown that *L. major* ATG8-like proteins are selectively cleaved by the *L. major* cysteine peptidases ATG4.1 and ATG4.2 (Williams *et al.*, 2009). *In vitro* cleavage assays were performed in which recombinant ATG8, ATG8A, ATG8B and ATG8C proteins with His and HA tags at the N- and C-termini were incubated with recombinant ATG4.1 or ATG4.2. The *L. major* ATG8 proteins were found to be selectively cleaved by the ATG4 cysteine peptidases, with ATG8, ATG8B and ATG8C undergoing proteolytic cleavage by ATG4.1, and ATG8A being specifically cleaved by ATG4.2 (figure 4.1, taken from (Williams *et al.*, 2009)). These data provide evidence that *Leishmania* ATG8 homologues can be processed in the same way as other characterised Atg8 proteins, and that they could potentially function in the ATG8 conjugation system in *Leishmania*.

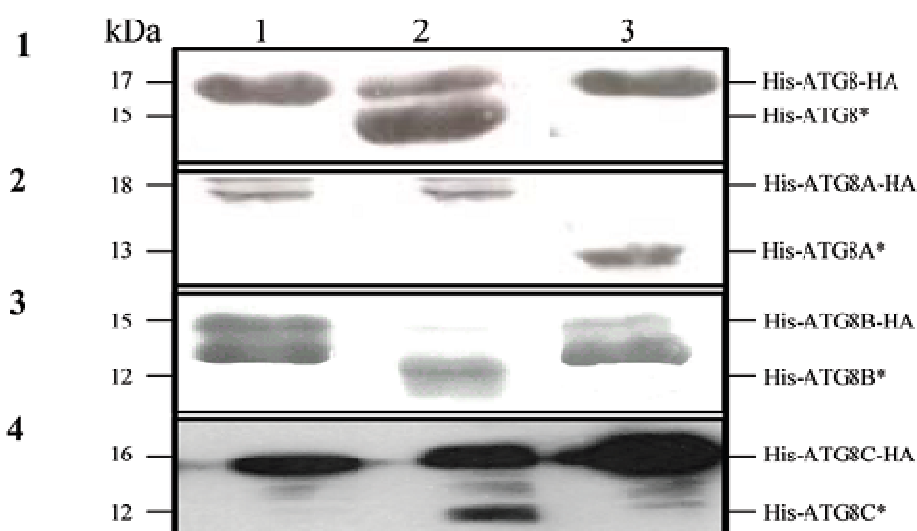


**Figure 4-1 Hydrolysis of *L. major* ATG8s by *L. major* ATG4s *in vitro* (Williams *et al.*, 2009).**

Soluble fractions of *E. coli* expressing His-ATG8-HA (row 1), His-ATG8A-HA (row 2), His-ATG8B-HA (row 3), His-ATG8C-HA (row 4) and His-ATG12-HA (row 5) alone (lane 1) or co-expressed with either ATG4.1 (lane 2) or ATG4.2 (lane 3) were incubated for 30 min at 30°C in 50 mM Tris-HCl pH 8.0, 125 mM NaCl and 40 mM  $\beta$ -mercaptoethanol and then analysed by western blot with anti-His antibody. The cleaved ATG8 bands are labelled with asterisk.

*L. major*  $\Delta atg4.2$  null mutants were previously shown to be defective in their ability to undergo differentiation, and significantly less able to survive under starvation conditions (Besteiro *et al.*, 2006b). GFP-ATG8A did not re-localise to punctate structures when  $\Delta atg4.2$  null mutants expressing GFP-ATG8A were subjected to starvation suggesting that ATG8A must be processed by ATG4.2 before they can be recruited to punctate structures, and supporting the data obtained from the *in vitro* cleavage assay described above (figure 4.2, Williams, *et al.*, 2009). Additionally, the reduced ability of  $\Delta atg4.2$  null mutants to withstand starvation provides some evidence that the correct processing and localisation of ATG8A is important for survival under starvation conditions.

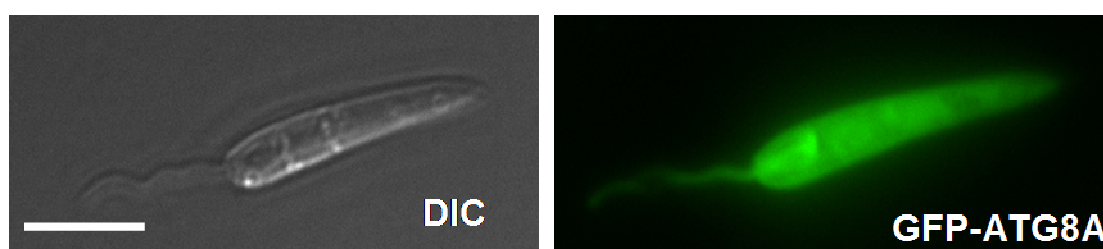


**Figure 4-2 The distribution of GFP-ATG8A in  $\Delta atg4.2$  null mutants after 4 hours in nutrient deprived medium.** *L. major*  $\Delta atg4.2$  null mutants expressing GFP-ATG8A were incubated in nutrient deprived media (PBS) for four hours and visualised by microscopy (Williams *et al.*, 2009).

### 4.1.2 Modification of yeast and mammalian Atg8 homologues with a phospholipid

The post-cleavage modification of Atg8 with phosphatidylethanolamine was first described by Ichimura and colleagues in pioneering work that identified a new mode of protein lipidation (Ichimura *et al.*, 2000). In subcellular fractionation experiments, more than half of Atg8 was recovered in the 100,000g pellet and was only solubilised by a detergent (1% deoxycholate), indicating a conversion to a tightly membrane bound form, termed Atg8-X (Kirisako *et al.*, 2000). Phase partitioning with the detergent Triton X-114 was used to separate aqueous and detergent-solubilisable forms of Atg8. Atg8-X was found to accumulate in the detergent phase, indicating a tight association with membranes upon modification, and a hydrophobic nature of the then unknown molecule, X (Ichimura *et al.*, 2000).

The structure of Atg8-X was studied using matrix-assisted laserdesorption ionization time of flight mass spectrometry (MALDI-TOFMS) of purified HisAtg8FG-X. Two signals were obtained, one at  $m/z$  14,368 which corresponded to HisAtg8FG (the cleaved but unlipidated form of ATG8), and another at 15,003. The difference in molecular mass between the two forms, and the hydrophobic nature of Atg8-X led to the proposal that the modifying moiety, X, was a glycerophospholipid (Ichimura *et al.*, 2000). The chemical nature of X and the attachment site were investigated by treating HisAtg8-X with a mild alkali, known to remove fatty acids from glycerophospholipids, followed by analysis by electonspray ionisation / tandem mass spectrometry. A difference in mass of Mr 197 was identified between Atg8-X and Atg8FG, leading to the identification of X as phosphatidylethanolamine (PE).

After processing by Atg4 to expose the carboxyl glycine residue, modification of the mammalian Atg8 homologues LC3-I, GABARAP-I and GATE-16-I to tightly membrane bound forms termed LC3-II, GABARAP-II and GATE-16-II also occurs (Kabeya *et al.*, 2000; Kabeya *et al.*, 2004; Tanida *et al.*, 2003). LC3-II has been shown to localise to autophagosome membranes (Kabeya *et al.*, 2000), and to accumulate in cells cultured under starvation conditions (Kabeya *et al.*, 2004). GATE-16 and GABARAP were also shown to be converted to membrane bound GATE-16-II and GABARAP-II forms, which could localise to autophagosome

membranes, and expression of which was upregulated during starvation (Kabeya *et al.*, 2004).

LC3-I and LC3-II can be separated by SDS-PAGE in the presence of 6 M urea, where LC3-II is found to migrate faster than LC3-I (Kirisako *et al.*, 2000). This is also true of GABARAP-II (Kabeya *et al.*, 2004) and GATE-16-II (Tanida *et al.*, 2003). Endogenous LC3-II and GABARAP-II were shown to be sensitive to treatment with phospholipase D, which releases phosphatidic acid from phospholipid conjugates, proving that LC3-II and GABARAP-II are lipidated forms of LC3 and GABARAP (Tanida *et al.*, 2004a). Similarly, treatment with phospholipase D altered the mobility of GATE-16-II suggesting that this protein too is modified by a phospholipid (Tanida *et al.*, 2003). In addition to its role as a processing enzyme, Atg4B was shown to be the deconjugating enzyme in the autophagy conjugation system responsible for removing the phospholipid moiety from LC3-II and GABARAP-II, and thus is proposed to be involved in the negative regulation of localisation of LC3 to autophagosomes (Tanida *et al.*, 2004a).

The phospholipid target of LC3-II was shown to be phosphatidylethanolamine (PE) by *in vivo* labelling experiments with [<sup>14</sup>C]-ethanolamine. HeLa cells transiently transfected with myc-tagged LC3 were labelled with [<sup>14</sup>C]-ethanolamine and immunoprecipitated with anti-myc antibody. These experiments revealed that only approximately 10% of LC3-I was converted to the LC3-II form, and that [<sup>14</sup>C] was preferentially incorporated into LC3-II, indicating that LC3-II is the PE-conjugated form (Kabeya *et al.*, 2004).

#### **4.1.3 Subcellular localisation of yeast and mammalian Atg8 homologues**

Subcellular fractionation experiments have been informative in determining the nature of the various forms of Atg8 and LC3. In wild type yeast, most Atg8 was detected in the pellet fraction after centrifugation at 100,000g for one hour (Kirisako *et al.*, 1999; Kirisako *et al.*, 2000). Approximately half of the Atg8 in the pelletable fraction was solubilised by NaCl, whereas almost all was solubilised by treatment with the detergent deoxycholate (1%), suggesting that some Atg8 was tightly bound to membranes. In  $\Delta atg4$  null mutants, almost all the pelletable Atg8 was solubilised by NaCl, demonstrating that the conversion

of Atg8 to a tightly membrane associated form was dependent on processing by Atg4. A further fractionation was performed, separating the lysate into low speed pellet (LSP) by centrifugation at 13000g, a high speed pellet (HSP) by centrifugation at 100,000g, and supernatant (HSS). Atg8 was found in all fractions in wild type yeast, and it was shown by solubilisation with NaCl that the LSP fraction contained Atg8-PE, while the HSP fraction contained both lipidated and non-lipidated forms of the protein (Kirisako *et al.*, 2000).

Similar to yeast Atg8, LC3 was found to be tightly bound to membranes only upon modification to LC3-II form (Tanida *et al.*, 2003). However GATE-16 and GABARAP were found to localise to membrane bound compartments even prior to modification, indicating that their biochemical characteristics are different to LC3 (Tanida *et al.*, 2003).

## **4.2 Optimisation of *L. major* ATG8, ATG8A, ATG8B and ATG8C specific antibodies for western blot analysis**

To analyse the expression and processing of ATG8-like proteins, polyclonal antibodies were raised in rabbit or in sheep against recombinant His tagged ATG8, ATG8A, ATG8B and ATG8C (protein produced by Dr R Williams). The antibodies were affinity purified against recombinant protein that was coupled to amino-link coupling gel (Pierce), and their specificity tested by western blot against cell lines expressing GFP-ATG8, GFP-ATG8A, GFP-ATG8B or GFP-ATG8C.  $\alpha$ -ATG8,  $\alpha$ -ATG8A and  $\alpha$ -ATG8B antibodies specifically recognised the GFP tagged versions of ATG8, ATG8A and ATG8B respectively (figure 4.3A, B, C).  $\alpha$ -ATG8B also detected endogenous ATG8B protein (figure 4.4C).  $\alpha$ -ATG8C was non-specific, recognising proteins of the expected size for both ATG8B and ATG8C, in addition to other proteins of unexpected sizes (figure 4.4D).  $\alpha$ -ATG8B was the only antibody to also detect endogenous protein in lysates which contained GFP tagged ATG8 proteins (figure 4.3C).

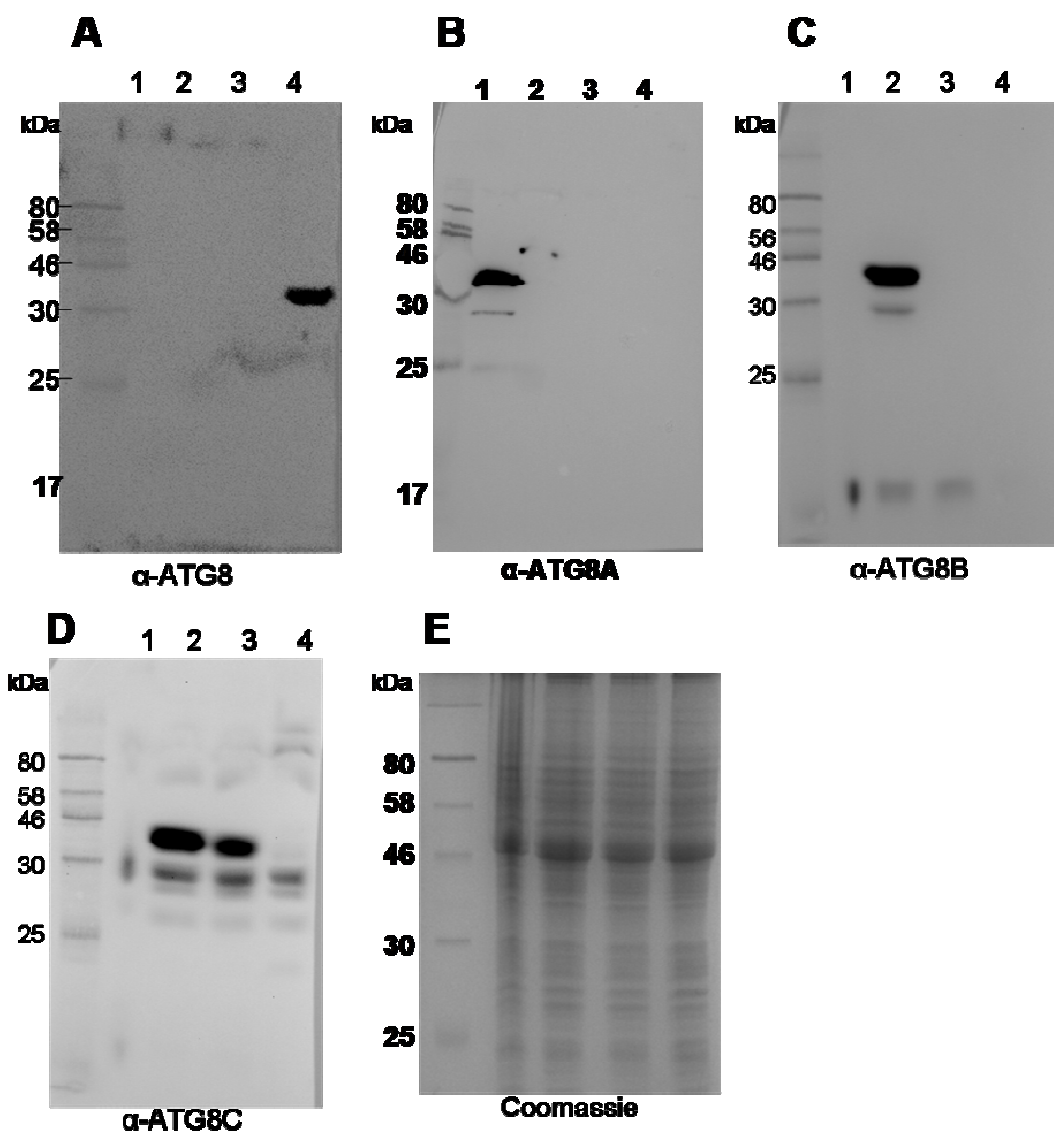


**Figure 4-3 Specificity of of anti-ATG8, anti-ATG8A, anti-ATG8B and anti-ATG8C antibodies.**

Western blot analyses performed on lysates of *Leishmania* late log phase promastigotes expressing GFP tagged ATG8, ATG8A, ATG8B and ATG8C. Cells were lysed in 0.2% Triton-X100 with protease inhibitors. Total lysates (equivalent to  $1 \times 10^7$  cells) were loaded on a 12% acrylamide gel and separated by SDS-PAGE. The gels were then transferred to a hybond-c nitrocellulose membrane and hybridised with rabbit anti-ATG8 or sheep anti-ATG8A, anti-ATG8B or anti-ATG8C. Primary antibodies were used at 1 in 500 dilution, secondary antibodies were used at a dilution of 1 in 10,000. The signal was detected using West Signal chemoluminescence detection system (Pierce). Lane 1 = WT(pN-ATG8A), Lane 2 = WT(pN-ATG8B), Lane 3 = WT(pN-ATG8C), Lane 4 = WT(pN-ATG8). A coomassie stained gel is used to demonstrate even loading.

#### 4.2.1 Detection of ATG8 paralogues in wild type *L. major*

Immunoblot analysis of endogenous proteins led to the discovery that ATG8, ATG8A and ATG8B are present in very low levels in early log phase of growth and significantly upregulated in the stationary phase of growth (figure 4.4). It appears that ATG8C expression is also upregulated in stationary phase parasite,

although the cross-reactivity of anti-ATG8C means that we cannot be certain that the detection of endogenous ATG8C is not being masked by other proteins. ATG8 expression appeared to be upregulated upon starvation where ATG8 expression, although very low, seems to be comparable to that of stationary phase cells, and higher than that seen in early log phase parasites (figure 4.4A, lane 4 compared to lane 1). No upregulation of ATG8A in response to starvation was observed (figure 4.4B, lane 4), despite the apparent involvement of ATG8A in a response to starvation.

Lipidated and non-lipidated versions of Atg8 and the mammalian homologues LC3, GATE-16 and GABARAP can be separated by SDS-PAGE in the presence of 6 M urea, where the lipidated form of the protein is found to migrate faster (Kabeya *et al.*, 2004; Kirisako *et al.*, 2000; Tanida *et al.*, 2003). Two proteins were detected when wild type *Leishmania* lysates were separated on an SDS gel containing 6 M urea and probed with anti-ATG8 antibodies (figure 4.4A, lanes 3 and 4). The signal detected with anti-ATG8 antibodies was very faint and somewhat difficult to detect, suggesting that anti-ATG8 antibodies were not very sensitive, or that *L. major* ATG8 is not expressed at a high level. The two proteins which migrated at approximately 12-15 kDa might be ATG8 and ATG8-PE, which have previously been detected as GFP tagged proteins in *Leishmania* (Besteiro *et al.*, 2006b). Interestingly, no faster migrating protein was detectable with anti-ATG8A, -ATG8B or -ATG8C, suggesting perhaps that a lipidated version of these proteins does not exist, or that it is at a very low concentration under the conditions examined.

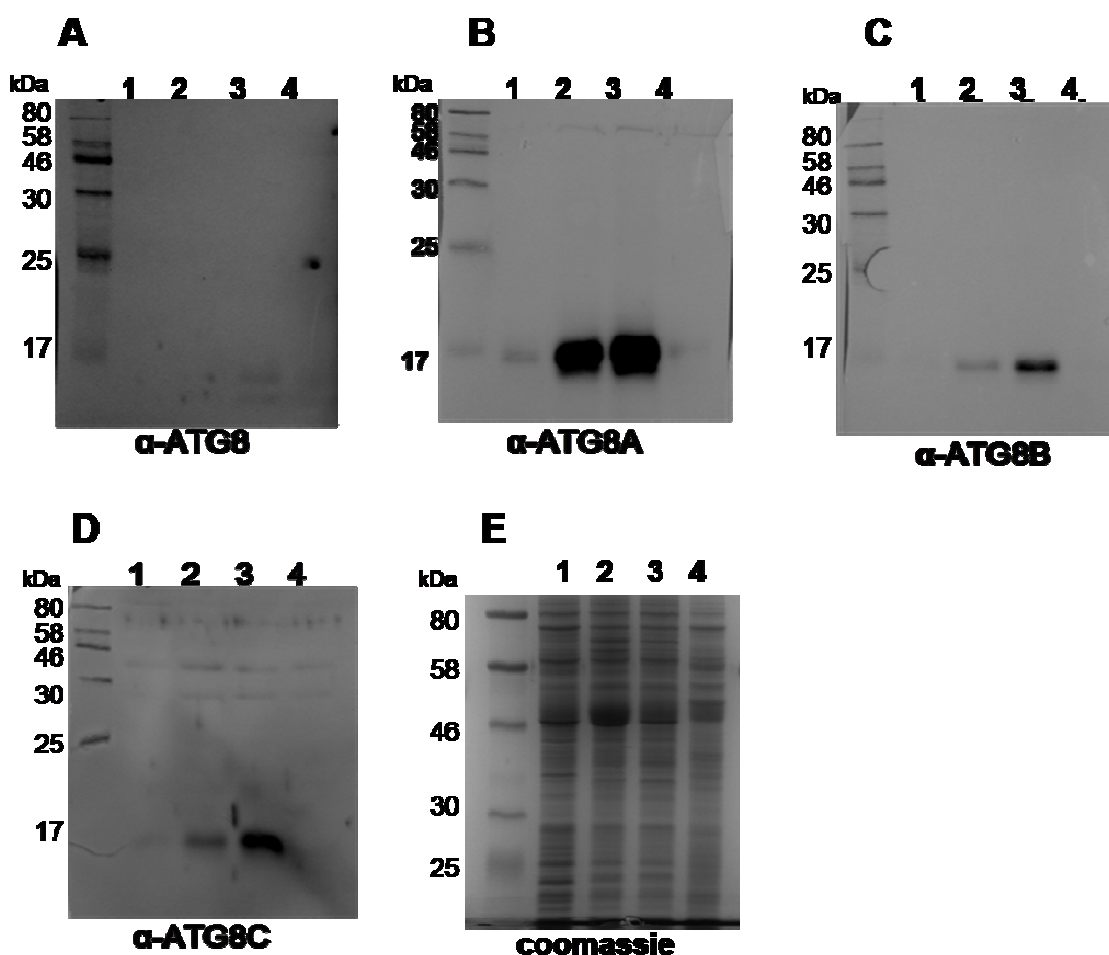


**Figure 4-4 Immunodetection of endogenous ATG8, ATG8A, ATG8B, and ATG8C in *Leishmania* promastigotes.** Western blot analyses performed on lysates of wild type *Leishmania* promastigotes harvested at different stages of their growth, or after starvation. Cells were lysed in 0.2% Triton-X100 with protease inhibitors. Total lysates were quantified using a Bradford Assay and 20  $\mu$ g was loaded on a 15% acrylamide gel containing 6 M urea, and separated by SDS-PAGE. The gels were then transferred to a hybrid-c nitrocellulose membrane and hybridised with rabbit anti-ATG8 (A), or sheep anti-ATG8A (B), anti-ATG8B (C) or anti-ATG8C (D). Primary antibodies were used at 1 in 100 dilution, secondary antibodies were used at a dilution of 1 in 10,000. The signal was detected using West Signal chemoluminescence detection system (Pierce). Lane 1 = early log phase promastigote, Lane 2 = mid-log promastigote, Lane 3 = early stationary phase promastigote, Lane 4 = starved early log phase promastigotes. Expected sizes are ATG8:13.9 KDa, ATG8A:14.8 KDa, ATG8B:12.6 KDa, ATG8C:12.5 KDa. E) A coomassie stained gel (15% gel with no urea) served as a loading control.

Further analysis of ATG8, A, B and C expression throughout the *Leishmania* growth phase confirmed the upregulation of ATG8A and ATG8B expression in stationary phase parasites (figure 4.5B and 4.5C). Neither ATG8A nor ATG8B could be detected in amastigote lysates, suggesting that their expression is significantly higher in promastigote stages. However, a loading control performed using anti-EF1 $\alpha$  antibodies showed that some degradation of the amastigote lysate had occurred (figure 4.5E). It is possible that the ATG8-like proteins were degraded in the amastigote lysate used, and so the lack of

expression of ATG8 and its homologues in amastigote stages cannot be stated with certainty, particularly as we would expect ATG8 at least to be expressed in amastigote stages, based on the occurrence of GFP-ATG8 puncta during differentiation from promastigote to amastigote (Williams *et al.*, 2006).

Endogenous ATG8 could barely be detected in this immunoblot using anti-ATG8 antibodies, again suggesting that the sensitivity of this antibody is very low or that the endogenous protein is expressed at a low level (figure 4.5A). However a protein of approximately 46 kDa was detected. Similarly, when a *Plasmodium* lysate was probed with *Plasmodium* anti-ATG8 antibodies, proteins of 53 and 57 kDa were detected along with ATG8 (Bonilla *et al.*, 2007), and the authors predicted that these proteins were conjugates between *P. falciparum* ATG3 (35 kDa) and lipidated and unlipidated forms of ATG8 (15 kDa). We might speculate that the 46 kDa protein detected with *L. major* anti-ATG8 antibodies could represent a conjugate formed between *L. major* ATG8 (13.9 kDa) and ATG3 (LmjF33.0295, predicted size 31.2 kDa). However, there are several reasons that make this explanation unsatisfactory; firstly that non-covalent interactions are most likely to be disrupted during SDS-PAGE, and secondly because the formation of ATG3-ATG7 intermediates with stable interactions have been reported to be short lived (Tanida *et al.*, 2002; Tanida *et al.*, 2006).

An ATG8-ATG7-ATG3 conjugate, if present in detectable quantities, would be predicted to correspond to a band of 115 kDa. A higher molecular mass protein was detected between 80 and 175 kDa when *L. major* lysate was probed with anti-ATG8 antibodies, which might be an ATG8-ATG7-ATG3 complex. Detection of endogenous ATG3 and ATG7 with specific anti-ATG3 and anti-ATG7 antibodies will be required to confirm the existence of ATG8 in such complexes in *Leishmania*.

Anti-ATG8A also detected multiple, higher molecular weight proteins. In particular, proteins were detected that were just larger than the 46 kDa marker, and between the 58 and 80 kDa markers in all promastigote lysates, and in early log phase promastigotes a band of approximately 26 kDa was detected (figure 4.5B). It is unclear whether these proteins are covalently-linked complexes that involve ATG8A, or whether this antibody is also detecting non-specific proteins.

Anti-ATG8C detected multiple proteins in all lysates (figure 4.5D). The lack of specificity of this antibody (figure 4.3D) reduced its utility for immunoblot analysis, and meant that it was not possible to obtain definitive data regarding the expression of ATG8C.

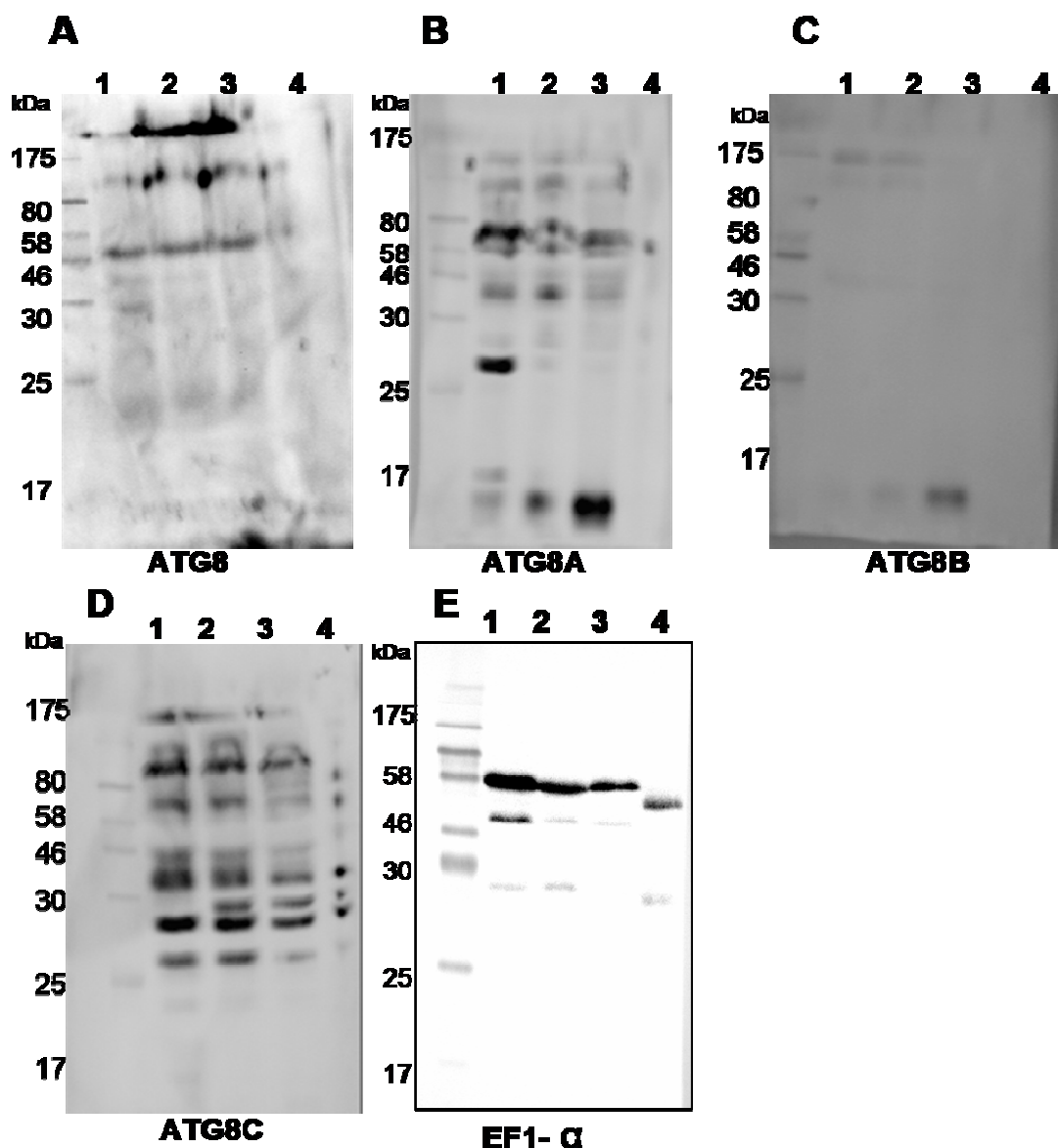


**Figure 4-5 Immunodetection of endogenous ATG8, ATG8A, ATG8B and ATG8C in *Leishmania* promastigotes and amastigotes.** Western blot analyses performed on lysates of wild type *Leishmania* promastigotes harvested at different stages of their growth and of amastigotes. Cells were lysed in 0.2% Triton-X100 with protease inhibitors. Total lysates were quantified using a Bradford Assay and 20  $\mu$ g was loaded on a 15% acrylamide gel and separated by SDS-PAGE. The gels were then transferred to a hybond-c nitrocellulose membrane and hybridised with rabbit anti-ATG8 or sheep anti-ATG8A, anti-ATG8B or anti-ATG8C. Primary antibodies were used at 1 in 100 dilution, secondary antibodies were used at a dilution of 1 in 10,000. A blot probed with anti-EF1- $\alpha$  (E) was used as a loading controls. The signal was detected using West Signal chemoluminescence detection system (Pierce). Lane 1 = early log phase promastigote, 2 = mid-log promastigote, 3 = early stationary phase promastigote, 4 = amastigotes. Expected sizes are ATG8:13.9 KDa, ATG8A:14.8 KDa, ATG8B:12.6 KDa, ATG8C:12.5 KDa.

#### 4.2.2 Subcellular fractionation of *Leishmania* promastigotes and immunodetection of ATG8-like proteins

*Leishmania* lysates were prepared and fractionated from early stationary phase cells as in (Coombs *et al.*, 1982). Parasites were harvested by centrifugation at 2000 x g for 10 minutes in the presence of protease inhibitors, washed twice in 0.25 M sucrose, and lysed without the use of detergent by mixing to a thick paste with alumina (Sigma). When more than 99% of the parasites were lysed (assessed by phase contrast microscopy) the paste was washed in 4 volumes of 0.25 M sucrose by low speed centrifugation, and the alumina discarded. The resultant supernatant was fractionated by differential centrifugation resulting in four fractions. The fraction termed P1 was collected by centrifugation at 2000 x g for 10 minutes, P2 was collected by centrifugation at 13000 x g for 30 minutes, and finally a one hour high-speed centrifugation step at 100,000 x g resulted in the pellet, P3, and the supernatant, S. A previous subcellular fractionation study in *Leishmania* showed by electron microscopy that the P1 (2000 g) fraction contained unlysed cells and nuclear components, P2 (13,000 g) was mainly comprised of plasma membrane profiles, and P3 (100,000 g) contained a population of spherical membrane bound vesicles which likely represent elements of the endocytic / exocytic compartments, leaving soluble, cytoplasmic proteins in the S fraction (Morgado-Diaz *et al.*, 2005). However, in order to confirm the success of the fractionation and accurately interpret data obtained here, the fractions obtained (P1, P2, P3 and S) should be analysed for the presence of proteins whose localisation are known.

A protein of ~13 kDa was detected in all fractions with anti-ATG8 (figure 4.6B), suggesting that as with yeast Atg8 (Kirisako *et al.*, 2000), *L. major* ATG8 is found in all fractions. In addition to this, a protein of ~ 17 kDa was detected in the P3 fraction, which is where the detection of the lipidated, membrane-bound form, ATG8-PE, would be expected. The products of the subcellular fractionation were separated by SDS-PAGE in the presence of 6M urea, known to cause ATG8-PE to migrate faster, so it was surprising that the additional protein detected in the P3 fraction migrated slower than ATG8, perhaps indicating that it is not a lipidated form of ATG8. It is possible that anti-ATG8 antibodies recognise a distinct protein of 17 kDa, unlikely to be ATG8A, ATG8B or ATG8C as all these were found to migrate below the 17 kDa protein marker (figures 4.4 and 4.5).

A protein with molecular weight slightly higher than 46 kDa was detected with anti-ATG8 antibodies in all pelletable fractions (P1, P2 and P3) that was absent from the S fraction (figure 4.6B). It could be that this protein is an ATG8-ATG3 conjugate (as suggested for figure 4.5A). The conjugation of ATG8 to ATG3 occurs just prior to the attachment to PE (Klionsky, 2005), and so would be associated with membrane bound species of ATG8, so the detection of a protein of this size in the membrane fractions and not in soluble fractions could indeed represent this complex.

Interestingly, ATG8A and ATG8B were only detectable in the P3 fraction, suggesting that ATG8A and ATG8B are totally localised to membrane compartments, at least in early stationary phase cells. The localisation of GFP-ATG8A and GFP-ATG8B to the cytoplasm in most cells (figure 3.5, 3.6) could possibly be an artefact due to the over-expression of the GFP tagged proteins, and it could be that ATG8A and ATG8B are in fact membrane associated proteins. It is interesting to note that GATE-16 and GABARAP, mammalian LC3 homologues, were found to localise to membrane bound compartments whether they were lipidated or not (Tanida *et al.*, 2003), suggesting that while these proteins can be processed and lipidated like ATG8 and LC3, their biochemistry is different.

An additional protein of ~27 kDa was detected with anti-ATG8A antibodies in the P3 fraction, as was seen previously (figure 4.5B, 4.6C). Proteins of ~35 kDa and ~46 kDa were detected with anti-ATG8B in pelletable and soluble fractions respectively (figure 4.5C), perhaps indicating that ATG8A and ATG8B exist *in vivo* as part of a protein complex. Multiple proteins were detected in all fractions with anti-ATG8C, although the lack of specificity of this antibody (figure 4.3D) meant that it was not possible to obtain definitive expression or localisation data for ATG8C. An analysis of the localisation of GFP-ATG8C might be informative.

The ATG8, ATG8A and ATG8B in the pellet fractions could be solubilised by treatment with a detergent (NP-40 or Triton-X-100 for immunoprecipitation experiments in section 4.3.3 and 4.4). However, their solubility in NaCl or other non-detergent based buffers was not tested, meaning that determination of the type of membrane association was not achieved in this experiment.

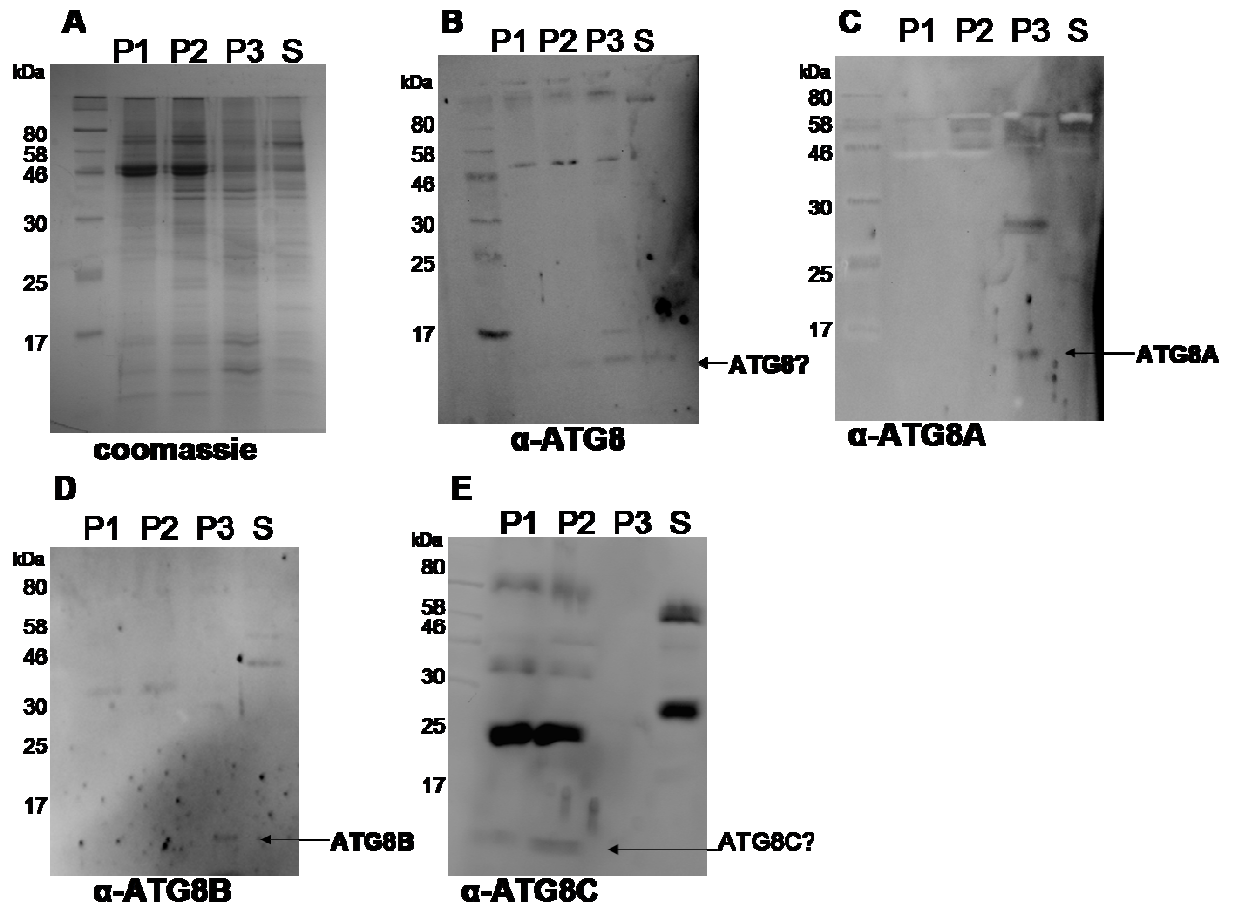


**Figure 4-6 Subcellular fractionation of wild type *L. major* and detection of endogenous ATG8, ATG8A and ATG8B.**  $3 \times 10^9$  *L. major* wild type cells (from 200 ml late log phase cells) were lysed by physical grinding in the presence of alumina and subcellular fractions were collected by differential centrifugation. In each case, P1 fraction was collected by centrifugation at 2000g, P2 was collected by 30 minutes centrifugation at 13000g, P3 was collected by ultracentrifugation at  $>100,000g$  for one hour and S is the supernatant. Pellets were solubilised in 0.2% Triton-X-100. Samples were quantified using a Bradford assay and 20  $\mu$ g of each sample was loaded onto a 15% acrylamide gel containing 6M urea and separated by SDS-PAGE. The gels were then transferred to a hybond-c nitrocellulose membranes and hybridised with affinity-purified rabbit anti-ATG8 or sheep anti-ATG8A or anti-ATG8B. Primary antibodies were used at 1 in 100 dilution, secondary antibodies were used at a dilution of 1 in 10,000. The signal was detected using West Signal supersubstrate chemoluminescence detection system (Pierce).

## 4.3 An analysis of the potential lipidation of *Leishmania* ATG8-like proteins

### 4.3.1 Treatment of GFP tagged ATG8 like proteins with phospholipase D

Lysates of *Leishmania* promastigotes expressing GFP-ATG8, GFP-ATG8A or GFP-ATG8B were subjected to treatment with phospholipase D (PLD), separated by SDS-PAGE in the presence of 6 M urea, and detected with anti-GFP antibodies (figure 4.7A, B and C respectively). *L. major* GFP-ATG8 was found to exist in two forms, with the top protein band correlating with the predicted size for GFP-ATG8 at 41.2 KDa, and a lower band that migrated faster in the presence of urea and was removed upon treatment with PLD (figure 4.7A, the lipidated form of GFP-ATG8 is marked with an asterisk). This result is the same as that described previously for *L. major* GFP-ATG8 (Besteiro *et al.*, 2006b), and validated the technique used for the analysis of GFP-ATG8A and GFP-ATG8B. Only one protein was detected when GFP-ATG8 is separated by normal SDS-PAGE without urea (figure 4.3A), confirming that the faster migrating protein is due to the hydrophobic nature of the lipid modifier and does not represent a degradation product.

Interestingly, anti-GFP antibodies detected four proteins when GFP-ATG8A lysates were probed with anti-GFP (figure 4.7B). The top protein corresponds to the predicted size of GFP-ATG8A of 42.5KDa. None of the lower proteins could be removed upon treatment with PLD in repeated attempts, suggesting that ATG8A is not modified by a lipid. When GFP-ATG8A lysates were probed with anti-ATG8A antibodies (figure 4.3B) only two proteins were detected. This might suggest that two of the four proteins that were consistently detected with anti-GFP antibodies are due to some GFP degradation products.

Two proteins were also detected when GFP-ATG8B lysates were probed with either anti-GFP or anti-ATG8B antibodies, with or without the presence of urea (figure 4.7C and 4.3C). Again, the top protein corresponds to the predicted size of GFP-ATG8B (40.5 KDa), and the lower protein could not be removed by phospholipase D (on multiple attempts), suggesting that ATG8B is not modified by a phospholipid.

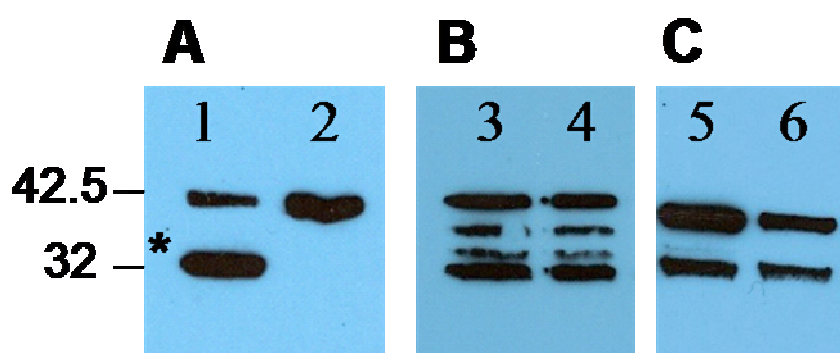


**Figure 4-7 Western blot analysis of GFP-ATG8, GFP-ATG8A and GFP-ATG8B.**

Western blot analysis was performed on lysates of *Leishmania* late log phase promastigotes expressing (A) GFP-ATG8, (B) GFP-ATG8A and (C) GFP-ATG8B. Autophagy was induced by starvation for four hours and cells lysed by sonication in the presence of protease inhibitors. A pellet was collected by ultracentrifugation at 100,000 x g and solubilised in 0.2% Triton-X-100. 20 µg of each sample was incubated with 10 units of phospholipase D (PLD) for one hour at 37°C, loaded alongside untreated sample onto 12% acrylamide gel containing 6 M urea, and separated by SDS-PAGE. The gels were then transferred to a hybond-c nitrocellulose membrane and hybridised with mouse anti-GFP antibodies. Anti-GFP antibody was used at 1 in 1000 dilution, anti-mouse antibody was used at a dilution of 1 in 5000. The signal was detected using West Signal chemoluminescence detection system (Pierce). Lane 1 = WT(pNATG8), Lane 2 = WT(pNATG8) + PLD, Lane 3 = WT(pNATG8A), Lane 4 = WT(pNATG8A) + PLD, Lane 5 = WT(pNATG8B), Lane 6 = WT(pNATG8B) + PLD. GFP-ATG8-PE is marked with an asterisk (lane 1).

### 4.3.2 Treatment of wild type promastigotes with phospholipase D

The effect of treatment with phospholipase D on wild type promastigotes was investigated, in order to support the data obtained with cells expressing GFP tagged proteins. Wild type promastigotes were harvested when they were at their early log phase or stationary phase of growth, and after starvation of early log phase parasites. The membrane bound version of the protein was enriched following the method of Tanida *et al* (2000). Cells were lysed by sonication and the pelletable fraction was collected by centrifugation at 100,000 x g, solubilised in Triton X-100, subjected to treatment with phospholipase D, and separated by SDS-PAGE in the presence of 6 M urea.

No endogenous ATG8 nor ATG8B, and only a very small amount of endogenous ATG8A was detected in early log phase parasites, regardless of PLD treatment (figure 4.8A, B and C, lanes 1 and 2). This observation supported the earlier finding that these proteins are expressed at a low level in early log phase promastigotes (figure 4.4). ATG8 was detected in lysates from early stationary phase parasites and those which had been starved, again supporting data presented in figure 4.4. Rather than detecting two proteins which differed in

their sensitivity to PLD, only one protein of the expected size of ~13 kDa was detected and this appeared to disappear upon treatment with PLD (figure 4.8A lanes 3-6, labelled with a red arrow). It has been reported that LC3-specific antibodies preferentially recognise LC3-II over the non-lipidated form of the protein (Mizushima and Klionsky, 2007). Similarly, yeast Atg8 antibodies are more sensitive to Atg8-PE than Atg8 (Ichimura *et al.*, 2004). In both yeast and mammalian systems this difference in immunogenicity is more pronounced when antibodies are generated against the N-terminal region of an LC3 or Atg8 peptide, suggesting that conjugation to PE results in some conformational change at the N terminus, allowing the exposure of an immunogenic epitope (Mizushima and Klionsky, 2007). Antibodies against *Leishmania* ATG8 proteins were raised against full length, His tagged recombinant protein. A difference in sensitivity to lipidated and non-lipidated forms of the protein could explain this apparent disappearance of ATG8 upon treatment with PLD. The detection of presumably unlipidated ATG8 in the supernatant fraction after subcellular fractionation (figure 4.6B) could be due to high levels of unlipidated ATG8 present in cells in which autophagy has not been induced by starvation. An additional protein of slightly higher molecular weight (~ 17kDa) was detected with anti-ATG8 antibodies in starved promastigotes that was absent in lysates from non-starved cells (labelled with a black arrow on figure 4.8A, lanes 5 and 6). This protein was unaffected by treatment with phospholipase D, indicating this is unlikely to be ATG8-PE, and might instead be a different protein that is recognised by anti-ATG8.

Endogenous ATG8A and ATG8B were detected in lysates both before and after treatment with PLD (indicated with red arrows on figure 4.8B and C, lanes 3-4), suggesting that these proteins are not modified by a lipid, and supporting the evidence generated with the GFP tagged proteins (figure 4.7). Antibodies specific to *L. major* oligopeptidase B (anti-OPB), known to be expressed at a consistent level in *L. major* promastigotes (Munday, 2008), was used as a loading control (figure 4.8D). More protein was present in lanes 3 and 4 (representing early stationary phase lysates), even though an attempt was made to normalise the amount of protein loaded in each gel by quantifying the samples with the Pierce BCA assay. Importantly however, the amount of protein loaded into lane 3 is the same as in lane 4, and that in lane 5 is the same as in lane 6, showing

that the apparent “disappearance” of the ATG8 signal after treatment with PLD is not due to uneven loading, and is indeed due to effect of PLD. Treatment with PLD involved incubation of samples at 37°C for one hour prior to analysis. The detection of ATG8A and ATG8B in PLD-treated samples demonstrated that incubation at 37°C did not result in the degradation of ATG8-like proteins.

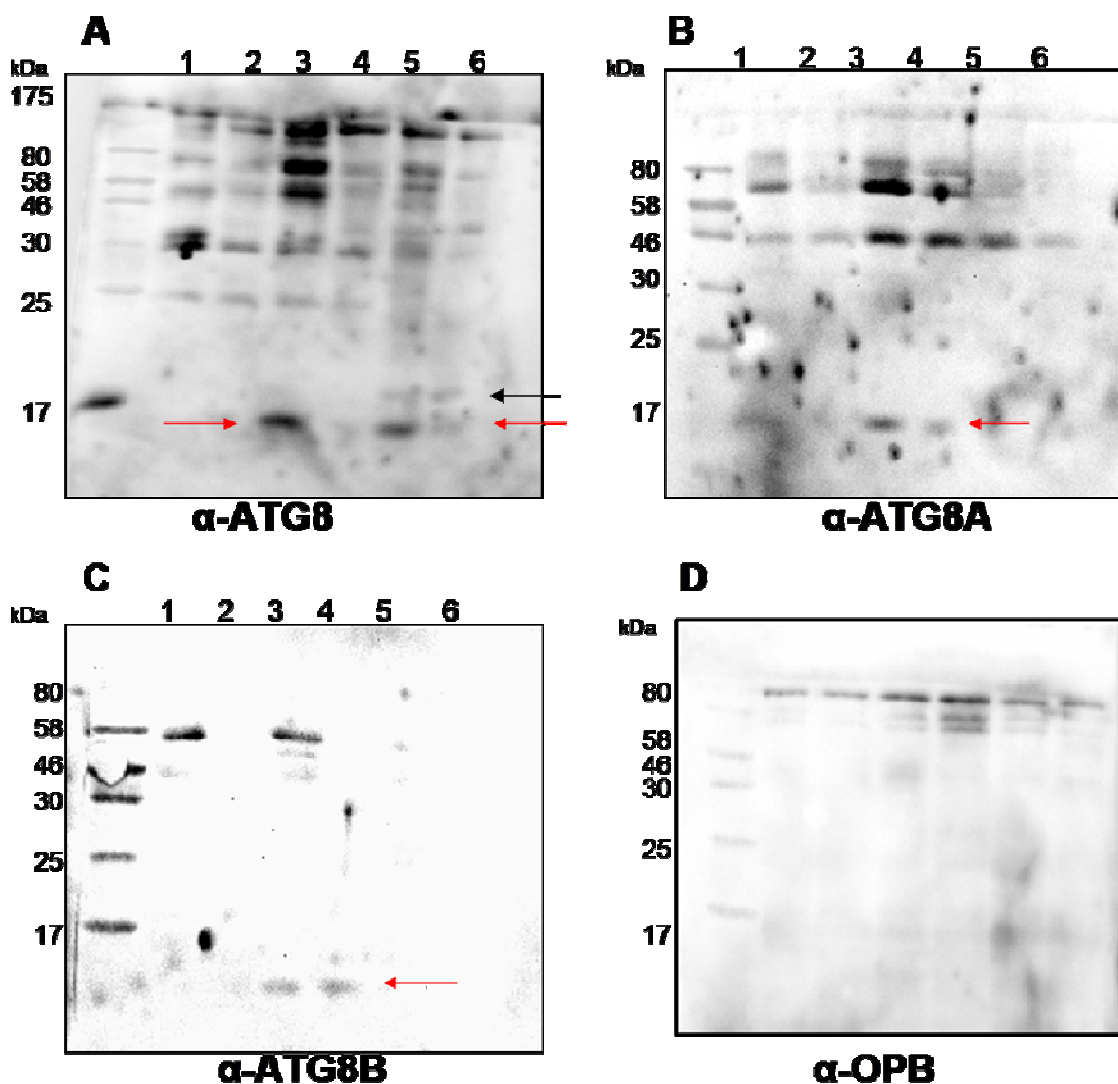


**Figure 4-8 Phospholipase D treatment of wild type *L. major* promastigotes and detection of endogenous ATG8, ATG8A and ATG8B.**

Western blot analysis was performed on lysates of early log phase, early stationary phase, and starved wild type *Leishmania* promastigotes. Cells were lysed by sonication in the presence of protease inhibitors. A pellet was collected by ultracentrifugation at 100,000 x g and solubilised in 0.2% Triton-X-100. 30 µg of each sample was incubated with 15 units of phospholipase D (PLD) for one hour at 37°C, loaded alongside untreated sample onto 15% acrylamide gel containing 6 M urea, and separated by SDS-PAGE. The gels were then transferred to a hybond-c nitrocellulose membranes and hybridised with rabbit anti-ATG8 or sheep anti-ATG8A or anti-ATG8B. Primary antibodies were used at 1 in 100 dilution, secondary antibodies were used at a dilution of 1 in 10,000. The signal was detected using West Signal supersubstrate chemiluminescence detection system (Pierce). For each gel, Lane 1 = early log phase, Lane 2 = early log phase + PLD, Lane 3 = stationary phase, Lane 4 = stationary phase + PLD, Lane 5 = starved log phase, Lane 6 = starved log phase + PLD.

### 4.3.3 Incorporation of radioactively labelled ethanolamine into *Leishmania* and immunoprecipitation of ATG8-like proteins

*In vivo* labelling experiments using radioactively labelled ethanolamine have been informative in confirming the lipid modifier of mammalian LC3 (Kabeya *et al.*, 2004), so dividing *Leishmania* promastigotes were incubated with [<sup>3</sup>H]ethanolamine and subjected to immunoprecipitation against anti-ATG8, anti-ATG8A and anti-ATG8B antibodies to attempt to determine whether they are modified by phosphatidylethanolamine. Log phase promastigotes were treated with 20 µCi [<sup>3</sup>H] ethanolamine and cultivated for 24 hours (following the method described by (Ralton *et al.*, 1998). 1 mg of purified antibody was covalently cross linked to aldehyde-activated beaded agarose (Pro-found co-IP kit, Pierce), producing reusable co-immunoprecipitation columns. Cell lysates were prepared from  $2 \times 10^8$  cells by sonication followed by high speed centrifugation to attempt to enrich for membrane bound forms of the proteins based on the information obtained from subcellular fractionation experiments, followed by solubilisation with the detergent NP-40. The lysate was incubated with immobilised antibody overnight, washed six times with PBS, and protein was eluted with 0.2 M glycine (pH 2.5). Total lysate, flow through, first and last washes and four elutions were loaded onto two 12% Bis-Tris gradient gels (Invitrogen). One gel was stained with coomassie, incubated with a fluorogenic reagent to detect [<sup>3</sup>H] labelled proteins (Amersham Amplify Fluoreogenic Reagent), and incubated with a Kodak film for one week and then two months at -80°C. To confirm the presence of ATG8, ATG8A or ATG8B in the elutions the proteins from a second gel in each case were transferred to a nitro-cellulose membrane and probed with affinity purified rabbit anti-ATG8, or sheep anti-ATG8A or anti-ATG8B antibodies. The detection of proteins of the expected size by western blot with anti-ATG8, anti-ATG8A and anti-ATG8B (and the apparent detection of ATG8A on a coomassie stained gel) confirmed that the immunoprecipitations were successful, although the signal obtained with anti-ATG8 was very weak (figure 4.9A, B, C).

Disappointingly, no radioactive signal was detected in any of the elutions after immunoprecipitation with anti-ATG8, anti-ATG8A nor anti-ATG8B (figures 4.10A, B and C), meaning that no conclusive data was obtained from this experiment. No radioactive signal was obtained even in the total cell lysate prior to

immunoprecipitation with anti-ATG8 or anti-ATG8A (figures 4.9A and B), suggesting that either the incorporation of [<sup>3</sup>H] ethanolamine into promastigotes or the detection process was unsuccessful in this experiment. A strong radioactive signal of the same size as ATG8B was detected in the flow through after immunoprecipitation against anti-ATG8B antibodies (figure 4.9C, lane 1). The presence of a radioactively labelled protein of such similar size to ATG8B in the flowthrough after immunoprecipitation with ATG8B meant that this could possibly represent ATG8-PE. However, in this experiment the total cell lysate was lost and was not analysed by SDS-PAGE.

The analysis of lipid extracts from promastigotes incubated with radioactively labelled ethanolamine has shown that radioactively labelled ethanolamine is incorporated into various species of glycosylphosphatidylinositol (GPI) glycolipids (Ralton and McConville, 1998). Less has been published on the profile of ethanolamine incorporated into parasite proteins. In *T. brucei* bloodstream forms, [<sup>3</sup>H] ethanolamine was incorporated into VSG, but into no proteins in procyclic *T. brucei*, *T. cruzi* epimastigotes or *L. mexicana* promastigotes (Rifkin and Fairlamb, 1985). In each case, most of the radioactivity was reported to migrate just before the dye front, and was assumed to be incorporated into phospholipids. However, [<sup>3</sup>H] ethanolamine has been detected in immunoprecipitated GP63 from *L. amazoniensis* cells (but not in secreted GP63) when analysed by SDS-PAGE (McGwire *et al.*, 2002). The absence of radioactively labelled bands corresponding to the predicted sizes of GP63 (69.2 KDa) in the total cell lysate in figure 4.9A and B (experiments with ATG8 and ATG8A) and the flow through in figure 4.9C (experiment with anti-ATG8B) suggests that the labelling procedure was unsuccessful, in this study and perhaps in that of Rifkin and Fairlamb (1985). On the other hand, the incorporation of [<sup>3</sup>H] ethanolamine into GP63 was only reported for immunoprecipitated protein and data for wild type cell lysates was not presented, so it could be that enrichment of GP63 by immunoprecipitation was required for detection (McGwire *et al.*, 2002).

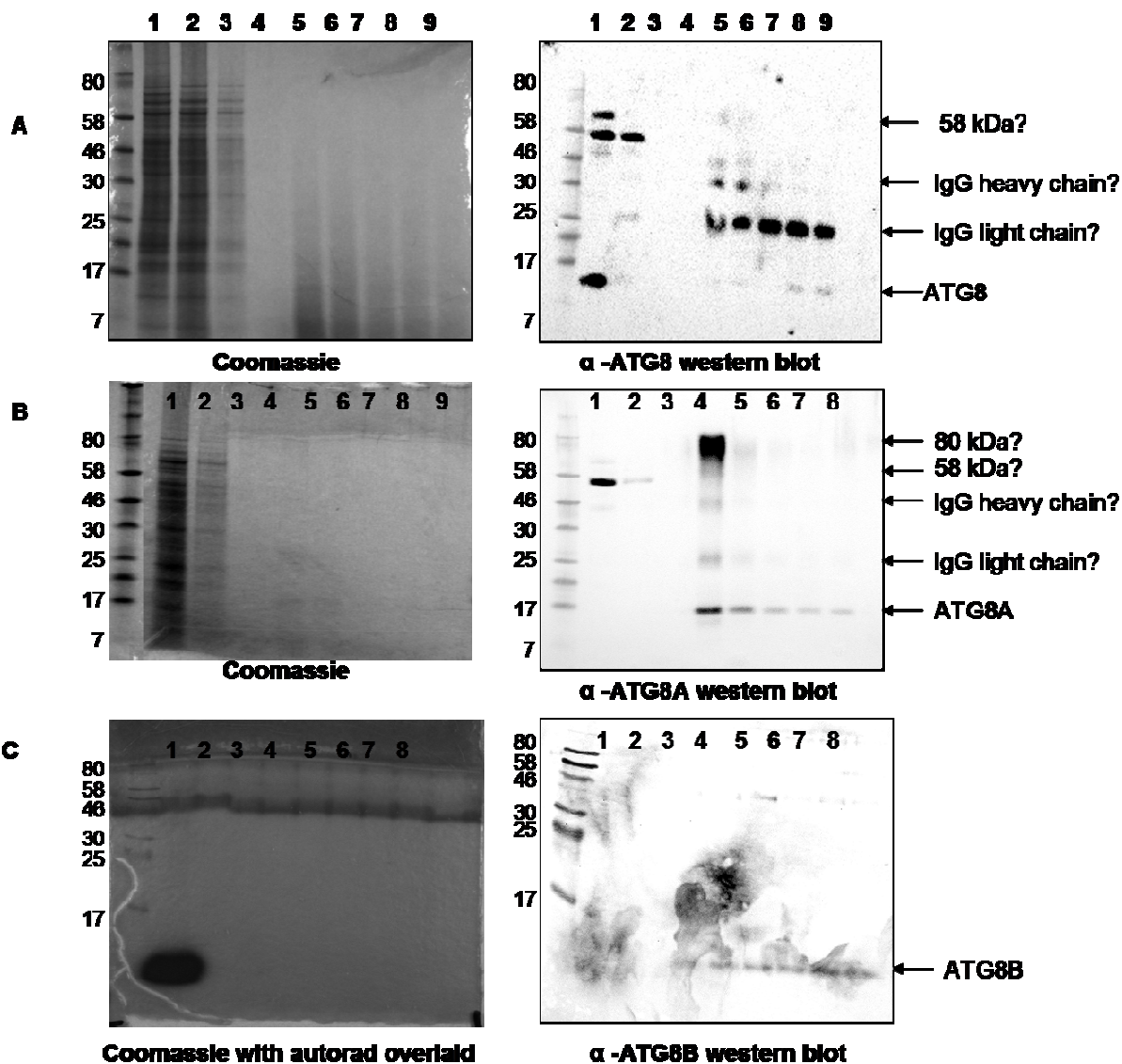


**Figure 4-9 Immunoprecipitation of radioactively labelled ATG8, ATG8B and ATG8A.**  $2 \times 10^8$  dividing promastigotes were resuspended in 10 ml fresh homem with 10% FCS and incubated with 20  $\mu$ Ci [ $^3$ H] ethanolamine for 24 hours. Autophagy was induced by starvation in PBS for four hours before immunoprecipitation with anti-ATG8 or anti-ATG8A antibodies (figure A, B). Cells were lysed by sonication followed by centrifugation at 100,000 x g and solubilisation of the pellet with NP-40 (0.2%). A reusable column for immunoprecipitation was produced by crosslinking 1 mg of purified antibody to protein X (using a co-IP column, Pierce). The lysate was incubated with the immobilised antibody overnight at 4°C. The column was washed six times in PBS, and protein was eluted from the column with 0.2 M glycine, pH 2.5. Samples were loaded onto two gradient Bis-Tris acrylamide gels and separated by SDS-PAGE. In each case, one gel was stained with Sigma Colloidal Brilliant Blue, impregnated with the fluorogenic reagent (Amersham Amplify), dried, and exposed to a Kodak film for up to two months at -80°C. The second gel was transferred to a hybond-C nitrocellulose membrane and hybridised with rabbit anti-ATG8 or sheep anti-ATG8A or anti-ATG8B (1 in 100 dilution).

**Figure 9A and 9B: Immunoprecipitation of ATG8 and ATG8A.** Left hand panel is coomassie stained gel, right hand panel is western blot. Lane 1 = total lysate, 2 = flow through, 3 = first wash, 4 = final wash, 5 – 9 = elutions 1-5. No signal was detected after incubation with the fluorogenic reagent and exposure to a film. A band of the predicted size for ATG8 or ATG8A is arrowed on the coomassie gel and on the western blot. **Figure 9C: Immunoprecipitation of ATG8B.** Left hand panel is coomassie stained gel with an autorad overlaid. Right hand panel is western blot. Lane 1 = flow through, 2 = first wash, 3 = final wash, 4 – 8 = elutions 1-5. A band of the predicted size is circled on the western blot.

## 4.4 Co-immunoprecipitation of *Leishmania* ATG8B with interacting partners

Based on the data obtained with cells expressing GFP-ATG8B it seems that ATG8B is unlikely to be involved in autophagy (chapter 3) and from the data presented here, does not appear to be modified by a phospholipid (figures 4.7C, 8C, 9C). ATG8B has been shown to be highly expressed in stationary phase parasites, where infective metacyclic promastigotes are abundant, indicating a potential role in virulence or transmission, and has been shown to be potentially derived from or maybe associated with the endosomal system (figure 3.15B). The existence of a highly specific antibody against ATG8B made a search for interacting proteins possible by immunoprecipitation.

200 ml stationary phase promastigotes were used to produce 1.5 - 1.8 mg lysate that had been enriched for membrane-bound ATG8B by subcellular fractionation, as described previously (section 4.2.2). Care was taken to perform all lysis steps at 4°C, in the presence of protease inhibitors, and to use a mild detergent (0.2% NP-40) for the solubilisation of the pellet, in order to avoid disrupting potential protein interactions. The lysate was incubated overnight with anti-ATG8B antibody that was covalently cross-linked to aldehyde-activated beaded agarose (Pierce Co-IP kit), and protein eluted as described above (section 4.3.3).

The experiment was performed three times (figure 4.10A, B and C). In the first experiment, the flow through, first wash and five elutions were loaded onto two 15% acylamide gels (figure 4.10A). In experiments two and three, total cell lysate and flow through were loaded onto two 12% Bis-Tris gradient gels (Invitrogen) along side the first and last washes and six elutions (figure 4.10B and C). One gel was stained with Colloidal Brilliant Blue Coomassie (Sigma) from which any detectable proteins in the gel were carefully removed using a clean blade and analysed, along with the concentrated eluant, by the determination of peptide mass fingerprints by electrospray ionisation mass spectrometry (table 4.1, 4.2, 4.3). The presence of ATG8B in the elutions was confirmed by transferring the second gel to a nitro-cellulose membrane and probing with anti-ATG8B antibodies (figure 4.10A, B and C, right hand panel).

For each protein identified, the protein band from which it was obtained was numbered, and the predicted size of the protein stated alongside the actual size at which that protein migrated on the gel. This was useful in some cases for identifying “false positive” results, likely the result of contamination. For example in experiment two, 2-oxoglutarate dehydrogenase E2 component (LmjF28.2420) was identified from a protein band of 23 kDa (protein 2(ii)), whereas the predicted size of the protein is 41.9 kDa, suggesting that this is very unlikely to be an interacting partner of ATG8B. In each case a probability based score was assigned, and scores of  $> 30$  indicate identity or extensive similarity (i.e.  $p < 0.05$ ).

Proteins of the ATG8B family were detected in gel slices and in the elution in experiments one and three. The fact that different ATG8B isoforms and not any of the other ATG8-like proteins were detected demonstrates the specificity of this antibody. The majority of proteins identified were abundant histones, ribosomal proteins and heat shock proteins, likely to be present in the elutions due to their high abundance in the lysate, rather than due to a direct interaction with ATG8B. Proteins of interest which are discussed in the text are highlighted in red, including alpha and beta-tubulin, ubiquitin fusion proteins LmjF14.1270 and LmjF31.1900, a putative SNARE protein LmjF06.0820, actin and ATG8B. All the proteins which are discussed have a predicted size close to or identical to the size of the protein band from which they were cut.

Proteins of ~27 kDa and ~50 kDa that were detected with anti-ATG8B antibodies by western blot are likely to be heavy and light IgG chains (labelled with arrows on figure 4.10). Although the antibodies were covalently cross-linked to the resin for co-immunoprecipitation, some antibody leaching may have occurred. In experiment two, additional, unknown proteins of ~30 and ~35 kDa were detected in the flow through and wash (labelled with arrows). Finally, two proteins of less than 17 kDa, very close in size, were detected in the elutions of experiment three. Previously, only a single protein of the predicted size for ATG8B has been detected from promastigote lysates (figures 4.4, 4.5, 4.6, 4.8, 4.9). It is possible that the use of a 12% Bis-Tris gradient gel, which allows greater resolution of small proteins, has allowed the discrimination between different isoforms of ATG8B, which are predicted to differ in size by 0.2 kDa (table 3.1).

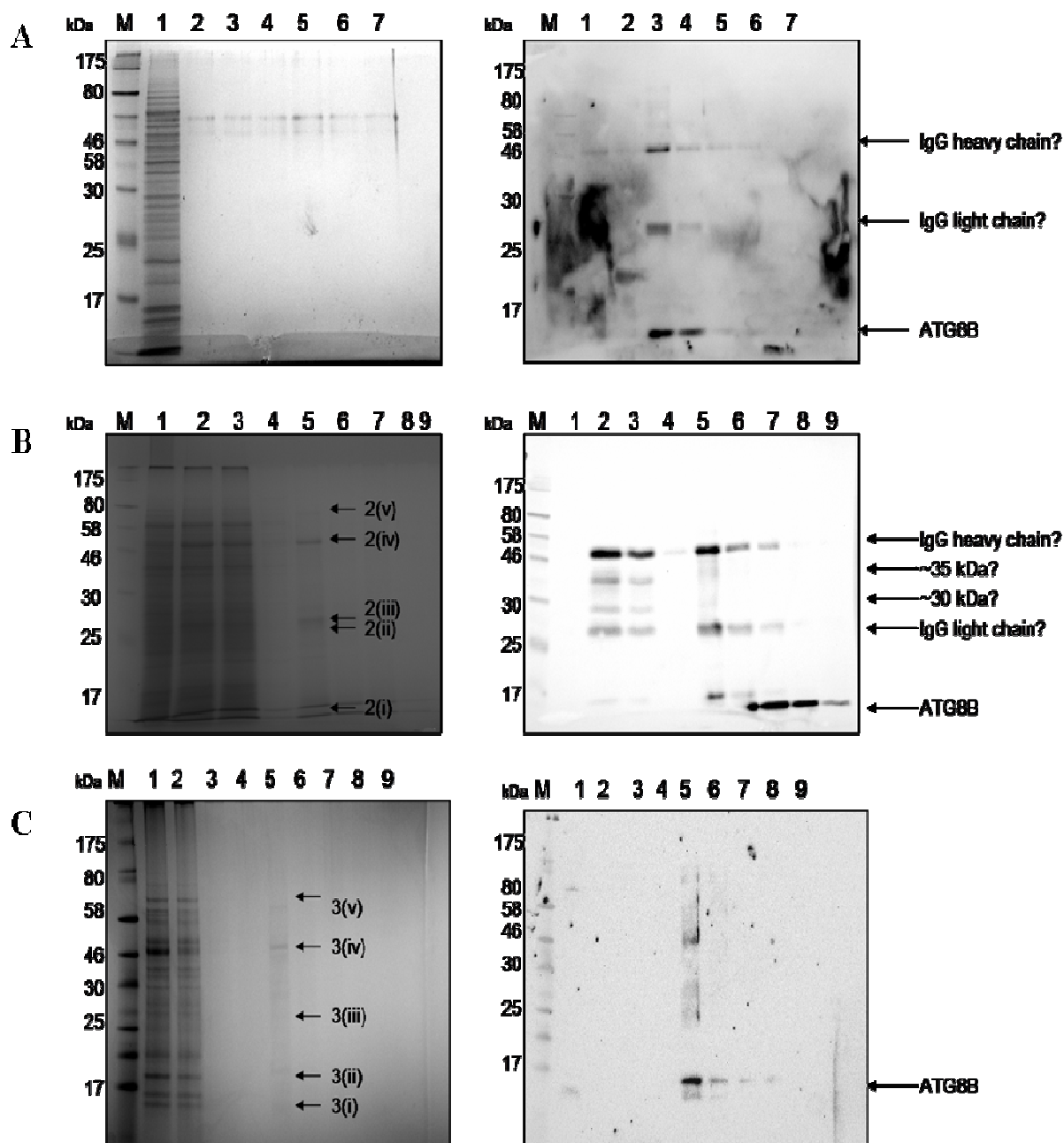


**Figure 4-10 Immunoprecipitation of ATG8B from wild type *L. major*.**

Three independent co-immunoprecipitation experiments were performed, labelled A, B and C. In each case, between 1.5 and 2 mg of parasite lysate enriched for ATG8B was obtained from 200 ml early stationary phase cells by physical lysis with alumina, ultracentrifugation at >100,000g and solubilisation of the pellet in 0.2% NP-40. A reusable column for immunoprecipitation was produced by crosslinking 1 mg of purified anti-ATG8B antibody to aldehyde-activated beaded agarose (AminoLink Plus Coupling Resin, Pierce). The lysate was incubated with the immobilised antibody overnight at 4°C. The column was washed six times in PBS, and ATG8B was eluted from the column in 0.2 M glycine, pH2.5. In each case, samples were loaded onto two gradient Bis-Tris acrylamide gels and separated by SDS-PAGE. One gel was stained with Sigma Colloidal Brilliant Blue, visible proteins are marked with an arrow and numbered (numbers correspond to data in table 4.1). Visible proteins were cut from the gel and provided for protein identification with MALDI-TOF along with concentrated elutions. The other gel was transferred to a hybond-c nitrocellulose membranes and hybridised with sheep anti-ATG8B (1 in 100 dilution). Signals for ATG8B and putative signals for IgG heavy and light chains are marked with arrows.

**Figure 4.10 A)** Lane 1 = flow through, 2 = first wash, 3 – 7 = elutions 1-5. **Figures 4.10 B and C.** Lane 1 = total lysate, 2 = flow through, 3 = wash 1, 4 = wash 6, 5 – 9 = elutions 1 – 5.

Gene ID	Annotation	Where detected?	Detected size on gel (kDa)	Predicted size (kDa)	Score
LmjF30.2460	Heat shock-70 related	Elution		68.9	120
LmjF02.0020	Histone h4	Elution		11.4	105
LmjF10.0070	Ribosomal protein 135a	Elution		16.4	71
LmjF32.2950	Nucleoside diphosphate kinase b	Elution		16.6	65
LmjF06.0010	Histone h4	Elution		11.3	64
LmjF29.2460	60S ribosomal protein L13	Elution		24.7	58
LmjF21.1060	40S ribosomal protein S23	Elution		15.9	58
<b>LmjF19.0860</b>	<b>Microtubule associated protein (ATG8B)</b>	<b>Elution</b>		<b>12.8</b>	<b>56</b>
LmjF19.0390	40S ribosomal protein S13	Elution		17.4	48
LmjF32.2690	Ribosomal protein L27	Elution		15.4	44
LmjF15.0020	60S ribosomal protein L13a	Elution		70.7	43
LmjF32.0080	60S ribosomal protein L18a	Elution		48.5	42
LmjF34.2580	hypothetical	Elution		22.5	40
LmjF26.0170	60S ribosomal protein L7	Elution		28.8	36
LmjF32.3900	60S ribosomal protein L2	Elution		28.2	36
LmjF24.0040	60S ribosomal protein L17	Elution		19.0	36
<b>LmjF14.1270</b>	<b>Ubiquitin/ribosomal protein s27a</b>	<b>Elution</b>		<b>17.0</b>	<b>35</b>
LmjF36.5850	Hypothetical	Elution		59.0	32
LmjF24.1980	Hypothetical	Elution		29.8	32
LmjF09.1340	Histone H2B	Elution		12.2	32

**Table 4-1 Potential interacting partners of ATG8B, experiment one.**

Gene ID	Annotation	Where detected?	Detected size on gel (kDa)	Predicted size (kDa)	Score
LmjF08.1230	Beta-tubulin	2(iv)	50	50.3	129
LmjF13.0280	Alpha tubulin	2(iv)	50	50.5	33
LmjF15.1040	Tryparedoxin peroxidase	2(ii)	23	23.3	101
LmjF28.2420	2-oxoglutarate dehydrogenase E2 component	2(ii)	23	41.9	68
LmjF25.2300	Hypothetical	2(ii)	23	75.4	37
LmjF16.0640	Hypothetical	2(ii)	23	74	39
LmjF20.0160	Hypothetical	2(iii)	25	87.6	36
LmjF32.2270	Membrane associated protein-like protein	2(v)	80	98	36
LmjF03.0820	Hypothetical	2(ii)	23	302.5	31
LmjF35.5180	Hypothetical	2(iv)	50	67.5	36
LmjF35.5390	Hypothetical	2(ii)	23	74.2	35
LmjF28.1650	Hypothetical	2(iii)	25	91	33
LmjF36.3970	Hypothetical	2(i)	14	146.6	30

Table 4-2 Potential interacting partners of ATG8B, experiment two

Gene ID	Annotation	Where detected?	Detected size on gel (kDa)	Predicted size (kDa)	Score
LmjF19.0820	ATG8B	3(i)	14	12.6	65
LmjF19.0860	ATG8B.5-9	3(i)	14	12.86, 12.6	54
LmjF20.1300	Calpain like cysteine peptidase	3(i)	14	14.9	45
LmjF36.6630	Hypothetical	3(i)	14	21.4	41
LmjF36.5550	Hypothetical	3(i)	14	14.6	40
LmjF32.3130	Ribosomal protein 13	3(i)	14	47.4	39
LmjF13.1220	40S ribosomal protein 13	3(i)	14	30.6	34
LmjF28.1200	Glucose related protein 78	3(iv)	50	72.1	104
LmjF31.1900	Ubiquitin fusion protein	3(i)	14	14.95	65
LmjF36.2030	Chaperone Hsp60	3(iv)	50	59.6	64
LmjF17.0870	Hypothetical	3(iv) and elution	50	49	60
LmjF14.0850	Calpain like cysteine peptidase	3(iv) and elution	50	13.04	55
LmjF13.0280	Alpha tubulin	3(iv) and elution	50	50.5	55
LmjF30.2460	Heat shock 70-related protein	3(iv)	50	69.5	54
LmjF35.3230	Cystathione gamma lyase	3(iv)	50	45	51
LmjF17.0080	Elongation factor 1-alpha	3(iv) and elution	50	49.48	46
LmjF04.1230	Actin	3(iv)	50	42.27	43
LmjF29.1270	ATP-dependent E1p protease subunit, heat shock protein 100	3(iv)	50	97.09	34
LmjF33.0850	Hypothetical	3(iv)	50	95.9	34
LmjF06.0820	Hypothetical	3(iv)	50	43.1	32
LmjF35.2210	Kinetoplastid membrane protein 11	3(iv)	50	11.2	32
LmjF32.1490	Hypothetical	3(iv)	50	22.8	31
LmjF05.0500	ATPase alpha subunit	Elution	n/a	62.79	37
LmjF21.0240	Hexokinase	Elution	n/a	51.6	89
LmjF34.2580	Hypothetical	Elution	n/a	22.5	88
LmjF15.1040	Tryparedoxin peroxidase	Elution	n/a	22.08	74

LmjF22.1310	Calpain like cysteine peptidase	Elution	n/a	14.97	62
LmjF30.3600	ATP synthase, epsilon chain	Elution	n/a	20.08	55
LmjF16.0460	60S ribosomal protein 121	Elution	n/a	18.01	46
LmjF32.0970	Calpain like cysteine peptidase	Elution	n/a	19.95	37
LmjF35.1880	60S ribosomal protein L5	Elution	n/a	33.96	37
LmjF05.0500	ATPase alpha subunit	Elution	n/a	62.5	34
LmjF36.5760	Hypothetical	Elution	n/a	188.1	34
LmjF32.0400	ATP-dependent RNA helicase	Elution	n/a	66.8	33
LmjF02.0020	Histone h4	Elution	n/a	11.4	30

**Table 4-2 Potential interacting partners of ATG8B, experiment three**

The identification of the hypothetical protein LmjF06.0820 in the immunoprecipitate was of interest, as this protein was identified (although not yet annotated) as a member of the Qc family of SNARES (Besteiro *et al.*, 2006a). SNARES are N-ethylmaleimide-sensitive factor (NSF) adaptor protein (SNAPs) receptors (SNARES), and belong to a large family of proteins involved in the docking process between donor and acceptor membranes, and considered essential for intracellular vesicular transport (Sagiv *et al.*, 2000). A recent analysis of the SNARE machinery in *Leishmania* identified 27 putative proteins, which were classified as R- and Q- groups based on the residues present in the central SNARE motif. The Q group is further classified into three; Qa (syntaxins), Qb (SNAP N-terminal) or Qc (SNAP C-terminal). Alternatively, SNARES can be classified as v-SNARES or t-SNARES based on their involvement with either the vesicle or the target membrane. The expression and localisation of members of the Qa family of *Leishmania* was studied with GFP tagged proteins, and localisations in the Golgi, late endosome / lysosome, and near the flagellar pocket were identified, indicative of roles in endo / exocytosis or intra-Golgi trafficking (Besteiro *et al.*, 2006a). Interestingly, co-immunoprecipitation experiments performed in mammalian cells have found that the mammalian ATG8 homologue GATE-16 interacts with NSF and the Golgi-specific v-SNARE GOS-28 (Sagiv *et al.*, 2000). The localisation of ATG8B to vesicle shaped structures near the flagellar pocket, and this apparent interaction with a member of the SNARE family provides some indication that ATG8B may be involved in intracellular, vesicle based trafficking. This possibility should be analysed further with co-localisation studies with members of the SNARE family, yeast-2-hybrid experiments, and further co-immunoprecipitation experiments using tagged proteins.

Two ubiquitin fusion proteins, identified in the *Leishmania* genome database as members of the ubiquitin protein family (pfam, GeneDB), were also identified as putative interacting partners of ATG8B (ribosomal protein 27a and “ubiquitin fusion protein” with a ribosomal protein L40 domain). Ubiquitin protein is usually found either freely in the cell, or conjugated via its carboxyl terminal Gly residue to a variety of proteins where it acts as a targeting signal to the proteasome. In the yeast genome, ubiquitin coding sequences were most often found either as a polymer of head-to-tail coding regions (polyubiquitins)

(Ozkaynak *et al.*, 1984), or as N-terminal fusions with ribosomal proteins L40 and S27a (Ozkaynak *et al.*, 1987, Redman and Rechsteiner, 1989), indicating that cellular ubiquitin is a product of posttranslational processing of precursor proteins in which ubiquitin is joined to itself (polyubiquitin) or to other amino acid sequences (other ubiquitin fusion proteins). It is thought that the fusion of ubiquitin to ribosomal proteins facilitates the assembly of these proteins into nascent ribosomes, so contributing to ribosomal biogenesis (Finley *et al.*, 1989). It has been shown in yeast that S27a and L40 are only capable of functioning when translated alone (not as a fusion) when over-expressed (Finley *et al.*, 1989).

In *L. major*, ubiquitin is transcribed as a fusion protein with ribosomal proteins s27a and L40 (LmjF14.1270 and LmjF31.1900 respectively) (GeneDB). In contrast, ATG8B does not exist as a gene fusion, so the putative interaction of ATG8B with LmjF14.1270 and LmjF31.1900 is not due to a gene fusion. It could be that this interaction does occur in nature, and that it represents an association of ATG8B with ubiquitin prior to its cleavage from the fusion proteins. However, it is also possible that these proteins were identified in these experiments as contaminants due to their abundance; LmjF31.1900 and LmjF14.1270 were both identified as two of the 106 most abundantly expressed transcripts in *L. major* metacyclic promastigotes (Guerfali *et al.*, 2008). Interestingly, actin (LmjF04.1230) was also identified as a putative interacting partner of ATG8B, and in the chlorarachniophyte algae actin has been identified as a novel ubiquitin fusion protein (Archibald *et al.*, 2003).

Alpha and beta-tubulin were also identified as putative interacting partners of ATG8B. Both have been identified as being highly abundant transcripts in *L. major* metacyclic promastigotes (Guerfali *et al.*, 2008), and were identified as being differentially upregulated in *L. major* metacyclic promastigotes (Mojtahedi *et al.*, 2008), so it could be that the co-immunoprecipitation of these proteins with ATG8B is simply due to their abundance. However, ATG8B shares identity with LC3, which is a member of the microtubule associated protein family (MAPs) (Halpain and Dehmelt, 2006), so this association could be genuine. Additionally, microtubules have been shown to be involved in the trafficking of ATG8 associated autophagosomes in *Leishmania* (Williams *et al.*, 2006). The potential association of ATG8B with microtubule associated proteins alpha and

beta tubulin should be further investigated, perhaps by performing immunoprecipitation experiments with anti-tubulin antibodies in *Leishmania*, or by analysing the effect of microtubule disrupting / stabilising compounds such as vinblastine or paclitaxel on the localisation and expression of ATG8B.

## 4.5 Discussion

This study has led to several interesting observations, although there are many remaining questions that need to be addressed. ATG8A, ATG8B and perhaps ATG8C appear to be highly expressed in stationary phase parasites, potentially indicating a role in transmission or virulence of the parasites. This result complements those found in a recent genome-wide analysis of gene expression in which the quantitative technique of serial analysis of gene expression of libraries constructed from mRNAs extracted from *L. major* parasites was utilised to identify mRNAs that were particularly highly expressed in the infective stage of the parasites (Guerfali *et al.*, 2008). In this paper, ATG8A and ATG8B were identified as being among the 106 most abundantly expressed transcripts in metacyclic promastigotes. It has been noted that in kinetoplastid genomes the genes of many abundant proteins exist as multicopy tandem arrays (Campbell *et al.*, 2003a). Additionally, members of the ATG8B and ATG8C families were identified in a gene expression profiling analysis of *L. major* developmental stages as being upregulated in promastigotes as compared to amastigote stages (a 2.5 fold increase). This study used a multispecies DNA oligonucleotide array to compare whole genome expression patterns of promastigote and amastigote stages between *L. major* and *L. infantum* (Rochette *et al.*, 2008). 9.3% of the *L. major* genome was found to be differentially expressed at the RNA level throughout development.

Subcellular fractionation experiments were informative, indicating that ATG8A and ATG8B, detectable only in high speed centrifugation fractions, exist as membrane associated proteins, likely associated with vesicles (Morgado-Diaz *et al.*, 2005). The data obtained using anti-ATG8C antibodies was not thought to be definitive, due to the lack of specificity of the antibody, and so data obtained with anti-ATG8C are not discussed. Interestingly, the localisation profile of ATG8B and ATG8A differed from ATG8, which was found in all fractions (although at very low levels). Similarly to *Leishmania* ATG8, mammalian LC3

was found in all fractions following subcellular fractionation, and its association with membranes as been found to be dependent on its modification with PE (Tanida *et al.*, 2003). It was shown that while GATE-16 and GABARAP are capable of being modified by PE, they were associated with membranes regardless of their state of modification by PE. In this study, the nature of the association of ATG8A and ATG8B with membranes was not investigated, and an analysis of their solubility in salt buffers and detergents would be informative as to the nature of such an association. It would be expected that ATG8A and ATG8B could be solubilised from the P3 fractions without the need for detergents, as a tight-association with a membrane (and so requiring detergent for the solubilisation) would require either a transmembrane domain, which is not present, or an association with a lipid or a GPI anchor, for which we have found no evidence. The detection of various higher molecular weight proteins in addition to ATG8A or ATG8B (for example figures 4.5B and 4.6C for ATG8A or figure 4.10B for ATG8B) might point to a direct conjugation with a membrane protein.

ATG8 was clearly shown to be post-translationally modified by a phospholipid, likely to be PE (Besteiro *et al.*, 2006, and this study figures 4.7 and 4.8). The lack of sensitivity of ATG8A and ATG8B to phospholipase D suggests that, despite being susceptible to cleavage by ATG4.1 and ATG4.2 (Williams *et al.*, 2009) these proteins are not modified by a phospholipid. Ethanolamine labelling experiments were not conclusive, as incorporated ethanolamine could not be detected in immunoprecipitated ATG8. This could be due either to a low level of ATG8 immunoprecipitation (the protein detected by immunoblotting with anti-ATG8 was very faint, figure 4.9A), or due to lack of uptake of ethanolamine by the promastigotes, as no radioactivity was detected in total cell lysate. The presence of a radioactively labelled molecule at ~ 15 KDa in the flow through after immunoprecipitation with ATG8B might represent lipidated ATG8. The absence of a detectable radioactive signal in ATG8B IP elutions may provide evidence that this protein is not modified by PE. However, without showing that the experiment was successful by the identification of [<sup>3</sup>H] ethanolamine in elutions after IP with anti-ATG8, conclusions cannot be drawn from this experiment.

[<sup>3</sup>H]ethanolamine was detected in immunoprecipitated GP63 from *L. amazonensis*, although the profile of [<sup>3</sup>H]ethanolamine incorporation into whole cell lysate was not shown (McGwire *et al.*, 2002). The biosynthetic incorporation of [<sup>3</sup>H]ethanolamine into proteins was investigated in human erythroleukemia cells (line K562), and a single predominant labelled protein was detected and shown to be elongation factor alpha (EF1- $\alpha$ ) (Rosenberry *et al.*, 1989). The lack of detection of radioactively labelled EF1- $\alpha$  or GP63 in *L. major* whole cell lysate might indicate that the uptake of [<sup>3</sup>H]ethanolamine was unsuccessful in this study. A useful control to ensure that ethanolamine was being taken up by promastigotes would be to perform immunoprecipitation experiments using anti-EF1 $\alpha$  antibodies. Additionally, scintillation measurements could be taken to ensure that that [<sup>3</sup>H]ethanolamine was taken up by the promastigotes.

PE is significantly upregulated in *Leishmania* stationary phase, and the analysis of *Leishmania* mutants either deficient in sphingolipids (sp2- mutant) (Zhang *et al.*, 2003, Denny *et al.*, 2004) or unable to degrade sphingolipids (spl- mutants, (Zhang *et al.*, 2007) identified defects in stationary phase differentiation and virulence which were shown to be directly attributable to a lack of ethanolamine (Zhang *et al.*, 2007). These data suggest that PE has an involvement in the differentiation into infective metacyclic promastigotes, perhaps through its conjugation to ATG8 and its involvement in autophagy, or perhaps due to independent roles of ethanolamine (Zhang *et al.*, 2007). In *Leishmania*, the majority of PE is found in the form of plasmalogen PE (Zhang *et al.*, 2003; Zufferey *et al.*, 2003), whereas in most organisms, PEs are a mix of diacyl and alkylacyl PEs (Nagan and Zoeller, 2001), perhaps making the enzymes involved in the biosynthesis of PE an interesting target for drug development.

The conjugation target of Atg8 is the amino group in the hydrophilic head of PE. Phosphatidylserine (PS) also has an amino group in the head moiety, and so could theoretically be a target of Atg8. When the conjugation system for mammalian Atg8 homologues was reconstructed *in vitro* using purified Atg proteins (Atg8, Atg7 and Atg3), ATP and synthetic phospholipid liposomes, LC3, GATE-16 and GABARAP were all found to conjugate to both PE and PS, showing that either phospholipid can act as the target of mammalian Atg8 homologues *in vitro*, although analysis of extracted phospholipids from purified LC3-II by thin layer chromatography demonstrated that PE and not PS is the *in vivo* target of

LC3 (Sou *et al.*, 2006). It was also shown in yeast that Atg8 can conjugate PS *in vitro* (Hanada *et al.*, 2007), although it was later shown however that the *in vitro* PS conjugation of Atg8 is markedly suppressed at physiological pH (Oh-oka *et al.*, 2008). The possibility that *L. major* ATG8 is modified by PS could be investigated by the incorporation of radioactively labelled serine.

In order to determine unequivocally the nature of the conjugation target of *Leishmania* ATG8 homologues, phospholipids extracted from purified ATG8-PE must be analysed by mass spectrometry, as has been done previously for yeast Atg8 (Ichimura *et al.*, 2000). To achieve this, lipidated ATG8 should be purified by immunoprecipitation, the phospholipids released either by the delipidating action of *L. major* ATG4.2 (Williams *et al.*, 2009) or by phospholipase D, and analysed by MALDI-TOF-MS. In this study, a sufficient amount of purified ATG8 was not obtained to achieve this, probably due to the low sensitivity of *L. major* anti-ATG8 antibodies. Further attempts to purify endogenous ATG8 should be made, perhaps by trying to make a co-immunoprecipitation column with larger quantities of anti-ATG8, or by performing the immunoprecipitation experiment with lysate produced from a larger number of cells.

The co-immunoprecipitation of ATG8B with ubiquitin fusion proteins, microtubule associated proteins and, perhaps most interestingly, a putative SNARE provides a good basis for future investigations. Although ATG8B itself was identified in two out of three experiments (experiments one and three), alpha tubulin was the only other protein to be detected more than once (in experiments two and three). This might suggest that the proteins identified were due to contamination or due to their high abundance in stationary phase promastigote lysates, rather than a genuine interaction with ATG8B. This lack of reproducibility could be due to the sensitivity of putative ATG8B conjugations to lysis methods, or perhaps the interaction of ATG8B with other proteins occurs transiently. The co-purification of ATG8B with a SNARE should be investigated further by fluorescent co-localisation studies and by performing pull down experiments from *Leishmania* promastigotes expressing tagged versions of ATG8B. Data produced in chapters 3 and 4 are considered together with recent analyses of the cysteine peptidases ATG4.1 and ATG4.2 (Williams *et al.*, 2009) in the general discussion.

## **5 Characterisation of *Leishmania major* Presenilin-1**

## 5.1 Introduction

### 5.1.1 General Introduction

An analysis of the completed *Trypanosoma brucei* genome revealed that approximately 2% of protein coding genes represent peptidases, and that just two aspartic peptidases can be found in the *L. major* genome (Ivens *et al.*, 2005). Aspartyl-peptidases have been identified as virulence factors in various pathogenic organisms and have potential as drug targets, making it of interest to study the potential roles of aspartic peptidases in *Leishmania* virulence. For example, an inhibitor of HIV-1 peptidase has been licensed for the treatment of AIDS (Scharpe *et al.*, 1991), and inhibitors of plasmepsins have been considered as viable targets for the treatment of malaria (Ersmark *et al.*, 2006).

The two aspartic peptidases encoded in the *Leishmania* genome share some sequence similarity with presenilin-1 (PS1) and signal peptide peptidase (SPP). PS1 is a polytopic integral membrane protein that in mammalian cells assembles with nicastrin, PEN-2 and APH-1 to form an active  $\gamma$ -secretase complex (Spasic *et al.*, 2006). Homologues of the  $\gamma$ -secretase co-factors, PEN-2, APH-1 and nicastrin, absolutely required for  $\gamma$ -secretase function in humans, are absent in *Leishmania*. Therefore, functions of PS1 that are independent from  $\gamma$ -secretase mediated proteolysis might be identified in *L. major*. PS1 is contained in clan AD of aspartic peptidases, (classified as endopeptidases that hydrolyse peptide bonds within biological membranes), family A22A (MEROPS data base <http://merops.sanger.ac.uk/>).

The best known role for PS1 (and the  $\gamma$ -secretase complex) is in the intramembrane proteolysis of the amyloid precursor protein (APP), leading to the liberation of amyloid  $\beta$  peptide (A $\beta$ ); a major feature and initiator of pathogenesis in Alzheimer's disease (De Strooper and Woodgett, 2003). In addition to this, PS1 has been implicated in a wide range of biological processes including a suggested role in the maturation of autophagic vacuoles (Eskelinen, 2005).

This study aimed to determine the role of PS1 in *L. major*, with the working hypothesis that PS1 could play a role in regulating autophagy and therefore be

involved in turnover of proteins and life cycle progression of the parasite. An analysis of PS1 expression and localisation of PS1 was attempted, and the production of and subsequent analysis of  $\Delta ps1$  mutants are described.

### 5.1.2 Presenilin-1 and it's role in Alzheimer's Disease

The human PS1 gene was first identified on chromosome 14 (14q24.3) during genetic linkage studies in families with a history of Alzheimer's disease (familial Alzheimer's disease, FAD) (Sherrington *et al.*, 1995, Levy-Lahad *et al.*, 1995). Four genes were identified in these studies that contribute to FAD; the E4 allele of the apolipoprotein E (APOE) gene modifies the risk of developing some forms of AD, and causative mutations have been described in the genes encoding  $\beta$ -Amyloid precursor protein ( $\beta$ -APP), presenilin-1 and presenilin-2 (Brunkan and Goate, 2005).

AD is pathologically characterised by the loss of neuronal cells and by the accumulation of neurofibrillary tangles (NFT) and senile plaques in the brain.  $A\beta$ , which is produced by the proteolytic processing of APP, is a primary component of such senile plaques, believed to be an important cause of the neuronal degeneration that is characteristic of AD. APP is cleaved in two places to generate amyloid- $\beta$ -peptide ( $A\beta$ ). The first cleavage event is carried out by  $\beta$ -secretase to produce the membrane bound carboxy-terminal fragment of APP which is subsequently cleaved by the  $\gamma$ -secretase complex, of which PS1 is an essential component (figure 5.1). Elevated levels of  $A\beta_{42}$  (the 42 residue form of  $A\beta$ , and the form which is most associated with familial AD) were identified in plasma of patients with PS1 or PS2 mutations (Scheuner *et al.*, 1996), and the overexpression of mutated PS1 or PS2 in mice led to the accumulation of  $A\beta_{42}$  (Xia *et al.*, 1997).

In addition to the proteolysis of APP,  $\gamma$ -secretase is also required for the cleavage of Notch, another type 1 membrane protein, and PS1 is required in mammalian cells, *C. elegans* and *Drosophila* to facilitate Notch signalling (Periz and Fortini, 2004, Levitan and Greenwald, 1995, Ye *et al.*, 1999).

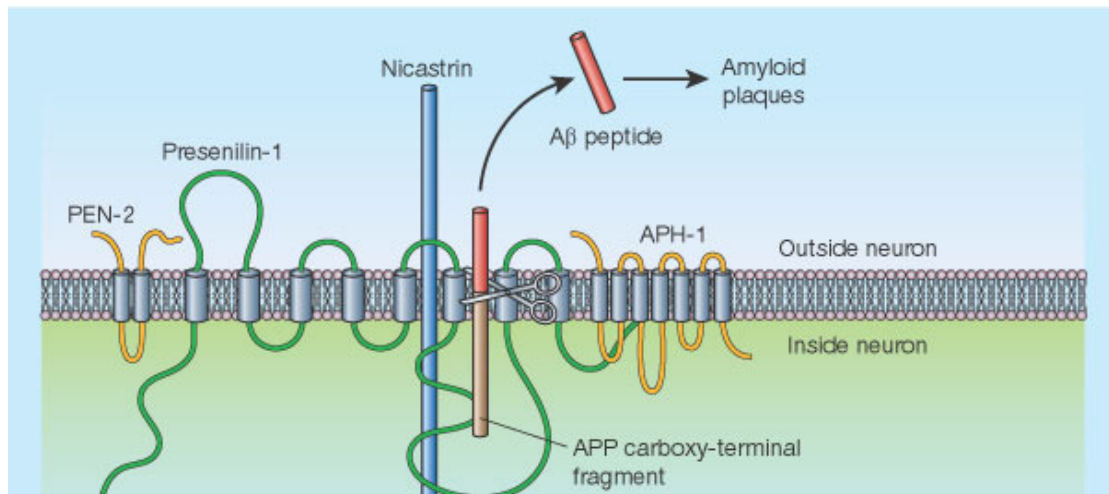


**Figure 5-1** The role of the  $\gamma$ -secretase complex in amyloid plaque formation in Alzheimer's Disease. (taken from de Strooper *et al.*, 2003).

### 5.1.3 Expression and Localisation of Presenilin-1

PS1 homologues have been identified in a range of multicellular organisms, including species from the mammals, frogs, flies, worms, fish and plants (Brunkan and Goate, 2005). Semi-quantitative reverse-transcribed RNA analysis (RT-PCR) and immunoblot analyses have demonstrated that PS1 and PS2 are expressed in most human adult tissues and in all brain regions (Brunkan and Goate, 2005), and that PS1 is upregulated in the cortex of new born mice, indicating a potential role in brain development and maturation (Lee *et al.*, 1996). PS1 mainly localises to the endoplasmic reticulum (ER) and the Golgi compartments (Baumann *et al.*, 1997, De Strooper *et al.*, 1997, Annaert and De Strooper, 1999), with a small proportion of PS1 detected at the cell surface and endosomal compartments (Dewji, 2005, Lah and Levey, 2000).

### 5.1.4 Structure and Processing of Presenilin-1

Human PS1 is a polytopic integral membrane protein of 467 amino acids, and a molecular weight of 57 kDa (Sherrington *et al.*, 1995). Ten hydrophobic regions are identified by hydropathy plots, leading to a prediction that PS1 contains seven to ten transmembrane domains (Brunkan and Goate, 2005). Several groups have attempted to determine the orientation of PS1 in the membrane and the number of membrane spanning domains, and in the absence of high-resolution X-ray crystallographic analysis of PS1 crystals, several different models have been proposed based on experimental evidence obtained mainly

with antibody staining and the use of tags placed at various places in the PS1 molecule (Brunkan and Goate, 2005).

Previously, an eight TM domain topology organization for PS1, where only 8 out of 10 hydrophobic domains cross the membrane, with both amino (N) and carboxy (C) tails facing the cytoplasm, was generally accepted (Li and Greenwald, 1996, Li and Greenwald, 1998, Kim and Schekman, 2004). However more recently, a nine TM domain topology was been suggested based on an N-linked glycosylation scanning approach (Laudon *et al.*, 2005, Spasic *et al.*, 2006, Laudon *et al.*, 2007). This model, which is supported by bioinformatics data (Henricson *et al.*, 2005) is in accordance with the other TM predictions, except for the localisation of the C terminus in the luminal side of the ER.

PS1 undergoes post translational endoproteolytic processing resulting in a 27-30 kDa N terminal fragment (NTF) and a 17-20 kDa C terminal fragment (CTF) with little full length PS1 detectable (Thinakaran *et al.*, 1996). The active site aspartate residues are each located in one fragment, D<sup>257</sup> in the NTF and D<sup>385</sup> in the CTF, and the two fragments remain associated to form the active PS molecule (Brunkan *et al.*, 2005). PS1 has been shown to be expressed predominantly in its cleaved form in all systems studied (Brunkan and Goate, 2005), and this NTF/CTF heterodimer is believed to be the biologically active form of PS1 in the  $\gamma$ -secretase complex (Laudon *et al.*, 2007). The enzyme responsible for this cleavage, termed “presenilinase”, remains unknown although it shares many characteristics of  $\gamma$ -secretase. Both proteases require the critical aspartate residues D<sup>257</sup> and D<sup>385</sup> for activity, both activities have been shown to be membrane associated, and both can be inhibited by pepstatin A and various  $\gamma$ -secretase inhibitors, leading to the suggestion that the same  $\gamma$ -secretase active site within PS that cleaves APP and Notch could also cleave and activate PS1 itself (Campbell *et al.*, 2002, Wolfe *et al.*, 1999). However, two potent inhibitors of  $\gamma$ -secretase activity, DAPT (Doverly *et al.*, 2001) and compound E (Seiffert *et al.*, 2000) had very little effect on presenilinase activity at 400  $\mu$ M, suggesting that presenilinase and  $\gamma$ -secretase are in fact pharmacologically distinct (Campbell *et al.*, 2003b).

### 5.1.5 Activity and Specificity of Presenilin-1

Two critical aspartic acid residues (positions 257 and 385 which reside within TM domain 6 and 8 respectively) were identified when it was shown that mutation of either of these residues in human recombinant PS1 resulted in defects in A $\beta$  secretion and an accumulation of C terminal fragments of APP (the substrate of  $\gamma$ -secretase). This led to the suggestion that PS1 is an unusual di-aspartyl peptidase that catalyses the intramembrane proteolysis of APP (Wolfe *et al.*, 1999). The catalytic active site of PS in the N terminal fragment (TM6) is embedded in a YD motif that is highly conserved across species (Steiner *et al.*, 2008). The equally highly conserved GXGD motif in TM 7 is similar to the putative aspartyl catalytic domain of the bacterial polytopic membrane protein prepilin peptidase (LaPointe and Taylor, 2000, Steiner *et al.*, 2000), indicating that this motif could be important for proteolytic cleavage within transmembrane domains. In addition to the conserved Asp residues in the YD and LGLGD motifs, the PALP residues in the carboxyl termini of the proteins are conserved in presenilin and “presenilin homologues” (PSH’s), and are required for normal conformation of the active site of  $\gamma$ -secretase and SPP (Wang *et al.*, 2006).

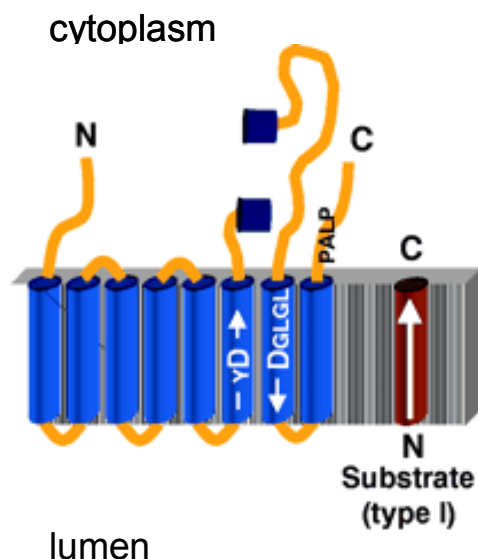


**Figure 5-2 A model of human PS1 (taken from Xia and Wolfe, 2003).** Eight transmembrane domains are shown, with both the N- and C-termini facing the cytoplasm. The active site motifs, YD and DGLGL are located in the TM domains 6 and 7 (where domain 7 consists of a cytoplasmic hydrophilic loop). The conserved PALP motif, thought to be required for the normal conformation of PS1 is located in the carboxyl terminus.

### 5.1.6 Biological Roles of Presenilin-1 independent of the $\gamma$ -secretase complex

In addition to its well documented role in the intramembrane proteolysis of APP as part of the  $\gamma$ -secretase complex, PS1 has also been implicated in the regulation of various cellular processes that are independent of  $\gamma$ -secretase (McCarthy, 2005). PS1 has been shown to interact with proteins involved in vesicle transport including Rab11 (Dumanchin *et al.*, 1999), syntaxin 5 (Suga *et al.*, 2004) and syntaxin 1A (Smith *et al.*, 2000). In addition to this, PS1 has been shown to play roles in calcium channel regulation (Leissring *et al.*, 2001), and trafficking of secretory proteins to the cell surface (Naruse *et al.*, 1998, Kaether *et al.*, 2002).  $\Delta ps1$  null mutant mice die *in utero*, and  $\Delta ps1$  embryos have multiple abnormalities including smaller size, skeletal malformations, nervous system hemorrhages, and fewer neurons (Wong *et al.*, 1997).

Some evidence has accumulated indicating that PS1 may have a role in the maturation of autophagic vacuoles. Two presynaptic membrane proteins, synuclein  $\alpha$  and  $\beta$ , were found to accumulate in enlarged vacuoles in the fibroblasts and primary neurons of  $\Delta ps1$  mouse embryos (Wilson *et al.*, 2004). The abnormally large vacuoles were shown to be autophagic or lysosomal in nature by TEM analysis, and also by the presence of Lamp-1, Lamp-2 and cathepsin D, all markers of autophagic vacuoles. The use of the  $\gamma$ -secretase inhibitors (transition-state analogues L-685,458 and III-21C, difluoroketone DFK-167, dipeptide aldehyde 2-Naphthyl-VF-CHO and LiCl) demonstrated that this phenotype was due to the loss of PS1, independent of  $\gamma$ -secretase. By manipulating the calcium levels in  $\Delta ps1$  neurons (with SKF 96365, a specific inhibitor of capacitative calcium channels in the plasma membrane), the authors showed that the formation of enlarged autophagic vacuoles might be due to the elevated levels of calcium stores in the ER (Wilson *et al.*, 2004).

An accumulation of the neuron-specific intracellular adhesion molecule telencephalin (TLN) was observed in abnormally large autophagic vacuoles of  $\Delta ps1$  hippocampal neurons, a phenotype that could be rescued with FAD linked F<sup>348A</sup> or D<sup>257A</sup> dominant negative  $\Delta ps1$  null mutants, demonstrating that this role

of PS1 was independent of  $\gamma$ -secretase (Esselens *et al.*, 2004). These enlarged vacuoles were positive for the autophagy markers LC3 and Atg12. While LC3 is an established marker of autophagosome membranes, Atg12 normally dissociates from the autophagosome prior to completion. Thus, the stable association of Atg12 with these structures suggested that the normal formation and maturation of autophagosomes is impaired in  $\Delta ps1$  neurons (Esselens *et al.*, 2004).

Autophagy has been described as an A $\beta$ -generating pathway in AD, and therefore a contributory factor to pathogenesis caused by AD (Yu *et al.*, 2005). The expression of LC3-II is significantly upregulated in the pre-pathological stages of AD in the brains of human AD patients and also in mouse models of AD in which a mutated form of PS1 and a variant of A $\beta$  are expressed (Nixon *et al.*, 2005; Yu *et al.*, 2005). In addition to this, autophagic vacuoles (AVs), rarely seen in normal adult brains, accumulated as disease progressed. PS1 and nicastrin were highly enriched within isolated AVs, and the use of autophagic inhibitors showed that A $\beta$  is generated within these AVs (Yu *et al.*, 2005; Yu *et al.*, 2004). Oxidative stress, an early determinant of AD, was shown to induce intralysosomal A $\beta$  accumulation via the induction of autophagy (Zheng *et al.*, 2006a; Zheng *et al.*, 2006b).

### **5.1.7 Aspartyl peptidase activity in *Leishmania***

The presence of aspartic-peptidase activity was detected for the first time in *Leishmania* in a study which monitored peptidase activities during differentiation in *L. amazonensis* from promastigote to amastigote form by incubating protein lysate with specific synthetic chromogenic substrates (N-Cbz-Pro-Phe-His-Leu-Leu-Val-Tyr-Ser  $\beta$ -naphthylamide for aspartic peptidases) (Alves *et al.*, 2005). The activity could be inhibited with the classic aspartyl inhibitor pepstatin. Metallo-, serine-, and aspartic peptidase activities were shown to be greater in promastigote stages, to gradually increase in the early hours of the *in vitro* differentiation process, before being down-regulated upon parasite transformation into amastigotes. On the other hand, cysteine peptidase activity gradually increased throughout transformation (Alves *et al.*, 2005).

More recently, an aspartyl peptidase activity that was detected in the soluble fraction of *L. mexicana* promastigote lysate was characterised (Valdivieso *et al.*,

2007). In this study, a synthetic substrate that is selective for Cathepsin D like aspartic-peptidases (benzoyl-Arg-Gly-Phe-Phe-Leu-4-methoxy- $\beta$ -naphthylamide) was used to detect activity. The aspartic-peptidase inhibitor diazo-acetyl-norleucinemethylester (DAN) (van Zandbergen *et al.* 2004) inhibited the proteolytic activity with an  $IC_{50}$  of 400  $\mu$ M, while 5  $\mu$ M pepstatin, a concentration sufficient to inhibit pepsin and cathepsin D, failed to inhibit aspartic peptidase activity in *Leishmania*. DAN was shown to inhibit *in vitro* proliferation of *L. mexicana*, with an  $LD_{50}$  of 466  $\mu$ M at 48 hours post treatment, with a drop of  $LD_{50}$  to 22  $\mu$ M after 72 hours of treatment. Promastigotes grown in the presence of DAN became spherical shaped and contained at least 2 nuclei per cell. These two studies represent the only published research on aspartic peptidases of *Leishmania*.

## **5.2 Alignments and phylogenetic analyses of *L. major* presenilin-1**

The *L. major* gene LmjF15.1530 encodes a protein (PS1) with 31% sequence identity at the protein level with human PS1. Based on the conservation of PALP residues in the carboxyl termini, two critical aspartic residues in the YD and LGLGD motifs, and the prediction of 7 probable transmembrane helices (at residues 16-38, 71-93, 100-122, 135-157, 164-186, 287-309 and 316-338) by TMHMM2.0 (GeneDB), LmjF15.1530 has been identified as a probable PS1 homologue. Interestingly, *L. major* lacks sequence within domain 7 where the site of endoproteolytic cleavage to produce N and C terminal fragments is, perhaps indicating that *L. major* PS1 may not be processed in the same way as the mammalian protein (figure 5.3A). *L. major* PS1 is predicted by SignalP 2.0 HMM to contain an N terminal signal sequence with a predicted cleavage site between residues 37 and 38 (figure 5.3B).

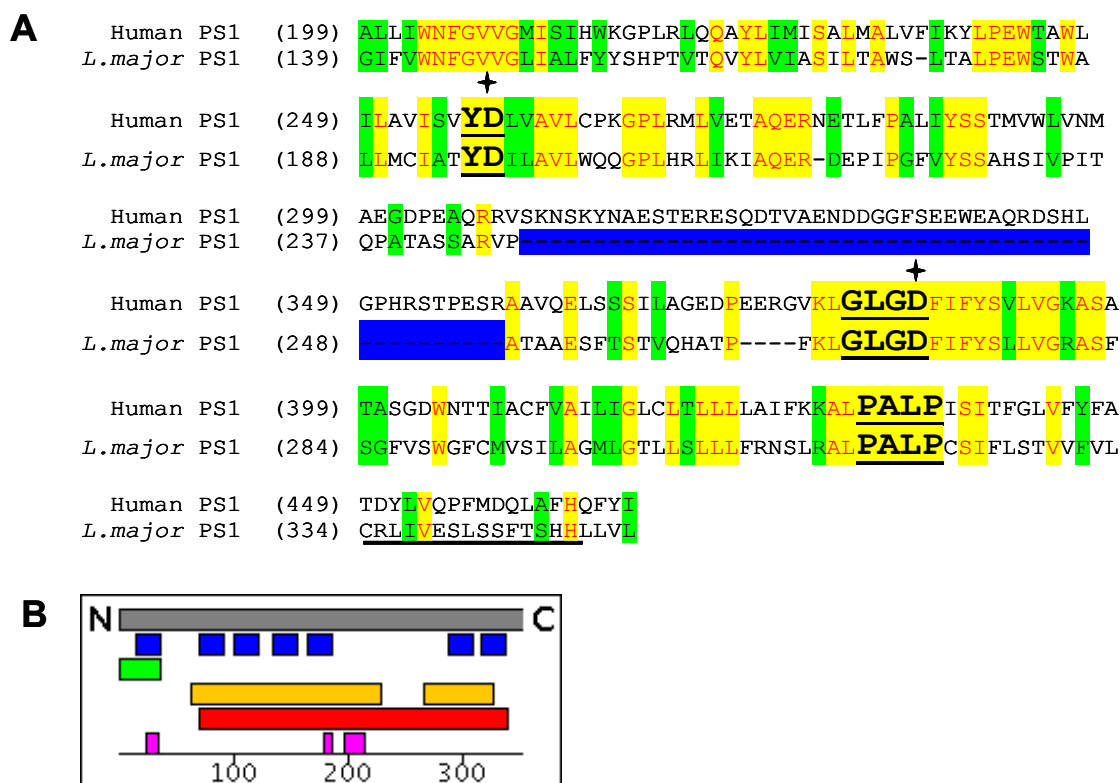


**Figure 5-3 Sequence analysis of *L. major* PS1** **A) Alignment of *L. major* and human PS1.** Identical amino acids are shown on a yellow background, while similar sequences are shown on a light green background. Sequences were aligned using the Clustal W algorithm of the Align X program (Vector NTI Advance 10 package, <http://www.informaxinc.com/>). Human PS1 accession number is AAB46371. Conserved motifs YD, GLGD and PALP are highlighted in bold and underlined, and conserved aspartate residues (positions 257 and 385 in human and 196 and 270) are marked with a star. *L. major* PS1 is missing the sequence that spans domain 7, and the position of the missing sequence is highlighted in blue. The peptide sequence that was used to raise antibodies specific to PS1 (amino acids 334 – 348) is underlined in black, and the signal sequence predicted by SignalP 2.0 HMM (Signal peptide probability 0.164, signal anchor probability 0.821 with cleavage site probability 0.088 between residues 37 and 38) is underlined in red. **B) Graphic representation of the PS1 gene.** 7 probable transmembrane helices were predicted for LmjF15.1530 by TMHMM2.0 at residues 16-38 (although this overlaps with an N terminal signal sequence), 71-93, 100-122, 135-157, 164-186, 287-309 and 316-338) are shown in blue. Predicted signal sequence is represented in green. Domains recognised by Pfam (Accession PF01080), SMART (Accession number SM00730) and PRINTS (PR01072) databases are represented in yellow, green and pink respectively.

PS1 homologues have been identified in the other trypanosomatid species, but are absent from *P. falciparum* and other apicomplexans. *L. major* PS1 shares 98% and 84% identity with *L. infantum* and *L. braziliensis* PS1 proteins, and 42% and 40% with *T. brucei* and *T. cruzi* proteins.

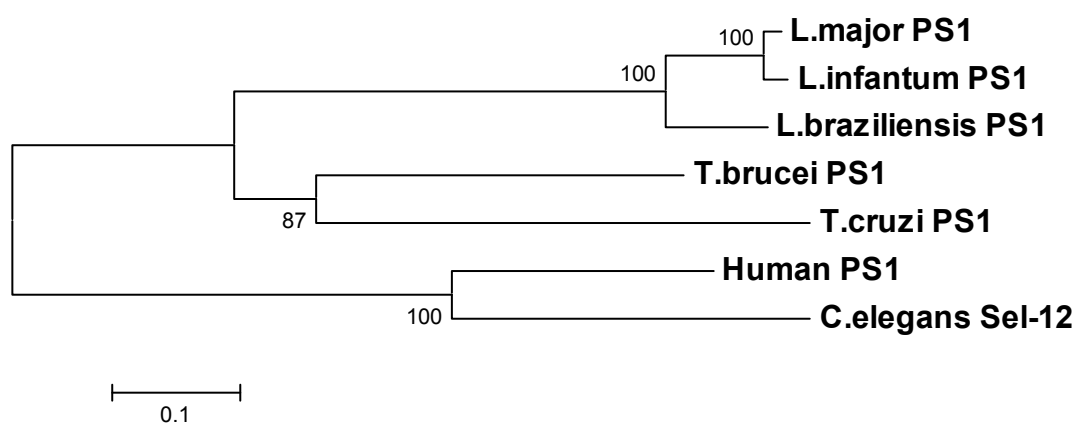


**Figure 5-4 Phylogenetic analysis of PS1 proteins from *C. elegans*, humans, *T. brucei*, *T. cruzi* and *Leishmania* spp.** The relationship between the PS1 protein of *L. major*, *T. brucei*, *T. cruzi*, *C. elegans* and *Homo sapiens* are shown on this tree. Bootstrap values from 10,000 pseudoreplicates are shown on the nodes. The scale bar represents a distance of 0.1 substitutions per site. The accession numbers and genedb designations are as follows: *L. major* PS1 (LmjF15.1530), *L. infantum* PS1 (LinJ15\_V3.1600), *L. braziliensis* PS1 (LbrM15\_V2.1530), *T. brucei* PS1 (Tb09.160.3510), *T. cruzi* (Tc00.1047053503543.10), Human PS1 (AAB46371), *C. elegans* Sel-12 (AAD50991)

### 5.3 Expression of *L. major* PS1 mRNA

To determine whether the gene for *L. major* PS1 was transcribed, total RNA from *L. major* promastigotes and amastigotes was isolated and converted to cDNA, and reverse transcriptase-PCR (RT-PCR) was performed using an mRNA-specific splice leader primer with a PS1 specific primer. The 39-41 nucleotide spliced leader RNA is added to the 5' terminus of all known protein-encoding RNAs. The spliced leader acceptor site is an AG dinucleotide immediately downstream of a polypyrimidine tract (Clayton and Shapira, 2007).

Transcript was detected in both promastigote and amastigote stages (figure 5.5A), while in controls carried out in the absence of the reverse transcriptase enzyme, no PCR product was obtained. Because in kinetoplastids, gene expression is often regulated at the level of translation, the presence of mRNA does not necessarily mean that the corresponding protein will be expressed (Clayton, 2002). The mRNA-derived PCR product was cloned into the subcloning vector pGEMT-easy, sequenced, and analysed to allow the determination of the splice leader addition site (marked on figure 5.5B with a red box), which was 115 bp upstream from the putative start codon of PS1. No other putative, in frame start codon was found upstream of the annotated initiator methionine in the PS1 sequence, confirming the GeneDB annotation for PS1.

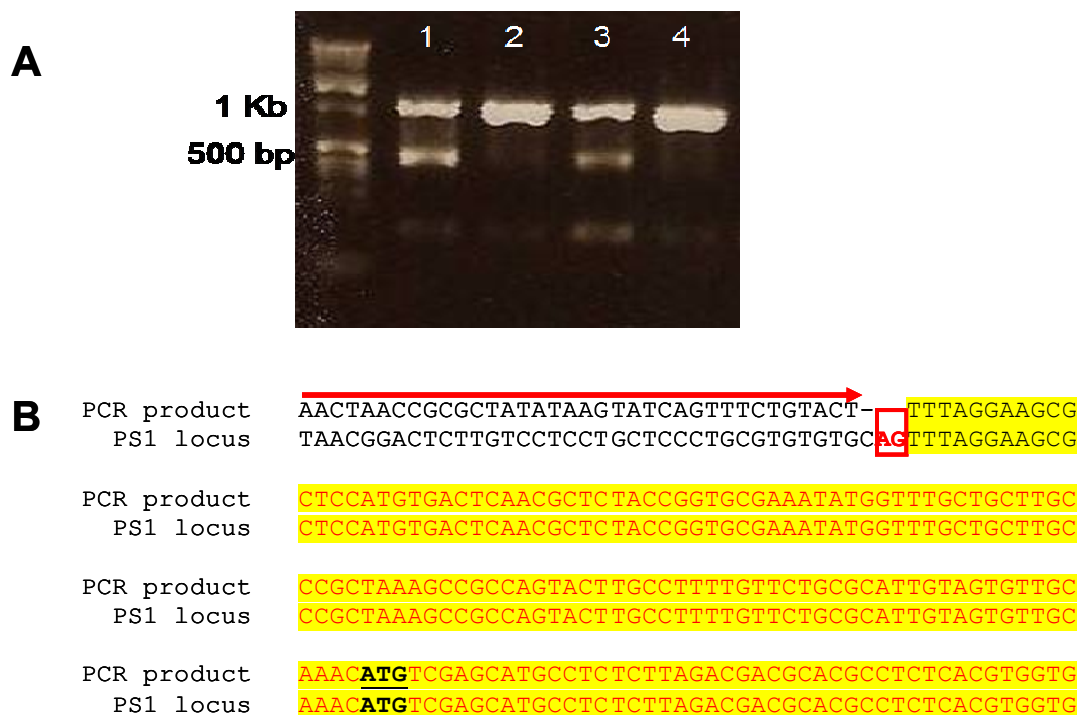


**Figure 5-5- Expression of PS1 mRNAs in promastigote and amastigote life cycle stages.** Total RNA from *L. major* promastigotes and amastigotes was isolated and converted to cDNA and two rounds of PCR were performed using an mRNA-specific splice leader primer (OL1760) with a PS1 specific primer (OL2588). Lanes 1 and 2 contain PCR product obtained from first and second rounds of PCR performed on promastigote cDNA, and lanes 3 and 4 are first and second rounds of PCR performed on amastigote cDNA. The mRNA derived PCR products were purified and cloned into the sub-cloning vector PGEMT-easy, sequenced, and the splice leader addition site was determined. B) **5'RACE mapping showing the splice leader addition site and ATG start codon for *L. major* PS1.** The sequence obtained from cloned RT-PCR products were aligned with the sequence of the PS1 gene and flanking regions obtained from GeneDB using the Clustal W algorithm of the Align X program (Vector NTI Advance 10 package, <http://www.informaxinc.com/>). Identical amino acids are shown on a yellow background. The position of the splice leader is shown with a red arrow. The splice leader addition site is highlighted with a red box.

## 5.4 Localisation of *L. major* PS1

### 5.4.1 Production of *L. major* expressing GFP and HA tagged PS1

*L. major* cell lines that expressed full length PS1 with a C terminal GFP or HA tag were produced in order to determine the subcellular localisation of PS1 (PS1-GFP and PS1-HA respectively). A C terminal tag was chosen due to the presence of a predicted N terminal signal sequence (Gene DB). While GFP tagging is a useful method for analysing the localisation of proteins in live cells, episomal expression can lead to heterogeneity in the level of protein expression and the intensity of GFP fluorescence, making analysis problematic (Benzel *et al.*, 2000). To ensure that the episomal expression of PS1-GFP did not lead to an analysis of

mislocalised protein, cell lines expressing PS1-HA under the control of the rRNA promoter were produced by stable integration into the 18S ribosomal RNA locus. The HA tag, derived from amino acids 98-106 of the human influenza hemagglutinin (HA) molecule, is extensively used as a general epitope tag in expression vectors, and is reported usually not to interfere with the bioactivity or the biodistribution of the recombinant protein.

For the expression of PS1-GFP, full length PS1 was amplified from the genome using the primer pair OL2204 and OL2205 (table 2.3) and cloned into the expression vector pGL1132 (section 2.2.1) using the restriction enzymes *NdeI* and *KpnI*, producing pGL1566 (figure 5.6B). For the expression of PS1-HA, full length PS1 was amplified from the genome with the primer pair OL2207 and OL2208 (table 2.3). The 3' primer (OL2208) contained the sequence corresponding to an HA tag (table 2.3). Full length PS1 with an additional C terminal HA tag was then cloned into the pRIB vector (pGL631) (table 2.1) using the restriction enzymes *XhoI* and *BglII* to produce pGL1564 (figure 5.6A). The construct was linearised using the restriction enzymes *PacI* and *PmeI*, and stably integrated into the 18S ribosomal RNA locus (figure 5.6C).

The correct integration of PS1-HA into the rRNA locus was determined by PCR using an oligo that recognises sequence upstream of the 5' flanking region of the rRNA (OL2380) in conjunction with an oligo specific for PS1 (OL1591) (figure 5.6C). A DNA fragment of the predicted size was obtained in clones transfected with PS1-HA, while no PCR product was obtained from wild type cells (figure 5.7A). Expression of PS1-HA was further tested by western blot using anti-HA antibodies. The resulting protein band detected at 46 kDa was slightly larger than the expected size of PS1 (38 kDa, GeneDB), but the absence of any signal in wild type cells suggested that PS1-HA was expressed in transfectants (figure 5.7B)

Plasmid	Backbone	Description	Drug resistance
pGL 1564	pGL1132	PS1 with C terminal HA tag	Puromycin
pGL 1566	pGL631	PS1 with C terminal GFP tag	Neomycin

**Table 5-1- Cell lines to study subcellular localisation of PS1**

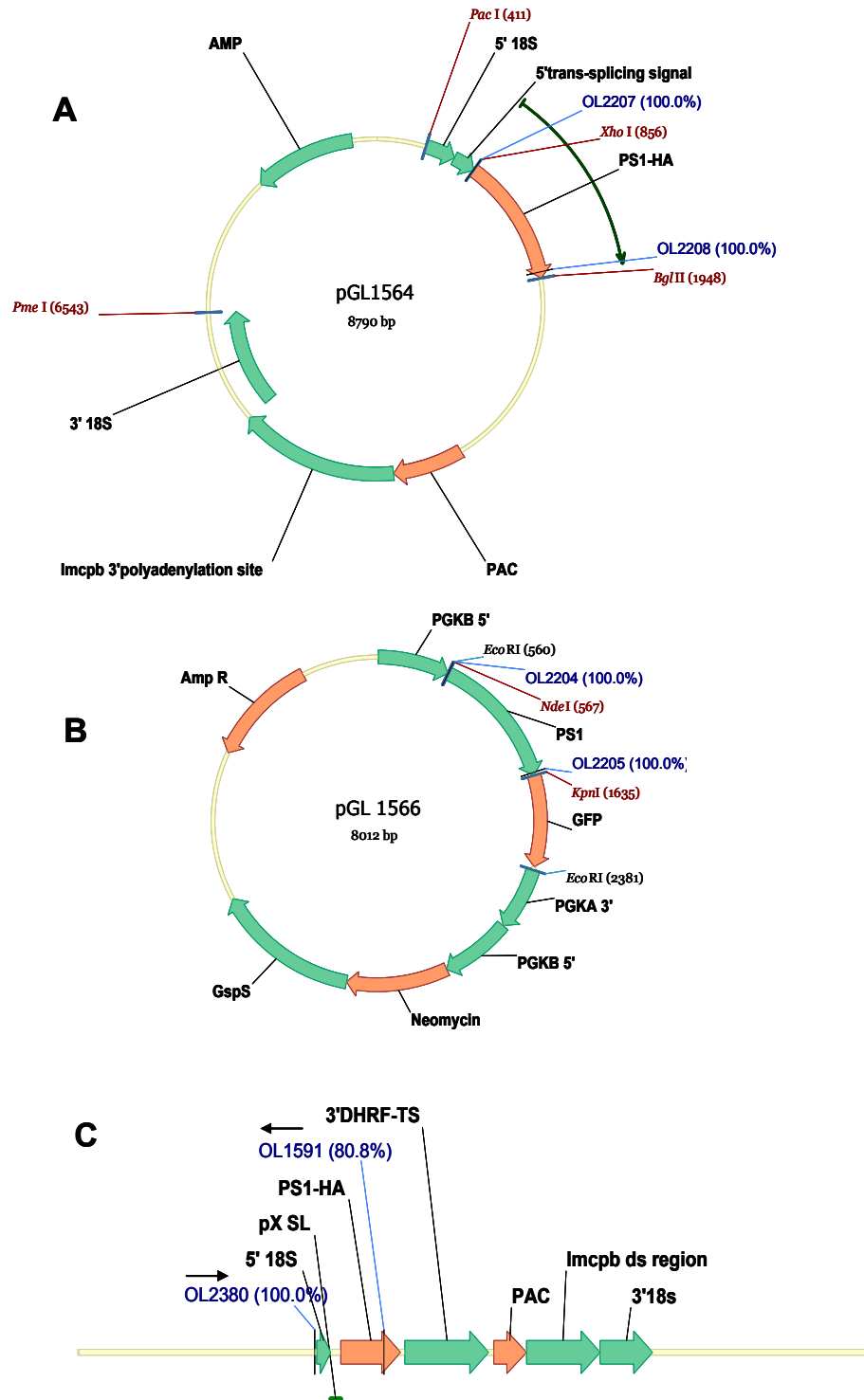


**Figure 5-6 Maps of plasmids for the expression of PS1-GFP and PS1-HA and integration of PS1-HA into the 18S rRNA locus.** Vector maps were produced using Vector NTI. A) pGL1564 was produced for the integration of PS1-HA at the rRNA locus. Oligos used for the amplification of PS1-HA, and restriction sites *PacI* and *PmeI* for the linearization of the construct for integration at the rRNA locus are shown. "PAC" refers to the puromycin resistance gene "puromycin N-acetyltransferase", required for selection of transfected parasites. 5' trans-splicing signals and 3-polyadenylation sites of dihydrofolate reductase (DHFR-TS) were included for the optimal expression of the gene of interest, while the 3' polyadenylation site of *L. mexicana* cysteine peptidase B (Imcpb) was included for the optimal expression of the antibiotic resistance gene.

B) pGL1566 for the episomal expression of PS1-GFP, based on the pNUS vectors (Tetaud *et al.*, 2002). C) Predicted integration of linearised pGL1564 at the 18S rRNA locus. Oligos used for PCR analysis of transformants are labelled and their orientation shown with an arrow.

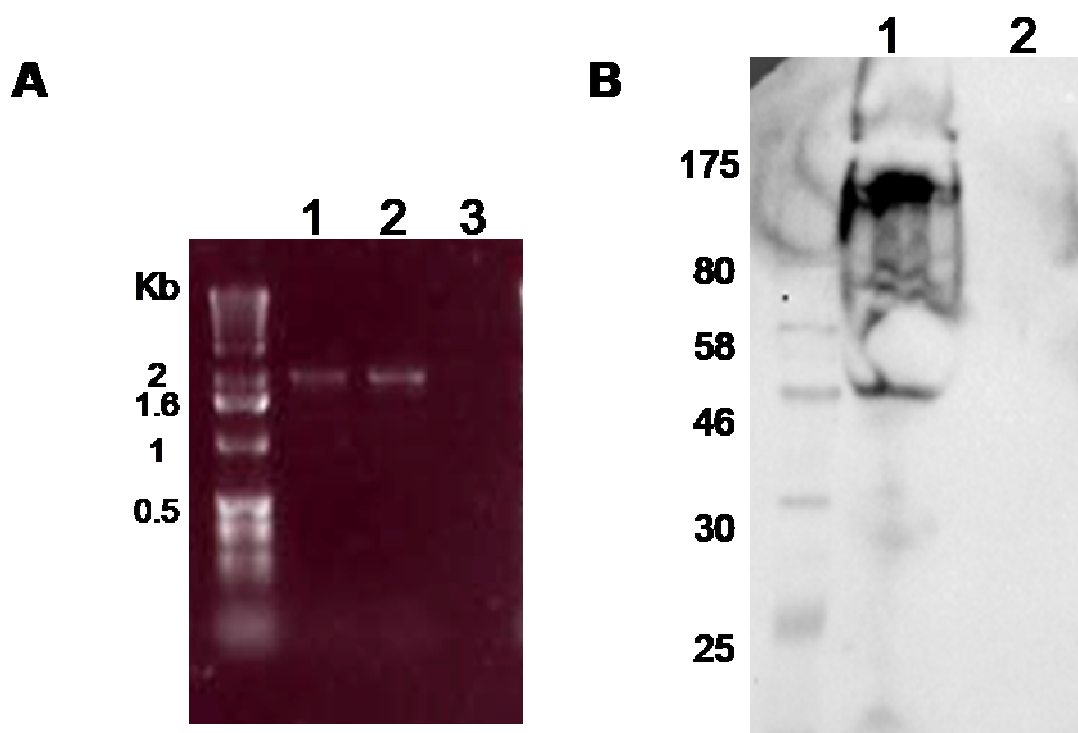


**Figure 5-7 Confirmation of PS1-HA cell lines by PCR and western blot.** A) PCR analysis of WT[PS1-HA]. Genomic DNA was extracted from two clones obtained after transfection with pGL1564 and analysed by PCR to determine whether integration of PS1-HA into the rRNA locus was achieved, using OL2380 and OL1591. Lane 1 = WT[PS1-HA] clone 1, Lane 2 = WT[PS1-HA] clone 2, lane 3 = wild type. B) Western blot analysis of WT[PS1-HA]. Cells were harvested and lysed with 0.2% Triton-X-100 and separated by SDS-PAGE. The gel was transferred to a hybond-c nitrocellulose membrane and hybridised with mouse anti-HA antibody (1 in 1000 dilution). HRP conjugated anti-mouse secondary antibody was used at 1 in 5000 dilution. The signal was detected using SuperSignal West Pico chemiluminescence detection system (Pierce). Lane 1 = WT[PS1-HA] clone1, Lane 2 = wild type.

### 5.4.2 Analysis of the localisation of PS1-GFP and PS1-HA

The expression of C terminally GFP tagged PS1 (PS1-GFP) was variable within and between populations of cells. In any one population a spectrum of expression levels was observed, ranging from cells with no fluorescence to intensely fluorescent cells. In those cells where PS1-GFP was detected, it generally showed a reticulated pattern that resembled the mitochondrion or endoplasmic reticulum (ER), or a punctate distribution in the cell that partially colocalised with lysotracker (figure 5.8), suggesting that PS1-GFP localises to various intracellular membranes.

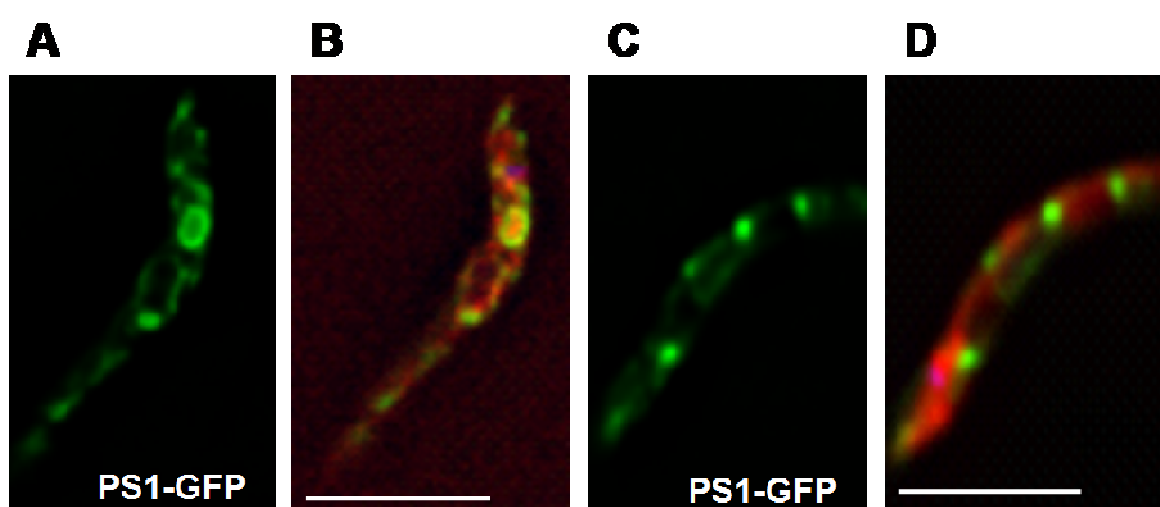


**Figure 5-8- Localisation of PS1-GFP (C terminal tag) in live *L. major* promastigotes.** **A) PS1-GFP, B) PS1-GFP with ER-tracker, C) PS1-GFP, D) PS1-GFP with lysotracker.** Live promastigotes expressing GFP tagged PS1 (PS1-GFP) were incubated with 1  $\mu$ l LysoTracker Red DND-99 (1 mM stock in DMSO, Molecular Probes) and incubated for 30 minutes at 25°C, or 1 nM ER-tracker (Molecular Probes, M7512, in DMSO) for 5 minutes at 25°C. Cells were washed twice in PBS, resuspended in ice-cold PBS, settled onto glass slides and viewed using an Applied Precision DeltaVision microscope. Scale bar is 10  $\mu$ m.

The localisation of PS1-HA was studied by indirect immunofluorescence analysis, using Alexa-Fluor (488) conjugated mouse anti-HA antibodies. Surprisingly, PS1-HA was found to localise to a region near the flagellar pocket in a different pattern to that seen with the PS1-GFP. Figure 5.9A and 5.9B show two examples of the localisation of PS1-HA from two independent transfections. The duplication of the signal observed in the dividing cell (figure 5.9B) suggests that PS1-HA localises to a particular structure that is duplicated during cell division. The localisation resembled that seen with *T. brucei* Rab11 antibodies on *L. major* cells, which has been shown to partially co-localise with ConA, a marker of the flagellar pocket (Ambit, 2006). To investigate the potential co-

localisation of PS1 with Rab11, immunofluorescence experiments were performed on fixed PS1-HA expressing cells using anti-HA and anti-Rab11 antibodies (figure 5.9C). The two signals did not over-lap, demonstrating that PS1 does not co-localise with, and is unlikely to interact with, Rab11. The cell line used for Rab11 staining was a  $\Delta ps1$  mutant (section 5.6) that had been complemented with PS1-HA. The tagged PS1 is less likely to be over-expressed when PS1-HA is expressed under the control of the rRNA promoter in a  $\Delta ps1$  mutant background.

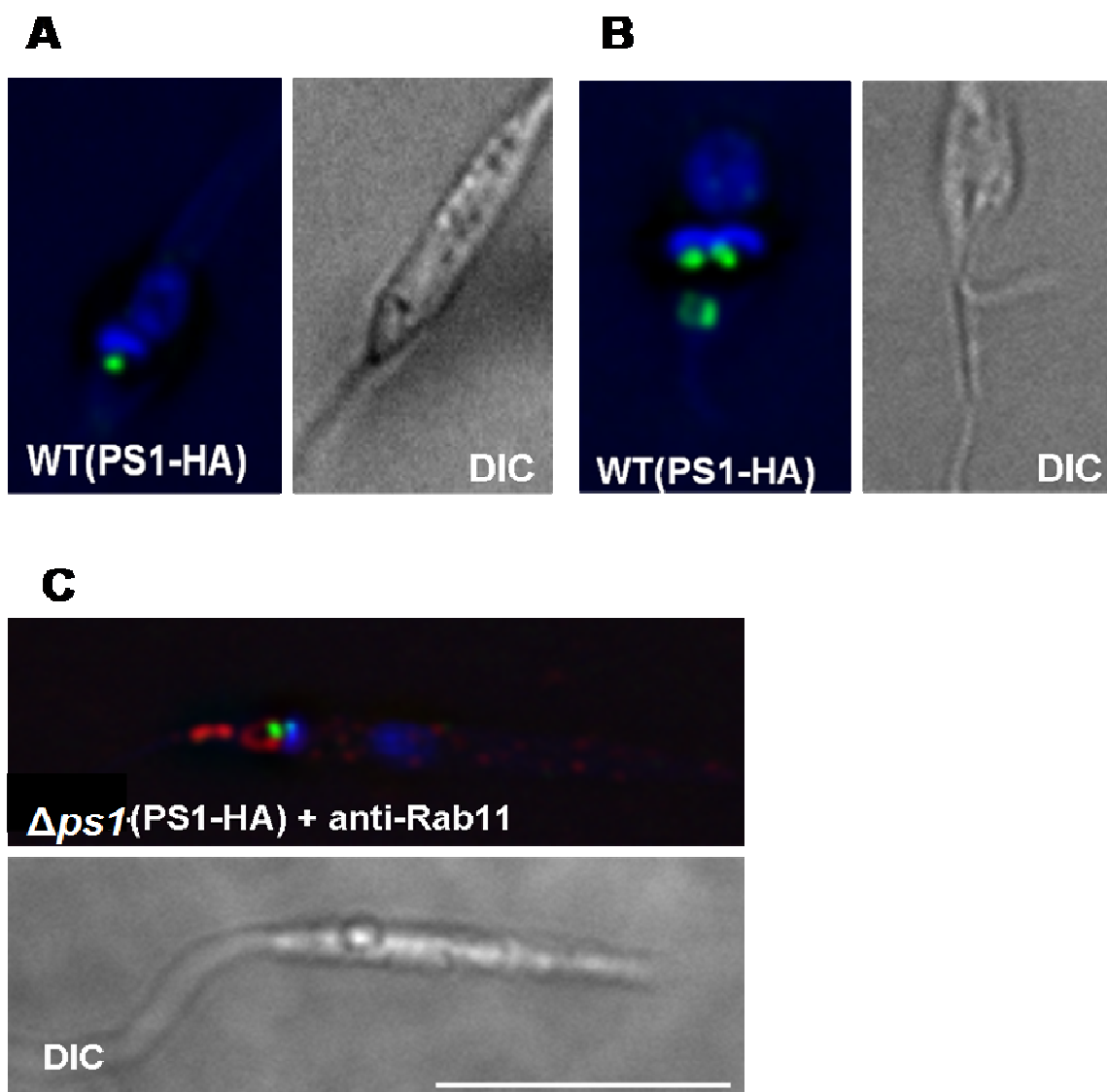


**Figure 5-9 Immunofluorescence analysis of *L. major* promastigotes expressing PS1-HA.** A) A non-dividing promastigote labelled with Alexa-Fluor 488 (green) mouse anti-HA antibodies B) a dividing promastigote from an independent transfection labelled with anti-HA antibodies and C) a non-dividing promastigote labelled with anti-HA and anti-TbRab11 antibodies. Promastigotes which expressed PS1-HA integrated at the ribosomal locus were fixed in 2% formaldehyde and labelled with mouse anti-HA (figure A and B) and rabbit anti-TbRab11 (figure C) and Alexa-Fluor 488 (green) conjugated anti-mouse and Alexa-Fluor 548 (red) conjugated anti-rabbit antibodies. Both primary antibodies were diluted 1 in 1000 prior to use, and the secondary antibodies used at a 1 in 2000 dilution. DAPI was added at a concentration of 0.5  $\mu\text{g ml}^{-1}$  to stain the nucleus and kinetoplast (blue).

## 5.5 Expression of *L. major* PS1 protein

Attempts were made to produce recombinant PS1 protein, with the aim of producing antibodies specific to PS1 that could be used to analyse the expression of PS1 throughout the life cycle, and to confirm the subcellular localisation of the protein. Because PS1 is an integral transmembrane protein, likely to be difficult to purify in its full length form, it was decided to attempt to purify a 10 kDa C terminal fragment, corresponding to the portion of the protein that is not predicted to be embedded in the membrane (amino acids 210 - 264).

### 5.5.1 Attempts to express a His tagged PS1 fragment

Prior to the start of this project, the pET28a(+) vector had been used to produce a construct with the desired fragment of PS1 protein tagged N terminally with a His tag (pGL1184) for expression in *E. coli* BL21 (DE3) cells. Expression trials and subsequent analysis by SDS-PAGE and western blotting with anti-His antibodies revealed that no expression of His-PS1 was achieved, despite trying multiple induction conditions (overnight expression at 19°C, 5 hour expression at 30°C or 3 hour expression at 37°C), with concentrations of Isopropyl- $\beta$ -D-thiogalactopyranoside (IPTG) ranging from 0.1 to 1 mM).

### 5.5.2 Expression of GST tagged PS1 fragment

In an attempt to increase expression levels of the PS1 fragment, a GST-fusion protein was produced. Although not specifically designed for this purpose, the 220 amino acid GST-Tag sequence has been reported to enhance the solubility of its fusion partners. The desired PS1 fragment was amplified from the genome using the primer pair OL2036 and OL2037 and cloned into the pGEX-5X1 vector (Amersham) using the restriction enzymes *Bam*HI and *Xho*I, producing a construct for the expression of a fusion protein with an N terminal GST tag (pGL1443). Various conditions were tested for the expression of GST-PS1, and the optimal expression was achieved when protein was induced with 1 mM IPTG, overnight at a temperature of 19°C. Fusion protein was purified using glutathione sepharose 4B, and eluted in 50 mM Tris, 20 mM glutathione, pH 7.0, as described in section 2.7.1 (figure 5.10). The predicted size of the GST-PS1 fusion protein is 35 kDa, and is the top protein on figure 5.10. GST (27 kDa) was also present in the elutions.

However, attempts to remove the GST tag from the PS1 fragment with the endopeptidase factor Xa (NEB) by incubating 1 µg of enzyme per 50 µg protein for 6 hours at room temperature, followed by purification with glutathione sepharose resin (and collection of the flow through) were unsuccessful and sufficient purified protein was not obtained for antibody production.

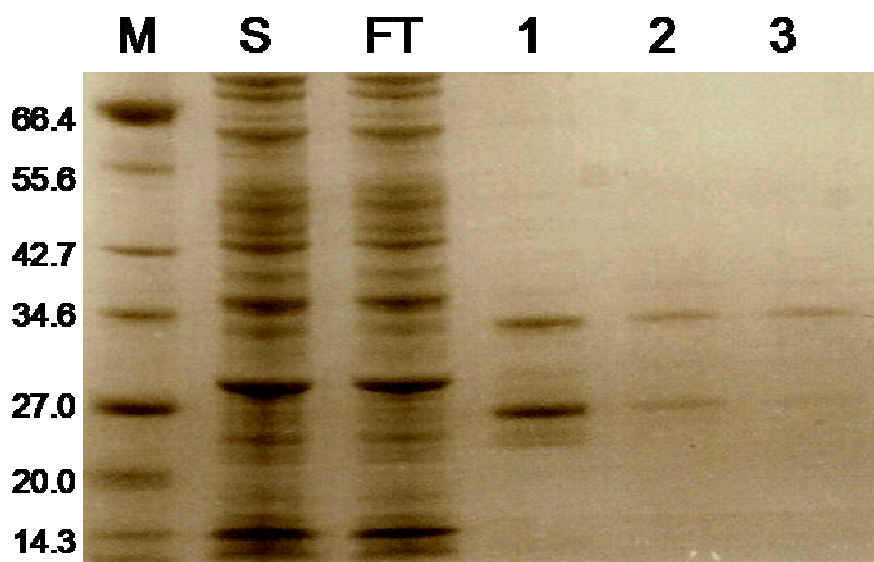


**Figure 5-10 Purification of GST-PS1 from *E. coli* cells.** Protein expression was induced in BL21-DE3 *E. coli* cells with 1 mM IPTG overnight at 19°C. The soluble fraction was incubated with 4 ml glutathione sparse 4B at room temperature for 30 – 60 minutes. The resin was washed three times in PBS, and the protein eluted in elution buffer (50 mM Tris, 20 mM glutathione sepharose, pH 7.0). The soluble fraction (S), the flow through (FT) and elutions 1-3 (lanes 1-3) were separated by SDS-PAGE on a 12% acrylamid gel, and the gel stained with coomassie K-250.

### 5.5.3 Peptide synthesis and antibody production

Due to failed attempts to produce sufficient recombinant protein for antibody production, a peptide corresponding to 15 amino acids in the C terminal domain of the predicted PS1 sequence (CRLIVESLSSFTSHH) was synthesised and used to immunise a rabbit (BioGenes). The peptide used is underlined on figure 5.3A. 5 mg of peptide was conjugated to a carrier protein and used to immunise a rabbit with three boosts over a three month period. Serum was extracted prior to immunisation (pre-immune serum) and three months after immunisation (immune-serum).

The specificity of anti-PS1 antibodies was tested by western blot analysis, comparing cell lysate from  $\Delta ps1$  mutants (produced as described in section 5.6) with wild type. Pre-immune serum detected several proteins of ~ 20, 46 and 60

kDa in both wild type and a  $\Delta ps1$  mutant (figure 5.11, A). In addition to the non-specific proteins recognised by the pre-immune sera, a protein of approximately 46 kDa was detected in the wild type sample and absent from two  $\Delta ps1$  mutant clones (figure 5.11.B lane 1). This protein is slightly larger than the predicted size of *L. major* PS1 (38.6 kDa, GeneDB), but the absence of the protein in lysates from  $\Delta ps1$  mutants suggests that this protein is likely to be PS1. PS1-HA was found to be slightly larger than 46 kDa when detected with anti-HA antibodies (figure 5.7B). Together, this provides some evidence that *L. major* PS1 has a molecular weight of ~ 46 kDa. Surprisingly, a protein of approximately 30 kDa was detected in both  $\Delta ps1$  mutants that were absent from wild type cells (figure 5.11.B lanes 2 and 3).

1 mg of the peptide was subsequently coupled to amino-link coupling gel and used to affinity purify the antibodies. Affinity purification did not seem to improve the specificity of the antibodies, and no protein likely to be endogenous PS1 was detected, despite trying various antibody concentrations and using wild type cells at various stages of growth (figure 5.12A for an example). The 30 kDa protein detected previously only in  $\Delta PS1$  mutants was detected in all samples tested (wild type,  $\Delta ps1$  mutants and WT[PS1-HA], suggesting that this is a protein unrelated to PS1. It seems that it was not possible to detect endogenous PS1, as no difference in proteins of the predicted size (~38 - 46 kDa) was observed between wild type and  $\Delta ps1$  mutant cell lysates. Although PS1-HA could be detected using anti-HA antibody (figure 5.7B), no protein was detected using the purified anti-PS1 antibody (figure 5.12A lane 4), again suggesting that these antibodies are not sufficiently sensitive to detect PS1 expressed endogenously, or under the control of the rRNA promoter.

Anti-PS1 serum (1 : 500 dilution) recognised GFP-PS1 (figure 5.12.C, lane 3). GFP has a molecular mass of 27 kDa, so the PS1-GFP fusion protein would be expected to have a size of ~65 - 73 kDa, depending on whether full length PS1 is in fact 38 kDa as predicted, or 46 kDa as it appears from western blot data. The protein that was detected from WT[PS1-GFP] lysates with both anti-GFP and anti-PS1 was approximately 58 kDa, which might correspond to a 30 kDa fragment of PS1 fused with the 27 kDa GFP molecule. In addition to the protein of ~58 kDa, a protein of higher molecular weight was also detected using both anti-GFP and anti-PS1 antibodies.

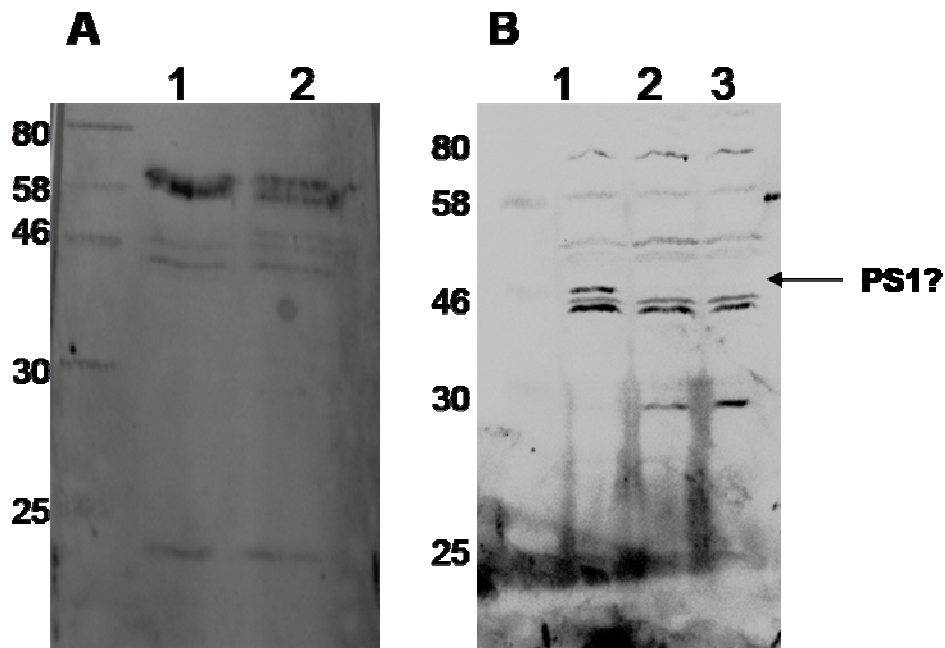


**Figure 5-11 Testing pre-immune rabbit serum and anti-PS1 rabbit serum by western blot.** Approximately  $1 \times 10^6$  wild type and  $\Delta ps1$  mutant cells were lysed with 0.2% triton-X-100 in the presence of protease inhibitors, and separated by SDS-PAGE on 12% acrylamide gels. The gels were transferred to hybond-c nitrocellulose membranes. **A) Detection of proteins in wild type (lane 1) and  $\Delta ps1-5$  (lane 2) lysates with serum extracted from a rabbit prior to immunisation with PS1 peptide.** **B) Detection of proteins in wild type (lane 1),  $\Delta ps1$ (clone 5) (lane 2), and  $\Delta ps1$ (clone B) (lane 3) lysates with rabbit anti-PS1 serum.** Immune sera were used at a 1 in 500 dilution, and HRP conjugated rabbit secondary antibody was used at 1 in 5000. The signal was detected using SuperSignal West Pico chemiluminescence detection system (Pierce).

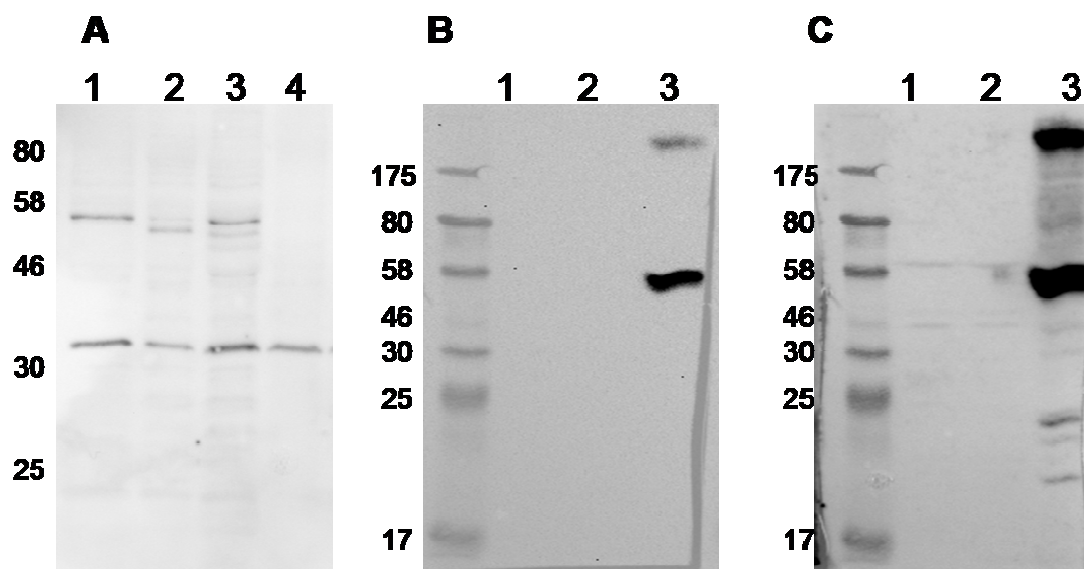


**Figure 5-12 Testing affinity purified rabbit anti-PS1 serum by western blot.** Approximately  $1 \times 10^8$  wild type and  $\Delta ps1$  mutant cells were lysed with 2% SDS, and separated by SDS-PAGE on 10% (figure A) or 12% (figures B and C) acrylamide gels. The gels were transferred to hybond-c nitrocellulose membranes. **A) Testing affinity purified anti-PS1 serum.** Lane 1 = wild type, lane 2 =  $\Delta PS1-5$ , lane 3 =  $\Delta PS1-B$ , lane 4 = WT[PS1-HA]. Immune sera were used at a 1 in 500 dilution. **B) Testing PS1-GFP cell lines with anti-GFP antibody.** Lane 1 = wild type, lane 2 =  $\Delta PS1-5$ , lane 3 = WT[GFP-PS1]. Anti-GFP antibody was used at a 1 in 2000 dilution. **C) Testing affinity purified anti-PS1 sera against WT[PS1-GFP] lysates.** Lane 1 = wild type, lane 2 =  $\Delta PS1-5$ , lane 3 = WT[GFP-PS1]. Rabbit anti-PS1 serum was used at a 1 in 500 dilution. In all cases, HRP conjugated secondary antibodies (rabbit or mouse) were used at a 1 in 5000 dilution.

## 5.6 Production of PS1 null mutant cell lines

In order to study the role of PS1 in *L. major*, PS1 null mutants ( $\Delta ps1$ ) were produced by targeted gene replacement. Because *Leishmania* is a diploid organism, two rounds of transfection were required to sequentially replace the two PS1 alleles by homologous recombination. Plasmids containing the 5' flanking region (FR) and 3' FR of PS1 had been produced prior to the start of the project for the replacement of wild type PS1 with the antibiotic resistance markers hygromycin (*HYG*) or blasticidin (*BSD*) (pGL1161 and pGL1162 respectively). The 5' trans-splicing signals and 3' polyadenylation sites of the *L. major* dihydrofolate reductase-thymidylate synthase (*DHFR-TS*) gene were included in the knock out construct and were integrated along with the resistance marker to allow expression of the *HYG* or *BSD* resistance genes (figure 5.13).

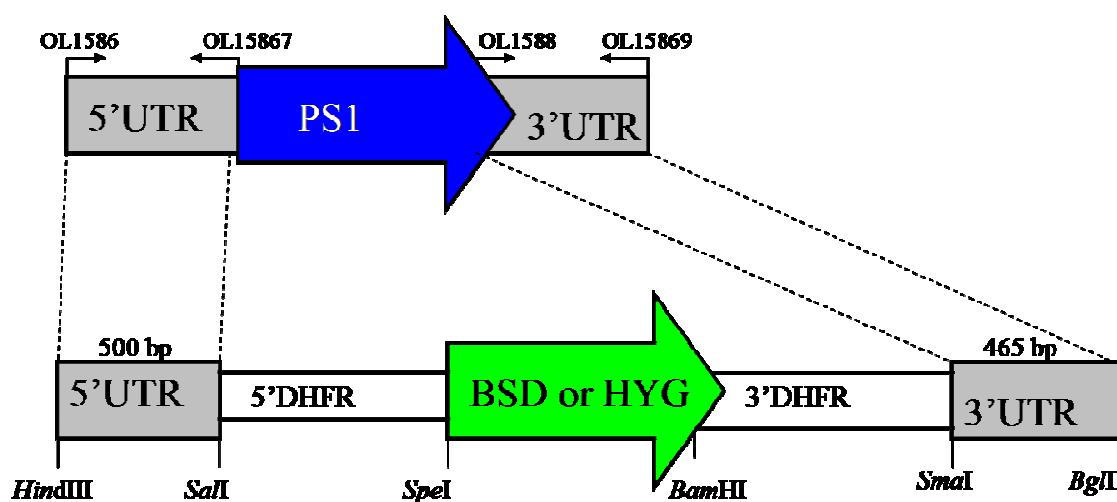


**Figure 5-13 Schematic of strategy used to produce PS1 null mutants.** ORFs are represented as arrows, intergenic and flanking DNA sequences are represented as boxes. The 5' and 3' untranslated flanking regions (5'UTR and 3'UTR) of PS1 were amplified using the primer pairs OL1586-OL1587 and OL1588-OL1589 respectively, and the 500 bp and 465 bp fragments were cloned into pGL345, using the *HindIII/SalI* and *SmaI/BglII* restriction sites respectively to produce pGL1161 and pGL1162.

### 5.6.1 Confirmation of *Leishmania* species by PCR

Prior to carrying out transfections, the *L. major* cell line to be used was confirmed as *L. major* by PCR amplification of the ribosomal internal spacer locus (ITS1) and subsequent analysis of *HaeIII* restriction fragment length

polymorphisms (Schonian *et al.*, 2003) (figure 5.14). This was done in order to avoid any confusion between stabilates and cell lines routinely used in the lab.

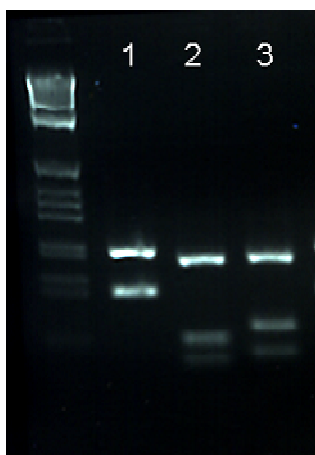


**Figure 5-14 - PCR confirmation of the *Leishmania* species used in this study**

The species of *Leishmania* used in this study was confirmed by PCR amplification of the ribosomal internal spacer locus with OL1853 and OL1854 and subsequent analysis of *Hae*III restriction fragment length polymorphisms by agarose gel electrophoresis, following the method described by Schonian *et al.*, 2003. 1 = wild type *L. major* for use in this study, 2 = *L. infantum* control, 3 = *L. mexicana* control.

### 5.6.2 Generation of $\Delta$ *PS1* null mutants and confirmation by PCR and Southern blot

Transfections were performed with 10  $\mu$ g of linearised DNA using the human T-cell Amaxa nucleofactor kit (Amaxa Biosystems) as described in section 2.4.6. To obtain heterozygotes, two independent transfections were performed in wild type cells, replacing the endogenous *PS1* locus with the *HYG* or *BSD* resistance cassettes, respectively. The day after transfection, serial dilutions of 1 in 5, 1 in 50 and 1 in 500 were produced from each overnight culture and plated out on 96 well microplates in order to obtain clones. This was done to ensure that the deletion of the *PS1* locus was due to a single recombination event rather than a combination of mutations, and to ensure the survival of any transfectants with deleterious phenotypes.

The vector NTI programme (Invitrogen) was used to design primers suitable for confirming the correct integration of the linearised plasmid in heterozygotes and *PS1*-deficient mutants by PCR, and restriction enzymes suitable for Southern blot analysis (figure 5.15 A, B, C). The predicted integration of full length *PS1* into

the 18S ribosomal locus in a  $\Delta ps1$  background (described in section 5.6.2.2) is shown in figure 5.15 D. Oligos OL2034 and OL2035 were designed to amplify the entire *PS1* locus, or for use in conjunction with drug resistant cassette specific oligos OL13, OL14, OL536 and OL537. The restriction enzyme *PciI* was utilised for Southern blot analysis, using the *PS1* 5' flanking region (5'FR) or the entire *PS1* ORF (figure 5.15, table 5.2).

After confirming the correct integration of linearised DNA into the *PS1* locus by PCR (described below), a second round of transfection was performed with the corresponding plasmid (hygromycin resistant clones were transfected with pGL1162, and vice versa). This was done in order to obtain two entirely independent clones. Eight clones (clones 1-8) were obtained from one transfection, and ten from another (clones A-J). These clones were initially screened by PCR to confirm the correct integration of DNA into the *PS1* locus, and then the absence of the *PS1* ORF was confirmed by Southern blot.

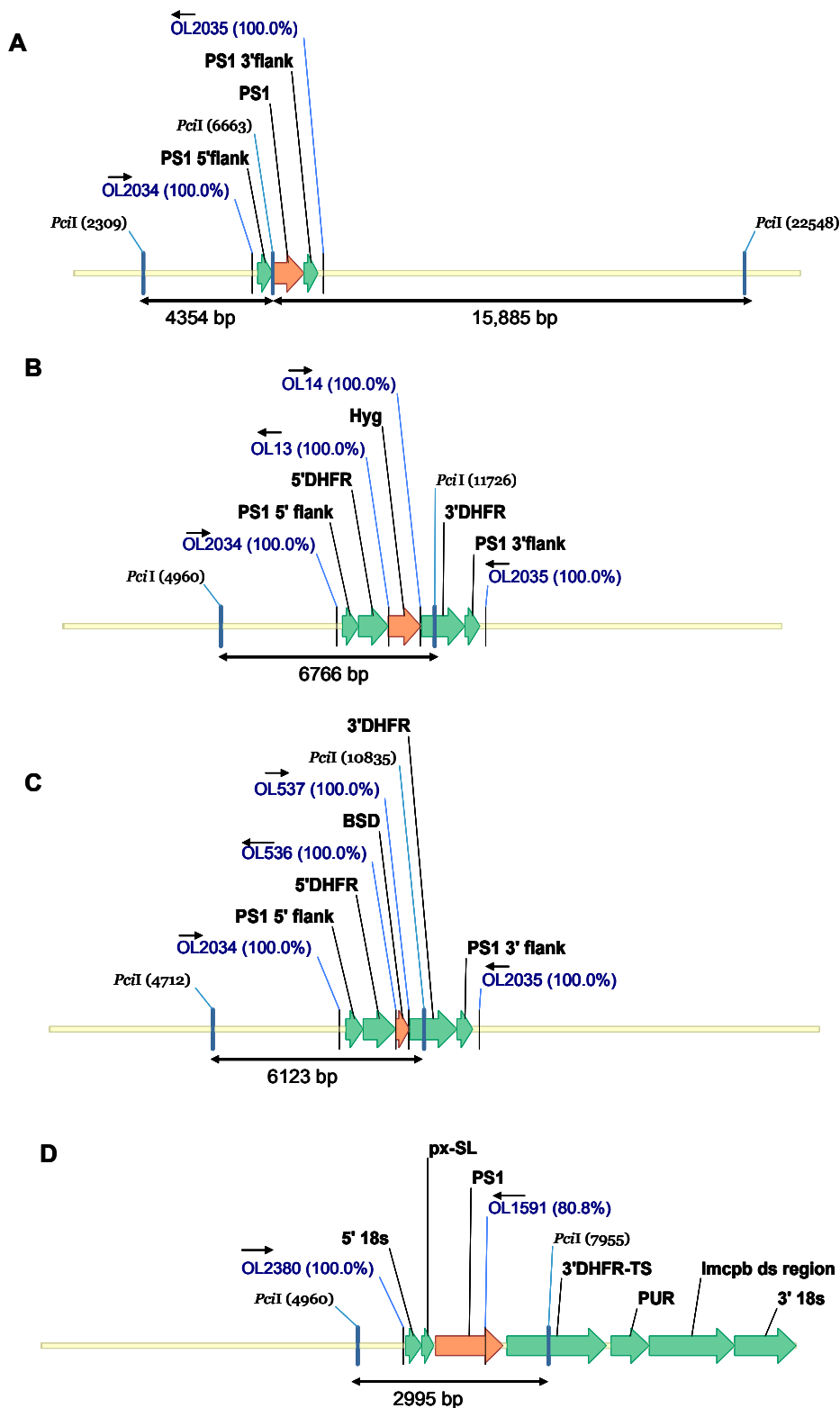


**Figure 5-15** Maps of wild type *PS1* locus, *PS1* loci with integration of *BSD* and *HYG* resistance genes, and the 18S ribosomal locus with integration of *PS1*. **A)** Wild type *PS1* locus, **B)** *PS1* locus with integration of the *BSD* resistance cassette, **C)** *PS1* locus with integration of the *HYG* resistance cassette. **D)** 18S ribosomal locus with integration of full length *PS1* gene. Molecule maps were produced using Vector NTI (Advance 10 package, <http://www.informaxinc.com/>). Oligos used for PCR analysis of clones are shown with an arrow indicating their orientation. The restriction fragments produced upon digest with *PciI* (used for Southern blot analysis) is shown. The 5' flank or the *PS1* ORF was used as a probe for Southern blot. DHFR-TS (dihydrofolate reductase thymidylate synthase) 5' and 3' regions were included for the expression of the gene of interest, and *Imcpb* (*L. mexicana* CPB) regions were included for expression of the drug resistance cassette. PUR refers to puromycin resistance.

Primers	Amplified product	Expected size of PCR product (bp)	Expected size (bp) of <i>PciI</i> restriction digest probed with 5' flank (left) or PS1 open reading frame (right)	
OL2035/ OL2035	Wild type PS1 locus	2387	4354	15,885
	PS1 locus with BSD integration	4060	6123	Nothing
	PS1 locus with HYG integration	4698	6766	Nothing
OL2034/ OL13	5' integration of HYG marker	1632		
OL2035/ OL14	3' integration of HYG marker	2062		
OL2034/ OL536	5' integration of BSD marker	1631		
OL2035/ OL537	3' integration of BSD marker	2065		
OL2380/ OL1591	Integration of PS1 at 18s ribosomal marker	1600		2955

**Table 5-2 Oligos and Enzymes used for PCR and Southern blot analysis of *PS1* mutants and re-expressing cell lines.** The expected size for PCR products obtained from different primer combinations and the expected size of *PciI* restriction digest probed with either the PS1 5' flanking region or with the PS1 open reading frame (Kaether et al.) are shown.

### 5.6.2.1 PCR analysis of $\Delta ps1$ mutants

Initial screens of drug resistant clones were carried out using OL2034 and OL2035 in conjunction with drug resistant cassette specific oligos OL13, OL14, OL536 and OL537, in order to test for the expected integration of the drug resistance cassettes (figure 5.15 B and C, table 5.2). An example of a PCR screen of a hygromycin resistant heterozygote with OL2034/OL13 and OL2035/OL14 (lanes 1 and 2 respectively) and a blasticidin resistant heterozygote with OL2034/OL536 and OL2035/OL537 (lanes 3 and 4, respectively) is shown in figure 5.16A. The expected sizes of PCR product are described in table 5.2. No PCR product was expected if the linearised DNA had not integrated as expected.

The replacement of the wild type *PS1* locus was confirmed by amplification of the entire locus with OL2034 and OL2035. Where the wild type locus was present, a PCR product of 2387 base pairs (bp) was expected. Amplification of the *PS1* locus in which the *BSD* or *HYG* resistance cassette had been integrated was expected to yield a PCR product of 4040 or 4698 bp respectively (figure 5.15 B and C, table 5.2). Figure 5.16 B shows the amplification of the entire *PS1* locus from wild type cells (lane 1) and 6 doubly-drug resistant clones (lanes 2-7). In this case, the locus had been replaced in one clone, called  $\Delta ps1$ -5. Where the wild type *PS1* locus was still present, a PCR product of 2.4 Kb was produced. Failure to replace the *PS1* locus might be because the drug resistance phenotype

was conferred due to the presence of the plasmid as an episome, or because the plasmid had integrated either upstream or downstream of the targeted gene in a position with sequence similarity to other parts of the plasmid, resulting in doubly drug-resistant cells that still retain a copy of the wild type locus.

Alternatively, *Leishmania* cells can become polyploid, containing both chromosomes in which the gene of interest has been replaced as expected, in addition to an extra chromosome that retains that gene (Clayton, 1999). Of 18 doubly drug-resistant clones that were obtained (clones 1-8 from transfection one and A-J from transfection two), the wild type *PS1* locus was absent in just four clones. Two independent clones, ( $\Delta ps1-5$  and  $\Delta ps1-B$ ), were chosen for all further analyses.

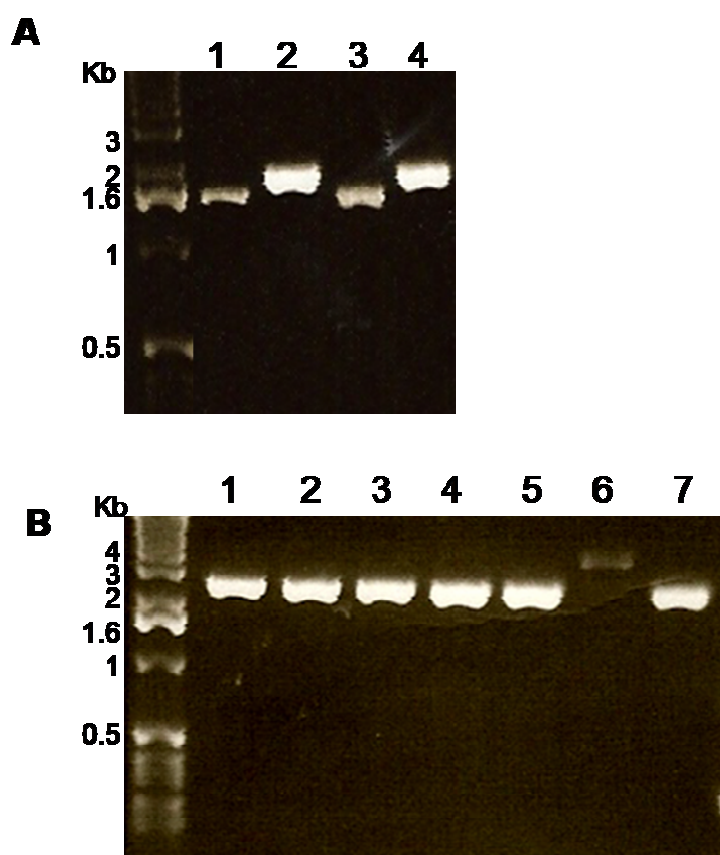


**Figure 5-16 PCR analysis of  $\Delta ps1$  mutant clones.** Genomic DNA was extracted from  $\Delta PS1$  mutant clones and analysed by PCR to determine whether integration of the knock out construct into the expected locus was achieved. **A) PCR analysis of integration of BSD or HYG resistance cassettes into heterozygotes.** DNA was extracted from hygromycin (lanes 1 and 2) or Blastidicin (lanes 3 and 4) resistant clones and analysed with OL2034 /OL13 (lane 1), OL2035/OL14 (lane 2), OL2034/OL536 (lane 3) or OL2035/OL537 (lane 4). **B) Amplification of the *PS1* locus of  $\Delta PS1$  mutant clones and wild type *L. major*.** Amplification of the entire *PS1* was achieved with OL2034/OL2035, and the polymerase *Phusion* (Finnzymes) was used. Lane 1 = wild type, lane 2-7 = clones 1-6.

### 5.6.2.2 Southern blot analysis of $\Delta ps1$ mutants and production of a $PS1$ re-expressing cell line ( $\Delta ps1[PS1]$ )

To confirm the data obtained by PCR, Southern blot analysis was performed on  $\Delta ps1$  mutants and wild type cells. Genomic DNA was extracted from the cell lines to be analysed, and digested overnight with the restriction enzyme *PciI*. Using the 5' untranslated region of *PS1* as a probe, the wild type allele could be detected as a DNA fragment of 4354 bp, and where integration with the hygromycin or blasticidin cassette had occurred, DNA fragments of 6766 bp or 6123 bp were detected (figure 5.17 A). The blot was then stripped and re-probed using the entire *PS1* ORF as a probe. A DNA fragment of 15,885 bp was detected in wild type cells and was absent in  $\Delta ps1$  mutants, demonstrating that these cell lines possessed no copy of the *PS1* gene (figure 5.17B)

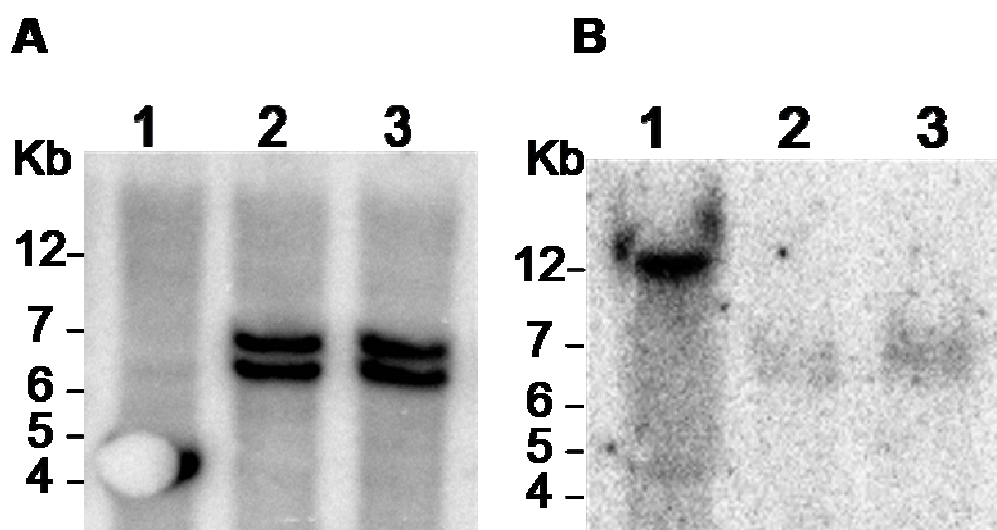


**Figure 5-17 Southern blot analysis of  $\Delta PS1-5$  and  $\Delta PS1-B$ .** A) Southern blot probed with the 5' flanking region. B) Southern blot, stripped and re-probed with the full length *PS1* ORF. Lane 1 = wild type, Lane 2 =  $\Delta PS1-5$ , Lane 3 =  $\Delta PS1-B$ . 3  $\mu$ g of genomic DNA was extracted from *L. major* promastigotes and digested overnight with 30 units (3  $\mu$ l) of the restriction enzyme *PciI*. The digested DNA was separated by electrophoresis on a 0.8% agarose gel which was subsequently transferred to a nitrocellulose membrane (hybond<sup>TM</sup>-N+) and covalently attached by UV cross-linking. 10 ng of the desired probe (either the *PS1* 5' flanking region or the *PS1* open reading frame) was purified, labelled with Alk-Phos<sup>TM</sup> Direct labelling kit (Amersham), and incubated with the membrane overnight. The signal was detected using a CDP-Star detection reagent (Amersham) and exposed using a Typhoon imager (GE Healthcare).

*PS1* was stably re-expressed at the *L. major* 18S ribosomal RNA small subunit (18S rRNA locus, GeneDB identifier LmjF27.rRNA.06) of  $\Delta ps1-5$ , producing  $\Delta ps1-5[PS1]$ . This was done in order to confirm that any phenotype observed in the mutants was due to the loss of *PS1*, rather than due to other problems that arose during culture. To achieve this, the full length *PS1* gene was cloned into the pRIB vector, the same vector used for the expression of *PS1*-HA, to produce pGL1567. The plasmid was linearised using the restriction enzymes *PacI* and *PmeI*, and stably integrated at the rRNA locus (please refer to figure 5.6 A for the structure of the vector). This allowed the re-expression of *PS1* under the control of the rRNA promoter (pol I) in the mutants which is known to drive high levels of transgene expression in trypanosomatids in both life cycle stages of the parasite (Misslitz *et al.*, 2000).

A second Southern blot was performed in which the genotype of  $\Delta ps1-5$  and  $\Delta ps1-B$  was confirmed after passaging through a mouse (section 5.7.3), to ensure that the replacement of the *PS1* locus was stable. Additionally, hygromycin and blasticidin resistant heterozygotes were analysed, along with the re-expressor cell line  $\Delta ps1-5[PS1]$  (figure 5.18 A). The stable re-expression of *PS1* in  $\Delta ps1-5[PS1]$  was confirmed by probing *PciI*-digested genomic DNA with the *PS1* ORF as a probe. A fragment of approximately 3 Kb was detected in the re-expressing cell line, as expected (figure 5.18 B), although in this case, a hybridising band of ~15 kDa was not detected in the wild type nor the heterozygote samples as would be expected.

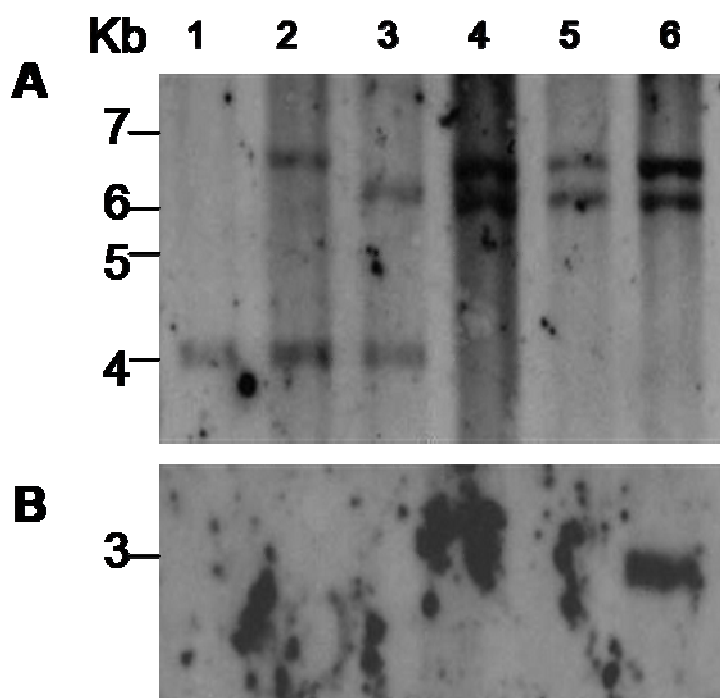


**Figure 5-18 Southern Blot Analysis of *L. major*  $\Delta ps1$  null mutants, heterozygotes and re-expressing cell lines.** Samples are: wild type (lane 1), PS1 heterozygotes (PS1 +/- HYG<sup>R</sup>, lane 2) and (PS1 +/- BSD<sup>R</sup>, lane 3),  $\Delta PS1$  5 (lane 4),  $\Delta PS1$  B (lane 5) and a re-expressing cell line ( $\Delta PS1$ /[PS1], lane 6). A) Southern blot probed with the 5'PS1 flank. B) Southern blot probed with the PS1 ORF. 3 $\mu$ g of genomic DNA was extracted from *L. major* promastigotes and digested overnight with 30 units (3  $\mu$ l) of the restriction enzyme *Pci*1. The digested DNA was separated by electrophoresis on a 0.8% agarose gel which was subsequently transferred to a nitrocellulose membrane (hybond<sup>TM</sup>-N<sup>+</sup>) and covalently attached by UV cross-linking. 10 ng of the desired probe (either the PS1 5' flanking region or the *PS1* open reading frame) was purified, labelled with Alk-Phos<sup>TM</sup> Direct labelling kit (Amersham), and incubated with the membrane overnight. The signal was detected using a CDP-*Star* detection reagent (Amersham) and exposed using a Kodak film.

## 5.7 Analysis of growth and virulence of $\Delta ps1$ mutants

### 5.7.1 Growth curves

*L. major* cultures were set up with a starting density of  $1 \times 10^5$  cells ml<sup>-1</sup>, and counted at the same time each day until stationary phase was reached, in order to analyse the ability of  $\Delta ps1$  promastigotes to grow. The growth curves of  $\Delta ps1$  promastigotes did not differ significantly from wild type cells, indicating that the loss of *PS1* was not detrimental to the parasite's ability to grow in normal culture media (figure 5.19).

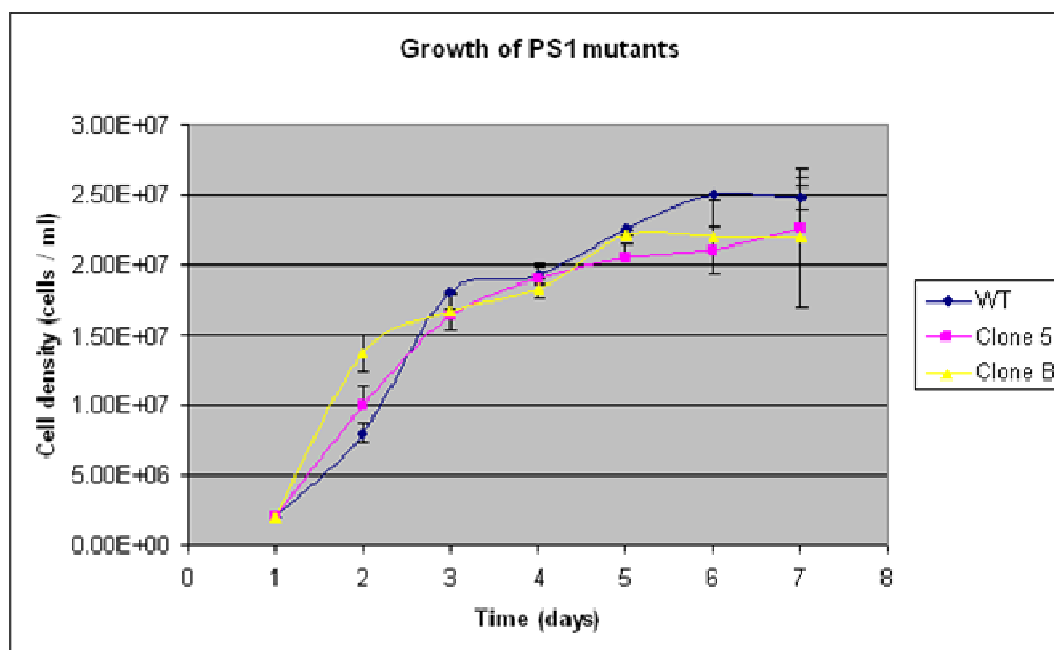


**Figure 5-19 Growth curve for  $\Delta ps1$  mutants**

Fresh cultures were set up with a starting cell density of  $1 \times 10^5$  cells  $\text{ml}^{-1}$ , and cells were counted at the same time each day until stationary phase was reached. Values shown are the mean  $\pm$  S.D from three independent experiments.

### 5.7.2 Differentiation into metacyclic promastigotes

The ability of  $\Delta ps1$  clones to differentiate into metacyclic promastigotes was investigated by analysing several properties which distinguish procyclic from metacyclic promastigote forms, including morphology (Sacks and Perkins, 1984), the expression of metacyclic-specific protein HASPB (Flinn *et al.*, 1994, Knuepfer *et al.*, 2001), and agglutination with peanut lectin (Sacks *et al.*, 1985). The development of infective metacyclic promastigotes is accompanied by glycosylation of the surface glycolipid, LPG, and it is this change in LPG structure that causes a loss of PNA agglutination in metacyclic promastigotes (Sacks and da Silva, 1987).

The analysis of these three markers of metacyclogenesis in conjunction has been useful in identifying subtle differences in the completion of differentiation. For example, although *L. major* VPS4<sup>E235Q</sup> promastigotes, defective in differentiation, did not express metacyclic specific proteins HASPB or SHERP and had reduced ability to infect and survive in macrophages, metacyclic-specific LPG was expressed on their cell surface (causing the non-agglutination of metacyclic like cells), leading to the suggestion that LPG assembly occurs earlier in the differentiation process than the expression of HASPB or SHERP (Besteiro *et*

*al.*, 2006b). On the other hand,  $\Delta atg4.2$  mutants analysed in the same study were negative for all markers of metacyclogenesis, leading to some speculation on the different roles of autophagy and endosome sorting in the completion of differentiation.

$\Delta ps1$  promastigotes looked morphologically similar to wild type cells by light microscopy, and cells with the characteristic shape of metacyclic promastigotes (shorter body with relatively longer flagellum) were identified in stationary phase cell cultures (figure 5.20 A). PNA negative cells were isolated from  $\Delta ps1$  promastigote cultures, demonstrating that the cells which appeared metacyclic-like in morphology also expressed the metacyclic specific version of LPG on their surface (figure 5.20 B). Wild type stationary phase cultures and  $\Delta ps1$  stationary phase promastigote cultures contained a similar proportion of PNA negative metacyclic promastigotes. Finally,  $\Delta ps1$  promastigotes were found to express the metacyclic specific protein HASPB at equivalent levels to wild type cells (figure 5.20 C). Together these data suggest that PS1 is not required for normal growth and differentiation of *Leishmania*.

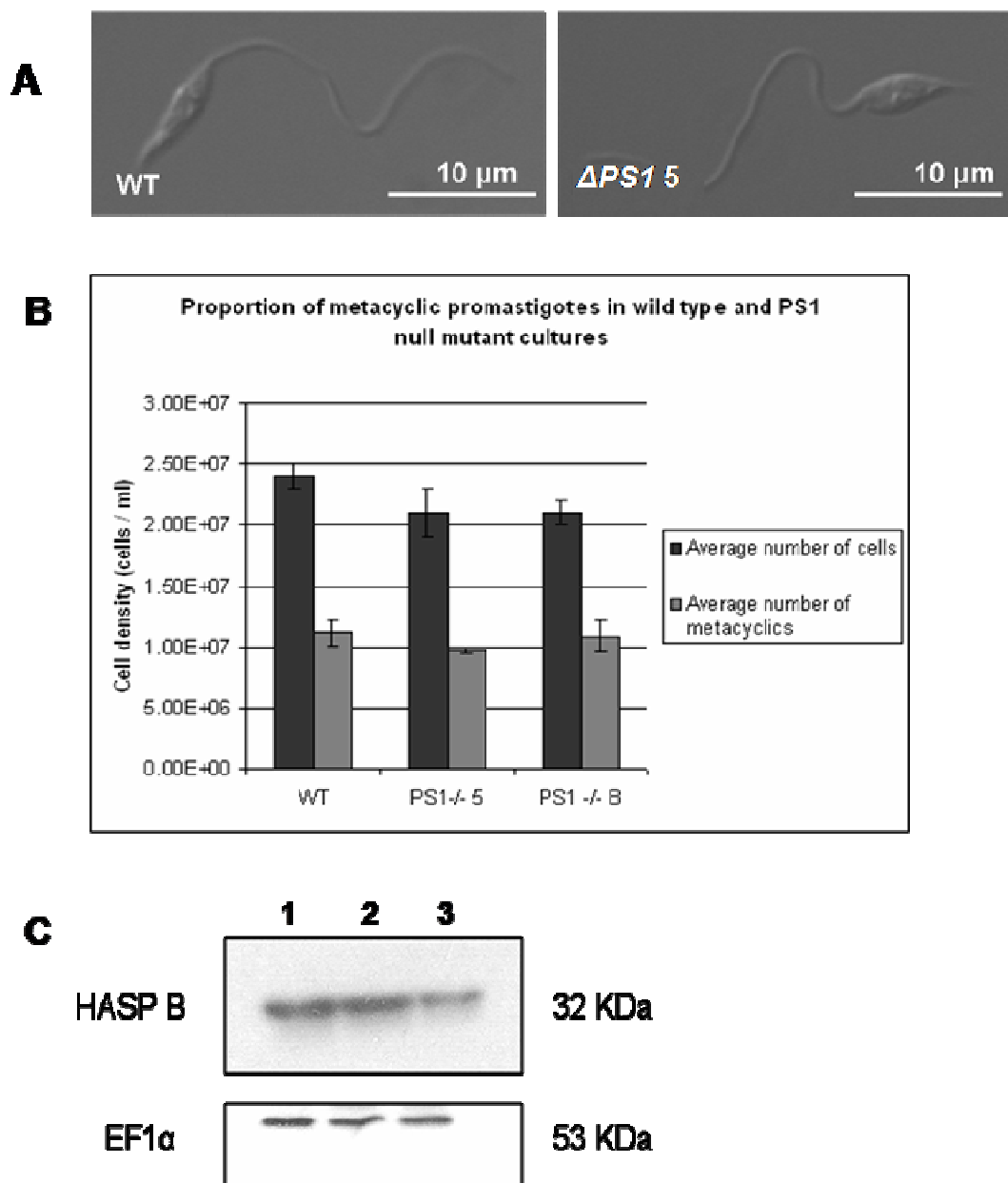


**Figure 5-20 Analysis of metacyclogenesis in *Δps1* null mutants.**

**A) DIC images of wild type and *Δps1* mutant (clone 5) metacyclic promastigotes.** Live cells were resuspended in ice-cold PBS and their morphology analysed by phase microscopy. One *Δps1* cell is compared to a wild type cell. **B) Agglutination of procyclic promastigotes by peanut lectin.** Peanut lectin (Sigma) was added at a concentration of  $50 \mu\text{g ml}^{-1}$  to 1 ml of stationary phase cells and incubated at room temperature for 10 minutes. Metacyclic promastigotes were separated from the agglutinated procyclic promastigotes by centrifugation at  $100 \times g$  for 5 minutes, and the cell density estimated by counting. Values shown are the mean  $\pm$  S.D from three independent experiments. **C) Expression of HASPB in wild type and *Δps1* mutant clones.** Stationary phase cells were harvested and lysed with 0.2% Triton-X-100 and separated by SDS-PAGE. The gels were transferred to a hybond-c nitrocellulose membrane and hybridised with rabbit anti-HASPB antibody (1 in 2000 dilution) or mouse anti-EF1 $\alpha$  antibody (1 in 5000 dilution) as a loading control. HRP conjugated secondary antibodies were used at 1 in 5000 dilution. The signal was detected using SuperSignal West Pico chemiluminescence detection system (Pierce). Lane 1 = wild type, Lane 2 = *Δps1-5*, Lane 3 = *Δps1-B*.

### 5.7.3 Infectivity to mammalian cells

In order to determine whether PS1 was required for virulence and infectivity of *L. major*, infectivity studies were carried out using peritoneal macrophages in an *in vitro* assay, and *in vivo* using BALB/C mice with footpad infections. The ability of parasites to infect macrophages was determined by counting the number of amastigotes within macrophages twenty four hours post infection. The initial infection rate was slightly lower in the mutants (31% and 26% of macrophages infected in clones 5 and B respectively compared with a 41% infection rate with wild type cells), however clearly the parasites were able to establish an infection *in vitro* (figure 5.21 A). The ability of the parasites to survive within the macrophages was assessed by counting the number of infected macrophages five days post infection. Again, the numbers of macrophages infected with  $\Delta ps1$  promastigotes was slightly lower than that for wild type cells (49% and 47% as compared to 58% infection rate for wild type cells) (figure 5.21 A). The ability of the parasites to replicate within macrophages was assessed by counting the number of amastigotes per infected macrophages. In both  $\Delta ps1$  mutant cell lines the numbers of amastigotes per infected macrophages had increased by day 5, with a small number of macrophages containing 16-20 amastigotes (figure 5.21 B). These data clearly demonstrate that  $\Delta ps1$  promastigotes are capable of infecting macrophages and replicating within the macrophage environment.

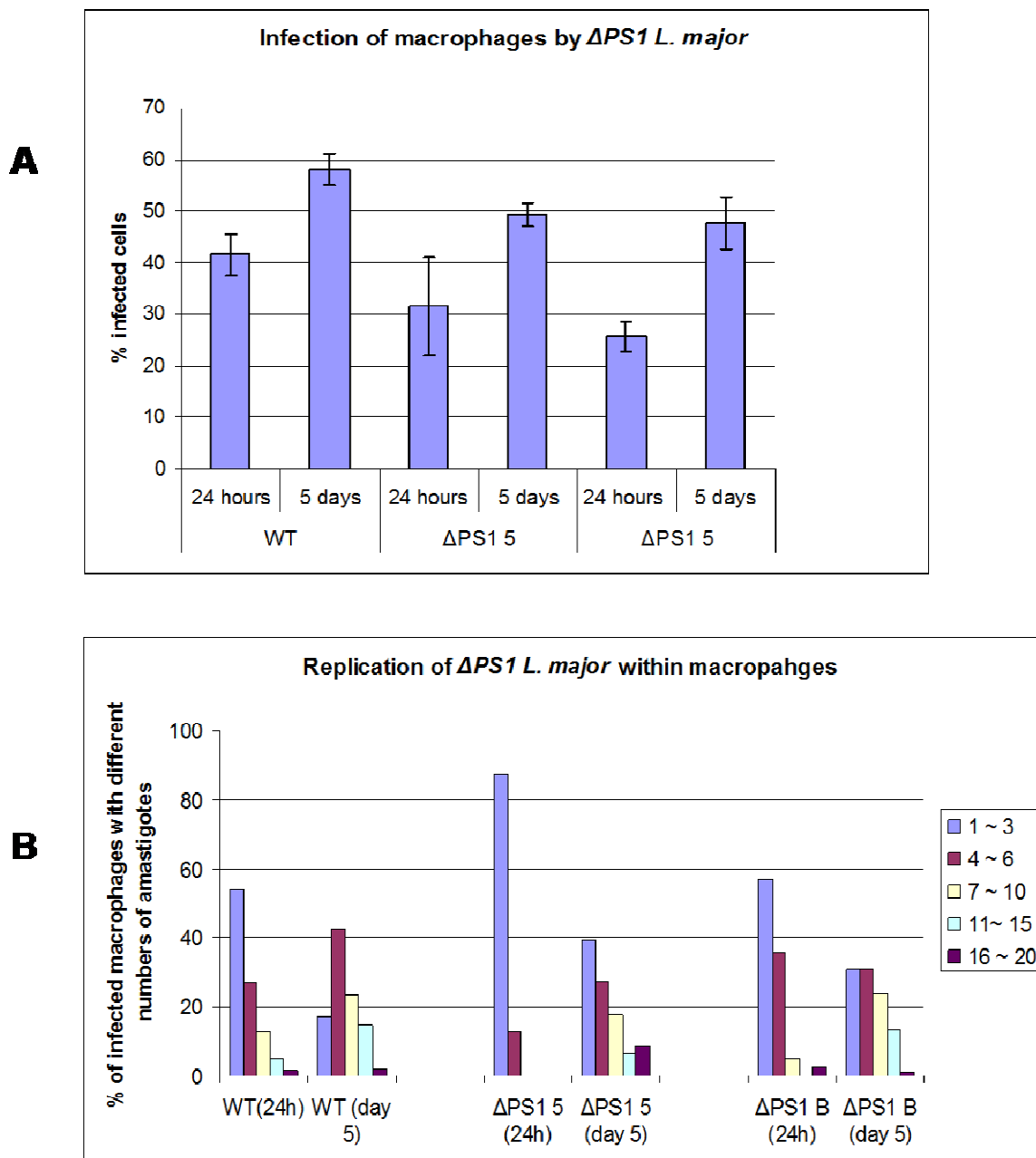


**Figure 5-21 Infection and survival of *L. major* wild type and  $\Delta ps1$  promastigotes within peritoneal macrophages**

Peritoneal macrophages were extracted from ICR mice and allowed to adhere to multi-well plates. Stationary phase parasites were added to the wells at a 10 to 1 ratio and washed three times with RPMI to remove non-internalised parasites after three hours. Cells were fixed in methanol 24 and 120 hours post infection, stained with Giemsa stain to visualise macrophage and parasite nuclei, and the percentage of macrophages containing parasites was recorded. **A) The proportion of macrophages containing amastigotes after 24 and 120 hours.** Values shown are the mean  $\pm$  S.D from three independent experiments. **B) The numbers of amastigotes within parasite-positive macrophages after 24 and 120 hours.**

An *in vivo* infection study was carried using wild type and  $\Delta ps1$  mutant stationary phase parasites. Five female BALB/c mice for each group (wild type,  $\Delta ps1$ -5 and  $\Delta ps1$ -B) were injected in the footpad with  $5 \times 10^5$  stationary phase parasites, and

the size of the footpad lesion was measured each week. The mutants formed footpad lesions at a comparable rate to wild type cells, with clone B producing a lesion of close to 5 mm one week earlier than the wild type control (figure 5.22). Amastigotes were isolated from footpad lesions, suggesting that the formation of lesions was not simply a non-specific inflammatory response. These data clearly demonstrate that PS1 is not a virulence factor for *L. major*, and is not required for growth, differentiation or infectivity.

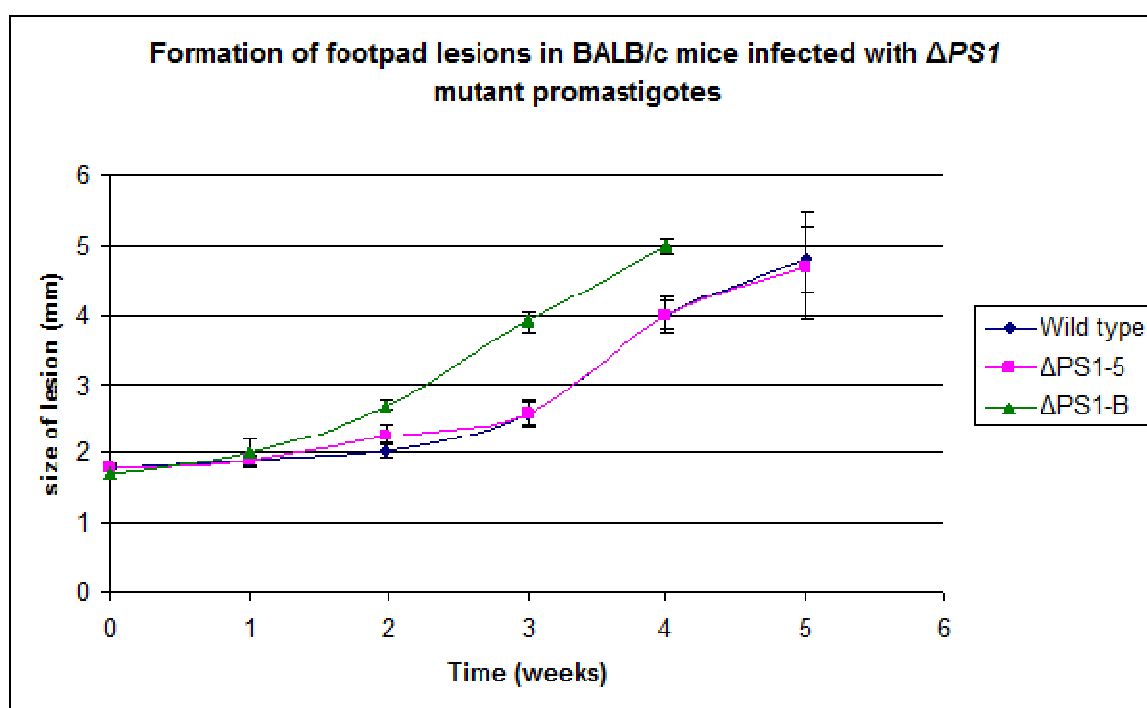


**Figure 5-22 Formation of footpad lesions in BALB/c mice infected with wild type and  $\Delta PS1$  mutant *L. major*.**  $5 \times 10^5$  stationary phase parasites (wild type,  $\Delta PS1 5$  and  $\Delta PS1 B$ ) were injected in BALB/c footpads, and a measurement of the footpad taken each week. Mice were culled before the footpad exceeded 5 mm thick. Values shown are the mean footpad measurement  $\pm$  S.D from five mice in each group.

## 5.8 Analysis of Autophagy in $\Delta ps1$ mutant promastigotes

The distribution of GFP-ATG8 labelled autophagosomes was analysed in  $\Delta ps1$  mutant promastigotes in order to investigate a putative role for PS1 in the maturation of autophagosomes. A plasmid which conferred the expression of GFP-ATG8 with neomycin resistance (pGL1686) was produced by replacing the hygromycin resistance gene of pGL1078 (the plasmid used for all previous GFP-

ATG8 expression analyses), with the purified neomycin resistance gene.  $\Delta ps1-5$ ,  $\Delta ps1-B$  and wild type promastigotes were transfected with pGL1686, and the production of autophagosomes during differentiation was analysed as described in chapter 3. Fewer  $\Delta ps1$  mutants were found to contain GFP-ATG8 labelled autophagosomes than wild type cells (figure 5.23 A), and in stationary phase  $\Delta ps1$  mutant cultures the average number of autophagosomes per positive cell increased (figure 5.23 B), indicating an accumulation of autophagosomes and perhaps a disruption in trafficking to the lysosome. In stationary phase  $\Delta ps1$  mutants, many autophagosomes were abnormally large compared to wild type cells, although some cells did contain “normal” autophagosomes (figure 5.24 A and B compared to C). GFP labelled MVT structures were rarely observed in  $\Delta ps1$  mutant promastigotes, suggesting that the ATG8 was not being trafficked to the lysosome in most cells. Although there was a small increase in the number of autophagosomes in response to starvation in  $\Delta ps1$  mutant promastigotes, the proportion of cells containing autophagosomes after four hours of starvation was very low compared to wild type cells (figure 5.23 C), suggesting that the autophagy response to starvation was also disrupted in  $\Delta ps1$  mutant promastigotes. Together, the results from these experiments indicated a role for PS1 in the regulation of autophagy, as was hypothesised.

To confirm that autophagy was deregulated in  $\Delta ps1$  mutant promastigotes, these experiments were repeated at a later date, using the analysis of GFP-ATG8 distribution in the  $\Delta ps1-5[PS1]$  cell line, in which the *PS1* ORF was expressed at the 18S rRNA locus, as a control. In order to show that the disruption of autophagy in  $\Delta ps1$  mutant promastigotes was due to the loss of *PS1*, rather than non-specific by stress due to transfection, new transfections were performed in which GFP-ATG8 was expressed in  $\Delta ps1-5$  and  $\Delta ps1-B$  mutant promastigotes that had been isolated from BALB/c footpad lesions.

The first set of data obtained was not reproducible, and the  $\Delta ps1$  mutant promastigotes appeared to undergo autophagy in the same manner as wild type cells. The percentage of cells containing autophagosomes, and the average number of autophagosomes per cell, were comparable in wild type and  $\Delta ps1$  mutant promastigotes (figure 5.25 A,B,C). It could be that this apparent “loss” of phenotype occurred because the  $\Delta ps1$  mutants had been allowed to adapt to compensate for the loss of PS1 during time in culture and within an animal host.

Alternatively, the accumulation of GFP-ATG8 observed in figures 5.24 and 5.25 might be an effect due to some unrelated post-transfection stress that the parasites were under. For example, protein aggregates that are positive for the autophagy marker LC3 were observed in macrophages and dendritic cells that were under stress due to transfection (Szeto *et al.*, 2006). On the other hand, it is clear that the accumulation of large GFP-ATG8 structures is not a general response to transfection stress as cells carrying this plasmid have been used repeatedly throughout this study. Further experiments using  $\Delta ps1$  mutant cell lines that were frozen immediately after obtaining them are required to resolve this issue.

The localisation and expression of *L. major* ATG8 homologues (GFP-ATG8A, GFP-ATG8B and GFP-ATG8C) also appeared to be unaffected in  $\Delta ps1$  mutants (figure 5.25 C and 5.26). GFP-ATG8A was recruited to punctate structures in response to starvation in  $\Delta ps1$  mutant promastigotes in the same manner as in wild type cells (figure 5.25 C and 5.26). GFP-ATG8B and GFP-ATG8C localised to a single punctum close to the flagellar pocket in  $\Delta ps1$  mutant promastigote, in a distribution resembling that seen in wild type cells (figure 5.26 compared to figure 3.4). The localisation of GFP-ATG8A, GFP-ATG8B and GFP-ATG8C appeared to be normal in mutant promastigotes, both before and after being allowed to adapt during infection in a mouse. Data shown (figures 5.25 and 5.26) were obtained from parasites that had been passaged through an animal.

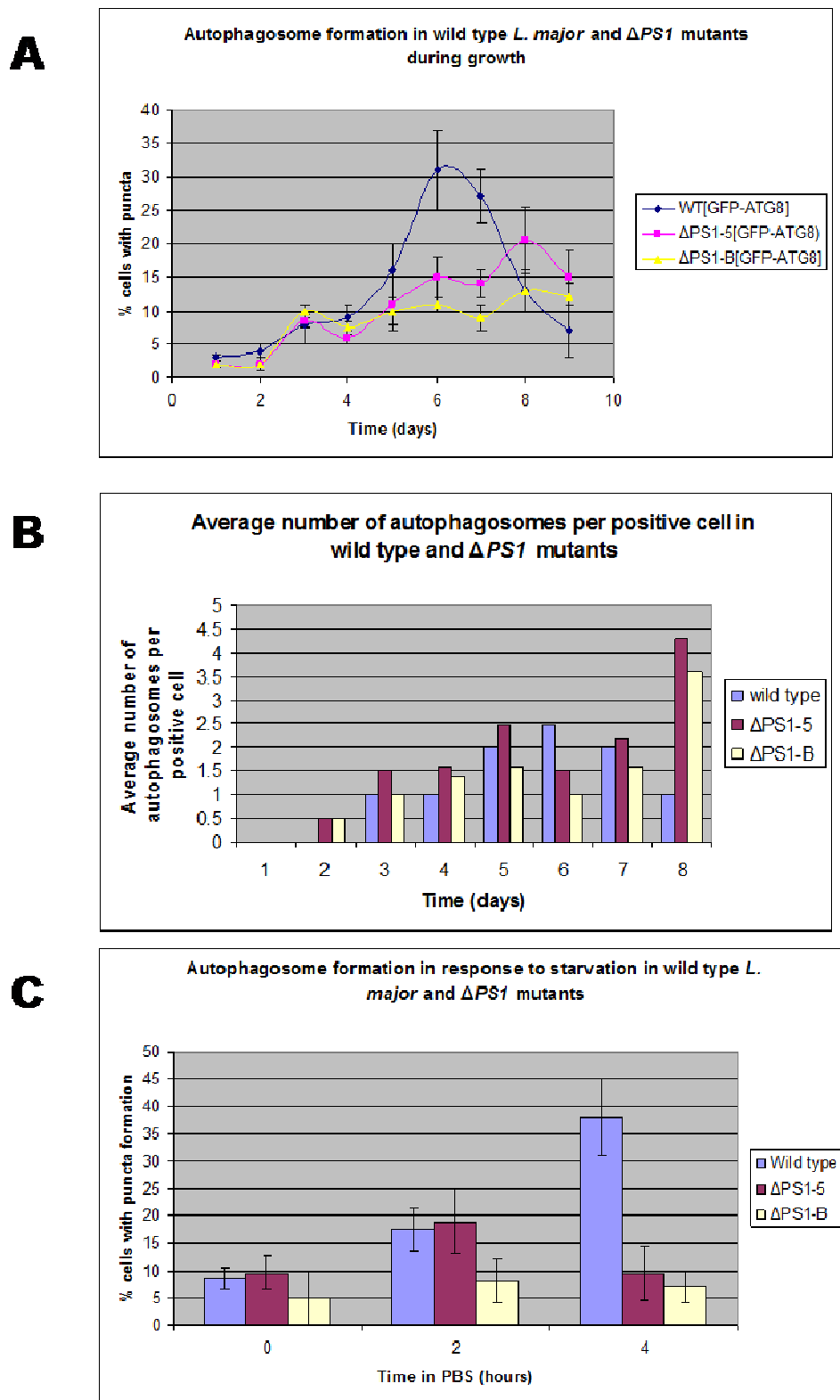


**Figure 5-23. Analysis of autophagy in  $\Delta ps1$  mutant promastigotes (experiment one).** A) Autophagosome formation in  $\Delta ps1$  mutants during growth. The percentage of promastigotes in a population containing GFP-ATG8 labelled punctate structures was counted every day until stationary phase was reached. Values shown are the mean  $\pm$  S.D from three independent experiments. B) The average number of autophagosomes per positive cell in wild type and in  $\Delta ps1$  mutants. The number of autophagosomes per positive cell (i.e. cells which contained one or more autophagosomes) was recorded every day during a growth curve. C) Autophagosome production in response to starvation in  $\Delta ps1$  mutant promastigotes. The percentage of cells containing autophagosomes was recorded after two hours and four hours of starvation. Values shown are the mean  $\pm$  S.D from three independent experiments.

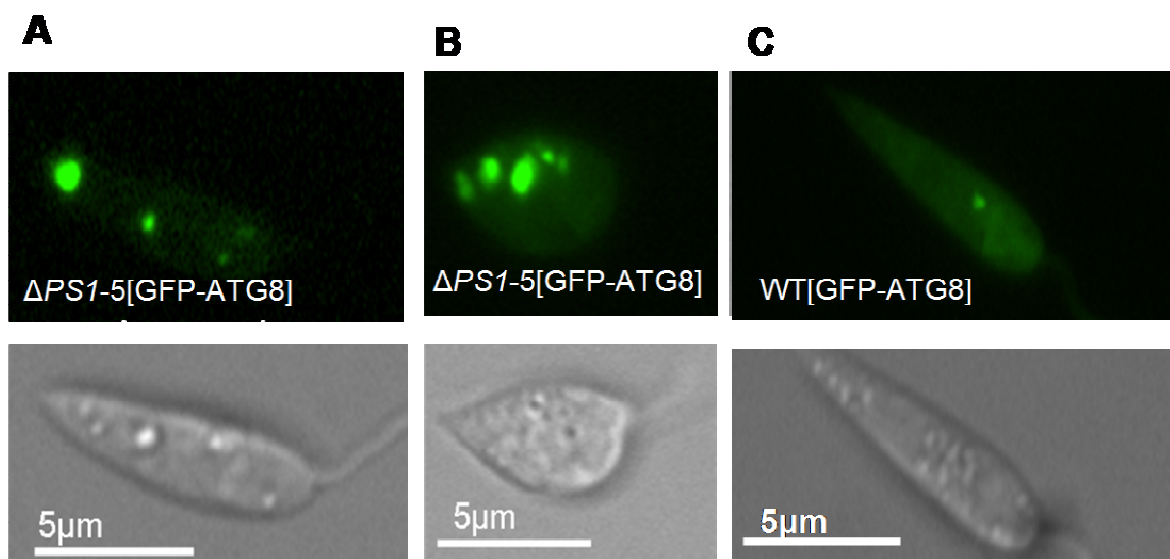


**Figure 5-24 Abnormally large autophagosomes accumulate in  $\Delta ps1$  mutant promastigotes.** Late log phase promastigotes were washed twice in PBS, resuspended in ice-cold PBS, settled onto glass slides and viewed using an Applied Precision DeltaVision microscope. Figures A and B show  $\Delta ps1-5$  [GFP-ATG8] and C is wild type [GFP-ATG8].

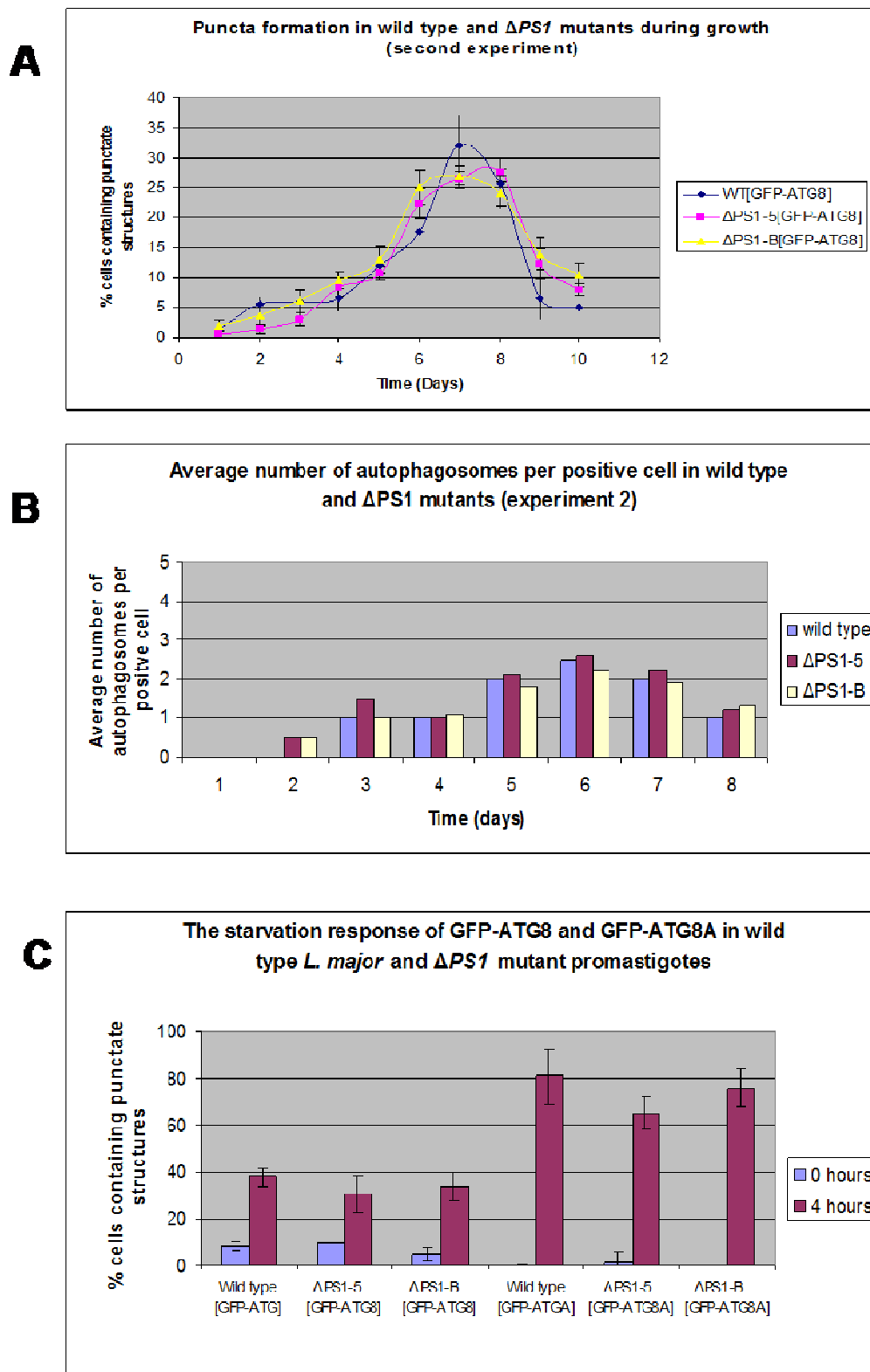


**Figure 5-25 Analysis of autophagy in  $\Delta ps1$  mutant promastigotes (experiment two).** All analyses performed for figure 5.11 were repeated using  $\Delta ps1$  mutant recently isolated from BALB/c footpad lesions. **A) Autophagosome formation in  $\Delta ps1$  mutants during growth.** The percentage of promastigotes in a population containing GFP-ATG8 labelled punctate structures was counted every day until stationary phase was reached. Values shown are the mean  $\pm$  S.D from three independent experiments. **B) The average number of autophagosomes per positive cell in wild type and in  $\Delta ps1$  mutants.** The number of autophagosomes per positive cell (i.e. cells which contained one or more autophagosomes) was recorded every day during a growth curve. **C) The starvation response of GFP-ATG8 and GFP-ATG8A in  $\Delta PS1$  mutant promastigotes.** The percentage of cells containing punctate structures labelled with GFP-ATG8 or GFP-ATG8A was recorded after two hours and four hours of starvation. Values shown are the mean  $\pm$  S.D from three independent experiments.

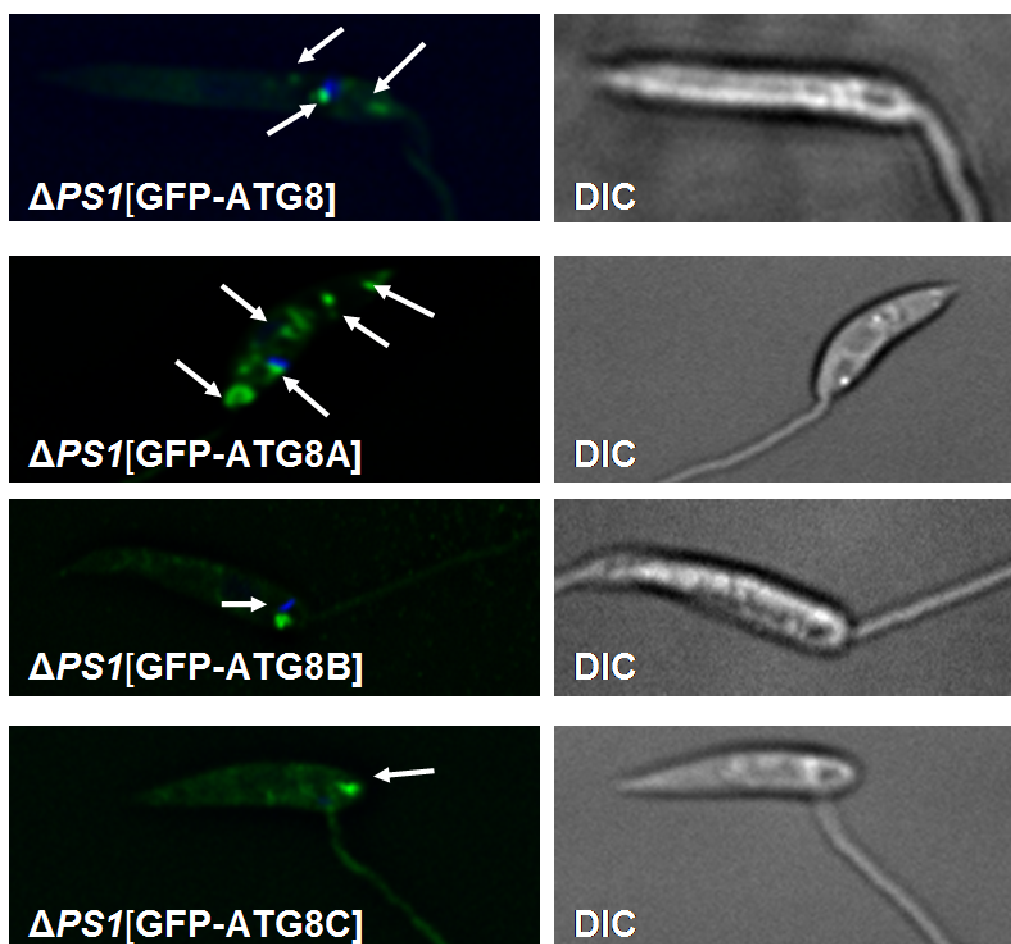


**Figure 5-26 Localisation of GFP-ATG8, GFP-ATG8A, GFP-ATG8B and GFP-ATG8C in  $\Delta PS1$  mutants.**  $\Delta ps1$  mutants were transfected with plasmids for the expression of GFP-ATG8, GFP-ATG8A, GFP-ATG8B or GFP-ATG8C with neomycin resistance. Promastigotes were washed twice in PBS, resuspended in ice-cold PBS, settled onto glass slides and viewed using an Applied Precision DeltaVision microscope.  $\Delta ps1-5$  [GFP-ATG8],  $\Delta ps1-5$  [GFP-ATG8B] and  $\Delta ps1-5$  [GFP-ATG8C] were viewed by microscopy in late log phase cells.  $\Delta ps1-5$  [GFP-ATG8A] were incubated in PBS for four hours prior to preparation for microscopy. Identical distribution of *L. major* ATG8 homologues was observed in  $\Delta PS1$ -B.

## 5.9 Analysis of endocytosis and protein trafficking in PS1 null mutants

Some evidence has accumulated suggesting that, in addition to its role in intramembrane proteolysis, PS1 functions in endocytosis, trafficking of membrane proteins and vesicle transport via mechanisms that are independent of  $\lambda$ -secretase activity (McCarthy, 2005).  $\Delta ps1$  deficient fibroblasts had a reduced ability to endocytose APP, APP-like protein (APLP) and other surface proteins, suggested to be due to competition for endocytosis-associated adaptor proteins by accumulated APP C-terminal fragments (CTFs) that had not been trafficked correctly (Kaether *et al.*, 2002). Additionally, the internalisation of extracellular lipoproteins by receptor mediated endocytosis was reduced in

$\Delta ps1/2$  double knock out mouse embryonic fibroblasts, although this was attributed to a loss of  $\lambda$ -secretase activity rather than a loss of PS1 itself (Tamboli *et al.*, 2008).

A role for PS1 has been identified in the ER-Golgi trafficking of select membrane proteins including APP, APLP1 (Naruse *et al.*, 1998), Notch (Ye *et al.*, 1999),  $\alpha$ -synuclein (Wilson *et al.*, 2004), telencephalin (Esselens *et al.*, 2004), and epidermal growth factor receptor (EGFR) (Repetto *et al.*, 2007). Additionally, PS1 has been shown to interact with Rab11, syntaxin 5 and syntaxin 1A, all proteins involved in vesicle transport (Dumanchin *et al.*, 1999, Suga *et al.*, 2004, Smith *et al.*, 2000).

### **5.9.1 Internalisation of the endocytic tracer FM4-64 in $\Delta ps1$ mutants**

Having shown that autophagosome formation with ATG8 was not impaired in  $\Delta ps1$  mutants (at least in cells that had undergone differentiation into amastigotes), the ability of the mutants to undergo endocytosis was studied utilising the endocytic tracer FM4-64. The marker initially accumulated in the flagellar pocket, as in wild type cells, and with time was progressively internalised (figure 5.27), suggesting that the endocytic pathway was not disrupted in  $\Delta ps1$  mutants.

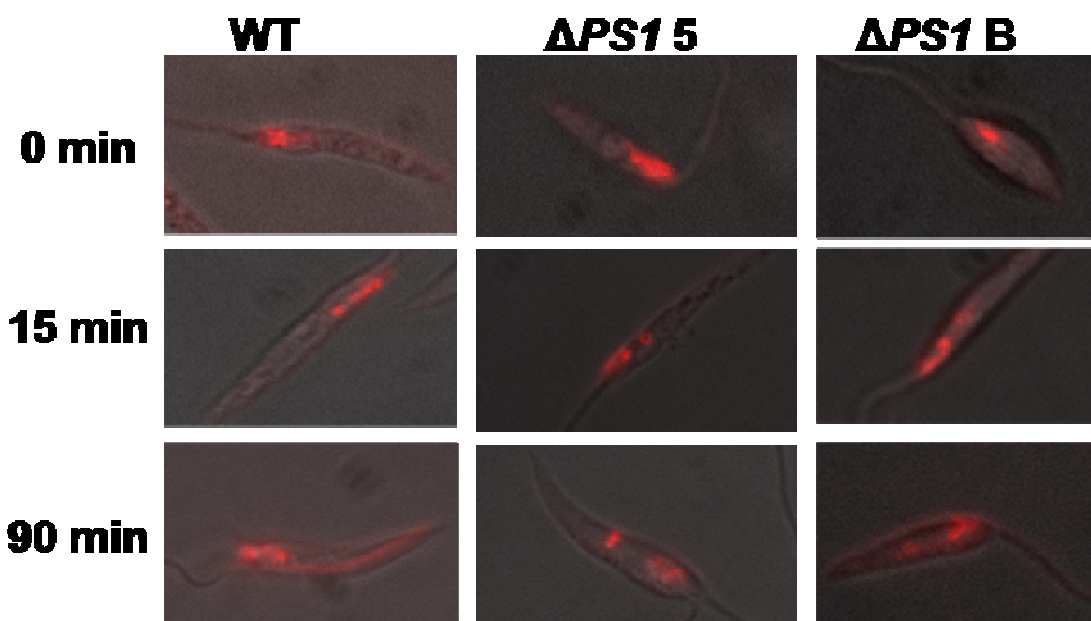


**Figure 5-27 Uptake of the endocytic tracer FM4-64 in  $\Delta ps1$  mutants.** Late log phase promastigote cultures were incubated with 40 $\mu$ M FM4-64 (Molecular probes) in a 100  $\mu$ l of serum free HOMEM at 4°C for 15 minutes. The cells were then washed and resuspended in HOMEM and incubated at 25°C for 15 minutes or 90 minutes. Cells were then washed and resuspended in ice cold PBS and viewed using the Rhodamine filter of an Applied Precision DeltaVision microscope.

### 5.9.2 Localisation of syntaxin 5 and syntaxin 1A in $\Delta ps1$ mutants

In addition to its putative role in trafficking membrane proteins, PS1 has been shown to interact with proteins involved in vesicle transport. An interaction with Rab11 (a protein associated with recycling endosomes) was shown by yeast-2-hybrid, immunoprecipitation and western blotting experiments (Dumanchin *et al.*, 1999). Interactions with the syntaxin 5 and syntaxin 1A, proteins involved in the regulation of vesicle transport, were shown by immunoprecipitation experiments with full length PS1 and the recombinant hydrophilic loop of PS1, respectively (Suga *et al.*, 2004, Smith *et al.*, 2000).

To investigate the possibility that SNARE-mediated vesicle trafficking might be disrupted in  $\Delta ps1$  mutants, *L. major* homologues of syntaxin 1A and syntaxin 5 (LmjF28.1470 and LmjF32.0070 respectively) were expressed with an N terminal GFP tag in wild type and mutant cells. The localisation of these proteins had been previously studied in wild type *L. major* and the syntaxin 1A homologue, LmjF28.1470, was found to localise in the flagellar pocket, while LmjF32.0070 (syntaxin 5) co-localised with the Golgi marker Rab1 (Besteiro *et al.*, 2006a). The localisation of both proteins was found to be identical in  $\Delta ps1$  mutants and

wild type cells (figure 5.28, Besteiro *et al.*, 2006a), demonstrating that a loss of PS1 did not lead to a disruption in the localisation and trafficking of these vesicle trafficking associated proteins. A striking similarity was noticed between the localisation of GFP-LmjF28.1470 and PS1-HA (figure 5.9), and co-localisation studies are required to investigate a possibility of interactions *in vivo*.

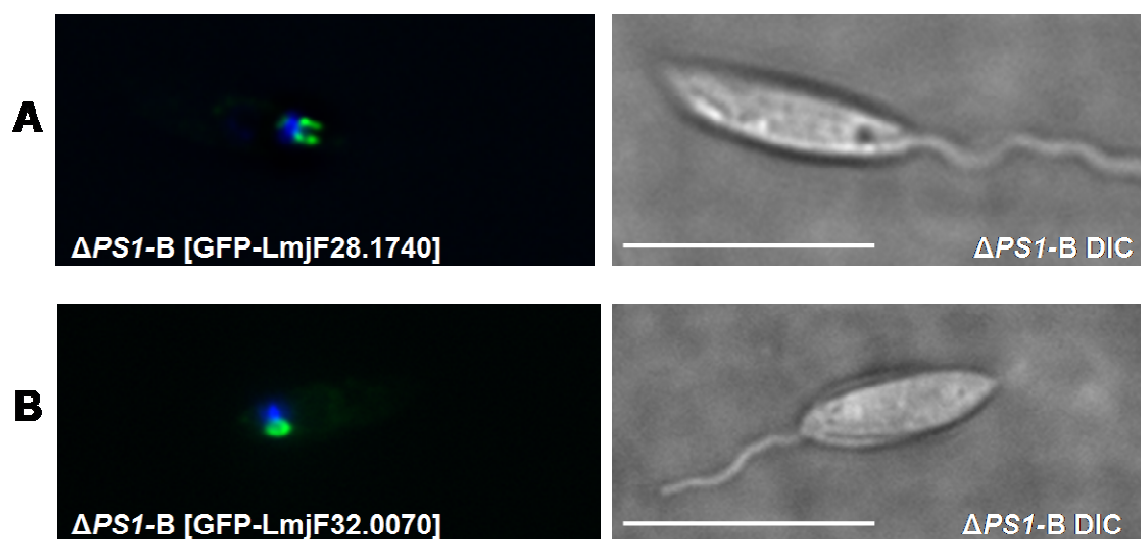


**Figure 5-28 Localisation of syntaxin 1A and syntaxin 5 in  $\Delta ps1$  promastigotes.**  $\Delta ps1$  mutants were transfected with pGL1431 and pGL1433 for the expression GFP fused LmjF28.1740 (syntaxin 1A) and LmjF32.0070 (syntaxin 5). Log phase promastigotes were washed twice in PBS, resuspended in ice-cold PBS, settled onto glass slides and viewed using an Applied Precision DeltaVision microscope. Scale bar is 10  $\mu\text{m}$ .

### 5.9.3 Trafficking of the vacuolar proton pyrophosphatase ( $\text{V-H}^+$ -PPase) in $\Delta ps1$ mutants

The possibility that PS1 was involved in the trafficking of membrane proteins was investigated by analysing the expression of GFP tagged wild type and mutated vacuolar proton pyrophosphatase  $\text{V-H}^+$ -PPase in  $\Delta ps1$  mutants.  $\text{V-H}^+$ -PPase is polytopic membrane protein that functions in the acidification of acidocalcisomes (Lustig *et al.*, 2007). It was recently shown, using indirect immunofluorescence and analysis of GFP tagged protein, that  $\text{V-H}^+$ -PPase was not correctly trafficked to acidocalcisomes in *L. major* mutants deficient in the adaptor protein subunit 3 ( $\Delta ap3\delta$ ) (Besteiro *et al.*, 2008). In fact, the GFP signal was not detectable in the mutants, leading to the suggestion that the mis-trafficked GFP- $\text{V-H}^+$ -PPase was being degraded by an unidentified peptidase.

Similarly, levels of endogenous V-H<sup>+</sup>-PPase were significantly reduced in a *T. brucei* signal-recognition particle (SRP)-deficient mutant, leading to the suggestion that the mis-translocated protein was subjected to proteolysis. Inhibition of the proteasome and lysosome did not inhibit proteolysis of V-H<sup>+</sup>-PPase, leading to the proposal that mis-targeted V-H<sup>+</sup>-PPase might be degraded by an unidentified intramembrane protease potentially localised on the face of the ER membrane (Lustig *et al.*, 2007).

Wild type GFP- V-H<sup>+</sup>-PPase (LmjF31.1220) was shown to localise to acidocalcisome membranes in  $\Delta ps1$  mutant promastigotes, and expression levels were similar to those seen in wild type cells (figure 5.29, (Besteiro *et al.*, 2008) indicating that PS1 is not required for the correct trafficking of this membrane protein. The hypothesis that PS1 could function as the “unidentified intramembrane protease” responsible for the proteolysis of mis-localised V-H<sup>+</sup>-PPase was investigated by studying the localisation of mutated V-H<sup>+</sup>-PPase in  $\Delta ps1$  mutants using GFP fusion proteins. Four tyrosine motifs, (<sub>115</sub>YTRI<sub>118</sub>, <sub>130</sub>YKYM<sub>133</sub>, <sub>467</sub>YRPV<sub>470</sub>, <sub>539</sub>YGPI<sub>542</sub>), were predicted to be the sites of recognition by the adaptor protein AP3, so it was hypothesised that mutating these residues would lead to the mis-localisation of V-H<sup>+</sup>-PPase in the same manner as depleting AP3 (Besteiro *et al.*, 2008). Plasmids were produced by D Tonn (Mottram lab) for the expression of V-H<sup>+</sup>-PPase in which Tyr<sub>467</sub> and Tyr<sub>539</sub> were mutated and replaced with alanine residues. Tyr<sub>115</sub> and Tyr<sub>130</sub> were disregarded as they were predicted to lie within the transmembrane domains and therefore unlikely to be involved in the trafficking of V-H<sup>+</sup>-PPase.

The mutation of the Tyr<sub>467</sub> and Tyr<sub>539</sub> was not sufficient however to disrupt the targeting of GFP-V-H<sup>+</sup>-PPase to acidocalcisome membranes, and GFP-V-H<sup>+</sup>-PPase<sup>Y437AY439A</sup> had a subcellular distribution resembling that seen with non-mutated GFP-V-H<sup>+</sup>-PPase in both wild type cells and  $\Delta ps1$  mutant cells (figure 5.29 B). The hypothesis that PS1 was the mysterious “unidentified membrane protease” could not be studied using these constructs, and the further mutation of the remaining two tyrosine motifs (<sub>115</sub>YTRI<sub>118</sub>, <sub>130</sub>YKYM<sub>133</sub>) should be considered for further investigation.

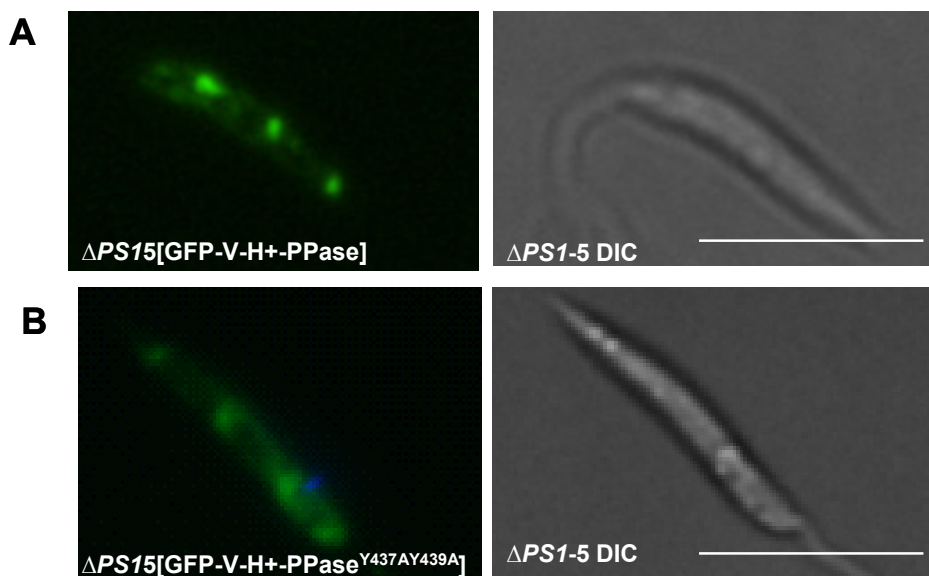


**Figure 5-29 Localisation of wild type and mutated V-H<sup>+</sup>-PPase in  $\Delta ps1$  mutants.**  $\Delta ps1$  mutants were transfected with pGL1681 and pGL1703 for the expression GFP fused with wild type V-H<sup>+</sup>-PPase or V-H<sup>+</sup>-PPase<sup>Y437AY439A</sup>. Log phase promastigotes were washed twice in PBS, resuspended in ice-cold PBS, settled onto glass slides and viewed using an Applied Precision DeltaVision microscope. Scale bar is 10  $\mu$ m.

## 5.10 Other aspartyl peptidases in *L. major*

Although PS1 and SPP are not highly similar in sequence (*L. major* SPP is 18% similar to PS1), they have an overall conservation of structural motifs (Ponting *et al.*, 2002). The YD and GLGD motifs which contain the catalytic aspartate residues are conserved and shown to be essential for activity in both proteases, although the orientation of those transmembrane regions is inverted in SPP compared to PS1 (Weihofen *et al.*, 2002). This inversion of the active site is significant in terms of function, as PS1 cleaves within the transmembrane domain of type 1 membrane proteins that are oriented in the membrane with their N terminus in the cytoplasm), and SPP cleaves type 2 membrane proteins that are orientated with their C terminus in the cytoplasm.

No PS1 homologue has been identified in *Plasmodium* species, while SPP appears to be ubiquitous in eukaryotic cells, and the only other predicted aspartyl peptidase in the *Leishmania* genome (Ivens *et al.*, 2005). The specific inhibition of SPP in *P. falciparum* impaired parasite viability in all stages of growth, and it was not possible to produce an SPP null mutant in *P. berghei*, indicative of an essential role (Bonilla, 2008). *P. falciparum* SPP localises to micronemes of

mature parasites, and antibodies to PfSSP were found to inhibit red blood cell invasion *in vitro* (Li *et al.*, 2008).

To investigate the possibility that SPP compensated for the loss of *PS1* in  $\Delta ps1$  *L. major* mutants, the effect of SPP and  $\gamma$ -secretase-specific inhibitors were compared in wild type and mutant cell lines using an alamar blue assay. Pentamidine, known to have anti-leishmanial activity was used as a positive control in each experiment. Three inhibitors were tested; *N*-[*N*-(3,5-difluorophenacetyl)-*L*-alanyl]-*S*-phenylglycine *t*-butyl ester (DAPT), a specific inhibitor of  $\gamma$ -secretase (Nyborg *et al.*, 2004), LY411,575, a derivative of DAPT that inhibits mammalian SPP only at high concentrations (Weihofen *et al.*, 2003), and (Z-LL)<sub>2</sub> ketone, a specific SPP inhibitor (Weihofen *et al.*, 2000, Lemberg and Martoglio, 2002). DAPT, LY411,575 and (Z-LL)<sub>2</sub> ketone were kindly provided by Dr J Bonilla, (University of Florida).

*L. major* wild type,  $\Delta ps1-5$ ,  $\Delta ps1-B$  and  $\Delta ps1[PS1]$  promastigotes were diluted to a concentration of  $2 \times 10^6$  cells ml<sup>-1</sup> in HOMEM media and incubated with concentrations of the drugs ranging from 1.5  $\mu$ M to 50  $\mu$ M, or DMSO alone as a negative control in 96 well plates. Four sets of data were obtained for each parasite / drug combination (2 different plates with duplicates on each plate).

Pentamidine inhibited parasite growth of wild type and mutants clones with an LD<sub>50</sub> between 3.6 - 6.10  $\mu$ M, and a distinct inhibition curve was produced for all cell lines, indicating that there were no technical problems with the assay (table 5.3). Concentrations of 50  $\mu$ M of the  $\gamma$ -secretase or SPP inhibitors were not sufficient to inhibit promastigote growth in any of the cell lines. However, the effect of these drugs against amastigotes, the disease-causing stage of the parasite, has not been investigated, and should be analysed.

Cell Line	LD <sub>50</sub> ( $\mu$ M) DAPT	LD <sub>50</sub> ( $\mu$ M) LY411,575	LD <sub>50</sub> ( $\mu$ M) (Z-LL) <sub>2</sub> ketone)	LD <sub>50</sub> ( $\mu$ M) Pentamidine
Wild type	>50 $\mu$ M	>50 $\mu$ M	>50 $\mu$ M	3.66
$\Delta PS1-5$	>50 $\mu$ M	>50 $\mu$ M	>50 $\mu$ M	5.44
$\Delta PS1-B$	>50 $\mu$ M	>50 $\mu$ M	>50 $\mu$ M	3.66
$\Delta PS1[PS1]$	>50 $\mu$ M	>50 $\mu$ M	>50 $\mu$ M	6.10

Table 5-3: LD<sub>50</sub> values for  $\gamma$ -secretase and SPP inhibitors on wild type and  $\Delta ps1$  *L. major*

## 5.11 Discussion

In this study, some progress has been made in analysing the expression and localisation of PS1 in *L. major*, although clarification of the subcellular localisation is needed, and further attempts to optimise conditions for the use of anti-PS1 antibodies are required. Through the production and analysis of  $\Delta ps1$  null mutants it has been shown that PS1 is not required for parasite viability or virulence, although a potential role for PS1 in regulating autophagy was uncovered, requiring further confirmation.

By isolating total RNA from promastigotes and amastigotes and performing reverse-transcriptase PCR (RT-PCR) using an mRNA-specific “splice-leader” (SL) primer in conjunction with a PS1 specific primer, it was demonstrated that the gene encoding *PS1* is transcribed in both life cycle stages of *L. major*. Cloning and sequencing of the PCR product allowed the confirmation of the predicted start codon annotated in GeneDB and led to the identification of the splice leader addition site.

Analysis of the localisation of PS1 in *L. major* was not conclusive. Episomally expressed PS1-GFP was detected on various intracellular membranes within any one population of transfected cells. Approximately half of the cells exhibited an ER-like distribution of PS1-GFP, while others exhibited a punctate distribution that partially co-localised with the MVT labelled with lysotracker. In fact, this distribution resembled that of acidocalcisomes, as labelled with lysotracker or acridine orange in wild type cells (Besteiro *et al.*, 2008). On the other hand, PS1-HA expressed in wild type and  $\Delta ps1$  mutants was detected close to the flagellar pocket, in a distribution similar to but not over-lapping with that of *L. major* Rab11 (figure 5.9C). The localisation of mammalian PS1 is equally as controversial, and the literature is full of contradictory reports.

Immunofluorescence performed on human neuronal cells transfected with wild type PS1 or PS1 with immunogenic tags inserted either at the N terminus (between residues 44 and 45) or at the carboxyl terminus found that PS1 was localised mainly on ER and early Golgi membranes (Cook *et al.*, 1996). Similarly, a reticular staining thought to be the ER with a more pronounced perinuclear staining was detected in COS-1 cells transfected with plasmids containing the

cDNA for human PS1 using antibodies raised against three distinct epitopes at the N terminus, the hydrophilic loop, and the second loop. In both studies, endogenous PS1 could not be detected in these cells probably due to low levels of expression (De Strooper *et al.*, 1997). Low levels of PS1 have also been detected at the cell surface in human neurons (Dewji and Singer, 1997, Dewji, 2005) and other divergent localisations have also been reported, including clathrin coated vesicles (Efthimiopoulos *et al.*, 1998), nuclear membrane, interphase kinetochores, and centrosomes (Li *et al.*, 1997). It has been suggested that some of the subcellular localisations described for PS1 might be artefacts due to the over-expression of full length PS1, rarely observed *in vivo* in this form (Annaert and De Strooper, 1999). For example, the abundant localisation of PS1 in the ER might be due to an accumulation of misfolded full length protein, and its association with centrosomes could be an artefact due to overexpression of misfolded full length PS1 leading to the formation of insoluble cytoplasmic structures, aggresomes, which accumulate at the microtubule-organising centre (Johnston *et al.*, 1998, Annaert and De Strooper, 1999).

Biologically functional PS1 tagged with GFP was used to analyse the localisation and function of PS1 in human kidney cells (Kaether *et al.*, 2002). GFP was inserted into the large cytoplasmic loop, shown to be irrelevant for PS1 function (Saura *et al.*, 2000), and the localisation analysed by live cell microscopy. PS1 was detected at the cell surface, surrounding the nuclear envelope, in the ER and in vesicular structures (Kaether *et al.*, 2002). The authors noted that the GFP fluorescence was very weak and significantly reduced upon fixation, suggesting low levels of expression of PS1. It was suggested that the low levels of PS1 expression and the requirement for sensitive detection methods could be the reason that conventional immunolabelling techniques had only detected PS1 at the ER and Golgi apparatus, and not at the plasma membrane.

Finally, subcellular fractionation and immunofluorescence analysis using antibodies raised against the hydrophilic loop of PS1 and an N terminal hydrophilic domain failed to detect endogenous PS1 in the Golgi and ER of PC12 cells, and instead found that PS1 co-localised with transferrin receptor, a marker of early endosomes (Lah and Levey, 2000). Other subcellular fractionation studies revealed that while full length protein, of which very little is thought to accumulate under normal physiological conditions, was primarily

localised to the ER, N terminal and C terminal fragments localised mainly to the Golgi (Zhang *et al.*, 1998).

While there is evidence in the literature that supports the intracellular membrane (mainly ER) localisation detected in live cells expressing PS1-GFP, episomal expression of GFP tagged proteins using the pNUS plasmids can lead to high levels of protein expression (Benzel *et al.*, 2000), so the over-expression of full length tagged PS1 might have led to the mis-folding of the protein in the ER (Johnston *et al.*, 1998). The localisation of PS1-HA near the flagellar pocket could indicate a role in endocytosis or exocytosis, and is supported by subcellular fractionation studies and immunofluorescence studies using antibodies that detected endogenous PS1 (Lah and Levey, 2000). The localisation of PS1-HA to the flagellar pocket region was consistent in wild type and  $\Delta ps1$  mutants (figure 5.9C), suggesting that this localisation was unlikely to be due to over-expression of the tagged protein. Confirmation of the localisation of PS1 might be obtained by inserting immunogenic tags into other regions of the PS1 protein (for example, a tagged version of the N terminal signal sequence or full length PS1 with a tag inserted at the site of missing sequence corresponding to the cytoplasmic hydrophilic loop, residue 248 in *L. major*, known not to be required for function in mammalian PS1), and analysing their distribution in a  $\Delta ps1$  mutant background to avoid issues associated with protein over-expression. Ideally, specific antibodies for the recognition of endogenous PS1 are required to solve the localisation of PS1, although it seems that detection of endogenous protein might prove to be problematic.

The consistent detection of endogenous PS1 by western blotting was unsuccessful using antibodies raised against a C terminal peptide, although some evidence was obtained that the antibodies raised in this study can recognise PS1 (the detection of a protein that was absent in  $\Delta ps1$  mutants in figure 5.11 and the detection of PS1-GFP in figure 5.12). A 46 kDa protein was detected in wild type cell lysate that was absent in  $\Delta ps1$  mutants (figure 5.11B), suggestive that this antibody could recognise endogenous PS1. However, in subsequent analyses after affinity purification of the antibody, a protein of 46 kDa could not be detected, and instead an apparently non-specific protein of ~30 kDa was detected in all samples (figure 5.12A). The detection of PS1-GFP in WT[PS1-GFP] cell lysates by western blot suggests that the antibody is capable of

recognising PS1 when over-expressed (figure 5.12B and C), and that the failure to consistently detect endogenous protein may be due to low levels of expression, or technical issues in the way in which the cells were lysed.

PS1-HA was detected by western blot using anti-HA antibodies (figure 5.7B), but not using anti-PS1 antibodies (figure 5.12A), suggesting that the level of expression of PS1-HA under the control of the rRNA promoter is not sufficiently high to be detected with anti-PS1 antibodies. PS1-HA was detected as a protein of ~ 46 kDa, slightly higher than the 38 kDa predicted by GeneDB, and an additional high molecular weight protein was detected. A protein of ~ 60 kDa was detected in WT[PS1-GFP] cell lysates using both anti-GFP and anti-PS1 antibodies (figure 5.12B and C). The predicted size of full length PS1 fused with GFP is ~63-76 kDa, suggesting that perhaps the protein band detected could be the result of some proteolytic cleavage event, resulting in a fusion protein shorter than expected. The fact that the size of PS1-HA is similar in size to the predicted fusion protein, while GFP-PS1 is found to be smaller than predicted could help to explain the differences in localisations of the two fusion proteins if PS1-GFP is somehow incorrectly processed.

Interestingly, the higher molecular weight protein that was detected in both WT[PS1-HA] and WT[PS1-GFP] lysates (figures 5.5B and 5.10B and C) has been described in various other systems. Performing immunoprecipitation experiments on NT2N neuronal cells expressing wild type PS1 and PS1-HA after lysis with detergent led to the detection of closely spaced doublets of 43 and 50 kDa in SDS-PAGE, in addition to smaller, proteolytic fragments and a protein of very high molecular weight (Cook *et al.*, 1996). Endogenous PS1 was not detectable in NT2N cells with anti-PS1 antibodies (raised against peptides from three different epitopes), again suggesting that PS1 expression is usually at a low level.

Similarly, diffuse protein bands with masses between 100 and 250 kDa were also detected in immunoprecipitates from COS1 hamster cells transfected with PS1 cDNA (no detection of endogenous protein was achieved) (De Strooper *et al.*, 1997). Denaturation of the immunoprecipitates at 37°C rather than 90°C led to increased amounts of the 45 kDa protein, suggesting that the aggregates probably consist mainly of oligomers of PS1. Clustering of PS1 in aggregates in

the ER has been observed by immuno-electron microscopy, suggesting that while the protein smears could be partly caused during sample preparation, it is likely to be physiologically significant (Selkoe, 1994). In both studies, PS1 was shown to not be glycosylated, nor modified by glycosaminoglycan chains (De Strooper *et al.*, 1997, Cook *et al.*, 1996). However PS1 was found to be phosphorylated on serine residues (De Strooper *et al.*, 1997). The relative intensities of the proteins detected with anti-PS1 antibodies varied depending on sample preparation (Cook *et al.*, 1996), and the authors suggested that while the doublet might represent post translational modifications, it was more likely to reflect different conformations of PS1 since hydrophobic regions are not always fully denatured by SDS treatment (Doms and Helenius, 1986).

Reports from the literature suggest that PS1 is expressed at a low level in many mammalian cells, and that success in detecting endogenous PS1 has been limited (De Strooper *et al.*, 1997, Cook *et al.*, 1996). Other methods of cell lysis should be attempted, for example the specific enrichment of membrane proteins by phase separation using the detergent Triton-X-114 (Bordier, 1981). The cell lysates analysed in this study were obtained from early to late log phase promastigotes by lysis with the detergent Triton-X-100 or SDS, and increased efforts to analyse cells from all stages of the life cycle should be attempted in case the expression of PS1 is developmentally regulated, and the “window” of expression has been missed in these studies. Further analysis of the expression of PS1-HA in a  $\Delta ps1$  mutant background by western blot might provide some useful information about the expression of the protein, but ultimately only detection of endogenous PS1 will provide expression data that is definitive.

Through genetic manipulation of the *PS1* locus it was demonstrated that PS1 is not required for parasite viability or virulence, and it has been established that PS1 is not a suitable target for drug development. A role for PS1 in the regulation of autophagy had been predicted, and initial experiments appeared to support this hypothesis (figures 5.23 and 5.24). GFP-ATG8 was recruited to fewer autophagosomes in  $\Delta ps1$  mutant cells, and enlarged autophagosomes appeared to accumulate in the late log stage of growth, suggesting that the autophagosomes were not correctly trafficked to the lysosome. However, when this experiment was repeated after the  $\Delta ps1$  mutants had been isolated from a mouse footpad lesion, perhaps allowing the cells to compensate for the loss of

PS1, no defect in autophagy was observed (figure 5.25). The localisation of other ATG8 homologues (GFP-ATG8A, GFP-ATG8B and GFP-ATG8C) was also found to resemble that of wild type cells regardless as to whether the parasites had been allowed to adapt, as did the dramatic response of ATG8A to starvation that was reported in chapter 3 (figure 5.25 and 5.26). It should be noted that  $\Delta ps1$  mutants were analysed again by Southern blot after passaging through mice and no wild type locus was detected, so the apparent loss in phenotype was not due to the mutants retaining a copy of the *PS1* gene (figure 5.18). While virulence studies were performed in recently obtained  $\Delta ps1$  mutants that had not infected an animal (figures 5.19 - 5.22), endocytosis and trafficking analyses (figure 5.27 - 5.29) were performed on parasites that had been allowed to differentiate within an animal host, and so should be repeated on freshly obtained  $\Delta ps1$  mutants to obtain a consistent set of data.

The ability of mutant parasites to adapt to the loss of a particular gene has been reported previously. For example, the sequential deletion of metacaspases *MCA2*, *MCA3* and *MCA5* from *T. brucei* caused an initial defect in growth, though the parasites rapidly recovered and after several weeks in culture resembled wild type cells (Helms *et al.*, 2006). In that case, depletion of *MCA2*, *MCA3* and *MCA5* by RNA interference (RNAi) was lethal, and the ability of the mutants to adjust to the deletion of the three genes was suggested to be due to a subsequent upregulation of other peptidases or by the activation of other signalling pathways. Further analyses of autophagy in  $\Delta ps1$  mutants that were frozen immediately after production and have not been kept in culture or passaged through animals might allow us to determine whether the disruption in autophagy is a real phenotype which the parasite must adapt to, or whether the apparent disruption of autophagy was due to some unrelated factor.

A role for PS1 in the trafficking of select membrane proteins or intracellular vesicles has been proposed by several groups (Repetto *et al.*, 2007). An accumulation of the C terminal fragments (CTFs) of APP, a well documented substrate of  $\gamma$ -secretase, has been reported in  $\Delta ps1$  mouse neurons, as might be expected given the well known role of PS1 as the catalytic core of  $\gamma$ -secretase (Naruse *et al.*, 1998). Additionally, and more surprisingly, the CTFs of APLP1, a homologue of APP, was also identified in  $\Delta ps1$  mouse neurons. The transmembrane domains of APP and APLP1, the proposed site of cleavage by  $\gamma$ -

secretase, share limited similarity, leading the authors to speculate that in addition to being required for  $\gamma$ -secretase, PS1 has a role in modulating the trafficking of residual CTFs derived from APP, APLP1, and maybe other transmembrane proteins to degradative compartments, for proteolysis by other peptidases (Naruse *et al.*, 1998). The glycosylation, trafficking and signalling of the membrane glycoprotein TrkB (tyrosine kinase receptor for brain derived neurotrophic factor (BDNF)), was also altered in *PS1* deficient mouse neurons, further validating the hypothesis that PS1 is involved in promoting intramembrane cleavage and degradation of a range of polytopic membrane proteins (Naruse *et al.*, 1998). The phenotype could be rescued by both wild type human *PS1* and *PS1* with FAD mutations, indicating that the role of PS1 in the trafficking of membrane proteins is distinct from  $\gamma$ -secretase function. The distinction between PS1 and  $\gamma$ -secretase activity is of importance when considering the potential role of PS1 in *L. major*, as the other components of the  $\gamma$ -secretase complex essential for its function, PEN-2, APH-1 and nicastrin, are apparently absent from *L. major*.

Levels of epidermal growth factor receptor (EGFR), a receptor tyrosine kinase, were increased in mouse fibroblasts that were deficient in both *PS1* and *PS2*, a phenotype that could be rescued by the re-expression of *PS1* but not *PS2*, and found to be independent of  $\gamma$ -secretase activity (Repetto *et al.*, 2007). The delay in turnover was found to be specifically due to a defect in trafficking of EGFR from early endosomes to lysosome, rather than due to defects in endocytosis or ubiquitination. Kaether *et al.*, (2002) suggest a  $\lambda$ -secretase independent role for PS1 in the endocytosis and trafficking of  $\beta$ -Amyloid precursor protein ( $\beta$ -APP) to post-Golgi compartments for proteolysis by  $\gamma$ -secretase. Those authors suggested that an accumulation of APP CTFs engaged a pool of adaptor proteins, compromising the ability of the cell to endocytose surface proteins (Kaether *et al.*, 2002). The proteins  $\alpha$ -synuclein and telencephalin, both found to accumulate in vacuoles resembling autophagosomes in  $\Delta ps1$  neurons, are both membrane proteins (Wilson *et al.*, 2004, Esselens *et al.*, 2004). Despite speculation that PS1 might have global effects on the metabolism and turnover of secretory proteins, an accumulation of anonymous polypeptides on the plasma membrane of  $\Delta ps1$  neurons or secreted in the culture medium has not been detected (Naruse *et al.*, 1998).

In this study, the integral membrane protein V-H+-PPase, which has 16 predicted transmembrane domains, was used to investigate the trafficking of membrane proteins in a  $\Delta ps1$  promastigotes. The localisation of GFP- V-H+-PPase was unaffected in  $\Delta ps1$  mutants, indicating that PS1 is not required for the correct trafficking of this membrane protein. However, we have not been able to show that the trafficking of other membrane proteins is not affected in the mutants, although we have shown that if there is any disruption in trafficking, it is not sufficient to reduce viability or virulence of the parasite. While *Leishmania* expresses many more membrane transport proteins that are required for the uptake of nutrients, efflux of metabolites, establishment of ion gradients and the take up and export of drugs, a lack of notable phenotype in  $\Delta ps1$  mutants makes it difficult to identify candidate membrane proteins that may be mis-trafficked due to a loss of PS1. A comparative proteomics approach in which proteins that are up or down regulated in  $\Delta ps1$  mutants might lead to the identification of proteins that accumulate due to mis-trafficking.

The expression and localisation of *L. major* syntaxin 1A and syntaxin 5 (fused to GFP) in  $\Delta ps1$  mutants were found to resemble that seen in wild type cells (Besteiro *et al.*, 2006a), suggesting that vesicle transport via SNARE proteins is not affected by a loss of PS1. Interestingly, the localisation of GFP-LmjF28.1470 (syntaxin 1A) appeared very similar to that of PS1-HA (figure 5. 28A compared to 5.7), and investigations into the potential co-localisation of these proteins may be interesting. Although Rab-11 was shown not to co-localise with PS1-HA, the expression of Rab11 in  $\Delta ps1$  mutants was not investigated in this study, and should be analysed using GFP fused protein or immunofluorescence using *T. brucei* anti-Rab11 antibodies.

Although the over-all process of endocytosis was shown to be unaffected in  $\Delta ps1$  mutants using the endocytic tracer FM4-64, other detailed analyses of the endosomal and lysosomal machinery were not carried out. The expression of two lysosomal *L. major* syntaxins, LmjF19.0120 and LmjF29.0070, was useful in studying trafficking to the lysosome and structure of the MVT in *L. major*  $\Delta ap3\delta$  mutants, and perhaps should be considered as tools to further analyse trafficking in  $\Delta ps1$  mutants (Besteiro *et al.*, 2008). Additionally, the structure of various organelles, including the mitochondrion, ER, acidocalcisomes and lysosome ought to be studied in  $\Delta ps1$  mutants using available markers including ER-

tracker, mitotracker and lysotracker (molecular probes). Many of the analyses carried out in this study were performed on cells isolated from mouse footpad lesions that may have compensated for the loss of PS1. All analyses ought to be repeated on fresh  $\Delta ps1$  stabilates that have not been exposed to an animal host.

Finally, the hypothesis that SPP, another integral membrane aspartyl protease that is related to PS1, compensated for the loss of PS1 was investigated in promastigotes by studying the effect of various  $\gamma$ -secretase and SP1 specific inhibitors on wild type,  $\Delta ps1$  mutant and re-expressing cell lines. None of the drugs were found to inhibit promastigote growth at concentrations as high as 50  $\mu\text{M}$  (figure 5.30). This could be because the drugs are not able to enter the cells, or because *L. major* PS1 and SPP are sufficiently different to mammalian or *Plasmodium* proteins and so the drugs are not effective. The effects of these drugs on the intracellular amastigote stage of the parasite were not investigated in this study, and should be analysed. Additionally, the generation of  $\Delta spp$  null mutants and a double null mutant that lacks both *PS1* and *SPP* might shed some light on the role of transmembrane aspartyl peptidases in *Leishmania*.

## **6 General Discussion**

The turnover of proteins or specific organelles by autophagy has been shown to be associated with differentiation in *Leishmania*, *T. cruzi* and *T. brucei*; and several *Leishmania* mutants have been produced which are both defective in autophagy and less able to differentiate into virulent metacyclic promastigotes or to establish infection *in vivo* (Alvarez *et al.*, 2008a; Besteiro *et al.*, 2006b; Herman *et al.*, 2008; Williams *et al.*, 2006). Together these data point to an important role for autophagy in differentiation and virulence of trypanosomatids, and so the identification of multicopy families of *ATG8*-like genes that are unique to *Leishmania* was intriguing (Williams *et al.*, 2006). In this study the expression and subcellular localisation of *ATG8A*, *ATG8B* and *ATG8C* proteins have been described, and the data presented here have allowed some predictions to be made as to their functions in *Leishmania*, particularly when considered together with recent work regarding the roles of the cysteine peptidases *ATG4.1* and *ATG4.2* (Besteiro *et al.*, 2006b; Williams *et al.*, 2009). In addition to this, a putative role for the transmembrane aspartic peptidase presenilin-1 in the regulation of autophagy has been proposed.

Some evidence accumulated suggesting that *ATG8A*, *ATG8B* and *ATG8C* might function in autophagy. First, by analysing the distribution of GFP-*ATG8A*, GFP-*ATG8B* and GFP-*ATG8C* in live promastigotes, it was shown that all *ATG8* paralogues localise to punctate structures resembling those labelled with GFP-*ATG8* under certain conditions (figures 3.6, 3.11). Secondly, *ATG8*, *ATG8A*, *ATG8B* and *ATG8C* genes have all been found to complement a yeast *ATG8*-defective strain (Williams *et al.*, 2009). And finally, recombinant *ATG8*, *ATG8A*, *ATG8B* and *ATG8C* were proteolytically processed by the cysteine peptidases *ATG4.1* or *ATG4.2*, indicative that these proteins undergo processing in the same manner as *ATG8* (Williams *et al.*, 2009). Further analyses of the localisation, expression and post-translational processing of *ATG8* paralogues led to the conclusion that *ATG8B* and *ATG8C* are likely to be associated with a cellular process that is distinct from autophagy. *ATG8A* does appear to play a role in starvation induced autophagy, although possibly a different type of autophagy that is induced under different circumstances to *ATG8*.

## 6.1 A role for ATG8A in an autophagy-like starvation response?

A putative role for ATG8A in withstanding starvation, perhaps during establishment of infection within the sandfly gut, has been proposed based on findings presented in this thesis. Using cells expressing GFP-ATG8A, it was demonstrated that ATG8A undergoes dramatic relocalisation to punctate structures in promastigotes in response to starvation (figure 3.10). Additionally it has been shown that *L. major*  $\Delta atg4.2$  mutants that are unable to process ATG8A and in which GFP-ATG8A is not redistributed to puncta during nutrient deprivation, are less able to withstand starvation than wild type cells (Besteiro *et al.*, 2006b; Williams *et al.*, 2009). Finally, western blot analysis using specific anti-ATG8A antibodies have revealed that ATG8A is highly expressed in stationary phase promastigote cultures (figure 4.5B), indicating that ATG8A might be required for or involved in the establishment of infective metacyclic populations. However, expression of ATG8A was not investigated specifically in purified metacyclic promastigotes, which might be informative in determining whether ATG8A is involved in differentiation, or in promoting metacyclic promastigote survival.

*Leishmania* metacyclic and leptomonad promastigotes are found at extremely high densities ( $\sim 1-2 \times 10^{10}$  cells  $\text{ml}^{-1}$ ) in the thoracic midgut of infected sandflies where they reside for several days in a tightly packed “plug” containing proteophosphoglycan rich promastigote secretory gel (PSG), and it is at the anterior and posterior poles of this plug that metacyclic promastigotes differentiate from leptomonad promastigotes (Rogers *et al.*, 2002). The parasites embedded in the plug appeared immobile in live preparations, but were able to swim away when the plug was disrupted in culture media, showing that they remained viable (Rogers *et al.*, 2002). In addition to there being limited nutrients available within the plug, the high density of promastigotes combined with the gelatinous nature of the plug would likely result in a local depletion of oxygen, and in fact, anaerobiosis has been shown to stimulate metacyclogenesis *in vitro* (Mendez *et al.*, 1999).

While *Leishmania* promastigotes depend on respiratory chain activity for the generation of energy, the ability of promastigotes to enter a state of reversible

metabolic arrest upon inhibition of the classical respiratory chain during culture in the absence of oxygen or presence of cyanide has been reported (Van Hellemond and Tielens, 1997., Van Hellemond *et al.*, 1997). *L. infantum*, *L. major* and *L. donovani* promastigotes were found to be resistant to anoxia for at least 48 hours, but prolonged inhibition of the respiratory chain (>100 hours) resulted in cell death (Van Hellemond and Tielens, 1997). During metabolic arrest, both the generation of energy by glucose catabolism and the consumption of energy through movement and proliferation were decreased, resulting in parasites that appeared “sluggish”, perhaps not unlike promastigotes that had been subjected to starvation in experiments performed in chapter 3. Analysing the response of *L. major* ATG8A (and other ATG8 paralogues) during anaerobic growth might provide some further clues as to their putative roles in life cycle progression.

Although both ATG8 and ATG8A are involved in a vesicle-associated response to nutrient deprivation, some differences between ATG8 and ATG8A have been identified. The occurrence of GFP-ATG8 labelled autophagosomes peaks during differentiation between morphological forms, indicative of a role in cellular remodelling during differentiation and life cycle progression (Besteiro *et al.*, 2006b; Williams *et al.*, 2006). On the other hand, promastigotes containing GFP-ATG8A puncta were rarely observed in healthy cells grown under nutrient rich conditions; no more than 6% of cells in a population were seen to contain puncta, and most of these were rounded in shape and appeared to be dying (figures 3.7, 3.8). This suggests that unlike ATG8, ATG8A is not involved in protein turnover by autophagy during differentiation.

ATG8A and ATG8 were found to co-localise at some punctate structures in many cells after autophagy was induced by starvation (figure 3.11). It was previously demonstrated that GFP-ATG8 labelled structures in *L. mexicana* are autophagosomes (Williams *et al.*, 2006), and so the recruitment of ATG8A to puncta that are also labelled by ATG8 provided some evidence that ATG8A was recruited to autophagosomes. However, in all cases after four hours of starvation, ATG8A labelled more puncta per cell than ATG8 (on average 6-7 GFP-ATG8A puncta per cell compared to 2-3 RFP-ATG8 puncta, figure 3.9), suggesting that while ATG8A is associated with autophagosomes during starvation, it is additionally recruited to another population of vesicles that might be a distinct

subset of autophagosomes specifically associated with starvation stress, or another stress-induced structure distinct from autophagosomes.

While ATG8 recruitment to autophagosomes was inhibited by the PI3 kinase inhibitor wortmannin (Besteiro *et al.*, 2006b; Williams *et al.*, 2006), no inhibition of GFP-ATG8A puncta formation was observed when WT[GFP-ATG8A] cells were subjected to starvation and treated with the same concentration of wortmannin (figure 3.13), indicating that the recruitment of ATG8A to puncta might not be regulated in the same manner as ATG8 recruitment.

The localisation of GFP-ATG8A to punctate structures was inhibited when cells were incubated in PBS supplemented with glucose or proline, demonstrating that the induction of ATG8A relocalisation is specifically associated with the availability of nutrients (figure 3.13). GFP-ATG8, however, was recruited to more autophagosomes in *L. mexicana* when suspended in PBS with glucose or proline, and autophagy was inhibited by the addition of individual amino acids (unpublished observations, Dr R Williams). These data demonstrate that the response of these two ATG8 proteins is induced under different conditions, and are suggestive of different roles for ATG8 and ATG8A. Further work is required to fully characterise the differences between ATG8 and ATG8A recruitment to vesicles in the presence of various energy sources, and additionally in response to other sources of stress, such as changes in pH and temperature and the presence of reactive oxygen species. Levels of H<sub>2</sub>O<sub>2</sub> rise in response to nutritional stress and other stress inducing compounds (Scherz-Schouval *et al.*, 2007), and a comparison of the response of ATG8 and ATG8A to the presence of H<sub>2</sub>O<sub>2</sub> might be informative in further characterising their roles in the response to stress.

Another interesting difference between ATG8 and ATG8A is in the selectivity of their processing by the cysteine peptidases ATG4.1 and ATG4. In an *in vitro* assay, recombinant ATG8A was found to be proteolytically processed by the cysteine peptidase ATG4.2, while ATG8, ATG8B and ATG8C were preferentially processed by ATG4.1, perhaps indicating an involvement in distinct pathways (Williams *et al.*, 2009). *L. major*  $\Delta atg4.2$  mutants are less able to withstand starvation, are defective in their ability to undergo differentiation, and have a reduced (but not completely abolished) ability to establish an infection in animal

models (Williams *et al.*, 2006; Williams *et al.*, 2009). In these mutants, GFP-ATG8-labelled autophagosomes and lipidated forms of ATG8 (ATG8-PE) accumulated, while GFP-ATG8A was unable to form punctate structures, suggesting that ATG4.2 is both an ATG8 deconjugating enzyme and an ATG8A processing enzyme (Besteiro *et al.*, 2006b; Williams *et al.*, 2009). In order to differentiate between the effects on withstanding starvation of ATG8-PE accumulation and the lack of ATG8A recruitment in  $\Delta atg4.2$  mutants,  $\Delta atg8a$  mutants are required.

## 6.2 An association of ATG8B and ATG8C with vesicle-trafficking?

ATG8B and ATG8C were found to have quite different localisation profiles to ATG8 and ATG8A. GFP-ATG8B and GFP-ATG8C were found to localise to punctate structures in 2-10% of healthy promastigotes, with no association observed between vesicle formation and life cycle progression (figure 3.6). Additionally no relocation of ATG8B and ATG8C was observed during starvation, indicating a different function to ATG8 and ATG8A.

In most cases where ATG8B or ATG8C were localised to a vesicle, it was to a single punctum close to (but not over-lapping with) the flagellar pocket, the sole site of endocytosis and exocytosis in the cell (figures 3.5, 3.15A). Occasionally the GFP-ATG8B vesicle appeared to be undergoing duplication in cells that had two flagella and were undergoing division (figure 3.15B). Vesicle duplication was observed very rarely, and only ever in cells undergoing division, and suggested that ATG8B might be associated with an organelle that is replicated and conserved during cell division. In some cases (again, very rarely seen) an additional GFP-ATG8B labelled punctum was seen that partially over-lapped with some compartments of the early endosomal system (figure 3.15B), perhaps indicating that ATG8B labels a vesicle or compartment that is derived from endosomal membranes. It might be informative to perform detailed analyses of ATG8B and ATG8C localisation during the cell cycle, using cell cycle markers such as anti beta-tubulin antibodies that label subpellicular microtubules and are useful in monitoring the progression of mitosis, and anti-Rab11 antibodies, proven to be useful in monitoring kinetoplast segregation (Ambit, 2006).

It was shown that ATG8B did not co-localise with ARL-1, a marker of the trans-golgi network (figure 3.17, Sahin *et al.*, 2008). However, the localisation of ATG8B and ATG8C in comparison to other markers of the Golgi should be investigated. For example, a GRIP domain has been identified that is sufficient to target proteins to the trans-Golgi network, and GFP-GRIP fusion proteins have been used to label the Golgi apparatus in *L. mexicana* (McConville *et al.*, 2002a). In those cases, the GFP-GRIP signal partially overlapped with endocytic marker FM4-64. *T. brucei* anti-Rab1 antibodies and a GFP fusion of the *L. major* syntaxin 5 orthologue LmjF32.0070 were found to localise to distinct subcompartments of the Golgi apparatus in *L. major* (Besteiro *et al.*, 2006a), and should be used to further characterise the position of ATG8B labelled vesicles in the cell relative to the Golgi apparatus.

A recent analysis of *L. major* SNARES, components of intracellular vesicle mediated transport, reported the localisation of SNARES of the Qa family, some of which exhibit a similar distribution to ATG8B; LmjF33.1340 and LmjF35.2720 labelled punctate structures near the flagellar pocket and throughout the cell, LmjF32.0070 associated with the Golgi, and LmjF28.1470 associated with the flagellar pocket (Besteiro *et al.*, 2006a). One putative SNARE protein of the Qc family, LmjF06.0820, was identified in an immunoprecipitation experiment with anti-ATG8B (figure 4.11, table 4.3), and a potential association should be investigated further by analysing their comparative localisations. *T. brucei* anti-Rab11 antibodies have been used to label a structure near the flagellar pocket in *L. major* (figure 5.9C), and the localisation of ATG8B in comparison to Rab11 recycling endosomes should be analysed. GFP-Rab5, thought to have a role in early endosomal trafficking, localised to punctate structures near the anterior end of *L. donovani* in a distribution similar to that of ATG8B, and it will be interesting to see if any over-lap in RAB5 and ATG8B localisation is seen (Marotta *et al.*, 2006). A possible role for ATG8B or ATG8C in endocytosis or vesicle-mediated transport could be investigated by analysing the expression and localisation of ATG8B and ATG8C in *Leishmania* mutants that are defective in endosomal processes, for example *L. major* that express dominant negative ATPase VPS4<sup>E235Q</sup> and are defective in endosomal sorting (Besteiro *et al.*, 2006b), or in cells in which the process of endocytosis has been blocked by incubation at 4°C.

Attempts to determine the ultrastructure of ATG8B labelled vesicles by immunoelectron microscopy using anti-ATG8B specific antibodies were unsuccessful in this study, and no specific signal was detected (immuno-EM analysis carried out with Dr L Tetley, data not shown). An electron microscopy ultrastructural study performed on high pressure frozen *L. mexicana* cells demonstrated that the anterior region of the cell was densely packed with poorly characterised vesicles that varied in appearance; some situated by the flagellar pocket were large and translucent, others found in close proximity to the trans-side of the Golgi were small and often coated (Weise *et al.*, 2000). The determination of the nature of the ATG8B associated puncta might be helpful in predicting the function of ATG8B; are the puncta cargo filled vesicles likely to be involved in protein trafficking, double membrane bound like an autophagosome, or associated with a particular organelle? Continued attempts to optimise the use of anti-ATG8B antibodies for immuno-EM should be made.

The production of  $\Delta atg8a/atg8b$  double null mutants is currently underway, and will hopefully help in determining their cellular functions.

### **6.3 Do ATG8 paralogues form conjugates with other proteins rather than a phospholipid?**

Data presented in chapter four indicate that, unlike ATG8, lipidated forms of ATG8A, ATG8B and ATG8C do not exist, as neither endogenous, nor GFP tagged versions of the proteins were sensitive to treatment with phospholipase D (figures 4.8, 4.9). On the other hand, it is possible that lipidated forms of the ATG8 paralogues occur only in small numbers of cells, or under particular conditions that were not investigated here. An attempt to investigate the nature of the lipid modifier of ATG8 by analysing the incorporation of [<sup>3</sup>H]ethanolamine into immunoprecipitated ATG8 was unsuccessful, although at this stage it is unclear whether this was due to a low level of immunoprecipitation of ATG8 (figure 4.10A), or because the ethanolamine was not taken up by the promastigotes. However, a radioactive signal of the predicted size for ATG8 (or ATG8 paralogues) was detected in the flow through after immunoprecipitation with ATG8B, leading to speculation that this might represent ATG8 conjugated to PE (figure 4.10C). Appropriate controls to prove

that radioactively labelled ethanolamine was taken up by the promastigotes are required before conclusions can be drawn from these experiments.

While no evidence was found that *L. major* ATG8 paralogues become conjugated to a phospholipid, western blot analyses showed that in most cases higher molecular weight proteins, or perhaps complexes, were detected in addition to endogenous ATG8 paralogues with antibodies specific to the ATG8A, ATG8B and ATG8C (figure 4.5, 4.6, 4.7, 4.9). It is of course possible that these are non-specific proteins recognised due to cross-reactivity of the antibodies. However, these might represent complexes with ATG8 proteins being conjugated to other proteins in the manner of other ubiquitin like proteins, rather than a phospholipid.

ATG8 is characterised as a ubiquitin-like protein (UBL) based on the conservation of the three dimensional structure, the ubiquitin or  $\beta$ -grasp fold (Hochstrasser, 2000). In fact, an entire family of UBLs has been defined, that, while often not sharing significant sequence similarity, possess the same three-dimensional structure (Hochstrasser, 2000, figure 3.4). Although the 3D structures of *L. major* ATG8 and ATG8 paralogues are not yet available, many of the residues thought to be required for maintenance of the ubiquitin structure are conserved in *L. major* ATG8, ATG8A, ATG8B and ATG8C (figure 3.3).

All UBLs become attached to their substrates via related enzyme pathways and must be processed by a cysteine peptidase, activated by an E1-like enzyme (ATG7 in the case of ATG8), and conjugated to its substrate (protein or a phospholipid in the case of ATG8) via the conjugating activity of an E2-like enzyme (ATG3) and an E3 ligase (possibly ATG5-ATG12 for ATG8). What makes ATG8 unique among the UBLs is the fact that its substrate is not a protein, rather a phospholipid, PE. Additionally, while other UBLs are termed “modifiers”, their function being to modify or target proteins for particular destinations, ATG8 itself is modified by its substrate, PE.

Currently, we know ATG8A, ATG8B and ATG8C are cleaved by ATG4.1 and ATG4.2 (Williams *et al.*, 2009), but we have no evidence for interaction with ATG7 or ATG3, and whether the ATG8 paralogues become conjugated to a phospholipid or to protein targets remains unclear. Putative interactions

between *L. major* ATG8 and its paralogues with ATG7 and ATG3 should be investigated in *in vitro* assays, as was reported previously for the human Atg8 homologues (Tanida *et al.*, 2006; Tanida *et al.*, 2001). In those studies, because the E1 reaction is subject to rapid turnover and is difficult to recognise as an intermediate stage, an active cysteine residue of the Atg7 was mutated to a serine (Atg7<sup>C572S</sup>), and over-expressed in human cells along with tagged versions of the substrate (GFP-LC3, GFP-GATE-16, GFP-GABARAP, Myc-Atg8L). This resulted in the detection of a stable, high molecular weight intermediate only in cells over-expressing the mutated Atg7. Similarly, intermediates were observed between all human Atg8 homologues and an active site mutant of the E2 enzyme Atg3 (Atg3<sup>C264S</sup>) (Tanida *et al.*, 2006; Tanida *et al.*, 2001, Tanida *et al.*, 2002). Determining whether *Leishmania* ATG8, ATG8A, ATG8B or ATG8C form intermediates with ATG3 and ATG7 would be informative in further dissecting the participation of these proteins in a ubiquitin-like conjugation system. The ability of Atg7 to activate both Atg8 and Atg12 is the only known example of two UBLs sharing the same E1 enzyme (Kerscher *et al.*, 2006), and it will be interesting to determine whether ATG8A, ATG8B and ATG8C are activated by the same E1 enzyme.

Immunoprecipitation experiments using anti-ATG8B identified various proteins in the elutions and excised from coomassie gels, many of which were thought to be contaminants (section 4.3). The identification of two ubiquitin fusion proteins (LmjF31.1900 and LmjF14.1270) was thought to be of interest, although without the use of an  $\Delta atg8b$  null mutant cell line to provide a control sample, or without confirming the results of immunoprecipitation experiments with a yeast-2-hybrid analysis, it is unclear whether ATG8B and ubiquitin related proteins really do interact, or whether they were detected due to their abundance. It has been reported that modification of one protein can occur by more than one UBL. For example, both SUMO (small ubiquitin-related modifier) and ubiquitin modify the same residues of several substrates (Schwartz and Hochstrasser, 2003). It is a possibility worth further investigation that ATG8B (and perhaps ATG8A and ATG8C) might be involved in protein modification of the same targets as ubiquitin, and perhaps that is why ATG8B co-purified with ubiquitin fusion proteins.

While the co-localisation of ATG8 and ATG8A at some punctate structures during starvation provided evidence that some ATG8A is associated with autophagosomes, we have no evidence that the majority of ATG8A labelled structures are autophagosomes. Some recent reports suggest that certain proteins, when tagged with GFP and over-expressed, can accumulate in protein aggregates that are punctate in distribution, sometimes label positive for LC3, and are unrelated to autophagy. It seems unlikely that the punctate distribution of GFP-ATG8A is simply due to an over-expression of misfolded protein, as punctate distribution was only observed under starvation conditions, and not in cells grown in normal media. However, the formation of aggresome-like induced structures (ALIS) which are punctate in appearance and are positive for LC3, has been reported in macrophages, dendritic cells and HeLa cells in response to several types of stress including transfection, oxidative stress and starvation (Szeto *et al.*, 2006). These structures were shown to contain ubiquitinated protein by immunofluorescence analysis with FK2 monoclonal antibodies (Fujimuro *et al.*, 1994), and were degraded via autophagy and proteasomal pathways (Szeto *et al.*, 2006). The formation of GFP-LC3 positive protein aggregates that are unrelated to autophagy was reported in mouse embryonic fibroblasts that are deficient in autophagy (Kuma *et al.*, 2007). Care must therefore be taken in interpreting results obtained from GFP-ATG8A expressing cells.

Immunofluorescence with anti-ATG8A antibodies performed on fixed, starved promastigotes revealed that endogenous ATG8A was localised to multiple punctate structures in a distribution similar to that seen with GFP-ATG8A (figure 3.16D). However, the analysis of non-starved cells revealed a very similar, punctate distribution of ATG8A, very different from the distribution of GFP-ATG8A in non-starved cells. Lacking definitive confirmation of the distribution of ATG8A by direct immunofluorescence, the analysis of tagged ATG8A (with GFP and perhaps the smaller immunogenic tag HA) that is stably integrated at the wild type locus rather than over-expressed might be useful.

A polyclonal anti-ubiquitin antibody (Santa Cruz Biotechnology) was used for immunoprecipitation of ubiquitinated proteins from *L. donovani* (Bhandari and Saha, 2007), and the possibility that GFP-ATG8A labels structures in which ubiquitinated proteins accumulate could be investigated in *L. major* using this

antibody. Puromycin, a translational inhibitor, has been used to induce the formation of ALIS, and the possibility that ATG8A could be involved in the turnover of defective proteins could be investigated using this drug (Szeto *et al.*, 2006).

Homologues of some UBLs have been identified in *L. major*, including ubiquitin (five genes), small ubiquitin-related modifier (SUMO, LmjF08.0470), ubiquitin related modifier (Urm1, LmjF34.2830) and of course ATG8 and ATG12. *L. major* has two genes encoding ubiquitin fused to ribosomal subunit S27a (LmjF36.0600, LmjF14.1270), two fused to ribosomal subunit L40 (LmjF31.1900, LmjF31.2030), one gene encoding polyubiquitin (LmjF36.3530) and one small, ubiquitin-like protein (LmjF34.2125). Other known UBLs, Nedd8, ISG15, FAT10 and Hub1 are apparently absent from the *Leishmania* genome (Ponder and Bogyo, 2007). Relatively little has been published about UBLs in *Leishmania*, and it will be interesting to investigate the possibility that ATG8 paralogues might in fact be novel UBLs. Ubiquitin-encoding genes in *T. cruzi* were found to be differentially regulated during life cycle progression (Manning-Cela *et al.*, 2006), and ubiquitin-dependent degradation of cytoskeletal flagellum proteins was shown to be associated with differentiation from trypomastigote to amastigote form (de Diego *et al.*, 2001). Recently, it was suggested that the posttranscriptional regulation of gene expression in *Leishmania* could be regulated through the ubiquitination of an RNA binding protein, LdCSBP (Bhandari and Saha, 2007). Other UBLs have divergent functions; the main function of SUMO is transcriptional regulation (Johnson, 2004), while Urm1 is involved in nutrient sensing and oxidative stress response in yeast but is apparently non-functional in higher eukaryotes (Goehring *et al.*, 2003a, 2003b; Xu *et al.*, 2006).

#### **6.4 A putative role for PS1 in the regulation of autophagy requires further confirmation**

Through the production of  $\Delta ps1$  mutants, it was demonstrated that PS1 is not required for differentiation or virulence and is not a good target for drug development (figures 5.20, 5.21, 5.22). An accumulation of large GFP-ATG8 labelled autophagosomes was observed in freshly obtained  $\Delta ps1$  mutants, indicating a disruption in correct trafficking of autophagosomes (figure 5.23, 5.24). However, this apparent disruption of autophagy in  $\Delta ps1$  mutants was not

sufficient to cause defects in differentiation or in their ability to infect mice, perhaps suggesting that *L. major* cells can cope with partial deregulation of the autophagy pathway. When the experiment was repeated in  $\Delta ps1$  mutants that had been allowed to adapt during 5 weeks within a mouse, autophagy appeared to have been restored to normal levels (figure 5.25), indicating that the cells were able to compensate for the loss of PS1, perhaps via the activity of other peptidases. It will be interesting to see if these data are reproducible, by analysing autophagy and protein trafficking in recently generated  $\Delta ps1$  mutants compared to  $\Delta ps1$  mutants that have been allowed to differentiate into amastigotes.

A priority for future investigation in this part of the project is to determine the subcellular localisation of PS1. It seems likely that the accumulation of PS1-GFP on intracellular membranes is due to over-expression and misfolding of the protein, and that localisation of PS1-HA on vesicle structures close to the flagellar pocket represents the true localisation of PS1. However, confirmation of this localisation is required and the expression of PS1 with immunogenic tags inserted at different points within the protein should be analysed. While some promising data was obtained that suggested that anti-PS1 antibodies could detect *L. major* PS1, limited success was obtained in detecting endogenous PS1. Further efforts to detect endogenous PS1 should be made, by attempting to enrich for membrane proteins in cell lysates. However, based on the lack of sensitivity of these antibodies demonstrated in chapter 5, and on reports of low levels of endogenous PS1 expression in many other organisms, it seems unlikely that anti-PS1 antibodies will be useful in confirming the subcellular localisation of PS1 by immunofluorescence (Cook *et al.*, 1996; De Strooper *et al.*, 1997).

## References

### A

- Alvarez, V. E., Kosec, G., Sant'Anna, C., Turk, V., Cazzulo, J. J., and Turk, B. (2008a). Autophagy is involved in nutritional stress response and differentiation in *Trypanosoma cruzi*. *J Biol Chem* **283**, 3454-64.
- Alvarez, V. E., Kosec, G., Sant Anna, C., Turk, V., Cazzulo, J. J., and Turk, B. (2008b). Blocking autophagy to prevent parasite differentiation: a possible new strategy for fighting parasitic infections? *Autophagy* **4**, 361-3.
- Alves, C. R., Corte-Real, S., Bourguignon, S. C., Chaves, C. S., and Saraiva, E. M. (2005). *Leishmania amazonensis*: early proteinase activities during promastigote-amastigote differentiation in vitro. *Exp Parasitol* **109**, 38-48.
- Amar, N., Lustig, G., Ichimura, Y., Ohsumi, Y., and Elazar, Z. (2006). Two newly identified sites in the ubiquitin-like protein Atg8 are essential for autophagy. *EMBO Rep* **7**, 635-42.
- Ambit, A. (2006). Characterisation of *Leishmania major* Metacaspase, University of Glasgow.
- Annaert, W., and De Strooper, B. (1999). Presenilins: molecular switches between proteolysis and signal transduction. *Trends Neurosci* **22**, 439-43.
- Antoine, J. C., Prina, E., Lang, T., and Courret, N. (1998). The biogenesis and properties of the parasitophorous vacuoles that harbour *Leishmania* in murine macrophages. *Trends Microbiol* **6**, 392-401.
- Archibald, J. M., Teh, E. M., and Keeling, P. J. (2003). Novel ubiquitin fusion proteins: ribosomal protein P1 and actin. *J Mol Biol* **328**, 771-8.
- Asanuma, K., Tanida, I., Shirato, I., Ueno, T., Takahara, H., Nishitani, T., Kominami, E., and Tomino, Y. (2003). MAP-LC3, a promising autophagosomal marker, is processed during the differentiation and recovery of podocytes from PAN nephrosis. *Faseb J* **17**, 1165-7.
- Atlashkin, V., Kreykenbohm, V., Eskelinen, E. L., Wenzel, D., Fayyazi, A., and Fischer von Mollard, G. (2003). Deletion of the SNARE vti1b in mice results in the loss of a single SNARE partner, syntaxin 8. *Mol Cell Biol* **23**, 5198-207.

**B**

- Baird, G. S., Zacharias, D. A., and Tsien, R. Y. (2000). Biochemistry, mutagenesis, and oligomerization of DsRed, a red fluorescent protein from coral. *Proc Natl Acad Sci U S A* **97**, 11984-9.
- Barquilla, A., Crespo, J. L., and Navarro, M. (2008). Rapamycin inhibits trypanosome cell growth by preventing TOR complex 2 formation. *Proc Natl Acad Sci U S A* **105**, 14579-84.
- Barquilla, A., and Navarro, M. (2009). Trypanosome TOR as a major regulator of cell growth and autophagy. *Autophagy* **5**.
- Bates, P. A. (2007). Transmission of *Leishmania* metacyclic promastigotes by phlebotomine sand flies. *Int J Parasitol* **37**, 1097-106.
- Baumann, K., Paganetti, P. A., Sturchler-Pierrat, C., Wong, C., Hartmann, H., Cescato, R., Frey, P., Yankner, B. A., Sommer, B., and Staufenbiel, M. (1997). Distinct processing of endogenous and overexpressed recombinant presenilin 1. *Neurobiol Aging* **18**, 181-9.
- Bavro, V. N., Sola, M., Bracher, A., Kneussel, M., Betz, H., and Weissenhorn, W. (2002). Crystal structure of the GABA(A)-receptor-associated protein, GABARAP. *EMBO Rep* **3**, 183-9.
- Bellu, A. R., Kram, A. M., Kiel, J. A., Veenhuis, M., and van der Klei, I. J. (2001). Glucose-induced and nitrogen-starvation-induced peroxisome degradation are distinct processes in *Hansenula polymorpha* that involve both common and unique genes. *FEMS Yeast Res* **1**, 23-31.
- Benzel, I., Weise, F., and Wiese, M. (2000). Deletion of the gene for the membrane-bound acid phosphatase of *Leishmania mexicana*. *Mol Biochem Parasitol* **111**, 77-86.
- Berg, T. O., Fengsrud, M., Stromhaug, P. E., Berg, T., and Seglen, P. O. (1998). Isolation and characterization of rat liver amphisomes. Evidence for fusion of autophagosomes with both early and late endosomes. *J Biol Chem* **273**, 21883-92.
- Berman, J. J. (2008). Treatment of leishmaniasis with miltefosine: 2008 status. *Expert Opin Drug Metab Toxicol* **4**, 1209-16.
- Besteiro, S., Coombs, G. H., and Mottram, J. C. (2006a). The SNARE protein family of *Leishmania major*. *BMC Genomics* **7**, 250.
- Besteiro, S., Williams, R. A., Morrison, L. S., Coombs, G. H., and Mottram, J. C. (2006b). Endosome sorting and autophagy are essential for differentiation and virulence of *Leishmania major*. *J Biol Chem* **281**, 11384-96.
- Besteiro, S., Williams, RA., Coombs, GH., Mottram, JC. (2007). Protein Turnover and differentiation in *Leishmania*. *Int J Parasitol* **37**(10): 1063-75

- Besteiro, S., Tonn, D., Tetley, L., Coombs, G. H., and Mottram, J. C. (2008). The AP3 adaptor is involved in the transport of membrane proteins to acidocalcisomes of *Leishmania*. *J Cell Sci* **121**, 561-70.
- Bhandari, D., and Saha, P. (2007). mRNA cycling sequence binding protein from *Leishmania donovani* (LdCSBP) is covalently modified by ubiquitination. *FEMS Microbiol Lett* **273**, 206-13.
- Blommaart, E. F., Krause, U., Schellens, J. P., Vreeling-Sindelarova, H., and Meijer, A. J. (1997). The phosphatidylinositol 3-kinase inhibitors wortmannin and LY294002 inhibit autophagy in isolated rat hepatocytes. *Eur J Biochem* **243**, 240-6.
- Blum, J. J. (1993). Intermediary metabolism of *Leishmania*. *Parasitol Today* **9**, 118-22.
- Bonen, L. (1993). Trans-splicing of pre-mRNA in plants, animals, and protists. *Faseb J* **7**, 40-6.
- Bonilla, J., Bonilla, TD., Yowell, C., Dame, JB., (2008). *Plasmodium falciparum* signal peptide peptidase (PfSPP) as a novel target for malarial chemotherapy. . In "Molecular Parasitology Meeting." Vol. Abstract 136A, Woods Hole.
- Bonilla, J. A., Bonilla, T. D., Yowell, C. A., Fujioka, H., and Dame, J. B. (2007). Critical roles for the digestive vacuole plasmepsins of *Plasmodium falciparum* in vacuolar function. *Mol Microbiol* **65**, 64-75.
- Bordier, C. (1981). Phase separation of integral membrane proteins in Triton X-114 solution. *J Biol Chem* **256**, 1604-7.
- Bray, P. G., Barrett, M. P., Ward, S. A., and de Koning, H. P. (2003). Pentamidine uptake and resistance in pathogenic protozoa: past, present and future. *Trends Parasitol* **19**, 232-9.
- Brooks, D. R., Denise, H., Westrop, G. D., Coombs, G. H., and Mottram, J. C. (2001). The stage-regulated expression of *Leishmania mexicana* CPB cysteine proteases is mediated by an intercistronic sequence element. *J Biol Chem* **276**, 47061-9.
- Brunkan, A. L., and Goate, A. M. (2005). Presenilin function and gamma-secretase activity. *J Neurochem* **93**, 769-92.
- Brunkan, A. L., Martinez, M., Walker, E. S., and Goate, A. M. (2005). Presenilin endoproteolysis is an intramolecular cleavage. *Mol Cell Neurosci* **29**, 65-73.
- Burchmore, R. J., Rodriguez-Contreras, D., McBride, K., Merkel, P., Barrett, M. P., Modi, G., Sacks, D., and Landfear, S. M. (2003). Genetic characterization of glucose transporter function in *Leishmania mexicana*. *Proc Natl Acad Sci U S A* **100**, 3901-6.

## C

- Campbell, D. A., Thomas, S., and Sturm, N. R. (2003a). Transcription in kinetoplastid protozoa: why be normal? *Microbes Infect* **5**, 1231-40.
- Campbell, W. A., Iskandar, M. K., Reed, M. L., and Xia, W. (2002). Endoproteolysis of presenilin in vitro: inhibition by gamma-secretase inhibitors. *Biochemistry* **41**, 3372-9.
- Campbell, W. A., Reed, M. L., Strahle, J., Wolfe, M. S., and Xia, W. (2003b). Presenilin endoproteolysis mediated by an aspartyl protease activity pharmacologically distinct from gamma-secretase. *J Neurochem* **85**, 1563-74.
- Chen, Z. W., and Olsen, R. W. (2007). GABAA receptor associated proteins: a key factor regulating GABAA receptor function. *J Neurochem* **100**, 279-94.
- Chiang, H. L., and Dice, J. F. (1988). Peptide sequences that target proteins for enhanced degradation during serum withdrawal. *J Biol Chem* **263**, 6797-805.
- Clayton, C., and Shapira, M. (2007). Post-transcriptional regulation of gene expression in trypanosomes and leishmanias. *Mol Biochem Parasitol* **156**, 93-101.
- Clayton, C. E. (1999). Genetic manipulation of kinetoplastida. *Parasitol Today* **15**, 372-8.
- Clayton, C. E. (2002). Life without transcriptional control? From fly to man and back again. *Embo J* **21**, 1881-8.
- Cook, D. G., Sung, J. C., Golde, T. E., Felsenstein, K. M., Wojczyk, B. S., Tanzi, R. E., Trojanowski, J. Q., Lee, V. M., and Doms, R. W. (1996). Expression and analysis of presenilin 1 in a human neuronal system: localization in cell bodies and dendrites. *Proc Natl Acad Sci U S A* **93**, 9223-8.
- Coombs, G. H., Craft, J. A., and Hart, D. T. (1982). A comparative study of *Leishmania mexicana* amastigotes and promastigotes. Enzyme activities and subcellular locations. *Mol Biochem Parasitol* **5**, 199-211.
- Coombs, G. H., Tetley, L., Moss, V. A., and Vickerman, K. (1986). Three dimensional structure of the *Leishmania* amastigote as revealed by computer-aided reconstruction from serial sections. *Parasitology* **92** ( Pt 1), 13-23.
- Courret, N., Frehel, C., Prina, E., Lang, T., and Antoine, J. C. (2001). Kinetics of the intracellular differentiation of *Leishmania amazonensis* and internalization of host MHC molecules by the intermediate parasite stages. *Parasitology* **122**, 263-79.

- Croft, S. L., and Coombs, G. H. (2003). Leishmaniasis--current chemotherapy and recent advances in the search for novel drugs. *Trends Parasitol* **19**, 502-8.
- Croft, S. L., Sundar, S., and Fairlamb, A. H. (2006). Drug resistance in leishmaniasis. *Clin Microbiol Rev* **19**, 111-26.
- Cruz, I., Nieto, J., Moreno, J., Canavate, C., Desjeux, P., and Alvar, J. (2006). Leishmania/HIV co-infections in the second decade. *Indian J Med Res* **123**, 357-88.
- Cuervo, A. M. (2004). Autophagy: in sickness and in health. *Trends Cell Biol* **14**, 70-7.
- Cunningham, I., and Slater, J. S. (1974). Amino acid analyses of haemolymph of *Glossina morsitans morsitans* (Westwood). *Acta Trop* **31**, 83-8.
- Cunningham, M. L., Titus, R. G., Turco, S. J., and Beverley, S. M. (2001). Regulation of differentiation to the infective stage of the protozoan parasite *Leishmania major* by tetrahydrobiopterin. *Science* **292**, 285-7.

## D

- Darsow, T., Rieder, S. E., and Emr, S. D. (1997). A multispecificity syntaxin homologue, Vam3p, essential for autophagic and biosynthetic protein transport to the vacuole. *J Cell Biol* **138**, 517-29.
- de Diego, J. L., Katz, J. M., Marshall, P., Gutierrez, B., Manning, J. E., Nussenzweig, V., and Gonzalez, J. (2001). The ubiquitin-proteasome pathway plays an essential role in proteolysis during *Trypanosoma cruzi* remodeling. *Biochemistry* **40**, 1053-62.
- De Strooper, B., Beullens, M., Contreras, B., Levesque, L., Craessaerts, K., Cordell, B., Moechars, D., Bollen, M., Fraser, P., George-Hyslop, P. S., and Van Leuven, F. (1997). Phosphorylation, subcellular localization, and membrane orientation of the Alzheimer's disease-associated presenilins. *J Biol Chem* **272**, 3590-8.
- De Strooper, B., and Woodgett, J. (2003). Alzheimer's disease: Mental plaque removal. *Nature* **423**, 392-3.
- Denninger, V., Koopmann, R., Muhammad, K., Barth, T., Bassarak, B., Schonfeld, C., Kilunga, B. K., and Duszynski, M. (2008). Kinetoplastida model organisms for simple autophagic pathways? *Methods Enzymol* **451**, 373-408.
- Denny, P. W., Goulding, D., Ferguson, M. A., and Smith, D. F. (2004). Sphingolipid-free *Leishmania* are defective in membrane trafficking, differentiation and infectivity. *Mol Microbiol* **52**, 313-27.

- Descoteaux, A., and Turco, S. J. (1999). Glycoconjugates in *Leishmania* infectivity. *Biochim Biophys Acta* **1455**, 341-52.
- Desjeux, P. (1996). Leishmaniasis. Public health aspects and control. *Clin Dermatol* **14**, 417-23.
- Desjeux, P. (2004). Leishmaniasis: current situation and new perspectives. *Comp Immunol Microbiol Infect Dis* **27**, 305-18.
- Dewji, N. N. (2005). The structure and functions of the presenilins. *Cell Mol Life Sci* **62**, 1109-19.
- Dewji, N. N., and Singer, S. J. (1997). Cell surface expression of the Alzheimer disease-related presenilin proteins. *Proc Natl Acad Sci U S A* **94**, 9926-31.
- Dice, J. F. (2007). Chaperone-mediated autophagy. *Autophagy* **3**, 295-9.
- Doelling, J. H., Walker, J. M., Friedman, E. M., Thompson, A. R., and Vierstra, R. D. (2002). The APG8/12-activating enzyme APG7 is required for proper nutrient recycling and senescence in *Arabidopsis thaliana*. *J Biol Chem* **277**, 33105-14.
- Dotz, G., Gould, S. J. (1996). Multiple PEX genes are required for proper subcellular distribution and stability of Pex5p, the PTS1 receptor: evidence that PTS1 protein import is mediated by a cycling receptor. *J Cell Biol.* **135**: 1763-1774.
- Doms, R. W., and Helenius, A. (1986). Quaternary structure of influenza virus hemagglutinin after acid treatment. *J Virol* **60**, 833-9.
- Dumanchin, C., Czech, C., Champion, D., Cuif, M. H., Poyot, T., Martin, C., Charbonnier, F., Goud, B., Pradier, L., and Frebourg, T. (1999). Presenilins interact with Rab11, a small GTPase involved in the regulation of vesicular transport. *Hum Mol Genet* **8**, 1263-9.
- Dunn, W. A., Jr., Cregg, J. M., Kiel, J. A., van der Klei, I. J., Oku, M., Sakai, Y., Sibirny, A. A., Stasyk, O. V., and Veenhuis, M. (2005). Pexophagy: the selective autophagy of peroxisomes. *Autophagy* **1**, 75-83.
- Duszenko, M., Ivanov, I. E., Ferguson, M. A., Plesken, H., and Cross, G. A. (1988). Intracellular transport of a variant surface glycoprotein in *Trypanosoma brucei*. *J Cell Biol* **106**, 77-86.

## E

- Efthimiopoulos, S., Floor, E., Georgakopoulos, A., Shioi, J., Cui, W., Yasothornsrikul, S., Hook, V. Y., Wisniewski, T., Buee, L., and Robakis, N. K. (1998). Enrichment of presenilin 1 peptides in neuronal large dense-core and somatodendritic clathrin-coated vesicles. *J Neurochem* **71**, 2365-72.

- Elazar, Z., Scherz-Shouval, R., and Shorer, H. (2003). Involvement of LMA1 and GATE-16 family members in intracellular membrane dynamics. *Biochim Biophys Acta* **1641**, 145-56.
- Ersmark, K., Samuelsson, B., and Hallberg, A. (2006). Plasmepsins as potential targets for new antimalarial therapy. *Med Res Rev* **26**, 626-66.
- Eskelinen, E. L. (2005). Maturation of autophagic vacuoles in Mammalian cells. *Autophagy* **1**, 1-10.
- Eskelinen, E. L., Illert, A. L., Tanaka, Y., Schwarzmann, G., Blanz, J., Von Figura, K., and Saftig, P. (2002). Role of LAMP-2 in lysosome biogenesis and autophagy. *Mol Biol Cell* **13**, 3355-68.
- Esselens, C., Oorschot, V., Baert, V., Raemaekers, T., Spittaels, K., Serneels, L., Zheng, H., Saftig, P., De Strooper, B., Klumperman, J., and Annaert, W. (2004). Presenilin 1 mediates the turnover of telencephalin in hippocampal neurons via an autophagic degradative pathway. *J Cell Biol* **166**, 1041-54.

## F

- Fass, E., Amar, N., and Elazar, Z. (2007). Identification of essential residues for the C-terminal cleavage of the mammalian LC3: a lesson from yeast Atg8. *Autophagy* **3**, 48-50.
- Felbor, U., Kessler, B., Mothes, W., Goebel, H. H., Ploegh, H. L., Bronson, R. T., and Olsen, B. R. (2002). Neuronal loss and brain atrophy in mice lacking cathepsins B and L. *Proc Natl Acad Sci U S A* **99**, 7883-8.
- Field, H., Farjah, M., Pal, A., Gull, K., and Field, M. C. (1998). Complexity of trypanosomatid endocytosis pathways revealed by Rab4 and Rab5 isoforms in *Trypanosoma brucei*. *J Biol Chem* **273**, 32102-10.
- Finley, D., Bartel, B., and Varshavsky, A. (1989). The tails of ubiquitin precursors are ribosomal proteins whose fusion to ubiquitin facilitates ribosome biogenesis. *Nature* **338**, 394-401.
- Flinn, H. M., Rangarajan, D., and Smith, D. F. (1994). Expression of a hydrophilic surface protein in infective stages of *Leishmania major*. *Mol Biochem Parasitol* **65**, 259-70.
- Fujimuro, M., Sawada, H., and Yokosawa, H. (1994). Production and characterization of monoclonal antibodies specific to multi-ubiquitin chains of polyubiquitinated proteins. *FEBS Lett* **349**, 173-80.
- Fujita, N., Itoh, T., Omori, H., Fukuda, M., Noda, T., and Yoshimori, T. (2008). The Atg16L complex specifies the site of LC3 lipidation for membrane biogenesis in autophagy. *Mol Biol Cell* **19**, 2092-100.

## G

- Geng, J., and Klionsky, D. J. (2008). The Atg8 and Atg12 ubiquitin-like conjugation systems in macroautophagy. 'Protein modifications: beyond the usual suspects' review series. *EMBO Rep* **9**, 859-64.
- Goehring, A. S., Rivers, D. M., and Sprague, G. F., Jr. (2003a). Attachment of the ubiquitin-related protein Urm1p to the antioxidant protein Ahp1p. *Eukaryot Cell* **2**, 930-6.
- Goehring, A. S., Rivers, D. M., and Sprague, G. F., Jr. (2003b). Urmylation: a ubiquitin-like pathway that functions during invasive growth and budding in yeast. *Mol Biol Cell* **14**, 4329-41.
- Gonzalez, U., Pinart, M., Reveiz, L., and Alvar, J. (2008). Interventions for Old World cutaneous leishmaniasis. *Cochrane Database Syst Rev*, CD005067.
- Gordon, P. B., Hoyvik, H., and Seglen, P. O. (1992). Prelysosomal and lysosomal connections between autophagy and endocytosis. *Biochem J* **283** ( Pt 2), 361-9.
- Gossage, S. M., Rogers, M. E., and Bates, P. A. (2003). Two separate growth phases during the development of *Leishmania* in sand flies: implications for understanding the life cycle. *Int J Parasitol* **33**, 1027-34.
- Grou, CP., Carvalho, AF, Pinto, MP., Alencaster, IS., Rodrigues, TA., Freitas, MO., Francisco, T., Sa-Miranda, C., and Azevedo, JE. (2009). The peroxisomal protein import machinery - a case report of transient ubiquitination with a new flavour. *Cell. Mol. Life Sci* **66**: 254-262
- Guerfali, F. Z., Laouini, D., Guizani-Tabbane, L., Ottones, F., Ben-Aissa, K., Benkahla, A., Manchon, L., Piquemal, D., Smandi, S., Mghirbi, O., Commes, T., Marti, J., and Dellagi, K. (2008). Simultaneous gene expression profiling in human macrophages infected with *Leishmania major* parasites using SAGE. *BMC Genomics* **9**, 238.
- Gull, K. (1999). The Cytoskeleton of Trypanosomatid Parasites. *Annu. Rev. Microbiol.* **53**, 629-655
- Gutierrez, M. G., Munafo, D. B., Beron, W., and Colombo, M. I. (2004). Rab7 is required for the normal progression of the autophagic pathway in mammalian cells. *J Cell Sci* **117**, 2687-97.

## H

- Halpain, S., and Dehmelt, L. (2006). The MAP1 family of microtubule-associated proteins. *Genome Biol* **7**, 224.

- Hamilton, J. G., and El Naiem, D. A. (2000). Sugars in the gut of the sandfly *Phlebotomus orientalis* from Dinder National Park, Eastern Sudan. *Med Vet Entomol* **14**, 64-70.
- Hanada, T., Noda, N. N., Satomi, Y., Ichimura, Y., Fujioka, Y., Takao, T., Inagaki, F., and Ohsumi, Y. (2007). The Atg12-Atg5 conjugate has a novel E3-like activity for protein lipidation in autophagy. *J Biol Chem* **282**, 37298-302.
- He, C., and Klionsky, D. J. (2006). Autophagy and neurodegeneration. *ACS Chem Biol* **1**, 211-3.
- Helms, M. J., Ambit, A., Appleton, P., Tetley, L., Coombs, G. H., and Mottram, J. C. (2006). Bloodstream form *Trypanosoma brucei* depend upon multiple metacaspases associated with RAB11-positive endosomes. *J Cell Sci* **119**, 1105-17.
- Hemelaar, J., Lelyveld, V. S., Kessler, B. M., and Ploegh, H. L. (2003). A single protease, Apg4B, is specific for the autophagy-related ubiquitin-like proteins GATE-16, MAP1-LC3, GABARAP, and Apg8L. *J Biol Chem* **278**, 51841-50.
- Henricson, A., Kall, L., and Sonnhammer, E. L. (2005). A novel transmembrane topology of presenilin based on reconciling experimental and computational evidence. *Febs J* **272**, 2727-33.
- Herman, M., Gillies, S., Michels, P. A., and Rigden, D. J. (2006). Autophagy and related processes in trypanosomatids: insights from genomic and bioinformatic analyses. *Autophagy* **2**, 107-18.
- Herman, M., Perez-Morga, D., Schtickzelle, N., and Michels, P. A. (2008). Turnover of glycosomes during life-cycle differentiation of *Trypanosoma brucei*. *Autophagy* **4**, 294-308.
- Herwaldt, B. L. (1999). Leishmaniasis. *Lancet* **354**, 1191-9.
- Hochstrasser, M. (2000). Evolution and function of ubiquitin-like protein-conjugation systems. *Nat Cell Biol* **2**, E153-7.
- Huang, J., and Klionsky, D. J. (2007). Autophagy and human disease. *Cell Cycle* **6**, 1837-49.
- Huang, W. P., and Klionsky, D. J. (2002). Autophagy in yeast: a review of the molecular machinery. *Cell Struct Funct* **27**, 409-20.

## I

- Ichimura, Y., Imamura, Y., Emoto, K., Umeda, M., Noda, T., and Ohsumi, Y. (2004). In vivo and in vitro reconstitution of Atg8 conjugation essential for autophagy. *J Biol Chem* **279**, 40584-92.
- Ichimura, Y., Kirisako, T., Takao, T., Satomi, Y., Shimonishi, Y., Ishihara, N., Mizushima, N., Tanida, I., Kominami, E., Ohsumi, M., Noda, T., and Ohsumi, Y. (2000). A ubiquitin-like system mediates protein lipidation. *Nature* **408**, 488-92.
- Ishihara, N., Hamasaki, M., Yokota, S., Suzuki, K., Kamada, Y., Kihara, A., Yoshimori, T., Noda, T., and Ohsumi, Y. (2001). Autophagosome requires specific early Sec proteins for its formation and NSF/SNARE for vacuolar fusion. *Mol Biol Cell* **12**, 3690-702.
- Ivens, A. C., Peacock, C. S., Worthey, E. A., Murphy, L., Aggarwal, G., Berriman, M., Sisk, E., Rajandream, M. A., Adlem, E., Aert, R., *et al.* (2005). The genome of the kinetoplastid parasite, *Leishmania major*. *Science* **309**, 436-42.

## J

- Johnson, E. S. (2004). Protein modification by SUMO. *Annu Rev Biochem* **73**, 355-82.
- Johnston, J. A., Ward, C. L., and Kopito, R. R. (1998). Aggresomes: a cellular response to misfolded proteins. *J Cell Biol* **143**, 1883-98.
- Joshi, P. B., Sacks, D. L., Modi, G., and McMaster, W. R. (1998). Targeted gene deletion of *Leishmania major* genes encoding developmental stage-specific leishmanolysin (GP63). *Mol Microbiol* **27**, 519-30.

## K

- Kabeya, Y., Kamada, Y., Baba, M., Takikawa, H., Sasaki, M., and Ohsumi, Y. (2005). Atg17 functions in cooperation with Atg1 and Atg13 in yeast autophagy. *Mol Biol Cell* **16**, 2544-53.
- Kabeya, Y., Mizushima, N., Ueno, T., Yamamoto, A., Kirisako, T., Noda, T., Kominami, E., Ohsumi, Y., and Yoshimori, T. (2000). LC3, a mammalian homologue of yeast Apg8p, is localized in autophagosome membranes after processing. *Embo J* **19**, 5720-8.
- Kabeya, Y., Mizushima, N., Yamamoto, A., Oshitani-Okamoto, S., Ohsumi, Y., and Yoshimori, T. (2004). LC3, GABARAP and GATE16 localize to autophagosomal membrane depending on form-II formation. *J Cell Sci* **117**, 2805-12.

- Kaether, C., Lammich, S., Edbauer, D., Ertl, M., Rietdorf, J., Capell, A., Steiner, H., and Haass, C. (2002). Presenilin-1 affects trafficking and processing of betaAPP and is targeted in a complex with nicastrin to the plasma membrane. *J Cell Biol* **158**, 551-61.
- Kamada, Y., Funakoshi, T., Shintani, T., Nagano, K., Ohsumi, M., and Ohsumi, Y. (2000). Tor-mediated induction of autophagy via an Apg1 protein kinase complex. *J Cell Biol* **150**, 1507-13.
- Kamhawi, S. (2006). Phlebotomine sand flies and *Leishmania* parasites: friends or foes? *Trends Parasitol* **22**, 439-45.
- Kanki, T., and Klionsky, D. J. (2008). Mitophagy in yeast occurs through a selective mechanism. *J Biol Chem* **283**, 32386-93.
- Kaushik, S., Massey, A. C., Mizushima, N., and Cuervo, A. M. (2008). Constitutive activation of chaperone-mediated autophagy in cells with impaired macroautophagy. *Mol Biol Cell* **19**, 2179-92.
- Kerscher, O., Felberbaum, R., and Hochstrasser, M. (2006). Modification of proteins by ubiquitin and ubiquitin-like proteins. *Annu Rev Cell Dev Biol* **22**, 159-80.
- Ketelaar, T., Voss, C., Dimmock, S. A., Thumm, M., and Hussey, P. J. (2004). *Arabidopsis* homologues of the autophagy protein Atg8 are a novel family of microtubule binding proteins. *FEBS Lett* **567**, 302-6.
- Kiel, J. A., Komduur, J. A., van der Klei, I. J., and Veenhuis, M. (2003). Macropexophagy in *Hansenula polymorpha*: facts and views. *FEBS Lett* **549**, 1-6.
- Kihara, A., Noda, T., Ishihara, N., and Ohsumi, Y. (2001). Two distinct Vps34 phosphatidylinositol 3-kinase complexes function in autophagy and carboxypeptidase Y sorting in *Saccharomyces cerevisiae*. *J Cell Biol* **152**, 519-30.
- Kim, J., Huang, W. P., Stromhaug, P. E., and Klionsky, D. J. (2002). Convergence of multiple autophagy and cytoplasm to vacuole targeting components to a perivacuolar membrane compartment prior to de novo vesicle formation. *J Biol Chem* **277**, 763-73.
- Kim, J., and Schekman, R. (2004). The ins and outs of presenilin 1 membrane topology. *Proc Natl Acad Sci U S A* **101**, 905-6.
- Kirisako, T., Baba, M., Ishihara, N., Miyazawa, K., Ohsumi, M., Yoshimori, T., Noda, T., and Ohsumi, Y. (1999). Formation process of autophagosome is traced with Apg8/Aut7p in yeast. *J Cell Biol* **147**, 435-46.
- Kirisako, T., Ichimura, Y., Okada, H., Kabeya, Y., Mizushima, N., Yoshimori, T., Ohsumi, M., Takao, T., Noda, T., and Ohsumi, Y. (2000). The reversible modification regulates the membrane-binding state of Apg8/Aut7

essential for autophagy and the cytoplasm to vacuole targeting pathway. *J Cell Biol* **151**, 263-76.

Kittler, J. T., Rostaing, P., Schiavo, G., Fritschy, J. M., Olsen, R., Triller, A., and Moss, S. J. (2001). The subcellular distribution of GABARAP and its ability to interact with NSF suggest a role for this protein in the intracellular transport of GABA(A) receptors. *Mol Cell Neurosci* **18**, 13-25.

Klionsky, D. J. (2005). The molecular machinery of autophagy: unanswered questions. *J Cell Sci* **118**, 7-18.

Klionsky, D. J., Abeliovich, H., Agostinis, P., Agrawal, D. K., Aliev, G., Askew, D. S., Baba, M., Baehrecke, E. H., Bahr, B. A., Ballabio, A., *et al.* (2008). Guidelines for the use and interpretation of assays for monitoring autophagy in higher eukaryotes. *Autophagy* **4**, 151-75.

Klionsky, D. J., Cregg, J. M., Dunn, W. A., Jr., Emr, S. D., Sakai, Y., Sandoval, I. V., Sibirny, A., Subramani, S., Thumm, M., Veenhuis, M., and Ohsumi, Y. (2003). A unified nomenclature for yeast autophagy-related genes. *Dev Cell* **5**, 539-45.

Knight, D., Harris, R., McAlister, M. S., Phelan, J. P., Geddes, S., Moss, S. J., Driscoll, P. C., and Keep, N. H. (2002). The X-ray crystal structure and putative ligand-derived peptide binding properties of gamma-aminobutyric acid receptor type A receptor-associated protein. *J Biol Chem* **277**, 5556-61.

Knuepfer, E., Stierhof, Y. D., McKean, P. G., and Smith, D. F. (2001). Characterization of a differentially expressed protein that shows an unusual localization to intracellular membranes in *Leishmania major*. *Biochem J* **356**, 335-44.

Koike, M., Nakanishi, H., Saftig, P., Ezaki, J., Isahara, K., Ohsawa, Y., Schulz-Schaeffer, W., Watanabe, T., Waguri, S., Kametaka, S., Shibata, M., Yamamoto, K., Kominami, E., Peters, C., von Figura, K., and Uchiyama, Y. (2000). Cathepsin D deficiency induces lysosomal storage with ceroid lipofuscin in mouse CNS neurons. *J Neurosci* **20**, 6898-906.

Komatsu, M., Kominami, E., and Tanaka, K. (2006). Autophagy and neurodegeneration. *Autophagy* **2**, 315-7.

Kuma, A., Matsui, M., and Mizushima, N. (2007). LC3, an autophagosome marker, can be incorporated into protein aggregates independent of autophagy: caution in the interpretation of LC3 localization. *Autophagy* **3**, 323-8.

Kumar, S., Tamura, K., and Nei, M. (2004). MEGA3: Integrated software for Molecular Evolutionary Genetics Analysis and sequence alignment. *Brief Bioinform* **5**, 150-63.

Kunz, J. B., Schwarz, H., and Mayer, A. (2004). Determination of four sequential stages during microautophagy in vitro. *J Biol Chem* **279**, 9987-96.

## L

- Lah, J. J., and Levey, A. I. (2000). Endogenous presenilin-1 targets to endocytic rather than biosynthetic compartments. *Mol Cell Neurosci* **16**, 111-26.
- Landfear, S. M., and Ignatushchenko, M. (2001). The flagellum and flagellar pocket of trypanosomatids. *Mol Biochem Parasitol* **115**, 1-17.
- LaPointe, C. F., and Taylor, R. K. (2000). The type 4 prepilin peptidases comprise a novel family of aspartic acid proteases. *J Biol Chem* **275**, 1502-10.
- Laskay, T., van Zandbergen, G., and Solbach, W. (2008). Neutrophil granulocytes as host cells and transport vehicles for intracellular pathogens: apoptosis as infection-promoting factor. *Immunobiology* **213**, 183-91.
- Laudon, H., Hansson, E. M., Melen, K., Bergman, A., Farmery, M. R., Winblad, B., Lendahl, U., von Heijne, G., and Naslund, J. (2005). A nine-transmembrane domain topology for presenilin 1. *J Biol Chem* **280**, 35352-60.
- Laudon, H., Winblad, B., and Naslund, J. (2007). The Alzheimer's disease-associated gamma-secretase complex: functional domains in the presenilin 1 protein. *Physiol Behav* **92**, 115-20.
- Lawrence, B. P., and Brown, W. J. (1992). Autophagic vacuoles rapidly fuse with pre-existing lysosomes in cultured hepatocytes. *J Cell Sci* **102 ( Pt 3)**, 515-26.
- Lee, M. K., Slunt, H. H., Martin, L. J., Thinakaran, G., Kim, G., Gandy, S. E., Seeger, M., Koo, E., Price, D. L., and Sisodia, S. S. (1996). Expression of presenilin 1 and 2 (PS1 and PS2) in human and murine tissues. *J Neurosci* **16**, 7513-25.
- Leissring, M. A., LaFerla, F. M., Callamaras, N., and Parker, I. (2001). Subcellular mechanisms of presenilin-mediated enhancement of calcium signaling. *Neurobiol Dis* **8**, 469-78.
- Lemberg, M. K., and Martoglio, B. (2002). Requirements for signal peptide peptidase-catalyzed intramembrane proteolysis. *Mol Cell* **10**, 735-44.
- Levitan, D., and Greenwald, I. (1995). Facilitation of lin-12-mediated signalling by sel-12, a *Caenorhabditis elegans* S182 Alzheimer's disease gene. *Nature* **377**, 351-4.
- Li, J., Xu, M., Zhou, H., Ma, J., and Potter, H. (1997). Alzheimer presenilins in the nuclear membrane, interphase kinetochores, and centrosomes suggest a role in chromosome segregation. *Cell* **90**, 917-27.

- Li, X., Chen, H., Oh, S. S., and Chishti, A. H. (2008). A Presenilin-like protease associated with *Plasmodium falciparum* micronemes is involved in erythrocyte invasion. *Mol Biochem Parasitol* **158**, 22-31.
- Li, X., and Greenwald, I. (1996). Membrane topology of the *C. elegans* SEL-12 presenilin. *Neuron* **17**, 1015-21.
- Li, X., and Greenwald, I. (1998). Additional evidence for an eight-transmembrane-domain topology for *Caenorhabditis elegans* and human presenilins. *Proc Natl Acad Sci U S A* **95**, 7109-14.
- Liou, W., Geuze, H. J., Geelen, M. J., and Slot, J. W. (1997). The autophagic and endocytic pathways converge at the nascent autophagic vacuoles. *J Cell Biol* **136**, 61-70.
- Lodge, R., and Descoteaux, A. (2005). Modulation of phagolysosome biogenesis by the lipophosphoglycan of *Leishmania*. *Clin Immunol* **114**, 256-65.
- Lucocq, J., and Walker, D. (1997). Evidence for fusion between multilamellar endosomes and autophagosomes in HeLa cells. *Eur J Cell Biol* **72**, 307-13.
- Lustig, Y., Vagima, Y., Goldshmidt, H., Erlanger, A., Ozeri, V., Vince, J., McConville, M. J., Dwyer, D. M., Landfear, S. M., and Michaeli, S. (2007). Down-regulation of the trypanosomatid signal recognition particle affects the biogenesis of polytopic membrane proteins but not of signal peptide-containing proteins. *Eukaryot Cell* **6**, 1865-75

## M

- Maarouf, M., Adeline, M. T., Solignac, M., Vautrin, D., and Robert-Gero, M. (1998). Development and characterization of paromomycin-resistant *Leishmania donovani* promastigotes. *Parasite* **5**, 167-73.
- Mann, S. S., and Hammarback, J. A. (1994). Molecular characterization of light chain 3. A microtubule binding subunit of MAP1A and MAP1B. *J Biol Chem* **269**, 11492-7.
- Manning-Cela, R., Jaishankar, S., and Swindle, J. (2006). Life-cycle and growth-phase-dependent regulation of the ubiquitin genes of *Trypanosoma cruzi*. *Arch Med Res* **37**, 593-601.
- Marotta, D. E., Gerald, N., and Dwyer, D. M. (2006). Rab5b localization to early endosomes in the protozoan human pathogen *Leishmania donovani*. *Mol Cell Biochem* **292**, 107-17.
- Massey, A., Kiffin, R., and Cuervo, A. M. (2004). Pathophysiology of chaperone-mediated autophagy. *Int J Biochem Cell Biol* **36**, 2420-34.

- Massey, A. C., Kaushik, S., Sovak, G., Kiffin, R., and Cuervo, A. M. (2006). Consequences of the selective blockage of chaperone-mediated autophagy. *Proc Natl Acad Sci U S A* **103**, 5805-10.
- Mazareb, S., Fu, Z. Y., and Zilberstein, D. (1999). Developmental regulation of proline transport in *Leishmania donovani*. *Exp Parasitol* **91**, 341-8.
- McCarthy, J. V. (2005). Involvement of presenilins in cell-survival signalling pathways. *Biochem Soc Trans* **33**, 568-72.
- McConville, M. J., and Blackwell, J. M. (1991). Developmental changes in the glycosylated phosphatidylinositols of *Leishmania donovani*. Characterization of the promastigote and amastigote glycolipids. *J Biol Chem* **266**, 15170-9.
- McConville, M. J., Collidge, T. A., Ferguson, M. A., and Schneider, P. (1993). The glycoinositol phospholipids of *Leishmania mexicana* promastigotes. Evidence for the presence of three distinct pathways of glycolipid biosynthesis. *J Biol Chem* **268**, 15595-604.
- McConville, M. J., de Souza, D., Saunders, E., Likic, V. A., and Naderer, T. (2007). Living in a phagolysosome; metabolism of *Leishmania* amastigotes. *Trends Parasitol* **23**, 368-75.
- McConville, M. J., Ilgoutz, S. C., Teasdale, R. D., Foth, B. J., Matthews, A., Mullin, K. A., and Gleeson, P. A. (2002a). Targeting of the GRIP domain to the trans-Golgi network is conserved from protists to animals. *Eur J Cell Biol* **81**, 485-95.
- McConville, M. J., Mullin, K. A., Ilgoutz, S. C., and Teasdale, R. D. (2002b). Secretory pathway of trypanosomatid parasites. *Microbiol Mol Biol Rev* **66**, 122-54; table of contents.
- McGwire, B. S., O'Connell, W. A., Chang, K. P., and Engman, D. M. (2002). Extracellular release of the glycosylphosphatidylinositol (GPI)-linked *Leishmania* surface metalloprotease, gp63, is independent of GPI phospholipolysis: implications for parasite virulence. *J Biol Chem* **277**, 8802-9.
- McKean, P. G., Denny, P. W., Knuepfer, E., Keen, J. K., and Smith, D. F. (2001). Phenotypic changes associated with deletion and overexpression of a stage-regulated gene family in *Leishmania*. *Cell Microbiol* **3**, 511-23.
- Meijer, A. J. (2008). Amino acid regulation of autophagosome formation. *Methods Mol Biol* **445**, 89-109.
- Meijer, W. H., van der Klei, I. J., Veenhuis, M., and Kiel, J. A. (2007). ATG genes involved in non-selective autophagy are conserved from yeast to man, but the selective Cvt and pexophagy pathways also require organism-specific genes. *Autophagy* **3**, 106-16.

- Melendez, A., Tallozy, Z., Seaman, M., Eskelinen, E. L., Hall, D. H., and Levine, B. (2003). Autophagy genes are essential for dauer development and life-span extension in *C. elegans*. *Science* **301**, 1387-91.
- Mendez, S., Fernandez-Perez FJ., de la Fuente, C., Cuquerella, M., Gomez-Munoz MR., Alunda, JM. (1999). Partial anaerobiosis induces infectivity of *Leishmania infantum* promastigotes. *Parasitol Res* **85**(6):507-9
- Michels, P. A., Bringaud, F., Herman, M., and Hannaert, V. (2006). Metabolic functions of glycosomes in trypanosomatids. *Biochim Biophys Acta* **1763**, 1463-77.
- Misslitz, A., Mottram, J. C., Overath, P., and Aebischer, T. (2000). Targeted integration into a rRNA locus results in uniform and high level expression of transgenes in *Leishmania* amastigotes. *Mol Biochem Parasitol* **107**, 251-61.
- Mizushima, N., and Klionsky, D. J. (2007). Protein turnover via autophagy: implications for metabolism. *Annu Rev Nutr* **27**, 19-40.
- Mizushima, N., Noda, T., and Ohsumi, Y. (1999). Apg16p is required for the function of the Apg12p-Apg5p conjugate in the yeast autophagy pathway. *Embo J* **18**, 3888-96.
- Mizushima, N., Noda, T., Yoshimori, T., Tanaka, Y., Ishii, T., George, M. D., Klionsky, D. J., Ohsumi, M., and Ohsumi, Y. (1998). A protein conjugation system essential for autophagy. *Nature* **395**, 395-8.
- Mizushima, N., Yamamoto, A., Hatano, M., Kobayashi, Y., Kabeya, Y., Suzuki, K., Tokuhiya, T., Ohsumi, Y., and Yoshimori, T. (2001). Dissection of autophagosome formation using Apg5-deficient mouse embryonic stem cells. *J Cell Biol* **152**, 657-68.
- Mizushima, N., Yamamoto, A., Matsui, M., Yoshimori, T., and Ohsumi, Y. (2004). In vivo analysis of autophagy in response to nutrient starvation using transgenic mice expressing a fluorescent autophagosome marker. *Mol Biol Cell* **15**, 1101-11.
- Mizushima, N., Yoshimori, T., and Ohsumi, Y. (2003). Role of the Apg12 conjugation system in mammalian autophagy. *Int J Biochem Cell Biol* **35**, 553-61.
- Mojtahedi, Z., Clos, J., and Kamali-Sarvestani, E. (2008). *Leishmania major*: identification of developmentally regulated proteins in procyclic and metacyclic promastigotes. *Exp Parasitol* **119**, 422-9.
- Moody, S. F., Handman, E., McConville, M. J., and Bacic, A. (1993). The structure of *Leishmania major* amastigote lipophosphoglycan. *J Biol Chem* **268**, 18457-66.
- Morgado-Diaz, J. A., Silva-Lopez, R. E., Alves, C. R., Soares, M. J., Corte-Real, S., and De Simone, S. G. (2005). Subcellular localization of an

intracellular serine protease of 68 kDa in *Leishmania (Leishmania) amazonensis* promastigotes. *Mem Inst Oswaldo Cruz* **100**, 377-83.

Morgan, G. W., Hall, B. S., Denny, P. W., Carrington, M., and Field, M. C. (2002). The kinetoplastida endocytic apparatus. Part I: a dynamic system for nutrition and evasion of host defences. *Trends Parasitol* **18**, 491-6.

Mottram, J. C., Souza, A. E., Hutchison, J. E., Carter, R., Frame, M. J., and Coombs, G. H. (1996). Evidence from disruption of the *lmcpc* gene array of *Leishmania mexicana* that cysteine proteinases are virulence factors. *Proc Natl Acad Sci U S A* **93**, 6008-13.

Mottram, J.C., Coombs, G.H., Alexander, J. (2004). Cysteine peptidases as virulence factors of *Leishmania*. *Curr. Opin. Microbiol.* **7**, 375-381.

Muller, J. M., Shorter, J., Newman, R., Deinhardt, K., Sagiv, Y., Elazar, Z., Warren, G., and Shima, D. T. (2002). Sequential SNARE disassembly and GATE-16-GOS-28 complex assembly mediated by distinct NSF activities drives Golgi membrane fusion. *J Cell Biol* **157**, 1161-73.

Mullin, K. A., Foth, B. J., Ilgoutz, S. C., Callaghan, J. M., Zawadzki, J. L., McFadden, G. I., and McConville, M. J. (2001). Regulated degradation of an endoplasmic reticulum membrane protein in a tubular lysosome in *Leishmania mexicana*. *Mol Biol Cell* **12**, 2364-77.

Munafo, D. B., and Colombo, M. I. (2001). A novel assay to study autophagy: regulation of autophagosome vacuole size by amino acid deprivation. *J Cell Sci* **114**, 3619-29.

Munday, J. (2008). Studies on oligopeptidase B of *Leishmania major*. University of Glasgow.

## N

Naderer, T., and McConville, M. J. (2008). The *Leishmania*-macrophage interaction: a metabolic perspective. *Cell Microbiol* **10**, 301-8.

Naderer, T., Vince, J. E., and McConville, M. J. (2004). Surface determinants of *Leishmania* parasites and their role in infectivity in the mammalian host. *Curr Mol Med* **4**, 649-65.

Nagan, N., and Zoeller, R. A. (2001). Plasmalogens: biosynthesis and functions. *Prog Lipid Res* **40**, 199-229.

Nakatogawa, H., Ichimura, Y., and Ohsumi, Y. (2007). Atg8, a ubiquitin-like protein required for autophagosome formation, mediates membrane tethering and hemifusion. *Cell* **130**, 165-78.

Nara, A., Mizushima, N., Yamamoto, A., Kabeya, Y., Ohsumi, Y., and Yoshimori, T. (2002). SKD1 AAA ATPase-dependent endosomal transport is involved in autolysosome formation. *Cell Struct Funct* **27**, 29-37.

- Naruse, S., Thinakaran, G., Luo, J. J., Kusiak, J. W., Tomita, T., Iwatsubo, T., Qian, X., Ginty, D. D., Price, D. L., Borchelt, D. R., Wong, P. C., and Sisodia, S. S. (1998). Effects of PS1 deficiency on membrane protein trafficking in neurons. *Neuron* **21**, 1213-21.
- Nixon, R. A., Wegiel, J., Kumar, A., Yu, W. H., Peterhoff, C., Cataldo, A., and Cuervo, A. M. (2005). Extensive involvement of autophagy in Alzheimer disease: an immuno-electron microscopy study. *J Neuropathol Exp Neurol* **64**, 113-22.
- Noda, T., and Ohsumi, Y. (1998). Tor, a phosphatidylinositol kinase homologue, controls autophagy in yeast. *J Biol Chem* **273**, 3963-6.
- Nyborg, A. C., Jansen, K., Ladd, T. B., Fauq, A., and Golde, T. E. (2004). A signal peptide peptidase (SPP) reporter activity assay based on the cleavage of type II membrane protein substrates provides further evidence for an inverted orientation of the SPP active site relative to presenilin. *J Biol Chem* **279**, 43148-56.

## O

- Obara, K., Sekito, T., and Ohsumi, Y. (2006). Assortment of phosphatidylinositol 3-kinase complexes--Atg14p directs association of complex I to the pre-autophagosomal structure in *Saccharomyces cerevisiae*. *Mol Biol Cell* **17**, 1527-39.
- Ogier-Denis, E., and Codogno, P. (2003). Autophagy: a barrier or an adaptive response to cancer. *Biochim Biophys Acta* **1603**, 113-28.
- Oh-oka, K., Nakatogawa, H., and Ohsumi, Y. (2008). Physiological pH and acidic phospholipids contribute to substrate specificity in lipidation of Atg8. *J Biol Chem* **283**, 21847-52.
- Onodera, J., and Ohsumi, Y. (2005). Autophagy is required for maintenance of amino acid levels and protein synthesis under nitrogen starvation. *J Biol Chem* **280**, 31582-6.
- Opperdoes, F. R., and Coombs, G. H. (2007). Metabolism of *Leishmania*: proven and predicted. *Trends Parasitol* **23**, 149-58.
- Orvedahl, A., and Levine, B. (2009). Eating the enemy within: autophagy in infectious diseases. *Cell Death Differ* **16**, 57-69.
- Otto, G. P., Wu, M. Y., Kazgan, N., Anderson, O. R., and Kessin, R. H. (2003). Macroautophagy is required for multicellular development of the social amoeba *Dictyostelium discoideum*. *J Biol Chem* **278**, 17636-45.
- Ouellette, M., Drummelsmith, J., and Papadopoulou, B. (2004). Leishmaniasis: drugs in the clinic, resistance and new developments. *Drug Resist Updat* **7**, 257-66.

Ozkaynak, E., Finley, D., Solomon, M. J., and Varshavsky, A. (1987). The yeast ubiquitin genes: a family of natural gene fusions. *Embo J* **6**, 1429-39.

Ozkaynak, E., Finley, D., and Varshavsky, A. (1984). The yeast ubiquitin gene: head-to-tail repeats encoding a polyubiquitin precursor protein. *Nature* **312**, 663-6.

## P

Paz, Y., Elazar, Z., and Fass, D. (2000). Structure of GATE-16, membrane transport modulator and mammalian ortholog of autophagocytosis factor Aut7p. *J Biol Chem* **275**, 25445-50.

Periz, G., and Fortini, M. E. (2004). Functional reconstitution of gamma-secretase through coordinated expression of presenilin, nicastrin, Aph-1, and Pen-2. *J Neurosci Res* **77**, 309-22.

Petiot, A., Ogier-Denis, E., Blommaert, E. F., Meijer, A. J., and Codogno, P. (2000). Distinct classes of phosphatidylinositol 3'-kinases are involved in signaling pathways that control macroautophagy in HT-29 cells. *J Biol Chem* **275**, 992-8.

Pimenta, P. F., Saraiva, E. M., and Sacks, D. L. (1991). The comparative fine structure and surface glycoconjugate expression of three life stages of *Leishmania major*. *Exp Parasitol* **72**, 191-204.

Plewes, K. A., Barr, S. D., and Gedamu, L. (2003). Iron superoxide dismutases targeted to the glycosomes of *Leishmania chagasi* are important for survival. *Infect Immun* **71**, 5910-20.

Ponting, C. P., Hutton, M., Nyborg, A., Baker, M., Jansen, K., and Golde, T. E. (2002). Identification of a novel family of presenilin homologues. *Hum Mol Genet* **11**, 1037-44.

Puentes, S. M., Sacks, D. L., da Silva, R. P., and Joiner, K. A. (1988). Complement binding by two developmental stages of *Leishmania major* promastigotes varying in expression of a surface lipophosphoglycan. *J Exp Med* **167**, 887-902.

## R

Ralton, J. E., and McConville, M. J. (1998). Delineation of three pathways of glycosylphosphatidylinositol biosynthesis in *Leishmania mexicana*. Precursors from different pathways are assembled on distinct pools of phosphatidylinositol and undergo fatty acid remodeling. *J Biol Chem* **273**, 4245-57.

Ramamoorthy, R., Donelson, J. E., Paetz, K. E., Maybodi, M., Roberts, S. C., and Wilson, M. E. (1992). Three distinct RNAs for the surface protease gp63

are differentially expressed during development of *Leishmania donovani chagasi* promastigotes to an infectious form. *J Biol Chem* **267**, 1888-95.

- Redman, K. L., and Rechsteiner, M. (1989). Identification of the long ubiquitin extension as ribosomal protein S27a. *Nature* **338**, 438-40.
- Reggiori, F., and Klionsky, D. J. (2005). Autophagosomes: biogenesis from scratch? *Curr Opin Cell Biol* **17**, 415-22.
- Reggiori, F., Wang, C. W., Nair, U., Shintani, T., Abeliovich, H., and Klionsky, D. J. (2004). Early stages of the secretory pathway, but not endosomes, are required for Cvt vesicle and autophagosome assembly in *Saccharomyces cerevisiae*. *Mol Biol Cell* **15**, 2189-204.
- Reithinger, R., Dujardin, J. C., Louzir, H., Pirmez, C., Alexander, B., and Brooker, S. (2007). Cutaneous leishmaniasis. *Lancet Infect Dis* **7**, 581-96.
- Repetto, E., Yoon, I. S., Zheng, H., and Kang, D. E. (2007). Presenilin 1 regulates epidermal growth factor receptor turnover and signaling in the endosomal-lysosomal pathway. *J Biol Chem* **282**, 31504-16.
- Rifkin, M. R., and Fairlamb, A. H. (1985). Transport of ethanolamine and its incorporation into the variant surface glycoprotein of bloodstream forms of *Trypanosoma brucei*. *Mol Biochem Parasitol* **15**, 245-56.
- Rigden, D. J., Herman, M., Gillies, S., and Michels, P. A. (2005). Implications of a genomic search for autophagy-related genes in trypanosomatids. *Biochem Soc Trans* **33**, 972-4.
- Roberts, P., Moshitch-Moshkovitz, S., Kvam, E., O'Toole, E., Winey, M., and Goldfarb, D. S. (2003). Piecemeal microautophagy of nucleus in *Saccharomyces cerevisiae*. *Mol Biol Cell* **14**, 129-41.
- Rochette, A., Raymond, F., Ubeda, J. M., Smith, M., Messier, N., Boisvert, S., Rigault, P., Corbeil, J., Ouellette, M., and Papadopoulou, B. (2008). Genome-wide gene expression profiling analysis of *Leishmania major* and *Leishmania infantum* developmental stages reveals substantial differences between the two species. *BMC Genomics* **9**, 255.
- Rogers, M. E., Chance, M. L., and Bates, P. A. (2002). The role of promastigote secretory gel in the origin and transmission of the infective stage of *Leishmania mexicana* by the sandfly *Lutzomyia longipalpis*. *Parasitology* **124**, 495-507.
- Rosenberry, T. L., Krall, J. A., Dever, T. E., Haas, R., Louvard, D., and Merrick, W. C. (1989). Biosynthetic incorporation of [3H]ethanolamine into protein synthesis elongation factor 1 alpha reveals a new post-translational protein modification. *J Biol Chem* **264**, 7096-9.
- Rosenzweig, D., Smith, D., Opperdoes, F., Stern, S., Olafson, R. W., and Zilberstein, D. (2008). Retooling *Leishmania* metabolism: from sand fly gut to human macrophage. *Faseb J* **22**, 590-602.

Russell, D. G., Xu, S., and Chakraborty, P. (1992). Intracellular trafficking and the parasitophorous vacuole of *Leishmania mexicana*-infected macrophages. *J Cell Sci* **103** ( Pt 4), 1193-210.

## S

Sacks, D. L. (2001). *Leishmania*-sand fly interactions controlling species-specific vector competence. *Cell Microbiol* **3**, 189-96.

Sacks, D. L., and da Silva, R. P. (1987). The generation of infective stage *Leishmania major* promastigotes is associated with the cell-surface expression and release of a developmentally regulated glycolipid. *J Immunol* **139**, 3099-106.

Sacks, D. L., Hieny, S., and Sher, A. (1985). Identification of cell surface carbohydrate and antigenic changes between noninfective and infective developmental stages of *Leishmania major* promastigotes. *J Immunol* **135**, 564-9.

Sacks, D. L., and Perkins, P. V. (1984). Identification of an infective stage of *Leishmania* promastigotes. *Science* **223**, 1417-9.

Sagiv, Y., Legesse-Miller, A., Porat, A., and Elazar, Z. (2000). GATE-16, a membrane transport modulator, interacts with NSF and the Golgi v-SNARE GOS-28. *Embo J* **19**, 1494-504.

Sahin, A., Espiau, B., Tetaud, E., Cuvillier, A., Lartigue, L., Ambit, A., Robinson, D. R., and Merlin, G. (2008). The *Leishmania* ARL-1 and Golgi traffic. *PLoS ONE* **3**, e1620.

Sakai, Y., Koller, A., Rangell, L. K., Keller, G. A., and Subramani, S. (1998). Peroxisome degradation by microautophagy in *Pichia pastoris*: identification of specific steps and morphological intermediates. *J Cell Biol* **141**, 625-36.

Santos, A. L., Branquinha, M. H., and D'Avila-Levy, C. M. (2006). The ubiquitous gp63-like metalloprotease from lower trypanosomatids: in the search for a function. *An Acad Bras Cienc* **78**, 687-714.

Santos, D. O., Coutinho, C. E., Madeira, M. F., Bottino, C. G., Vieira, R. T., Nascimento, S. B., Bernardino, A., Bourguignon, S. C., Corte-Real, S., Pinho, R. T., Rodrigues, C. R., and Castro, H. C. (2008). Leishmaniasis treatment--a challenge that remains: a review. *Parasitol Res* **103**, 1-10.

Saura, C. A., Tomita, T., Soriano, S., Takahashi, M., Leem, J. Y., Honda, T., Koo, E. H., Iwatsubo, T., and Thinakaran, G. (2000). The nonconserved hydrophilic loop domain of presenilin (PS) is not required for PS endoproteolysis or enhanced abeta 42 production mediated by familial

- early onset Alzheimer's disease-linked PS variants. *J Biol Chem* **275**, 17136-42.
- Schaible, U. E., Schlesinger, P. H., Steinberg, T. H., Mangel, W. F., Kobayashi, T., and Russell, D. G. (1999). Parasitophorous vacuoles of *Leishmania mexicana* acquire macromolecules from the host cell cytosol via two independent routes. *J Cell Sci* **112** ( Pt 5), 681-93.
- Scharpe, S., De Meester, I., Hendriks, D., Vanhoof, G., van Sande, M., and Vriend, G. (1991). Proteases and their inhibitors: today and tomorrow. *Biochimie* **73**, 121-6.
- Scherz-Shouval, R., and Elazar, Z. (2007). ROS, mitochondria and the regulation of autophagy. *Trends Cell Biol* **17**, 422-7.
- Scherz-Shouval, R., Sagiv, Y., Shorer, H., and Elazar, Z. (2003). The COOH terminus of GATE-16, an intra-Golgi transport modulator, is cleaved by the human cysteine protease HsApg4A. *J Biol Chem* **278**, 14053-8.
- Scheuner, D., Eckman, C., Jensen, M., Song, X., Citron, M., Suzuki, N., Bird, T. D., Hardy, J., Hutton, M., Kukull, W., *et al.*, (1996). Secreted amyloid beta-protein similar to that in the senile plaques of Alzheimer's disease is increased in vivo by the presenilin 1 and 2 and APP mutations linked to familial Alzheimer's disease. *Nat Med* **2**, 864-70.
- Schonian, G., Nasereddin, A., Dinse, N., Schweynoch, C., Schallig, H. D., Presber, W., and Jaffe, C. L. (2003). PCR diagnosis and characterization of *Leishmania* in local and imported clinical samples. *Diagn Microbiol Infect Dis* **47**, 349-58.
- Schwartz, D. C., and Hochstrasser, M. (2003). A superfamily of protein tags: ubiquitin, SUMO and related modifiers. *Trends Biochem Sci* **28**, 321-8.
- Scott, S. V., Hefner-Gravink, A., Morano, K. A., Noda, T., Ohsumi, Y., and Klionsky, D. J. (1996). Cytoplasm-to-vacuole targeting and autophagy employ the same machinery to deliver proteins to the yeast vacuole. *Proc Natl Acad Sci U S A* **93**, 12304-8.
- Seifert, K., Matu, S., Javier Perez-Victoria, F., Castanys, S., Gamarro, F., and Croft, S. L. (2003). Characterisation of *Leishmania donovani* promastigotes resistant to hexadecylphosphocholine (miltefosine). *Int J Antimicrob Agents* **22**, 380-7.
- Selkoe, D. J. (1994). Cell biology of the amyloid beta-protein precursor and the mechanism of Alzheimer's disease. *Annu Rev Cell Biol* **10**, 373-403.
- Sherrington, R., Rogaev, E. I., Liang, Y., Rogaeva, E. A., Levesque, G., Ikeda, M., Chi, H., Lin, C., Li, G., Holman, K., and *et al.* (1995). Cloning of a gene bearing missense mutations in early-onset familial Alzheimer's disease. *Nature* **375**, 754-60.

- Shintani, T., Mizushima, N., Ogawa, Y., Matsuura, A., Noda, T., and Ohsumi, Y. (1999). Apg10p, a novel protein-conjugating enzyme essential for autophagy in yeast. *Embo J* **18**, 5234-41.
- Shu, X., Shaner, N. C., Yarbrough, C. A., Tsien, R. Y., and Remington, S. J. (2006). Novel chromophores and buried charges control color in mFruits. *Biochemistry* **45**, 9639-47.
- Silvestre, R., Cordeiro-da-Silva, A., and Ouaiissi, A. (2008). Live attenuated *Leishmania* vaccines: a potential strategic alternative. *Arch Immunol Ther Exp (Warsz)* **56**, 123-6.
- Slavikova, S., Shy, G. m., Yao, Y., Glzman, R., Levanony, H., Pietrokovski, S., Elazar, Z., and Galili, G. (2005). The autophagy-associated Atg8 gene family operates both under favourable growth conditions and under starvation stresses in *Arabidopsis* plants. *J Exp Bot* **56**, 2839-49.
- Smith, S. K., Anderson, H. A., Yu, G., Robertson, A. G., Allen, S. J., Tyler, S. J., Naylor, R. L., Mason, G., Wilcock, G. W., Roche, P. A., Fraser, P. E., and Dawbarn, D. (2000). Identification of syntaxin 1A as a novel binding protein for presenilin-1. *Brain Res Mol Brain Res* **78**, 100-7.
- Sommer, J. M., Peterson, G., Keller, G. A., Parsons, M., and Wang, C. C. (1993). The C-terminal tripeptide of glycosomal phosphoglycerate kinase is both necessary and sufficient for import into the glycosomes of *Trypanosoma brucei*. *FEBS Lett* **316**, 53-8.
- Sou, Y. S., Tanida, I., Komatsu, M., Ueno, T., and Kominami, E. (2006). Phosphatidylserine in addition to phosphatidylethanolamine is an in vitro target of the mammalian Atg8 modifiers, LC3, GABARAP, and GATE-16. *J Biol Chem* **281**, 3017-24.
- Spasic, D., Tolia, A., Dillen, K., Baert, V., De Strooper, B., Vrijens, S., and Annaert, W. (2006). Presenilin-1 maintains a nine-transmembrane topology throughout the secretory pathway. *J Biol Chem* **281**, 26569-77.
- Steiner, H., Fluhrer, R., and Haass, C. (2008). Intramembrane proteolysis by gamma-secretase. *J Biol Chem* **283**, 29627-31.
- Steiner, H., Kostka, M., Romig, H., Basset, G., Pesold, B., Hardy, J., Capell, A., Meyn, L., Grim, M. L., Baumeister, R., Fichteler, K., and Haass, C. (2000). Glycine 384 is required for presenilin-1 function and is conserved in bacterial polytopic aspartyl proteases. *Nat Cell Biol* **2**, 848-51.
- Suga, K., Tomiyama, T., Mori, H., and Akagawa, K. (2004). Syntaxin 5 interacts with presenilin holoproteins, but not with their N- or C-terminal fragments, and affects beta-amyloid peptide production. *Biochem J* **381**, 619-28.
- Sugawara, K., Suzuki, N. N., Fujioka, Y., Mizushima, N., Ohsumi, Y., and Inagaki, F. (2004). The crystal structure of microtubule-associated protein light chain 3, a mammalian homologue of *Saccharomyces cerevisiae* Atg8. *Genes Cells* **9**, 611-8.

- Sundar, S., Jha, T. K., Thakur, C. P., Sinha, P. K., and Bhattacharya, S. K. (2007). Injectable paromomycin for Visceral leishmaniasis in India. *N Engl J Med* **356**, 2571-81.
- Suzuki, K., Kirisako, T., Kamada, Y., Mizushima, N., Noda, T., and Ohsumi, Y. (2001). The pre-autophagosomal structure organized by concerted functions of APG genes is essential for autophagosome formation. *Embo J* **20**, 5971-81.
- Szeto, J., Kaniuk, N. A., Canadien, V., Nisman, R., Mizushima, N., Yoshimori, T., Bazett-Jones, D. P., and Brumell, J. H. (2006). ALIS are stress-induced protein storage compartments for substrates of the proteasome and autophagy. *Autophagy* **2**, 189-99.

## T

- Tamboli, I. Y., Prager, K., Thal, D. R., Thelen, K. M., Dewachter, I., Pietrzik, C. U., St George-Hyslop, P., Sisodia, S. S., De Strooper, B., Heneka, M. T., *et al.*, (2008). Loss of gamma-secretase function impairs endocytosis of lipoprotein particles and membrane cholesterol homeostasis. *J Neurosci* **28**, 12097-106.
- Tanaka, Y., Guhde, G., Suter, A., Eskelinen, E. L., Hartmann, D., Lullmann-Rauch, R., Janssen, P. M., Blanz, J., von Figura, K., and Saftig, P. (2000). Accumulation of autophagic vacuoles and cardiomyopathy in LAMP-2-deficient mice. *Nature* **406**, 902-6.
- Tanida, I., Mizushima, N., Kiyooka, M., Ohsumi, M., Ueno, T., Ohsumi, Y., and Kominami, E. (1999). Apg7p/Cvt2p: A novel protein-activating enzyme essential for autophagy. *Mol Biol Cell* **10**, 1367-79.
- Tanida, I., Tanida-Miyake, E., Ueno, T., and Kominami, E. (2001). The human homolog of *Saccharomyces cerevisiae* Apg7p is a Protein-activating enzyme for multiple substrates including human Apg12p, GATE-16, GABARAP, and MAP-LC3. *J Biol Chem* **276**, 1701-6.
- Tanida, I., Tanida-Miyake, E., Komatsu, M., Ueno, T., and Kominami, E. (2002). Human Apg3p/Aut1p homologue is an authentic E2 enzyme for multiple substrates, GATE-16, GABARAP, and MAP-LC3, and facilitates the conjugation of hApg12p to hApg5p. *J Biol Chem* **277**, 13739-44.
- Tanida, I., Komatsu, M., Ueno, T., and Kominami, E. (2003). GATE-16 and GABARAP are authentic modifiers mediated by Apg7 and Apg3. *Biochem Biophys Res Commun* **300**, 637-44.
- Tanida, I., Sou, Y. S., Ezaki, J., Minematsu-Ikeguchi, N., Ueno, T., and Kominami, E. (2004a). HsAtg4B/HsApg4B/autophagin-1 cleaves the

carboxyl termini of three human Atg8 homologues and delipidates microtubule-associated protein light chain 3- and GABAA receptor-associated protein-phospholipid conjugates. *J Biol Chem* **279**, 36268-76.

Tanida, I., Ueno, T., and Kominami, E. (2004b). Human light chain 3/MAP1LC3B is cleaved at its carboxyl-terminal Met121 to expose Gly120 for lipidation and targeting to autophagosomal membranes. *J Biol Chem* **279**, 47704-10.

Tanida, I., Ueno, T., and Kominami, E. (2004c). LC3 conjugation system in mammalian autophagy. *Int J Biochem Cell Biol* **36**, 2503-18.

Tanida, I., Sou, Y. S., Minematsu-Ikeguchi, N., Ueno, T., and Kominami, E. (2006). Atg8L/Apg8L is the fourth mammalian modifier of mammalian Atg8 conjugation mediated by human Atg4B, Atg7 and Atg3. *Febs J* **273**, 2553-62.

Ter Kuile, B. H., and Opperdoes, F. R. (1992). A chemostat study on proline uptake and metabolism of *Leishmania donovani*. *J Protozool* **39**, 555-8.

Tetaud, E., Lecuix, I., Sheldrake, T., Baltz, T., and Fairlamb, A. H. (2002). A new expression vector for *Crithidia fasciculata* and *Leishmania*. *Mol Biochem Parasitol* **120**, 195-204.

Thinakaran, G., Borchelt, D. R., Lee, M. K., Slunt, H. H., Spitzer, L., Kim, G., Ratovitsky, T., Davenport, F., Nordstedt, C., Seeger, M., Hardy, J., *et al.*, (1996). Endoproteolysis of presenilin 1 and accumulation of processed derivatives in vivo. *Neuron* **17**, 181-90.

Tooze, J., Hollinshead, M., Ludwig, T., Howell, K., Hoflack, B., and Kern, H. (1990). In exocrine pancreas, the basolateral endocytic pathway converges with the autophagic pathway immediately after the early endosome. *J Cell Biol* **111**, 329-45.

Tsukada, M., and Ohsumi, Y. (1993). Isolation and characterization of autophagy-defective mutants of *Saccharomyces cerevisiae*. *FEBS Lett* **333**, 169-74.

Tuon, F. F., Amato, V. S., Graf, M. E., Siqueira, A. M., Nicodemo, A. C., and Amato Neto, V. (2008). Treatment of New World cutaneous leishmaniasis-- a systematic review with a meta-analysis. *Int J Dermatol* **47**, 109-24.

Turco, S. J., and Sacks, D. L. (1991). Expression of a stage-specific lipophosphoglycan in *Leishmania major* amastigotes. *Mol Biochem Parasitol* **45**, 91-9.

Tuttle, D. L., and Dunn, W. A., Jr. (1995). Divergent modes of autophagy in the methylotrophic yeast *Pichia pastoris*. *J Cell Sci* **108** ( Pt 1), 25-35.

Tuttle, D. L., Lewin, A. S., and Dunn, W. A., Jr. (1993). Selective autophagy of peroxisomes in methylotrophic yeasts. *Eur J Cell Biol* **60**, 283-90.

## U

- Ueda-Nakamura, T., da Conceicao Rocha Sampaio, M., Cunha-e-Silva, N. L., Traub-Cseko, Y. M., and de Souza, W. (2002). Expression and processing of megasome cysteine proteinases during *Leishmania amazonensis* differentiation. *Parasitol Res* **88**, 332-7.
- Uetz, P., Giot, L., Cagney, G., Mansfield, T. A., Judson, R. S., Knight, J. R., Lockshon, D., Narayan, V., Srinivasan, M., Pochart, P., *et al.*, (2000). A comprehensive analysis of protein-protein interactions in *Saccharomyces cerevisiae*. *Nature* **403**, 623-7.

## V

- Valdivieso, E., Dagger, F., and Rascon, A. (2007). *Leishmania mexicana*: identification and characterization of an aspartyl proteinase activity. *Exp Parasitol* **116**, 77-82.
- van Zandbergen, G., Klinger, M., Mueller, A., Dannenberg, S., Gebert, A., Solbach, W., and Laskay, T. (2004). Cutting edge: neutrophil granulocyte serves as a vector for *Leishmania* entry into macrophages. *J Immunol* **173**, 6521-5.
- Vida, T. A., and Emr, S. D. (1995). A new vital stain for visualizing vacuolar membrane dynamics and endocytosis in yeast. *J Cell Biol* **128**, 779-92.

## W

- Walden, H., Podgorski, M. S., Huang, D. T., Miller, D. W., Howard, R. J., Minor, D. L., Jr., Holton, J. M., and Schulman, B. A. (2003). The structure of the APPBP1-UBA3-NEDD8-ATP complex reveals the basis for selective ubiquitin-like protein activation by an E1. *Mol Cell* **12**, 1427-37.
- Waller, R. F., and McConville, M. J. (2002). Developmental changes in lysosome morphology and function *Leishmania* parasites. *Int J Parasitol* **32**, 1435-45.
- Wang, H., Bedford, F. K., Brandon, N. J., Moss, S. J., and Olsen, R. W. (1999). GABA(A)-receptor-associated protein links GABA(A) receptors and the cytoskeleton. *Nature* **397**, 69-72.
- Wang, J., Beher, D., Nyborg, A. C., Shearman, M. S., Golde, T. E., and Goate, A. (2006). C-terminal PAL motif of presenilin and presenilin homologues required for normal active site conformation. *J Neurochem* **96**, 218-27.
- Weihofen, A., Binns, K., Lemberg, M. K., Ashman, K., and Martoglio, B. (2002). Identification of signal peptide peptidase, a presenilin-type aspartic protease. *Science* **296**, 2215-8.

- Weihofen, A., Lemberg, M. K., Friedmann, E., Rueeger, H., Schmitz, A., Paganetti, P., Rovelli, G., and Martoglio, B. (2003). Targeting presenilin-type aspartic protease signal peptide peptidase with gamma-secretase inhibitors. *J Biol Chem* **278**, 16528-33.
- Weihofen, A., Lemberg, M. K., Ploegh, H. L., Bogyo, M., and Martoglio, B. (2000). Release of signal peptide fragments into the cytosol requires cleavage in the transmembrane region by a protease activity that is specifically blocked by a novel cysteine protease inhibitor. *J Biol Chem* **275**, 30951-6.
- Weise, F., Stierhof, Y. D., Kuhn, C., Wiese, M., and Overath, P. (2000). Distribution of GPI-anchored proteins in the protozoan parasite *Leishmania*, based on an improved ultrastructural description using high-pressure frozen cells. *J Cell Sci* **113 Pt 24**, 4587-603.
- Williams, R. A., Tetley, L., Mottram, J. C., and Coombs, G. H. (2006). Cysteine peptidases CPA and CPB are vital for autophagy and differentiation in *Leishmania mexicana*. *Mol Microbiol* **61**, 655-74.
- Williams, R. A., Woods, K. L., Juliano, L., Mottram, J. C., and Coombs, G. H. (2009). Characterization of unusual families of ATG8-like proteins and ATG12 in the protozoan parasite *Leishmania major*. *Autophagy* **5-2(1-14)**
- Wilson, C. A., Murphy, D. D., Giasson, B. I., Zhang, B., Trojanowski, J. Q., and Lee, V. M. (2004). Degradative organelles containing mislocalized alpha- and beta-synuclein proliferate in presenilin-1 null neurons. *J Cell Biol* **165**, 335-46.
- Wolfe, M. S., Xia, W., Ostaszewski, B. L., Diehl, T. S., Kimberly, W. T., and Selkoe, D. J. (1999). Two transmembrane aspartates in presenilin-1 required for presenilin endoproteolysis and gamma-secretase activity. *Nature* **398**, 513-7.
- Wong, P. C., Zheng, H., Chen, H., Becher, M. W., Sirinathsinghji, D. J., Trumbauer, M. E., Chen, H. Y., Price, D. L., Van der Ploeg, L. H., and Sisodia, S. S. (1997). Presenilin 1 is required for Notch1 and Dll1 expression in the paraxial mesoderm. *Nature* **387**, 288-92.

## X

- Xia, W., and Wolfe, M. S. (2003). Intramembrane proteolysis by presenilin and presenilin-like proteases. *J Cell Sci* **116**, 2839-44.
- Xia, W., Zhang, J., Kholodenko, D., Citron, M., Podlisny, M. B., Teplow, D. B., Haass, C., Seubert, P., Koo, E. H. c., and Selkoe, D. J. (1997). Enhanced production and oligomerization of the 42-residue amyloid beta-protein by

Chinese hamster ovary cells stably expressing mutant presenilins. *J Biol Chem* **272**, 7977-82.

- Xie, Z., and Klionsky, D. J. (2007). Autophagosome formation: core machinery and adaptations. *Nat Cell Biol* **9**, 1102-9.
- Xie, Z., Nair, U., and Klionsky, D. J. (2008). Atg8 controls phagophore expansion during autophagosome formation. *Mol Biol Cell* **19**, 3290-8.
- Xu, J., Zhang, J., Wang, L., Zhou, J., Huang, H., Wu, J., Zhong, Y., and Shi, Y. (2006). Solution structure of Urm1 and its implications for the origin of protein modifiers. *Proc Natl Acad Sci U S A* **103**, 11625-30.

## Y

- Yang, Y. P., Liang, Z. Q., Gu, Z. L., and Qin, Z. H. (2005). Molecular mechanism and regulation of autophagy. *Acta Pharmacol Sin* **26**, 1421-34.
- Yao, C., Donelson, J. E., and Wilson, M. E. (2003). The major surface protease (MSP or GP63) of *Leishmania* sp. Biosynthesis, regulation of expression, and function. *Mol Biochem Parasitol* **132**, 1-16.
- Ye, Y., Lukinova, N., and Fortini, M. E. (1999). Neurogenic phenotypes and altered Notch processing in *Drosophila* Presenilin mutants. *Nature* **398**, 525-9.
- Yoo, A. S., Cheng, I., Chung, S., Grenfell, T. Z., Lee, H., Pack-Chung, E., Handler, M., Shen, J., Xia, W., Tesco, G., Saunders, A. J., Ding, K., Frosch, M. P., Tanzi, R. E., and Kim, T. W. (2000). Presenilin-mediated modulation of capacitative calcium entry. *Neuron* **27**, 561-72.
- Yu, W. H., Cuervo, A. M., Kumar, A., Peterhoff, C. M., Schmidt, S. D., Lee, J. H., Mohan, P. S., *et al.*, (2005). Macroautophagy--a novel Beta-amyloid peptide-generating pathway activated in Alzheimer's disease. *J Cell Biol* **171**, 87-98.
- Yu, W. H., Kumar, A., Peterhoff, C., Shapiro Kulnane, L., Uchiyama, Y., Lamb, B. T., Cuervo, A. M., and Nixon, R. A. (2004). Autophagic vacuoles are enriched in amyloid precursor protein-secretase activities: implications for beta-amyloid peptide over-production and localization in Alzheimer's disease. *Int J Biochem Cell Biol* **36**, 2531-40.

## Z

- Zhang, J., Kang, D. E., Xia, W., Okochi, M., Mori, H., Selkoe, D. J., and Koo, E. H. (1998). Subcellular distribution and turnover of presenilins in transfected cells. *J Biol Chem* **273**, 12436-42.

- Zhang, K., Pompey, J. M., Hsu, F. F., Key, P., Bandhuvula, P., Saba, J. D., Turk, J., and Beverley, S. M. (2007). Redirection of sphingolipid metabolism toward de novo synthesis of ethanolamine in *Leishmania*. *Embo J* **26**, 1094-104.
- Zhang, K., Showalter, M., Revollo, J., Hsu, F. F., Turk, J., and Beverley, S. M. (2003). Sphingolipids are essential for differentiation but not growth in *Leishmania*. *Embo J* **22**, 6016-26.
- Zheng, L., Marcusson, J., and Terman, A. (2006a). Oxidative stress and Alzheimer disease: the autophagy connection? *Autophagy* **2**, 143-5.
- Zheng, L., Roberg, K., Jerhammar, F., Marcusson, J., and Terman, A. (2006b). Oxidative stress induces intralysosomal accumulation of Alzheimer amyloid beta-protein in cultured neuroblastoma cells. *Ann N Y Acad Sci* **1067**, 248-51.
- Zheng, Z., Butler, K. D., Tweten, R. K., and Mensa-Wilmot, K. (2004). Endosomes, glycosomes, and glycosylphosphatidylinositol catabolism in *Leishmania major*. *J Biol Chem* **279**, 42106-13.
- Zijlstra, E. E., Musa, A. M., Khalil, E. A., el-Hassan, I. M., and el-Hassan, A. M. (2003). Post-kala-azar dermal leishmaniasis. *Lancet Infect Dis* **3**, 87-98.
- Zufferey, R., Allen, S., Barron, T., Sullivan, D. R., Denny, P. W., Almeida, I. C., Smith, D. F., Turco, S. J., Ferguson, M. A., and Beverley, S. M. (2003). Ether phospholipids and glycosylinositolphospholipids are not required for amastigote virulence or for inhibition of macrophage activation by *Leishmania major*. *J Biol Chem* **278**, 44708-18.

